On the role of amino acids in plant disease resistance:

Interplay between pipecolic acid and salicylic acid in plant systemic acquired resistance

Inaugural-Dissertation

Zur Erlangung des Doktorgrades der

Mathematisch-Naturwissenschaftlichen Fakultät

der Heinrich-Heine-Universität Düsseldorf

vorgelegt von

Friederike Elisabeth Maria Bernsdorff

aus Eutin

Düsseldorf, Oktober 2014

Aus dem Institut für Molekulare Ökophysiologie der Pflanzen

der Heinrich-Heine Universität Düsseldorf

Gedruckt mit der Genehmigung der

Mathematisch-Naturwissenschaftlichen Fakultät

der Heinrich-Heine Universität Düsseldorf

Referent: Prof. Dr. Jürgen Zeier

Koreferent: Prof. Dr. Michael Feldbrügge

Tag der mündlichen Prüfung: ....

I. SUMMARY

Recognition of microbes by plants leads to both local and systemic immune responses. Systemic acquired resistance (SAR) is a long-lasting, broad-spectrum disease resistance that occurs in uninfected parts of the plant. The establishment of SAR requires the accumulation of the phenolic compound salicylic acid (SA) in distal leaves, but SA itself is not the mobile signal. A number of potential SAR signals have recently been proposed in the last decade, such as methyl salicylate (MeSA), dehydroabietenal (DA), glycerol-3-phosphate (G3P), azelaic acid (AzA) and the lipid transfer protein DEFECTIVE IN INDUCED RESISTANCE 1 (DIR1), but the true identity of the mobile signal is still controversial. Our laboratory has recently identified the lysine (Lys)-derived non-proteinogenous amino acid pipecolic acid (Pip) as a novel important regulator of local and systemic acquired resistance, as well as defense priming, in *Arabidopsis thaliana*. In addition to Pip, massive changes in free amino acid levels were also observed upon pathogen recognition, revealing an unexpected role for these molecules in plant immunity.

In this thesis, we investigated the role of free amino acids during plant defense, the mechanisms underlying Pip-induced resistance, and the relationship between Pip and SA during SAR and defense priming in *Arabidopsis thaliana*. We observed that the profile of amino acids changes was similar when plants were treated with virulent or avirulent strains of the bacterium *Pseudomonas syringae* pv. *maculicola*, or upon treatment with the bacterial pathogen-associated molecular pattern (PAMP) flg22. To test whether pathogen-induced free amino acid changes depend on immune hormone signaling pathways, we measured free amino acid levels in mutants affected in SA, jasmonic acid or ethylene biosynthesis and/or signaling. Interestingly, the lipase-like PHYTOALEXIN-DEFICIENT4 (PAD4) differentially regulated changes of distinct amino acids, revealing an unexpected uncoupling of amino acid induced biosynthesis during defense.

To uncover the relationship between Pip and SA, we monitored amino acid levels and gene expression changes in distal leaves of the SA-deficient mutant *sid2-1* during SAR. Surprisingly, we observed that it still exhibited a systemic increase in Pip levels, an increased expression of the genes encoding *AGD2-LIKE DEFENSE RESPONSE PROTEIN1* (*ALD1*; as an important Pip biosynthetic enzyme) and *FLAVIN-DEPENDENT MONOOXYGENASE1* (*FMO1*; as a critical regulator of Pip-mediated resistance), and resistance induced by exogenous Pip treatment, albeit to lower levels than in wild-type distal leaves. Furthermore, we found that Pip and SA contributed additively to basal resistance, and that SA-deficient mutants exhibited a modest, but significant SAR response, which was otherwise absent in Pip-deficient mutants. Together, these results indicate an SA-independent role of Pip during

SAR. To further study this novel SA-independent regulatory node of SAR, we analyzed transcriptional changes during SAR in wild-type, SA- and Pip-deficient plants. We observed a transcriptional reprogramming in distal leaves and found that SAR as a state with activated defense responses was further associated with decreased photosynthesis rates and anabolic metabolism. Interestingly, we identified a subset of SAR genes whose expression was partially SA-independent, and strikingly observed that the Pip-deficient mutant *ald1* hardly mounted any transcriptional reprogramming during SAR, confirming that Pip is an SA-independent, central regulator of gene expression during SAR.

We further wanted to characterize the role of Pip in the priming of defense responses by SAR. We found that defense priming is orchestrated by Pip and FMO1 in both an SA-dependent and -independent manner. Combined and single treatments with Pip and SA revealed that they employ two distinct pathways that lead to a synergistic effect on the priming of *PR1* gene expression and disease resistance.

Lastly, we sought to characterize the close ALD1 homolog, the diaminopimelate-aminotransferase ABERRANT GROWTH AND CELL DEATH 2 (AGD2) and found that *agd2* accumulates an unknown compound that may partly explain the constitutive disease resistance observed in this mutant. To gain further insight in the enzymatic processes of the Pip biosynthetic pathway, we selected candidate genes with a potential role upstream and downstream of Pip biosynthesis based on expression patterns and homology in other organisms. Despite altered Pip levels, mutant lines in these genes did not show impaired SAR, suggesting potential functional redundancy and/or the involvement of other enzymes. Finally, we examined the sub-cellular localization of ALD1 and FMO1, which are required for Pip accumulation and signaling, respectively. We found that ALD1 localizes in the chloroplasts and FMO1 in the endoplasmic reticulum, suggesting that Pip biosynthesis and signaling act in different organelles. In summary, this thesis revealed Pip as a crucial regulator of local and systemic immunity and priming against bacteria, that acts via both SA-dependent and -independent pathways.

I. ZUSAMMENFASSUNG

Die Erkennung von Mikroorganismen hat eine lokale und systemische Immunantwort in Pflanzen zur Folge. Systemisch erworbene Resistenz (SAR = Systemic acquired resistance) ist eine langfristig Abwehrreaktion, die wirksam gegen einen breiten Kreis von Pathogenen in nicht-infizierten Teilen der Pflanze ist. Für die Etablierung von SAR bedarf es der Akkumulation des phenolischen Phytohormons Salicylsäure (SA = Salicylic acid) im distalen Blatt. SA selbst ist jedoch nicht das mobile SAR-Signal. Eine Reihe anderer potentieller Kandidaten, wie etwa Methylsalicylat (MeSA), Dehydroabietinal (DA), Glycerol-3-Phosphat (G3P) und das Lipidtransferprotein DEFECTIVE IN INDUCED RESISTANCE 1 (DIR1), wurden innerhalb der letzten 10 Jahre diskutiert, die wahre Identität des SAR-Signals konnte bis jetzt jedoch nicht geklärt werden. Vor Kurzem wurde in unserer Arbeitsgruppe die von Lysin abgeleitete, nicht proteinogene Aminosäure Pipecolinsäure (Pip) als wichtiger Regulator von lokaler und systemisch erworbener Resistenz und Abwehrpriming in *Arabidopsis thaliana* identifiziert. Eine massive Änderung freier Aminosäurelevel, inklusive Pip, nach Pathogenerkennung, verdeutlicht die unerwartete Rolle von Aminosäuren in der Pflanzenimmunität.

In dieser Arbeit wird die Rolle freier Aminosäuren während der Pflanzenabwehr, die Mechanismen die hinter der Pip-induzierten Resistenz stehen und die Beziehung zwischen Pip und SA während SAR und Abwehrpriming in *Arabidopsis thaliana* untersucht. Wir konnten zeigen, dass das Aminosäureprofil nach der Infektion mit virulenten oder avirulenten Stämmen des Bakteriums *Pseudomonas syringae* pv. *maculicola*, oder nach Behandlung mit dem bakteriellen Pathogen-assoziierten molekularen Muster (PAMP = Pathogen associated molecular pattern) flg22, sehr ähnlich war. Um zu überprüfen, ob diese durch Pathogene induzierten Änderungen der Aminosäuregehalte von hormonellen Signalwegen abhängen, haben wir Mutanten, beeinträchtigt in der Biosynthese, oder Signalweitergabe von SA, Jasmonsäure und Ethylen, für unsere Analysen verwendet. Interessanterweise regulierte das lipase-ähnliche Protein PHYTOALEXIN-DEFICIENT4 (PAD4) die Akkumulation bestimmter Aminosäuren und deutete dadurch auf eine unerwartete Entkopplung der Aminosäurebiosynthese während der Pflanzenabwehr hin. Um die Beziehung zwischen Pip und SA zu entschlüsseln wurden die Aminosäuregehalte und die Expression von Abwehrgenen in distalen Blättern der SA-defizienten Mutante *sid2-1* während der SAR untersucht. Überraschenderweise konnten wir eine systemische Akkumulation von Pip, eine Erhöhung der Expression von AGD2-LIKE DEFENSE RESPONSE PROTEIN1 (ALD1; spielt eine wichtige Rolle in der Pip-Biosynthese) und FLAVIN-DEPENDENT MONOOXYGENASE1 (FMO1; entscheidend für die Regulation von Pip-vermittelter

Resistenz), wie auch eine Erhöhung der Resistenz durch externe Pip-Gabe feststellen, wenn auch zu einem niedrigeren Niveau als in Blättern des Wildtyps. Weiterhin konnten wir einen additiven Beitrag von Pip und SA innerhalb der basalen Resistenz und eine moderate, jedoch signifikante SAR-Antwort, die in Pip-defizienten Mutanten fehlte, in *sid2-1* feststellen. Zusammengefasst deuten diese Ergebnisse darauf hin, dass eine SA-unabhängige Rolle für Pip während der SAR existiert. Um diesen neuen Aspekt von SA-unabhängiger SAR näher zu untersuchen, analysierten wir die transkriptionellen Änderungen innerhalb des distalen Blattes von SA- und Pip-defizienten Mutanten während der SAR. Wir beobachteten eine transkriptionelle Re-Programmierung in distalen Blättern und stellten fest, dass SAR, als Zustand aktivierter Pathogenabwehr, weiterhin mit einer Reduktion der Photosynthese und anabolischen Stoffwechselprozessen assoziiert war. Interessanterweise konnten wir eine SA-unabhängige Gruppe von SAR-Genen identifizieren und beachtenswerterweise feststellen, dass die Pip-defiziente *ald1* Mutante kaum transkriptionelle Veränderungen während der SAR aufweist. Diese Ergebnisse bestätigen, dass Pip ein SA-unabhängiger, zentraler Regulator der Genexpression während der SAR ist. Weiterhin wollten wir die Rolle von Pip im SAR-induzierten Priming von Abwehrreaktionen charakterisieren. Wir konnten zeigen, dass Abwehrpriming in SA-abhängiger und -unabhängiger Weise von ALD1 und FMO1 reguliert ist. Kombinierte und Einzelbehandlungen von Pip und SA konnten zusätzlich zeigen, dass unterschiedliche Signalwege genutzt werden und es einen synergistischen Effekt auf *PR-1* Expression und Resistenz gibt. Schließlich wollten wir die Rolle des ALD1 Homologs, der L,L-Diaminopimelate Aminotransferase ABERRANT GROWTH AND CELL DEATH 2 (AGD2), charakterisieren. Wir beobachteten die Akkumulation einer bis dato nicht identifizierten Substanz in *agd2-1*, die helfen könnte den konstitutiven Resistenzphänotyp dieser Mutante zu erklären. Um besseren Einblick in die enzymatischen Prozesse des Pip-Biosyntheseweges zu bekommen, selektierten wir Kandidatengene mit möglicher Funktion stromauf- und stromabwärts der Pip-Biosynthese, begründet auf Genexpressionsdaten und Homologien in anderen Organismen. Trotz veränderter Pip-Gehalte zeigten diese Mutanten keine Verschlechterung in der SAR, was darauf schließen lässt, dass die selektierten Kandidaten funktionell redundant und/oder dass noch andere Enzyme in diese Prozesse involviert sind. Zuletzt untersuchten wir die subzelluläre Lokalisation von ALD1 und FMO1, die jeweils für die Akkumulation von Pip und die Signalweitergabe notwendig sind. Wir konnten zeigen, dass ALD1 im Chloroplasten und FMO1 im Endoplasmatischen Retikulum lokalisiert ist, was darauf schließen lässt, dass die Pip-Biosynthese und Signalweitergabe in unterschiedlichen Organellen stattfindet.

Zusammenfassend konnte diese Arbeit zeigen, dass Pip ein zentraler Regulator der lokalen und systemischen Immunität und Priming gegen Bakterien ist und dass die Pip vermittelte Resistenzantwort über SA-abhängige und –unabhängige Signalwege läuft.

II.   INTRODUCTION

II.1. GENERAL PLANT IMMUNITY

II.1.1. PAMP-triggered immunity

Plants develop a defense system that consists of constitutive barriers on the surface of the plant like wax layers and rigid cell walls and inducible defenses that render the plant into an unsuitable source for proliferation and nutrition of the pathogen (Thordal-Christensen, 2003). In order to be ahead and prepared for an early recognition of the pathogen, a multi-layered defense system exists, that allows the plant to fight off infection from the very beginning. Bacteria and fungi carry specific motifs conserved among species that will be recognized by the plants. The so called pathogen or microbe associated molecular patterns (PAMPs/MAMPs) are indispensable, highly conserved among entire groups and classes of pathogens and not easily modified by mutagenesis to avoid recognition by the host. MAMPs are general elicitors of plant defense and include flagellin and polysaccharides from bacteria and chitin and ergosterol from fungi or damage associated molecular patterns (DAMPs) that are released by the plant upon infection (Boller et *al.*, 1995; Dow et *al.*, 2000; Felix et *al.*, 1993; Granado et *al.*, 1995, Lotze et *al.*, 2007).

PAMPs are recognized by the plants through pattern recognition receptors (PRRs) that are located in the plasma membrane and trigger PAMP-triggered immunity (PTI). PRRs can be divided into two groups, the receptor kinases (RKs) and the receptor like proteins (RLPs) (Shiu and Bleecker, 2001). The two receptor classes differ structurally. Whereas RKs consist of an extracellular ligand-binding domain, a transmembrane and a cytoplasmic kinase signaling domain, the RLPs lack the intracellular signaling domain (Fritz-Laylin et *al.*, 2005). Two of the best studied MAMPs are flagellin and the elongation factor Tu (EF-Tu). Flagellin is the subunit building filament of the bacterial flagellum. Plants and mammals share similar recognition mechanisms, as flagellin is also recognized by the Toll-like receptor TLR5 (Smith et *al.*, 2003). The most N-terminal conserved domain of flagellin, the peptide flg22, is recognized by the LRR-type receptor kinase FLS2 (flagellin sensing 2) in Arabidopsis (Zipfel et *al.*, 2004; Felix et *al.*, 1999; Gómez-Gómez and Boller, 2000). Upon recognition of flg22, FLS2 forms a heterodimer complex with BRI1-associated kinase 1 (BAK1; Sun et *al.*, 2013). BAK1 is a LRR-RK that also acts as a co-receptor for the brassinolide receptor BRASSINOSTEROID-INSENSITIVE 1 (BRI1), a positive mediator of BR-mediated growth (Kim and Wang, 2010; Gómez-Gómez and Boller, 2000). The complex formation of FLS2 and BAK1 triggers downstream signaling via a mitogen-activated protein kinase pathway, composed of AtMEKK1, AtMKK4/AtMKK5 and AtMPK3/AtMPK6 followed by initiation of

defense responses (Asai et *al.*, 2002). EF-Tu is involved in translation processes in the bacteria and like flagellin highly conserved. The active peptide of EF-Tu, elf18 is recognized by the LRR-RK EFR (EF-TU RECEPTOR) and, like FLS2, relies on the regulatory LRR-BAK1 for signaling (Kunze et *al.*, 2004; Monaghan and Zipfel, 2012). The first line of defense during PTI upon PAMP recognition consists of altered ion fluxes, production of reactive oxygen species (ROS), and activation of mitogen-activated protein kinases (MAPKs) and Calcium-dependent protein kinases (CDPKs; Felix et *al.*, 1999; Gómez-Gómez et *al.*, 1999; Grant et *al.*, 2000; Asai et *al.*, 2002). MAP kinase signaling cascades induce numerous defense-related genes in *A. thaliana* including transcription factors, protein kinases, and phosphatases and proteins that regulate protein turnover (Navarro et *al.*, 2004).

II.1.2. Effector triggered immunity

Innate immunity can be overcome by adapted pathogens that secrete effectors directly inside the plant cell cytosol. The so-called effector triggered immunity can overcome the basal defense level of the plant and is the next step in the arms race of the plant and the pathogen. In response to the delivery of pathogen effectors, the plant develops a more specialized second way of recognition and evolves resistance-proteins (R-proteins) that specifically recognize the effectors in a direct or indirect manner (Flor, 1956). This gene-for-gene-resistance is established when an adapted pathogen that is carrying an avirulence (avr) gene encounters a host plant that carries the matching resistance gene (R-gene). During this incompatible interaction, bacterial growth is suppressed after a short proliferation phase by the host, by triggering a sudden cell death called the hypersensitive response (HR). If one of the factors is absent, the interaction is compatible and the virulent pathogen is able to infect the host plant. Plants and pathogens constantly try to overcome an evolved advantage of the counterpart and develop themselves new R-genes and avr-genes, respectively, to suppress in an „arms race" pathogenicity or ETI (Chrisholm et *al.*, 2006). Gram-negative bacteria have evolved an important mechanism to overcome plant resistance called type III protein secretion system (T3SS; Büttner and He, 2009). Bacteria are enabled to deliver effector proteins through the T3SS directly into the host cell to manipulate cellular functions (Block and Alfano, 2011). The structure of an R-gene that will recognize these effector proteins consists of a variable N-terminal region, a nucleotide-binding site (NB) and a C-terminal LRR-domain. The majority of the NB-LRR receptors can be grouped according to their N-terminus, which consists either of a 'toll, interleukin 1R and resistance'- (TIR) or a coiled-coil (CC)-domain (Maekawa et *al.*, 2011; Bonardi and Dangl, 2012). Well studied NB-LRR protein/*avr* protein interactions in the *Arabidopsis/Pseudomonas syringae* pathosystem with

a TIR-domain is *RPS4/AvrRps4* and with a CC-domain *RPM1/AvrRpm1* and *AvrB*, *RPS5/AvrPphB*, *RPS2/AvrRpt2*. In an unchallenged state RPM1 and RPS2 interact with RIN4 to ensure an inactive state (Axell and Staskawicz, 2003). As soon as the corresponding effectors are recognized by the R-proteins, RIN4 is phosphorylated, mediated by a protein kinase, RPM1 becomes activated and downstream signaling is then induced (Liu et *al.*, 2011a). TIR-NB-LRRs require lipase-like proteins ENHANCED DISEASE SUSCEPTIBILITY1 (EDS1) and its interaction partners PHYTOALEXIN DEFICIENT 4 (PAD4) and SENESCENCE-ASSOCIATED GENE 101 (SAG101). EDS1 is required to regulate *RPP2-*, *RPP4-*, *RPP5-*, *RPP21-*, and *RPS4-*mediated resistance to the biotrophic oomycete *Peronospora parasitica*, and to *Pseudomonas* bacteria expressing the avirulence gene *avrRps4* (Aarts et *al.*, 1998; Coppinger et *al.*, 2004). In contrast, for the activity of CC-NB-LRR protein NON RACE SPECIFIC DISEASE RESISTACE1 (NDR1) is needed. NDR1 is a glycosylphosphatidylinositol-anchored plasma membrane protein that is interacting with RIN4 and thus required for the function of RPS2, RPS5 and RPM1-mediated immunity against *P. syringae* pv. *tomato* DC3000 (Coppinger et *al.*, 2004).

PTI and ETI both activate defense responses in the local leaf. One of the earliest defense responses upon infection with virulent and avirulent pathogens is the regulation of ion-channel permeability that stimulates ion fluxes (Ca^{2+} and H^+ influx, K^+ and Cl^- efflux) over plasma membranes (Scheel, 1998). Ca^{2+} channels that are activated by elicitors, will lead to a reallocation of extracellular Ca^{2+} to increase cytosolic Ca^{2+} levels (Zimmermann et *al.*, 1997). CALCIUM-DEPENDENT PROTEIN KINASE (CDPK) was identified as one of the earliest elicitor-responsive downstream targets of Ca^{2+} as treatment with AVR9 resulted in rapid phosphorylation and activation of this CDPK in a Ca^{2+} dependent manner (Romeis et *al.*, 2000). Ca^{2+} binds to the calmodulin-like domain of CDPK and causes conformational change of the enzyme. This conformational change leads to activation and phosphorylation of the enzyme (Romeis et *al.*, 2000).

Another important component of early pathogen defense and defense signaling is the oxidative burst (Blume et *al.*, 2000). Transient increases of cytosolic Ca^{2+} levels lead to production of ROS like superoxide such as superoxide anions (O_2^-), hydrogen peroxide (H_2O_2), hydroxyl radicals (OH^-) and active species of nitric oxide (NO), among others in the apoplast (Dempsey et *al.*, 1999; Holuigue et *al.*, 2007). The accumulation of ROS may kill the pathogen directly and/or leads to reinforcement of the cell walls (Dempsey and Klessig, 1999; Durner et *al.*, 1997). ROS also induces the development of a hypersensitive response (HR) which leads to necrosis of the infected cell (Vlot et *al.*, 2009) Mitogen-activated protein kinases (MAPKs) are important regulators in signaling upon pathogen induced stresses and are activated by a large variety of abiotic and biotic stimuli (Nürnberger and Scheel, 2001). The MAPK signaling cascade consists of protein kinases that will be phosphorylated upon

perception of a stimulus. In this cascade MAPK kinase kinase (MAPKKK) is phosphorylated to a MAPK kinase (MAPKK), which is phosphorylated to a MAPK. Arabidopsis MAPK signaling triggered by flagellin leads to the activation MEKK1, MKK4/MKK5, and MPK3/MPK6 which in the end induces the transcription factors WRKY29 and FRK1 and defense responses like tissue necrosis (Asai et *al.*, 2002). An important signal for PTI and ETI activation is salicylic acid (SA; DebRoy et *al.*, 2004; Dempsey et *al.*, 1999; Klessig and Malamy, 1994). The burst of reactive oxygen species during incompatible interactions induces SA-dependent systemic acquired resistance (SAR; Cameron et *al.*, 1994). However, SAR establishment is not dependent on a hypersensitive response of necrotic disease symptoms during non-host *Pseudomonas syringae* interaction with Arabidopsis (Mishina and Zeier, 2007; Liu et *al.*, 2010; Vlot et *al.*, 2009; Fu and Dong, 2013).

II.2. PLANT DEFENSE HORMONES

II.2.1. SALICYLIC ACID (SA)

II.2.1.1. SA-biosynthesis

In plants salicylic acid (SA) is synthesized from chorismate via two distinct enzymatic pathways (Garcion and Metraux, 2006; Mao et *al.*, 2007).

The first pathway is characterized by the conversion of L-phenylalanine, a chorismate-derived amino acid, via the intermediates benzoate or coumaric acid to SA. This reaction is catalyzed by PHENYLALANINE AMMONIA LYASE (PAL). Although PAL is produced upon pathogen infection, it is not the major pathway for SA synthesis after infection (Lee et *al.*, 1995). The second enzymatic pathway synthesizes SA via isochorismate wich requires the catalytic enzymes ISOCHORISMATE SYNTHASE (ICS) and ISOCHORISMATE PYRUVATE LYASE (IPL; Wildermuth et *al.*, 2001). Pathogen-induced accumulation of SA in Arabidopsis is conducted via the isochorismate pathway. Two *ICS* genes, *ICS1* and *ICS2,* exist in Arabidopsis and *ICS1* is making up mostly 90% of the SA produced upon pathogen infection or UV light (Garcion et *al.*, 2008; Wildermuth et *al.*, 2001). Basal levels in *ics1 ics2* mutants indicate a different source for SA in Arabidopsis (Garcion et *al.*, 2008). Two allelic SA-deficient mutants, *sid2-2/eds16-1* and *sid2-1*, were mapped close to the *ICS* locus on chromosome 1 of *Arabidopsis thaliana. SID2* encodes a chloroplast-localized *ICS1* and expression patterns follow those observed after infection with a pathogen (Wildermuth et *al.*, 2001). In the mutant *sid2-2*, a fast-neutron-generated mutant, the *ICS1* transcript was not expressed after infection with *Golovinomyces orontii* or a virulent strain of the bacterial hemi-

14

biotroph, *P. syringae* pv. *maculicola*. A significant deletion/ rearrangement in exon IX by DNA blot analysis confirmed that *sid2-2* indeed carries a mutation in *ICS1*. The mutant *sid2-1* was generated by treatment with ethylmethane sulfonate (EMS) and contains a mutation in *ICS1*. *ICS1* genomic DNA from *sid2-1* was sequenced and a point mutation was found that results in a stop codon in exon IX. The mutations in both *sid2* alleles disrupt the chorismate binding domain (Wildermuth et *al.*, 2001). The *sid2* mutants are severely affected in basal and systemic disease resistance and *ICS1* expression, SA accumulation and *PR* gene expression were significantly reduced. After infection with pathogens SA levels were reduced to 5-10% of the wild type level in the *sid2* mutants (Wildermuth et al., 2001). Basal SA synthesis however is not completely abolished in *sid2* mutants and might be produced via the isochorismate synthase ICS2, or the phenylpropanoid pathway. The multidrug and toxin extrusion (MATE) family of transporter protein ENHANCED DISEASE SUSEPTIBILITY5 (EDS5/SID1) also is required for SA accumulation and relocating SA or a precursor out of the plastid after biosynthesis (Nawrath and Metraux, 1999; Wildermuth et *al.*, 2001; Serrano et *al.*, 2013).

Free SA is mostly converted into an inactive storage form in the vacuole like SA O-β-glucoside (SAG) and less abundant into salicyloyl glucose ester (SGE). Pathogen-inducible SA glucosyltransferases (SAGT) UGT74F1 and UGT74F2 are converting SA into either SAG or SGE. As ICS1 and ICS2 colocalize with chlorophyll autofluorescence signals in transient localization assays, SA is likely synthesized in the chloroplast, whereas SAGT in tobacco localizes to the cytosol (Garcion et *al.*, 2008; Dean et *al.*, 2005). SAGT designated UGT74F1 forms only SAG, while UGT74F2 forms both SAG and SGE (Dean and Delaney, 2008). SAG synthesized in the cytosol is transported into the vacuole unless it is converted back into active SA (Dean and Mills, 2004; Dean et *al.*, 2005; Hennig et *al.*, 1993). Volatile methyl salicylate (MeSA), synthesized via the S-adenosyl-L-methionine SA-METHYLTRANSFERASE1 (SAMT1), and/or its glucosylated derivative MeSAG accumulate to high levels *in vivo* (Dean et *al.*, 2005, Park et *al.*, 2007, Seskar et *al.*, 1998; Attaran et *al.*, 2009). However, MeSA is like SAG biologically inactive (Koo et *al.*, 2007). SA and auxin indole acetic acid (IAA) can be conjugated to amino acids via an acyl-adenylate/thioester-forming enzyme (GH3.5). Arabidopsis plants overexpressing GH3.5 accumulated more SA, higher *PR* gene expression and showed elevated disease resistance to *P. syringae* pv. *tomato* strain DC3000 (Park et *al.*, 2007). Because the GH3.5 loss of function mutants is compromised in SAR it was proposed that GH3.5 acts as a positive regulator of SA-signaling (Zhang et *al.*, 2007).

II.2.1.2. SA role in resistance

The first evidence that SA might play a role in resistance arose when infiltration of aspirin or SA in the leaves of resistant tobacco cultivar Xanthi-nc prior to infection with tobacco mosaic virus (TMV) led to a 90%-reduction of lesion formation and induction of *PR* gene expression (White, 1979). In TMV-resistant tobacco cultivars, SA accumulated more than 20-fold in the inoculated leaves and 5-fold in the distal leaves, together with induced *PR* gene expression (Malamy et *al.*, 1990). SA accumulation was also found in the phloem exudates of cucumber after inoculation with tobacco necrosis virus, *Colletotrichum lagenarium*, and prior to SAR establishment (Metraux et *al.*, 1990). Injection of SA at concentrations found in the exudates of cucumber plants inoculated with *Pseudomonas syringae* induced resistance and increased peroxidase activity (Rasmussen et *al.*, 1991). Elevated SA levels correlated with enhanced resistance to pathogen infection, as expression of *ICS1* is constitutively elevated in three gain-of-resistance mutants*, cpr1, cpr5*, and *cpr6* (*constitutive expresser of PR genes1/5/6*; Wildermuth et *al.*, 2001). Loss of SA has severe impact on plant disease resistance. Tobacco and Arabidopsis plants that express the bacterial *NahG* gene (a salicylate hydroxylase converting SA to catechol) are unable to accumulate SA or development of SAR and *PR* gene expression. These plants were highly susceptible to virulent and avirulent pathogens (Delaney et *al.*, 1994; Gaffney et *al.*, 1993). The same phenotype was observed in Arabidopsis plants that are defective in SA biosynthesis, caused by mutations in SID2/EDS16 (encodes *ICS1*) or SID1/EDS5, and in tobacco plants with suppressed PAL expression (Nawrath and Metraux, 1999; Nawrath et *al.*, 2002; Pallas et *al.*, 1996, Wildermuth et *al.*, 2001). Plants expressing *NahG* or having defects in SA-biosynthesis showed restored resistance phenotypes after treatment with SA or the synthetic analog 2,6-dichloro-isonicotinic acid (INA; Vernooij, 1995). Furthermore, overexpression of genes involved in SA metabolism like the *SA GLUCOSYLTRANSFERASE1* (*AtSGT1*) or *SA METHYLTRANSFERASE* (*OsBSMT1*) lead to reduced endogenous SA levels, reduced PR expression and enhanced susceptibility to pathogens (Song et *al.*, 2008; Koo et *al.*, 2007).

II.2.1.3. Regulation of SA signaling

The SA signal transduction pathway plays a key role in plant defense signaling (Vlot et *al.*, 2009). All Arabidopsis mutants that are either impaired in SA signaling such as (*non expressor of PR genes 1*) *npr1*, *eds1* and *pad4* or are defective in pathogen induced SA accumulation such as *eds5* and *sid2-1*, are highly susceptible to pathogen infection and show reduced expression of *PR* gene s (Cao et *al.*, 1997; Falk et *al.*, 1999; Nawrath et *al.*,

2002; Wildermuth et *al.*, 2001 and Jirage et *al.*, 1999). The *NPR1* gene encodes a transcription co-activator that has an important role SA-mediated signaling during basal resistance and SAR (Durrant and Dong, 2004; Chaturvedi and Shah, 2007; Spoel and Dong, 2012). Furthermore NPR1 is required for induced systemic resistance (ISR), which is triggered by microbes in the rhizosphere conferring resistance in aerial parts of the plant (Durrant and Dong, 2004). The NPR1 protein contains, besides a bipartite nuclear localization sequence (NLS) and a phosphorylation site, two protein interaction domains: one ankyrin-repeat domain and one BTB/POZ (broad-complex, tramtrack, and bricà-brac/poxvirus, zinc finger; Cao et *al.*, 1998; Kinkema et *al.*, 2000) The Arabidopsis *npr1* mutant was isolated in a genetic screen for plants that failed to express *PR* genes after SAR induction. More *npr1* alleles (*nim1*) were found in screens for components of the SAR signaling pathway (Cao et *al.*, 1994; Delaney et *al.*, 1995; Glazebrook et *al.*, 1996). SAR is not restored in *npr1* mutants upon treatment with either SA, its synthetic analogs INA and benzo-(1,2,3)-thiadiazole-7-carbothioic acid S-methyl ester (BTH) and avirulent pathogens they are fully compromised in basal resistance and SAR and show enhanced disease symptoms when infected with virulent pathogens (Dong, 2004). However, some SA-dependent responses are independent of *NPR1*, since the synthesis of the phytoalexin camalexin requires SA but not NPR1 (Glazebrook et *al.*, 1994; Zhao and Last, 1996). The cytosolic oligomer NPR1 regulates the antagonism of SA- and JA-signaling. Accumulation of SA upon pathogen attack changes the cellular reduction potential and monomeric NPR1 is formed to facilitate the transport into the nucleus (Spoel et *al.*, 2003; Mou et *al.*, 2003; Kinkema et *al.*, 2000). In the nucleus, monomeric NPR1 interacts with members of the DNA-binding protein TGA-family of TFs, TGA2, TGA3, TGA5, TGA6 and TGA7, but not with TGA1 and TGA4, and regulates the expression of proteins in the secretory pathway such as PR proteins (Despres et *al.*, 2000; Zhang et *al.*, 2003; Wang et *al.*, 2005). To control NPR1 levels in the nucleus and to facilitate the next round of binding of NPR1 to TGA transcription factors to ensure maximal expression of *PR* genes during SAR, phosphorylation, ubiquitination and degradation of NPR1 is promoted by SA (Wang et *al.*, 2005; Spoel et *al.*, 2009). It is not fully clarified whether NPR1 is an SA-receptor, because of the conflicting results of two groups: Fu et *al.* (2012), detected SA-binding activity for NPR1, whereas Wu et *al.* (2012) did not. However, the NPR1 paralogues NPR3 and NPR4 were identified as SA receptors with different SA binding affinities. They function as adaptors of the Cullin 3 ubiquitin E3 ligase to mediate NPR1 degradation in an SA-regulated manner. Since the *npr3 npr4* double mutant accumulated higher levels of NPR1 and was insensitive to induction of SAR, it was suggested that NPR3 and NPR4 promote the SA-dependent turnover of NPR1 by the proteasome and regulate the function of NPR1 in SA signaling (Fu et *al.*, 2012). PAD4 and SAG101 were identified as interaction partners of EDS1 and regulate ETI through

TIR-type NB-LRR proteins and PTI against virulent pathogens or PAMP treatment (Feys et al., 2001; 2005; Wiermer et al, 2005). Pathogen-induced SA accumulation depends on NDR1, which regulates ETI through CC-type NB-LRR proteins and/or on EDS1 in interaction with PAD4 and SAG101 (Wiermer et al., 2005). Exogenous SA treatment can induce defense gene expression in *eds1*, *pad4* and *ndr1* mutants and *EDS1, PAD4* and *NDR1* gene expression in the wild type (Wiermer et al., 2005). These results indicate that downstream signaling is still functional in these mutants and that EDS1, PAD4 and NDR1 possibly act upstream of SA-biosynthesis in a positive signal amplification loop that is required for *PR-1* expression and other defense responses (Wiermer et al., 2005). In this model a pathogen infection creates a signal that leads to elevated SA levels that trigger the expression of *PAD4* which in turn would then stimulate SA biosynthesis (Jirage et al., 1999). Exogenous SA treatment is sufficient to trigger *PAD4* expression, but is also required for full *PAD4* expression during defense (Jirage et al., 1999). EDS1 forms a homodimer mostly in the cytoplasm, whereas EDS1-PAD4 heterodimers are localized in the cytoplasm and nucleus and EDS1-SAG101 heterodimers are located exclusively in the nucleus (Feys et al., 2005). EDS1 however is required in both compartments for the full establishment of plant innate immunity (García et al, 2010). In the heteromeric complexes EDS1 has a stabilizing effect on PAD4 and this complex is crucial for basal resistance and SAR (Rietz et al., 2011). The function of PAD4 and SAG101 seems to be partially redundant, since the *pad4* and *sag101* single mutants are less susceptible compared to the *pad4 sag101* mutants and *eds1* (Feys et al, 2005). The *pad4* mutant was identified in an EMS screen of Col-0 for mutants with enhanced susceptibility to *Psm* ES4326 (Glazebrook et al., 1996). The mutation in *pad4-1* is a recessive allele of a single gene that causes reduced camalexin levels and enhanced susceptibility upon *Psm* ES4326 infection (Glazebrook et al., 1996). Other mutants affected in camalexin induction include *pad1, pad2,* and *pad5.* Mutations in *PAD1*, *PAD2* and *PAD4* cause increased susceptibility to *Psm* E4326, whereas mutations in *PAD5* have no effect on resistance (Glazebrook et al., 1997).

Chloroplastic localized ENHANCED DISEASE SUSCEPTIBILITY5 (EDS5) shows homology to transporters of the MATE (Multidrug And Toxic compound Extrusion) family, which transport small organic molecules, but the exact function remains unclear (Dempsey et al., 2009; Kuroda and Tsuchiya, 2009; Nawrath et al, 2002). A possible function for EDS5 is the transport of a regulator for SA biosynthesis into the chloroplast, or to export SA from the plastid to the cytosol to ensure cytosolic functions and prevent feedback inhibition of SA biosynthesis (Dempsey et al., 2009). Expression of *EDS5* is induced by exogenous SA treatment, but its function can also be placed upstream of SA biosynthesis in the SA signaling pathway, as exogenous SA induced SA production and elevated levels of *PR-1* expression in *eds-5* mutants and in the wild type. Furthermore SA is not essential for stress

induced *EDS5* expression (Volko et *al*, 1998; Nawrath and Métraux, 1999; Nawrath et *al.*, 2002). *eds5* mutants, identified in a screen for enhanced disease susceptibility towards *Psm* E4326, are impaired in resistance to virulent pathogens development of SAR and show reduced levels of free and conjugated SA after biotic and abiotic stress (Glazebrook et *al.*, 1996; Rogers and Ausubel, 1997; Volko et *al,* 1998; Nawrath and Métraux, 1999). Very recently Métraux and colleagues could show that EDS5 is a MATE-like SA transporter that is localized at the chloroplast envelope, where it functions in the export of SA (Serrano et *al.*, 2013). Reduced levels of SA in *eds5* mutants might be explained by an autoinhibitory feedback regulation of SA accumulation in the chloroplast (Serrano et *al.*, 2013).

AVRPPHB SUSCEPTIBLE3 (PBS3/WIN3/GDG1/GH3.12) encodes the GH3 acyl adenylase thioester-forming enzyme GH3.12 and *pbs3* mutants were identified in a screen for reduced disease resistance (Nobuta et *al.*, 2007; Jagadeeswaran et *al.*, 2007; Lee et *al.*, 2007; Warren et *al.*, 1999). *pbs3* mutants show severely reduced levels of glycosidically bound SA (SAG) and total levels of SA and *PR-1* transcripts (Nobuta et *al.*, 2007). However, exogenous SA and BTH application can rescue *pbs3* plants and GH3.12 is thus proposed to act upstream of SA biosynthesis. It was proposed that the GH3.12 product 4-hydroxybenzoate-glutamic acid, might induce or prime SA biosynthesis and induce resistance (Okrent et *al.*, 2009).

ICS1 expression and thus SA biosynthesis is positively regulated by the transcription factors Calmodulin-Binding Protein 60-like g (CBP60g) and SAR-Deficient 1 (SARD1). SA accumulation and resistance to bacterial pathogens was compromised in PTI, ETI and SAR (Zhang et *al.*, 2010; Wang et *al.*, 2011). *SARD1* overexpressing lines showed a marked rise in total SA, induction of SA-responsive gene expression and resistance responses (Zhang et *al.*, 2010). An ICS1-promoter binding motif was found in both CBP60g and SARD1 (Wang et *al.*, 2011). CBP60g was identified to be important in early defense responses and in PTI and may induce SA-synthesis through the activation of Ca^{2+} signals, while SARD1 is important for later disease responses during ETI and SAR (Wang et *al.*, 2009; Zhang et *al.*, 2010; Wang et *al.*, 2011).

II.2.1.4. SA functions beside defense

SA is not only an important player in direct contribution to basal and induced plant defenses, it is also important for several processes affecting physiological functions in the plant; including seed germination, photosynthesis, respiration, thermogenesis, growth, flowering, seed production and senescence (Rivas-San Vincente and Plasencia, 2011). Additionally, SA might play a role in cellular redox homeostasis through regulation of antioxidant enzyme activity and induction of the alternative respiratory pathway (Durner and Klessig, 1995, 1996;

Slaymaker et al., 2002; Moore et al., 2002). SA is a known defense metabolite, but also plays an important role in photosynthesis and growth. Trade-offs between defense and growth have been intensively discussed (Huot et al., 2014).

SA can influence photosynthesis through alterations in leaf structure, chlorophyll structure and content, stomatal closure, the activity of RuBisCo (ribulose-1,5-bisphosphate carboxylase/oxygenase) and carbonic anhydrase (Rivas-San Vincente and Plasencia, 2011). Depending on the concentration of exogenous SA, the photosynthetic parameters differ. A high SA concentration (1-5 mM) cause reduction of the photosynthetic rate and RuBisCo in barley (Hordeum vulgare L.), and reduced chlorophyll content in Arabidopsis (Pancheva et al., 1996; Rao et al., 1997). The observed reduction of RuBisCo activity was due to a reduction in protein levels up to 50%. A reduction in photosynthetic activity at high SA concentrations might be due to changes in leaf morphogenesis that affect the structure of chloroplasts, thylakoids and stroma (Uzunova and Popova, 2000). On the contrary, exogenous SA at low concentrations (10 µM) also had a positive effect on the photosynthetic net CO_2 assimilation in mustard seedlings which lead to an increase in carboxylation efficiency, chlorophyll content and activities of carbonic anhydrase and nitrate reductase (Fariduddin et al., 2003). SA also protects against oxidative stress, possibly through rapid detoxification of ROS (Rivas-San Vincente and Plasencia, 2011). Arabidopsis mutants with constitutively high SA levels, like defense-no-death1 (dnd1) and cpr5-1, exhibit decreased maximum of PSII (F_v/F_m), reduced quantum yield of PSII (ΦPSII), increased thermal dissipation of absorbed light energy (NPQ) and reduced stomatal conductance in low light (LL; 100 µmol m^{-2} s^{-1}) conditions (Rivas-San Vincente and Plasencia, 2011). Arabidopsis mutants with low SA contents like sid2-1 and NahG are slightly impaired in PSII operating efficiency and increase heat dissipation in LL and also impaired in acclimation to high light (HL; 750 µmol m-2 s-1), whereas dnd1 and cpr5-1 acclimate like wild type plants (Mateo et al., 2006). Light acclimation by SA is most likely the result of hormonal and ROS signaling pathway contribution, because ET and ROS accumulate prior to SA in response to excess excitation energy (EEE; Mühlenbock et al., 2008). The response to EEE is regulated by LSD1 (LESION SIMULATING DISEASE1; At4g20380) a negative regulator of SA-dependent programmed cell death and the positive SA regulators PAD4 and EDS1. PAD4 and EDS1 modulate ET and ROS production upon EEE stress and LSD1 limits the spread of cell death through regulation of superoxide dismutase and catalase (Mühlenbock et al., 2008). Another important factor for photosynthesis is the regulation of stomatal aperture through hormonal regulation by abscisic acid (ABA), auxin, cytokinin, ET, brassinosteroids, JA and SA (Acharya and Assmann, 2009). Exogenous SA (0.4 mM) induces rapid stomata closure with an up to 4-fold reduction of stomatal gas exchange (Mateo et al., 2004). Since SA-deficient mutants like sid2-1 and NahG and the ABA-deficient mutants aba3-1 fail to close stomata in

response to virulent and avirulent pathogens, it was suggested that a positive cross-talk between SA- and ABA-signaling is required to promote stomatal closure during defense (Melotto et al., 2006). A growth-stimulating effect of low SA concentrations (50 µM) has been shown for soybean, wheat, maize and chamomile (Gutiérrez-Coronado et al., 1998; Shakirova et al., 2003; Gunes et al., 2007; Kovácik et al., 2009). Higher concentrations of SA (100 µM to 1 mM) had negative effects on trichome development in Arabidopsis (Traw and Bergelson, 2003). Constitutive defense mutants with elevated SA biosynthesis and signaling generally showed a dwarfed growth phenotype, but it is not ensured whether this is only linked to SA and not due to perturbed cellular processes (Clarke et al., 2000). Repeated BTH application reduced plant biomass in a dose-dependent manner and mutants identified in a screen for BTH-resistance were mostly identified as non-functional alleles of NPR1 (Canet et al., 2010b). It was shown that SA inhibits growth by suppression of the AUX signaling pathway by stabilization of the AUX/IAA repressor proteins (Wang et al., 2007).

II.2.2. JASMONATE (JA)

Jasmonate (JA) is a lipid-derived hormone originating from α-linolenic acid from the plastid membrane that regulates primarily the defense against insect herbivores and necotrophic pathogens (Pieterse et al., 2012; Schaller and Stintzi, 2009). Beside its role in plant defense, JA is involved in regulation of physiological processes like abiotic stress responses, flower development and leaf senescence and primary and secondary metabolism (Wasternack, 2007; Browse, 2009). There are several forms of biologically active jasmonates: The (+)-7-iso-jasmonoyl-L-isoleucine (JA-Ile) is the key player in jasmonate signaling in leaves and flowers, Jasmonoyl-L-tryptophan inhibits auxin signaling in roots and the JA precursors 12-oxo-phytodienoate (OPDA) and dinor-OPDA possess signaling properties within the jasmonate machinery (Fonseca et al., 2009b; Staswick, 2009; Ribot et al., 2008). The biosynthesis of JA is initiated in the plastids, completed in the peroxisomes and the active form of JA is then exported to the cytosol (Schaller and Stintzi, 2009). JA is esterified to methyl (+)-7-iso-jasmonate (MeJA) or conjugated with an amino acid to form (+)-7-iso-jasmonoyl-isoleucine (JA-Ile) which is the active form of the hormone (Schaller and Stintzi, 2009). The nuclear 18 leucine-rich repeat (LRR) F-box protein of an SCF-(Skip-cullin-F-box)-type E3 ubiquitin ligase CORONATINE INSENSITIVE 1 (COI1) forms a receptor complex with the JASMONATE ZIM-DOMAIN (JAZ) which binds Ja-Ile (Xie et al., 1998; Katsir et al., 2008; Chini et al., 2009a). JAZ proteins repress JA signaling by directly binding to MYC family of transcription factors that are required for the expression of JA-responsive genes in the nucleus (Chini et al., 2007; Thines et al., 2007; Yan et al., 2007; Withers et al., 2012) In

basal conditions transcription factors are repressed by JAZ proteins and the co-repressor TOPLESS (TPL) and TPL-related proteins (TPR) by the adaptor protein NINJA (Pauwels et al., 2010). A rise in JA-Ile level leads to binding of JAZ proteins to COI1 and degradation of JAZ by the 26S proteasome (Sheard et al., 2010). Upon ubiquitination and degradation of JAZ proteins, MYC2 and other transcription factors will induce the expression of JA responsive genes and the increase of JA-Ile levels in the local and distal tissues (Chini et al., 2007; Thines et al., 2007; Sheard et al., 2010, Fonseca et al., 2009b). coi1 mutants show elevated resistance to the P. syringae strain PstDC3000, which is correlated with accumulation of salicylic acid (SA) and PR-1 transcripts, and the necrotrophic pathogen F. oxysporum (Kloek et al., 2001; Thatcher et al., 2009). In contrast, coi1 plants are more susceptible to the fungal pathogens Alternaria brassicicola and Boytritis cinerea and are unable to induce PLANT DEFENSIN1.2 (PDF1.2) and pathogensis related genes PR-3, and PR-4 upon pathogen challenge (Thomma et al., 1998).

II.2.3. JA–SA CROSS TALK

To optimize the immune response against different types of pathogens, plants often suppress JA-dependent defenses, triggered during the interaction with necotrophic pathogens or herbivores, when infected with SA-inducing biotrophic pathogens and vice versa (Spoel et al., 2007; Uppalapati et al., 2007). The SA-mediated suppression of the JA pathway includes MPKs, NPR1, glutaredoxins and nuclear localized transcription factors like TGAs and WRKYs (Pieterse et al., 2012). MPK4 is a negative regulator of SA signaling and SAR and positively regulates JA signaling, involving the defense regulators EDS1 and PAD4 (Petersen et al., 2000; Brodersen et al., 2006). The SA master regulator NPR1 interacts with TGA TFs in the nucleus and activates SA-responsive PR genes (Dong, 2004). Although the nuclear localization of NPR1 is required to activate SA-responsive defense genes, it is not necessary for the SA-mediated suppression of the JA pathway as cytosolic NPR1 is likely to be involved in the control of JA-responsive gene expression (Spoel et al., 2003). Furthermore, NPR1 regulates SA-dependent TGA and WRKY transcription factors required for the suppression of JA-gene expression (Robert-Seilaniantz et al., 2011). Glutaredoxins (GRXs) like GRX480 are important regulators of the crosstalk and the SA- and JA-mediated signaling and mediate redox regulation of protein activity via catalyzation of disulfide transitions (Ndamukong et al., 2007; Zander et al., 2012). In interaction with TGA transcription factors, GRXs positively regulate SA-responsive genes like PR genes and negatively regulate JA-responsive genes such as PLANT DEFENSIN1.2 (PDF1.2) and OCTADECANOID-RESPONSIVE ARABIDOPSIS AP2/ERF-domain protein 59 (ORA59;

Ndamukong et *al.*, 2007; Zander et *al.*, 2012). WRKY transcription factors like WRKY50, WRKY51, WRKY70, and WRKY62 also regulate the interaction of SA and JA signaling (Pieterse et *al.*, 2012). Overexpression of WRKY70 for example leads to constitutively elevated levels of SA and *PR* gene transcripts during interaction with the biotrophic pathogen *Erysiphe cichoracearum* and to repression of the JA-responsive marker gene *PDF1.2* and compromised resistance during interaction with the necotroph *Alternaria brassicicola* (Li et *al.*, 2004).

II.2.4. ETHYLENE

The unsaturated hydrocarbon ethylene (ET) is a gaseous signal molecule that controls many processes in plants including senescence of plant organs, influences plant growth, morphogenetic effects and acts as a stress hormone during biotic and abiotic stress conditions (Bleecker and Kende, 2000). The ET precursor 1-aminocyclopropane-1-carboxylic acid (ACC) is synthesized from *S*-adenosyl-L-Met by ACC synthase (ACS; Yang and Hoffman, 1984). ACC is further converted to CO_2, cyanide (HCN), and ET by ACC oxidase. The formed HCN is rapidly detoxified by β-cyano-Ala synthase (CAS; Yip and Yang, 1988). SA is generally important for immunity to biotrophs, while ET and JA signaling is important for immunity to necotrophs, for example *Alternaria brassicicola* and acts antagonistically (Glazebrook, 2005). ET, JA and SA are produced upon perception of PAMPs by plant pattern-recognition receptors (PRRs) and all three signaling molecules are required for local resistance to pathogens (Tsuda et *al.*, 2009). ET modulates EF-Tu RECEPTOR (EFR)-triggered immunity by potentiation of salicylate-based immunity and the repression of a jasmonate-related branch in an amplification loop that is required for long lasting PTI and growth responses (Tintor et *al.*, 2013; Liu et *al.*, 2013). ET signaling is important for responses triggered by the recognition of the EF-Tu epitope elf18, such as the reactive oxygen species (ROS) burst, transcriptional reprogramming, callose deposition, but not MAP kinase activation (Tintor et *al.*, 2013). ET seems to regulate responses triggered by recognition of endogenous damage associated molecular patterns (DAMPs), like PROPEP2 which is part of a seven member family and induces immune responses similar to PAMPs (Huffaker et *al.*, 2006; Krol et *al.*, 2010). Recognition of Pep propeptides by the LRRs-RKs PEPR1 and PEPR2, with sequence and functional homologies to FLS2 and EFR, might contribute to responses triggered by elf18 (Krol et *al.*, 2010; Yamaguchi et *al.*, 2010; Tintor et *al.*, 2013, Zipfel et *al.*, 2013). Furthermore, the PEPR pathway was shown to coactivate SA- and JA/ET-dependent immune branches and to promote systemic immunity (Ross et *al.*, 2014). In *pepr1 pepr2* plants *PR1* and *PR2* expression in local leaves following infection with

Pst DC3000 *AvrRpm1* remains unaffected, whereas the systemic expression is severely reduced. Besides retained local defense responses upon infection with *Pst* DC3000 *AvrRpm1*, SAR is impaired in *pepr1 pepr2* mutants. SA levels however do not differ from wild type levels, indicating that the PEPR pathway contributes to SAR independently of SA (Ross et al., 2014).

II.3. SYSTEMIC ACQUIRED RESISTANCE (SAR)

Systemic acquired resistance is an inducible inmmune response that confers long lasting resistance against a broad spectrum of pathogens (Durrant and Dong, 2004). The initial trigger for SAR remains elusive as it is established to differential triggers such as, virulent and avirulent pathogens and MAMPs (Hammerschmidt et al., 1999a; Mishina and Zeier, 2007). However, it was shown that local and systemic SA accumulation is crucial for expression of *PR* genes and SAR induction in the systemic leaf of cucumber, tobacco and Arabidopsis (Vernoij et al., 1994; Gaffney et al., 1993; Dong, 1998). Repression of SA accumulation has a severe impact on plant resistance, as expression of the bacterial *NahG* gene, a salicylic acid hydroxylase that converts SA into catechol, leads to a phenotype of enhanced disease susceptibility, suppression of genetic resistance and abolishment of SAR (Delaney et al., 1994).

II.3.1. SA AND SYSTEMIC ACQUIRED RESISTANCE

SA accumulation in the distal leaf is indispensable for the development of SAR (Vernooij et al., 1994; Gaffney et al., 1993). Also, mutants defective in the hypersensitive response (*rsp2-201* and *rsp2-1-1C*) are unable to establish SAR and show a delayed and reduced expression of *PR-1* (Cameron et al., 1999). However, *rsp2-201* accumulates SA to the wild type level and *rsp2-101C* shows a reduction in SA compared to the wild type suggesting an HR-specific defect. Therefore the ability to establish SAR is not necessarily associated with a systemic accumulation of SA (Cameron et al., 1999). More evidence for a SA-independent pathway leading to SAR was coming from the observation that very high light intensities (500 mmol photons m^{-2} s^{-1}) induced SAR in the absence of systemic SA accumulation or *PR-1* expression (Zeier et al., 2004). It was believed that SA could be the mobile signal triggering SAR in the distal leaf, but several studies revealed that this is unlikely. Cucumber leaves that were infected with *Pseudomonas syringae* were removed before the SA levels had increased in the petiole exudates and still SAR was established in

the rest of the plant (Rasmussen et *al.*, 1991). Grafting experiments with *NahG*-expressing and wild-type tobacco plants showed that a rootstock that was unable to accumulate SA still was able to induce SAR in the scion, showing that the SAR signal was still produced and translocated into the distal part of the plant. Importantly the experiments also showed that for successful SAR establishment, distal tissue must be able to accumulate SA (Vernooij et *al.*, 1994; Gaffney et *al.*, 1993). These results confirm that SA is not the mobile signal.

II.3.2. THE ELUSIVE SAR SIGNALS

II.3.2.1. Methyl salicylate (MeSA)

The biologically inactive, volatile methylated form of SA (MeSA) was also discussed as potential mobile SAR signal. The inactive MeSA is converted through MeSA esterase acitivity (MES) of *SALICYLIC ACID-BINDING PROTEIN2* (*SABP2;* At1g26360) to active SA. Klessig and colleagues found that scions from *SABP2*-silenced plants, grafted on wild-type scions and challenged with tobacco mosaic virus (TMV), failed to accumulate SA and to induce SAR (Park et *al.*, 2007). *SA METHYLTRANSFERASE1* (*SAMT1;* At4g39460) is responsible for MeSA biosynthesis. *SAMT1*-silenced tobacco lines are unable to convert SA into MeSA and to induce SAR. *NtSAMT1* activity, and thus MeSA biosynthesis, is required in the primary infected leaves where the SAR signal is produced (Liu et *al.*, 2011). It was hypothesized that SA, produced in the infected leaf, is converted to MeSA by SAPB2. MeSA perceived in the distal leaf would then be reconverted to active SA and induce SAR. It was speculated that the activity of SABP2 was inhibited by SA in order to regulate intracellular SA levels (Forouhar et *al.*, 2005). Volatile MeSA emitted from TMV-infected tobacco or *P. syringae*-infected Arabidopsis plants, expressing the *SALICYLIC ACID/BENZOIC ACID CARBOXYL METHYLTRANSFERASE1* gene (*OsBSMT1)* from *Oryza sativa*. Furthermore, Arabidopsis overexpressing *OsBSMT1* accumulated considerably higher amounts of MeSA, failed to accumulate SA or SAG and showed reduced *PR* gene expression upon infection with *Pseudomonas syringae* or the fungal pathogen *Golovinomyces orontii* (Koo et *al.*, 2007). It was shown that MeSA serves as an airborne signal for plant-to-plant communication and induces *PR* gene expression in other plants (Koo et *al.*, 2007). However, Zeier and colleagues showed that Arabidopsis knockout mutants of *BSMT1* (At3g11480), *bsmt1-1* and *bsmt1-2,* establish a wild-type-like SAR response, SA levels and *PR gene* expression. The MeSA content in these mutants did not increase and only marginal emission from distal leaves upon pathogen treatment indicated that a flow of MeSA from inoculated to systemic leaves is negligible. This demonstrates that MeSA is not responsible for systemic SA accumulation and SAR in Arabidopsis. Furthermore, MeSA does not act as an airborne

signal as *bsmt1* mutants still conduct wild-type SAR without being able to produce or emit MeSA (Attaran et *al.*, 2009). Indeed, differences in the experimental design, like developmental age of the plant, time of infection and provided light intensity may influence the ability to establish SAR (Liu et *al.*, 2011). Klessig and colleagues showed that SAR was restored in MeSA metabolism of *bsmt1-3* when the first inoculation with *Psm AvrRpt2 cor⁻* was conducted in the morning (9:00 – 9:30 AM), but that no SAR was elicited after evening inoculations (5:30–6:00 PM). The time of the second inoculation was of minor importance for SAR establishment. It has been shown that the duration of available light provided before the dark period after inoculation, rather than the circadian rythm, was important for SAR establishment and resistance levels (Griebel and Zeier, 2008, Liu et *al.*, 2011).

II.3.2.2. DIR1 is required for long distance communication in SAR

DEFECTIVE IN INDUCED RESISTANCE1 (DIR1; At5g48485*)* belongs to the LTP2 family of lipid-transfer proteins, is expressed in the phloem sieve elements and companion cells and was identified in a genetic screen for SAR-defective mutants (Maldonado et *al.*, 2002). DIR1 contains an N-terminal signal peptide for secretion to the cell surface and two SH3 domains that facilitate interaction between proteins (Champigny et *al.*, 2011; Lascombe et *al.*, 2008). *dir1* mutants exhibit normal local defense responses, but were unable to confer SAR (Maldonado et *al.*, 2002). Taking this into account, DIR1 could be a good candidate for synthesis or translocation of the SAR signal (Maldonado et *al.*, 2002). Klessig and colleagues also showed for *dir1* that depending on the time point of the first inoculation either morning or evening, mutants exhibited SAR or not. Furthermore, petiole exudates collected from *dir1* mutants after inoculation with avirulent pathogens failed to induce *PR* gene expression and resistance in the distal leaves of the wild type (Maldonado et *al.*, 2002; Chaturvedi et *al.*, 2008).

II.3.2.3. Diterpenoid dihydroabietinal (DA)

The diterpenoid dihydroabietinal (DA) was identified as a SAR inducing compound and purified from petiole exudates of Arabidopsis leaves treated with an avirulent pathogen (Chaturvedi et *al.*, 2012). Abietane diterpenoids are components of oleoresin, produced by conifers and angiosperms (Trapp and Croteau, 2001; Hanson, 2009). Chemically synthesized DA induces resistance against virulent *P. syringae* strains and the fungal pathogen *Fusarium graminearum*. Most interestingly radioactive-labeled DA is translocated

into the distal leaves within 15 minutes after infiltration and induces SAR in Arabidopsis, tomato and tobacco (Chaturvedi et *al.*, 2012). DA-induced SAR was dependent on SA and SA-signaling, since SAR was attenuated in transgenic *NahG* plants, *ics1 ics2* double mutants and required NPR1. DA obviously functions upstream of SA accumulation and signaling. FMO1 (FLAVIN-DEPENDENT MONOOXYGENASE1) was required for systemic SA accumulation and SAR in DA-treated plants. In pathogen inoculated leaves and exudates DA contents did not further increase, but were enriched in the biologically active high molecular weight fraction (HMW), of petiole exudates derived from leaves infiltrated with an avirulent pathogen (Chaturvedi et *al.*, 2012). However, when Avr Pex collected from Avr pathogen-treated leaves and was subjected to molecular sieve chromatography, DA was found to be enriched in the biologically active HMW fraction (>100 kD). In contrast, petiole exudates from mock leaves showed DA enrichment in the low molecular weight fraction (LMW) (<30 kD) that was not able to induce SAR (Chaturvedi et *al.*, 2012). It was speculated whether DA in the unchallenged leaf was stored in the LMW fraction until it is remobilized in case of defense. Trypsin protease treatment of petiole exudates not only reduced the SAR-inducing capacity of Avr Pex, they also reduced DA levels, indicating an association of DA with proteins (Chaturvedi et *al.,* 2012). DA-induced SAR was also dependent on DIR1 (Dempsey and Klessig, 2012). Nonetheless, no genetic evidence, for DA as a SAR signal was found yet, since no genes was identified that is involved in the biosynthesis of DA and therefore no knock-out lines could be tested for the ability to elicit SAR.

II.3.2.4. SFD1-synthesized glycerol-3-phosphate (G3P)

Glycerol-3-phosphate (G3P), a precursor for membrane and storage lipids, was shown to be involved in SAR development (Lorenc-Kukula et *al.*, 2012). G3P is synthesized by SUPPRESSOR OF FATTY ACID DESATURASE DEFICIENCY 1 (SFD1; At2g40690) a plastid-localized dihydroxyacetone phosphate (DHAP) reductase (Nandi et *al.*, 2004). This suggests that SFD1's DHAP reductase activity is required for the accumulation and/or long-distance transport of a SAR signal (Lorenc-Kukula et *al.*, 2012). *sfd1* mutants in the accession Nössen have been identified in a suppressor screen of the lipid metabolism *ssi2* (*suppressor of SA-insensitivity 2*) mutant, a suppressor of the *npr1* mutant, which exhibits a dwarf phenotype and constitutive disease resistance (Nandi et *al.,* 2003 & 2004; Shah et *al.*, 2001). *sfd1* showed compromised biological SAR, failed to accumulate SA or induce *PR* gene expression systemically (Nandi et *al.*, 2004; Chaturvedi et *al.*, 2008 & 2012). *sfd1* responded to the SAR signal, as exogenous SA and wild type Avr Pex induced SAR (Chaturvedi et *al.*, 2008). Avr Pexs collected from *sfd1* mutants on the other hand failed to

induce SAR in wild type, suggesting that the mobile signal cannot accumulate or is not transported into the phloem sap anymore (Chaturvedi et *al.*, 2008). The *sfd1* mutant also showed reduced sensitivity to DA (Chaturvedi et *al.*, 2012). Recently a mutant named *gly1* has been discovered that carries a mutation in the *SFD1* gene in Arabidopsis accession Columbia that was also attenuated in SAR (Chanda et *al.*, 2011). Unlike *sfd1*, *gly1* was able to accumulate SA and express *PR* genes upon pathogen infection up to wild-type levels. *gly1* was defective in SAR, but it could be restored through exogenous application of G3P. However, locally applied 14C-labeled G3P could not be recovered in the systemic leaves (Chanda et *al.*, 2011). This means that G3P itself was not the systemically translocated SAR signal and that G3P was synthesized *de novo* in the systemic leaf. Furthermore, in SAR experiments comparing the time point of the first inoculation *Psm AvrRpt2 cor⁻* (morning 9:00–9:30 AM and evening 5:30-6:00 PM) inoculation it was observed that *gly1-1* mutants, like *bsmt1-3*, exhibited SAR following a first inoculation of pathogen in the morning (Liu et *al.*, 2011). More likely is that a G3P-dependent factor is involved in long-distance SAR signaling. G3P only induced SAR when co-applied with petiole exudate from mock, or pathogen inoculated leaves, which suggested that an exudate-derived host factor was required for G3P-triggered SAR (Chanda et *al.*, 2011). Avr Pex from *sfd1* and *dir1* induced SAR when co-applied, indicating a cross-complementation of the SFD1- and DIR1-dependent factors in long distance signaling (Chaturvedi et *al.*, 2008). G3P seems to require DIR1 protein to enhance systemic resistance and to accumulate in the petiole exudates (Chanda et *al.*, 2011). It also has been shown that there is an interaction between G3P and other potential SAR signals. G3P coapplied with petiole exudates up-regulates the expression of *MES9* (At4g37150), a putative esterase that converts MeSA into SA, in the distal leaves. At the same time the expression of *BSMT1*, involved in MeSA synthesis, is down-regulated (Chanda et *al.*, 2011). As the G3P induced alteration of *MES9* and *BSMT1* expression did not lead to a shift in SA or SAG contents. It only can be reasoned that MES9 and BSMT1 are not important for G3P conferred SAR (Shah and Zeier, 2013).

II.3.2.5. C9 dicarboxylic acid azelaic acid (AzA)

Azelaic acid (AzA) has been suggested to be involved in plant defense priming enabling a faster and stronger SA accumulation in response to pathogen inoculation (Jung et *al.*, 2009). The exact biosynthetic pathway is unknown, but AzA is potentially synthesized from 9-oxononanoic acid (ONA) in the plastids, where ONA is generated through free radical-catalyzed oxidative fragmentation. Further radical-catalyzed oxidation of esterified ONA leads to accumulation of esterified AzA in galactolipids (Zoeller et *al.*, 2012). AzA

accumulates in petiole exudates of leaves inoculated with an avirulent pathogen and local application of AzA induced systemic resistance (Jung et *al.,* 2009). Deuterium labeled AzA was found in petiole exudates and systemic leaves, confirming the mobility of AzA in plants (Jung et *al.*, 2009). As AzA did not induce SA accumulation or *PR* gene expression, but rather priming of SA biosynthesis and *PR* genes for a faster response upon a pathogen infection, it was suggested that AzA is more a priming factor than a mobile SAR signal (Jung et *al.*, 2009). AzA accumulates in the petiole exudates of leaves infected with *P. syringae* expressing the effector *AvrRpt2* (Jung et *al.*, 2009; Yu et *al.*, 2013). Through microarray analysis *AZELAIC ACID-INDUCED1* (*AZI1;* At4g12470), a putative lipid transfer protein, required for AzA- and biologically-induced SAR, priming of SA-accumulation and –signaling, was identified (Jung et *al.*, 2009). Petiole exudates collected from *azi1* mutants after inoculation with avirulent pathogen did not enhance systemic resistance when applied locally to wild-type plants. Arabidopsis plants expressing dexamethasone inducible *AvrRpm1*-HA, accumulate besides AzA, the precursor ONA in an EDS1-dependent manner (Wittek et *al.*, 2014). SAR-deficient *eds1*-mutants are not compromised in local resistance to avirulent pathogens, which would associate ONA and AzA specifically to SAR (Rietz et *al.* 2011, Wittek et *al.*, 2014). Vlot and colleagues propose furthermore that the *eds1* SAR deficiency is linked to the reduced levels of ONA and AzA (Wittek et *al.*, 2014). ONA induces SAR with a 4-fold lower concentration than AzA, indicating that exogenous ONA is rapidly oxidized to AzA in Arabidopsis leaves, but still remains detectable above basal levels and might have SAR-inducing capacity independent of AzA (Zoeller et *al.*, 2012; Wittek et *al.*, 2014). *AZI1* was locally, but not systemically induced upon local treatment with ONA and AzA (Jung et *al.*, 2009; Yu et *al.*, 2013; Wittek et *al.*, 2014). It was proposed that AzA acts upstream of G3P in the infected tissue and like AZI1 would be required for the local signal generation, but not for systemic SAR signal perception (Jung et *al.*, 2009; Gao et *al.*, 2014). The ability of exogenous ONA to induce SAR depends, like exogenous AzA, on accumulation of G3P (Wittek et *al.*, 2014; Yu et *al.*, 2013). Zeier and colleagues showed that SAR induced by petiole exudates of leaves inoculated with virulent bacterial pathogen occurs independently of AzA and no increase in AzA was observed in petiole exudates upon SAR induction with *Psm* (Návarová et *al.* 2012). This goes in line with the observation that AzA content in virulent-pathogen-inoculated leaves was only marginally higher than in mock-inoculated leaves (Zoeller et *al.*, 2012). However, translocation of AzA might not be essential for the establishment of SAR, but can enforce systemic immunity during SAR (Shah and Zeier, 2013). No strong genetic evidence for the role of AzA in SAR has been provided, since AzA is not enzymatically produced, no gene and thus knock out line was identified yet (Zoeller et *al.*, 2012).

II.3.2.6. Potential feedback loop between DIR1, AZI1 and G3P in SAR

DIR1, or a DIR-dependent factor, and G3P seem both to be required for long–distance signaling in SAR, since co-applied Avr-Pex from *sfd1* and *dir1* mutants induced SAR in wild-type plants (Chaturvedi et *al.*, 2008). DIR1 might facilitate the systemic translocation of radiolabeled G3P, as it was enhanced after exogenous DIR1 application (Chanda et *al.*, 2011). DIR1 is required for the accumulation of G3P and G3P-induced immunity during SAR as G3P is required for the stability of DIR1, as well as *AZI1* transcripts (Yu et *al.,* 2013). DIR1 and AZI1 are also required for AzA- and G3P-induced immunity (Jung et *al.*, 2009; Yu et al., 2013). Overexpressed *DIR1* and *AZI1* complemented the defects of *azi1* and *dir1* mutants, respectively, indicating that DIR1 and AZI1 could have a shared function and work together during SAR (Yu et *al.*, 2013; Shah et *al.*, 2014). A regulatory feedback loop was proposed in which DIR1 and AZI1 proteins are required for AzA-induced accumulation of G3P that would stabilize *DIR1* and *AZI1* transcripts and levels of DIR1 and AZI1 proteins in turn (Yu et *al.*, 2013). It was shown that FLAVIN-DEPENDENT MONOOXYGENASE 1 (FMO1) was required for DA- and AzA-resistance induction and that AzA enhanced resistance in an AGD2-LIKE DEFENSE RESPONSE PROTEIN 1 (ALD1) -dependent manner (Jung et *al.*, 2009; Chaturvedi et *al.*, 2012). Zeier and colleagues proposed an amplification loop in the distal leaf, that leads to *de novo* synthesis of the non-proteinogenous amino acid Pipecolic acid (Pip) through activation of ALD1 expression and induction of *FMO1* expression. A rise in *FMO1* transcripts then activates SA accumulation and *PR* gene expression, which then would lead to the full SAR response (Návarová et *al.*, 2012). Taking the requirement of FMO1 for DA- and AzA-induced resistance into account (and in case of AzA also ALD1) at least a subset of mobile SAR signals are dependent on a functional Pip/FMO1-dependent amplification loop to mediate SAR (Návarová et *al.*, 2012).

II.3.3. FLAVIN-DEPENDENT MONOOXYGENASE1 (FMO1)

Flavin-containing mono-oxygenases have been detected in various organisms, like bacteria, fungi, plants and animals (Schlenk, 1998). In animals they have an important role in xenobiotic biotransformation and detoxification, i.e. molecules that are foreign to the organism. There are five classes of FMOs known in animals, identified based on amino acid sequence similarity (Lawton et *al.*, 1994). Often of broad substrate specificity, FMO will oxigenize any soft nucleophile that can make contact with FMOs, for example iodide, boronic acids, phosphines, functional groups with sulphur and selenium, amines, hydrazines and aromatic aldehydes (Schlenk, 1998).

The Arabidopsis gene family of flavin-dependent monooxygenases (FMOs) consists of 29 members which are part of three different FMO subgroups. Members of the YUCCA clade convert tryptamine to N-hydroxyl-tryptamine. YUCCA1, a FMO1-like protein, is a member of the YUCCA subgroup and was described to be involved in auxin biosynthesis (Zhao et *al.*, 2001). FMOs that belong to the S-oxygenation group (FMOGS-OX) generate the secondary metabolites methylsulfinylalkyl glucosinolates through oxidation of sulfide groups of Met-derived methylthioalkyl glucosinolates (Li et *al.*, 2008; Hansen et *al.*, 2007). FMO1 together with a pseudogene forms its own subgroup (Olszak et *al.*, 2006; Schlaich, 2007). *FMO1-3D* was described as an Arabidopsis gain-of-function activation-tagged dominant mutant, that showed increased basal resistance to *H. parasitica* and *Pst + avrRpt2*. Due to the over-expression of a class 3 FMO, *FMO1-3D* showed increased basal resistance, but no alterations in SA levels or morphological changes upon pathogen attack (Koch et *al.*, 2006). *FMO1-3D* mutants exhibit no disease symptoms after pathogen infection and bacterial titres are reduced. These results indicated that over-expression of the class 3 FMO in Arabidopsis reduced the virulence of the pathogen (Koch et *al.*, 2006).

FLAVIN-DEPENDENT MONOOXYGENASE1 (*FMO1*; At1g19250) is a critical SAR regulator in Arabidopsis that is also indispensable for effective local resistance against bacterial and oomycete pathogens (Bartsch et *al.*, 2006; Koch et *al.*, 2006; Mishina and Zeier, 2006; Jing et *al.*, 2011). FMO1 was identified as pathogen-responsive gene and SA-independent positive regulator of EDS1-derived resistance and cell death (Bartsch et *al.*, 2006). Intact FAD- and NADPH-binding sites in *FMO1* are required for basal resistance to virulent strain *H. parasitica* (Bartsch et *al.*, 2006). The conserved Gly residues in the FAD- and NADPH-binding sites are important for cofactor binding and enzymatic activity and thus crucial for the functionality of FMO1 (Bartsch et *al.*, 2006).

FMO1 is up-regulated in local and systemic leaves upon pathogen attack (Mishina & Zeier 2006). *fmo1* mutants are fully compromised in systemic defense responses like SA accumulation, expression of defense-related genes and establishment of SAR (Mishina and Zeier, 2007). When inoculated with *H. parasitica* isolate Cala2 (recognized by RPP2) the *fmo1-1 sid2-1* double mutant was more susceptible compared to either *sid2-1* or *fmo1-1* alone. The effects of both *fmo1* and *sid2-1* on resistance were therefore additive and suggest that FMO1 acts independently of SA in the EDS1 resistance pathway. SA biosynthesis and FMO1 are both required for full disease resistance (Bartsch et *al.*, 2006).

Pip accumulated in pathogen-inoculated leaves of *fmo1* and *sid2-1* mutants and therefore was independent of FMO1- and SA-mediated signaling (Návarová et *al.*, 2012). In local leaves of *fmo1* mutants Pip even overaccumulated after pathogen treatment. Because FMO1 is required for SAR and Pip-induced resistance and Pip overaccumulates in infected

leaves of *fmo1* mutants, it was proposed that FMO1 acts downstream of Pip and is required for Pip-induced resistance (Návarová et *al.*, 2012).

FMO1 expression is primed during SAR and exogenous Pip treatment in the wild type (Návarová et *al.*, 2012). This result points towards a role of FMO1 in a defense amplification loop during SAR with Pip as a central metabolite. Furthermore, *fmo1* mutants were fully blocked in BABA-induced resistance and exogenous Pip was neither able to restore SAR nor BABA-induced resistance in *fmo1* (Návarová et *al.*, 2012). Independent of the time of inoculation (morning/evening), *fmo1* mutants were unable to establish SAR, unlike *bsmt1-3*, g*ly1-1* and *dir1-1* mutants that conferred wild type like SAR following a first inoculation in the morning. Therefore FMO1 can be considered as crucial for the induction of systemic defense responses during SAR irrespective of the light environment applied (Liu et *al.*, 2011). Induction of SAR and salicylic-acid-dependent systemic defense reactions is compromised in double mutants of the photoreceptor phytochrome A and B (*phyA phyB*). Phytochrome regulation of SAR involves the essential SAR component FMO1 (Griebel and Zeier, 2008).

Flavin-dependent monooxygenases in plants, animals and fungi are known to oxidize substrates of small organic molecules with either N- or S-containing functional groups (Schlaich, 2007). Recent metabolite analyses suggest that the FMO1 monooxygenase converts Pip into an oxidized derivative and thereby transduces the Pip signal (Návarová et *al.*, 2012; Zeier, 2013).

II.3.4. LONG LASTING IMMUNITY - RESISTANCE PRIMING

Defense priming of cells in local and systemic tissue can be induced upon perception and recognition of pathogen-, microbe- or damage-associated molecular patterns, PAMPs, MAMPs and DAMPs, respectively, pathogen-derived effectors or wounding (Boller and Felix, 2009; Conrath, 2011). The priming phenomenon is described as a faster and stronger response to a subsequent infection by pathogens or abiotic stresses and induces basal and systemic immune responses (Conrath et *al.*, 2011). Priming is involved in SAR, β-amino butyric acid (BABA) -induced resistance, wound-induced resistance as well as induced systemic resistance (ISR; Jung et *al.*, 2009; Pieterse et *al.*, 1996; Zimmerli et *al.*, 2000 and Pozo et *al.*, 2009). It was shown that SAR priming after pathogen inoculation is associated by a potentiated and strong induction of camalexin and Pip biosynthesis (Návarová et *al.*, 2012). The accumulation of SA is also primed during SAR, resulting from an additive effect of SA produced upon the first inoculation together with the SA produced after the second challenge infection in the distal leaves (Návarová et *al.*, 2012; Jung et *al.*, 2009). The SAR regulators *ALD1* and *FMO1*, as well as the SA-inducible *PR-1* gene are primed upon biologically activated SAR (Návarová et *al.*, 2012; Jung et *al.*, 2009). The SAR-associated priming

response is absent in *ald1* mutants, emphasizing the critical role of Pip as an endogenous mediator of SAR induced defense priming (Návarová et *al.*, 2012). Very recently it was found that *BABA-INDUCED DISEASE IMMUNITY* (*IBI1*; At4g31180) and immunity induced by exogenous BABA treatment, control plant immunity and growth via separate pathways, so that the negative effect of BABA on plant growth might be uncoupled from broad-spectrum disease resistance in the future (Luna et *al.*, 2014). More priming-inducing compounds, with a positive effect on SA accumulation through inhibition of SA glucosyltransferases (SAGTs) and resistance to *Pseudomonas syringae,* have been identified in a chemical screening (Noutoshi et *al.*, 2012). Biologically induced SAR and exogenous azelaic acid (AzA) treatment leads to priming of the distal leaves and elevated levels of SA and *PR-1* transcripts, although it is not clear yet whether AzA indeed is responsible for priming of SA biosynthesis and a faster defense response during SAR (Jung et *al.*, 2009; Shah and Zeier, 2013). MAPK-signaling is also involved in BTH-induced priming, as mitogen-activated protein kinases (MPK) MPK3 and MPK6 reacted stronger to mechanical stress after BTH pretreatment and that priming of *PR-1* was dependent on both MPKs (Beckers et *al.,* 2009). Furthermore WRKY transcription factor genes WRKY29, WRKY6 and WRKY53 were primed upon BTH-treatment and biologically activated SAR through inoculation of *P. syringae* followed by pressure infiltration, whereas BTH-treatment alone only had minor effects on gene expression levels (Jaskiewicz et *al.*, 2011). SA itself conditions and primes defense genes for enhanced epression in parsley to induce resistance upon a subsequent pathogen infection (Thulke and Conrath, 1998). Genes associated with induced resistance and antimicrobial activity were grouped into nine gene families of so called 'SAR' genes or PR proteins and are used as molecular markers for the induction of an induced resistance state (Ward et *al.*, 1998). The BTH- and *Psm-* priming stimulus set marks in the chromatin of *WRKY* promoters, suggesting, that these genes were then activated and the histone modifications were the result of the memory of a previous stress (Jaskiewicz et *al.,* 2011). The memory of a previous attack might be even passed on to the next generation as a recent study by Ton and colleagues indicated (Luna et *al.*, 2012). The plants of the next progeny of SAR plants exhibited a more robust expression of defense-associated genes such as *PR-1* and *WRKY*-genes (*WRKY6, WRKY53* and *WRKY70*) when treated with SA. The next generation priming was dependent on NPR1 and promoter regions of NPR1 regulated genes like *PR-1*, *WRKY6* and *WRKY53* where changed through methylation and acetylation (Luna et *al.*, 2012).

II.4. ROLE OF AMINO ACIDS IN PLANT DISEASE RESISTANCE

II.4.1. ASPARTATE DERIVED AMINO ACIDS

Lysine (Lys), threonine (Thr), methionine (Met) and isoleucine (Ile) are aspartate derived amino acids produced in plants, bacteria and fungi, but not in mammals and belong to the group of essential amino acids that have to be taken up with the diet or through other source like for example endosymbiontic bacteria (Douglas, 1998). The biosynthesis of all four amino acids starts with two common steps that require an Aspartate kinase (AK) to catalyze the formation of L-aspartyl-4-phosphate and L-aspartate-4-semialdehyde dehydrogenase (Asd) to commit the next step towards L-aspartate-4-semialdehyde from which the pathways divide either into the Lys biosynthesis pathway via a dihydrodipicolinate synthase (DHDPS) or towards Thr, Met and Ile via a homoserine dehydrogenase (HSDH; Fig. 1). AKs are subject to allosteric regulation through the pathway endproducts Lys, S-adenosylmethionine and L-threonine and L-Leucine (Fig. 1; Jander and Joshi, 2009; Zeier, 2013). In Arabidopsis AKs are encoded by five different genes including three monofunctional AKs At5g13280 (AK1), At5g14060 (AK2) and At3g02020 (AK3) and two bifunctional AKs At1g31230 (AK-HSDH1) and At4g19710 (AK-HSDH2) with aspartate kinase and homoserine dehydrogenase activity. Asd is only encoded by At1g14810 in Arabidopsis emphasizing the importance of aspartate kinases in amino acid biosynthesis (Jander and Joshi, 2009).

II.4.1.1. Lysine

The biosynthesis of L-Lys (Fig. 1 (2)) continues in an independent pathway with the degradation of L-aspartate-4-semialdehyde to L-2,3-dihydrodipicolinate catalyzed by dihydrodipicolinate synthase (DHDPS). DHDPS is negatively regulated by Lys and important for the regulation of Lys production (Galilli, 2002). *A. thaliana* genes encoding DHDPS are At3g60880 (*DHDPS1*) and At2g45440 (*DHDPS2*). Studies have shown that unlike bacteria, plants convert tetrahydrodipicolinate into diaminopimelate in just one reaction step. The catalyzing enzyme L,L-diaminopimelate aminotransferase (L,L-DAP-AT) is encoded by *ABBERANT-GROWTH AND CELL DEATH2* (*AGD2*; At4g33680) in Arabidopsis (Fig. 1; Hudson et *al*., 2006; Zeier, 2013).

Lys is degraded in plants via saccharopine and α-amino adipic acid into glutamate (Glu), pipecolic acid (Pip) and acetyl-CoA (Arruda et *al*., 2000). Two enyzmes linked on a single bifunctional polypeptide commit the first two reaction steps. Lysine ketoglutarate reductase

(LKR) combines lysine and α-ketoglutarate producing saccharopine and saccharopine dehydrogenase (SDH) converts saccharopine into α-amino adipic semialdehyde and glutamate. Additional reaction steps lead to the conversion of α-amino adipic semialdehyde, via α-amino adipic acid (AAD), into acetyl-CoA and additional glutamate molecules (Galili, 2002). In mammals a functional Lys catabolism and glutamate production is crucial for undisturbed nerve signal transmission and brain function, whereas in plants the Lys catabolic pathway is involved in developmental processes like seed germination and associated in responses to abiotic stresses (Galili, 2002). Osmotic stress for example was described to have a severe impact on Lys degradation at the level of LKR and SDH in *Brassica napus*. LKR and SDH activities were enhanced by decreasing osmotic potential and in osmotically-stressed tissues. The LKR/SDH activity produced α-aminoadipate semialdehyde, which could be further converted into α-aminoadipate a possible precursor of Pip and acetyl CoA. Pip was described as an osmoprotectant in bacteria and co-accumulated with proline in halophytic plants. It was demonstrated that Lys catabolism through LKR/SDH activity was involved in the osmo-induced synthesis of Pip (Moulin et *al.*, 2006). In the absence of stress LKR and SDH activities are low and approximately equal. A first response upon osmotic stress is the induction of SDH activity, but not LKR. This is possibly due to an excess production of SDH, which may allow a slight increase in the flux of Lys catabolism.
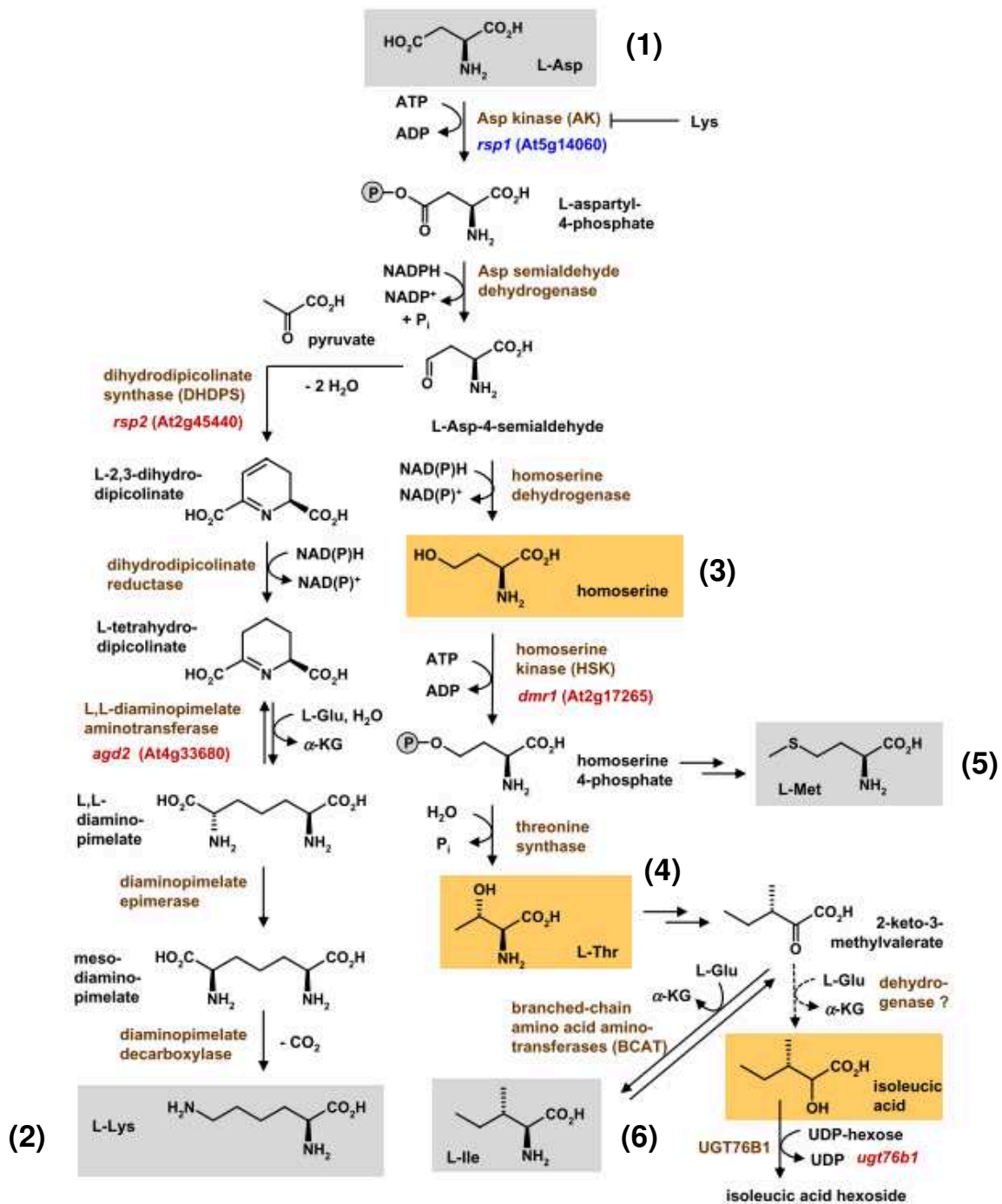
Figure 1. Overview of the biosynthesis of the Asp (1)-derived amino acids L-Lys (2), homoserine (3), L-Thr (4), L-Met (5) and L-Ile (6). Possible Ile catabolic reactions are depicted. Arabidopsis mutations that alter pathogen resistance are indicated (red: knockdown/knockout mutant, blue: loss-of-inhibition mutant). Metabolites which positively affect plant immunity are highlighted in orange (Zeier, 2013).

More severe osmotic stress induces differential expression of LKR, due to differential production of monofunctional LKR and/or stimulation of LKR activity by phosphorylation (Galili et al., 2001). The bifunctional peptide LKR/SDH is subject of intense regulation via (post-) transcriptional and posttranslational control and negatively regulated by the SDH domain controlled by Lys. This SDH-derived regulation operates apparently via the

phosphorylation/dephosphorylation of LKR by casein kinase-II and a putative protein phosphatase (Galili, 2002). The level of LKR/SDH was strongly enhanced by ABA, jasmonate, and sugar starvation, but reduced upon an excess of sugars and nitrogen starvation. Glutamate is a product of the Lys catabolic pathway and a major precursor for the synthesis of stress-associated metabolites like Pro, Arg, polyamines, γ-amino butyric acid (GABA), and nitric oxide (NO) accumulate (Galili et *al.*, 2001). This emphasizes the contribution of Lys catabolism in stress-associated metabolism.

II.4.1.2. Threonine

L-Threonine is formed by catalyzation of a homoserine dehydrogenase (HSDH) in a first committing step in the biosynthetic pathway (Fig. 1 (4); Zeier 2013). The *A. thaliana* enzymes that catalyze the formation of homoserine, AK-HSDH1 and AK-HSDH2, are bifunctional and, in addition to the dehydrogenase activity, exhibit functions as aspartate kinases that catalyze the first step in the aspartate-derived amino acid pathway. A homoserine kinase (HSK) is encoded by a single gene in Arabidopsis (At4g35395) and is not allosterically inhibited by Thr, Ile, Val or S-adenosylmethionine. HSK converts homoserine to O-phospho-homoserine (Lee and Leustek, 1999). *METHIONINE OVER-ACCUMULATOR2* (*MTO2;* At4g29840) is the only gene that was identified as threonine synthase in Arabidopsis, catalyzing the final reaction of threonine biosynthesis and the first reaction in the Ile biosynthetic pathway. Threonine catabolism proceeds via a Threonine deaminase, which catalyzes the conversion of threonine to 2-oxobutanoate and is encoded by a single gene, *L-O-METHYLTHREONINE RESISTANT1* (*OMR1*; At3g10050; Mourad et *al.*, 1995) in Arabidopsis. The threonine deaminase is used as a target for herbicides resulting in growth inhibition which implies that threonine deaminase is essential for plants. Another catabolic step from Thr yields glycine and acetaldehyde that are formed from threonine by threonine aldolase (Joshi et *al.*, 2006).

II.4.1.3. Methionine

L-Methione (L-Met) is derived from O-phosphohomoserine via a cystathionine γ-synthase (CGS) encoded by At3g01120 in Arabidopsis (Fig. 1 (5); Zeier, 2013). Cystathionine γ-synthase competes with threonine synthase for O-phosphohomoserine and is a key regulatory point for the biosynthesis of Thr and Met (Amir et *al.*, 2002). S-adenosylmethionine synthase (SAM) is, after ATP, the most important cofactor and essential for DNA, protein and lipid methylation and biosynthesis of cell wall components such as chlorophyll and lignin. SAMs also play a role in the biosynthesis of plant metabolites like

ethylene, vitamin B1, polyamines, biotin and the iron chelator mugineic acid. The four SAM genes in Arabidopsis *SAM1* (At1g02500), *SAM2* (At4g01850), *SAM3, MTO3* (At3g17390), and *SAM4* (At2g36880) show reduced activity and protein accumulation upon enhanced Lys concentrations (Peleman et *al.*, 1989a; Peleman et *al.*, 1989b; Shen et *al.*, 2002; Hacham et *al.*, 2007). Met also serves as substrate for Ile biosynthesis, which is activate in response to drought stress (Amir et *al.*, 2002; Anderson, 1990; Hernández et *al.*, 2007; Nambara et *al.*, 1998).

II.4.1.4. Role of Aspartate derived amino acids in plants disease resistance

Infection with virulent and avirulent bacteria and PAMPs triggers the accumulation of amino acids like Lys, aliphatic and aromatic amino acids (Návarová et *al.*, 2012). Aspartate derived amino acids like homoserine, Thr, Met, Ile and Lys seem to have an especially high impact on resistance in plants against hemibiotrophic bacteria, but also obligate biotrophic fungi.

In the Lys biosynthesis pathway ABBERANT GROWTH AND DEATH2 (AGD2), a L,L-diaminopimelate-aminotransferase, is thought to convert L-tetrahydropidipicolinate into L,L-diaminopimelate and its epimerized form meso-diaminopimelate (Fig. 1; Hudson et *al.*,2006). The *AGD2* gene encodes a novel chloroplast-localized aminotransferase with highest activity for Lys (Song et *al.*, 2004a). A point mutation in *AGD2* leads to a severely altered growth phenotype and constitutive disease resistance with elevated levels of SA and *PR* gene expression (Song et *al.*, 2004a). AGD2 was originally recognized in association with pathogen resistance and was subsequently identified as the diaminopimelate aminotransferase (DAP-AT) enzyme involved in Lys biosynthesis and localized to the chloroplasts (Rate and Greenberg, 2001; Song et *al.*, 2004a). Since AGD2 is able to complement *E. coli* mutants defective in bacterial Lys biosynthesis it was concluded that AGD2 catalyzes the forward step leading to Lys production in plants (Hudson et *al.* 2006). A complete knockout of *AGD2* results in embryo lethality and heterozygous *agd2-1*/AGD2 (*agd2-1*) plants exhibit mild dwarfism and altered leaf shapes (Song et *al.* 2004a). *agd2-1* showed elevated levels of SA, *PR* gene expression and increased resistance to the bacterial pathogen *Pseudomonas syringae* and *Hyaloperonospora arabidopsidis* (*Hpa*). Parker and colleagues detected a twofold increase in Thr content in *agd2-1* which was claimed to contribute to *Hpa* resistance (Stuttmann et *al.*, 2011).

DOWNY MILDEW RESISTANT1 (*DMR1*), identified through Map-based cloning, encodes a homoserine kinase (HSK), a chloroplast enzyme that is involved in the biosynthesis of Asp-derived amino acids Met, Thr and Ile and catalyzes the conversion of homoserine to homoserine-4-phosphate, within the Thr biosynthesis pathway (Fig. 1; van Damme et *al.* 2005; van Damme et *al.* 2009; O'Connell & Panstruga 2006). The *dmr1* mutants showed a severe reduction in the HSK activity of the *DMR1* protein and accumulation of homoserine (van Damme et *al.* 2009). Levels of the amino acids located downstream of HSK in the Asp pathway, Thr, Met and Ile, were not reduced in *dmr1*, and were possibly synthesized via a *DMR1*-independent route. The knockdown in *dmr1* provides protection against *Hpa* but not against the powdery mildew fungus *Golovinomyces orontii* and *Pseudomonas syringae* (van Damme et *al.* 2009). Furthermore, homoserine was able to induce resistance to *Hpa* in wild type and mutant plants impaired in defense signaling when applied exogenously, but was not directly toxic to oomycete pathogens *in vitro* (van Damme et *al.* 2009).

Enhanced resistance to *Hpa* was also identified in a screen for genetic suppressors of susceptibility of *Arabidopsis thaliana* ecotype *Landsberg erecta* to *Hpa* (isolate Noco2) caused by a *rar1* mutation disabling RPP5 (NLR) recognition (Muskett et *al.* 2002). Two alleles were identified, named *rsp1* and *rsp2* that enhance resistance at early stages of infection to *Hpa*, but not to *G. orontii* or *P. syringae* (Stuttmann et *al.*, 2011). Because the mutants were smaller than the wild type it was tested whether they exhibit characteristics of constitutive disease resistance, but no constitutive SA-associated defense responses or accelerated inducible defenses against the oomycete pathogen were activated. The *rsp1* mutant carries a point mutation in ASPARTATEKINASE 2 (AK2) which encodes a monofunctional Asp kinase that catalyzes the conversion of Asp to L-aspartyl-4-phosphate and is feedback-inhibited by Lys (Stuttmann et *al.*, 2011; Curien et *al.* 2007). This mutations lead to an increase in Asp kinase activity due to the Val to Met exchange in the AK2 *rsp1* protein, because the feedback inhibition by Lys is not functional anymore. The *rsp2* mutant carries a lesion in DIHYDRODIPICOLINATE SYNTHASE2 (DHDPS2) one of two *Arabidopsis* DHDPS, DHDPS1 and DHDPS2, enzymes catalyzing the conversion of L-aspartate-4-semialdehyde to L-2,3-dihydrodipicolinate as the committing step in Lys biosynthesis (Jander and Joshi 2010). Loss of the major isoform of DHDPS leads to increased accumulation of products of the Lys, Met, Thr and Ile branch in the *rsp1* mutant and Met, Thr and Ile in *rsp2* (Stuttmann et *al.*, 2011). Thr and homoserine, but not Ile increased resistance to *Hpa*, by suppressing *in planta* growth of the pathogen (Stuttmann et *al.*, 2011). Homoserine induced resistance to *Hpa* to a lesser extent than Thr and was also only faintly elevated in *rsp* lines, so that Thr was more likely to confer resistance to *Hpa* than homoserine (Stuttmann et *al.*, 2011). *rsp2* mutants did not perform programmed cell death at infection sites and so it was

speculated that the reduced *Hpa* growth was because of loss of susceptibility and not because of activation of classical immune responses (Stuttmann et *al*., 2011). Parker and colleagues hypothesized that the accumulation of Thr perturbed the amino acid metabolism and as a result rendered the plant tissue an unsuitable substrate for *Hpa* (Stuttmann et *al*., 2011). Concluding, plant-derived Thr could have a negative impact on the Asp pathway in the oomycete and be differently regulated among distant related pathogens, which might be the reason for the observed specific suppression of susceptibility for *Hpa* (Stuttmann et *al*., 2011).

Taken together, the *agd2-1* mutant did not resemble the *rsp2* phenotype since it was constitutive disease resistant (Song *et al*., 2004). *dmr1* plants, defective in a homoserine kinase, showed resistance to *Hpa* without being constitutive resistant and the same resistance phenotype was observed in *rsp2* mutants. Since both, *dmr1* and *rsp2*, were affected in the biosynthesis of enzymes of the Lys superpathway, it was hypothesized that *DMR1* and *DHDPS2* share a mechanism in resistance against *Hpa* (van Damme et *al*., 2009; Stuttmann et *al*., 2011). *AGD2*, *DMR1* and *DHDPS2* encode enzymes of the Lys superpathway that have an effect on plant immune responses, but confer resistance to different pathogens.

II.4.2. PIPECOLIC ACID (PIP)

The non proteinogenous amino acid pipecolic acid (Pip) was first detected in fruits and seeds of legumes by Steward and colleagues, who isolated 800 mg of L-pipecolic acid from 10 kg of fresh green beans (*Phaseolis vulgaris;* Zacharius et *al*., 1952). Besides, Pip was detected in various other plants species, fungi, microorganisms and animals (Morrison, 1953, Wickwire et *al*., 1990; Zabriskie and Jackson, 2000; Fletcher et *al*., 2001; Murthy and Janardanasarma, 1999). L-Pip is an L-Lys derived catabolite and the Pip biosynthesis pathway was described as the main degradation pathway for Lys in mammals (Broquist, 1991; Chang, 1976).

II.4.2.1. AGD2-like defense response protein1 (ALD1)

An AGD2 homolog with 62% idendity and 77% similarity with AGD2 at the amino acid level was identified as a Lys aminotransferase and named AGD2-LIKE DEFENSE RESPONSE PROTEIN1 (ALD1; Song et *al*., 2004a). Biosynthesis of the Lys-derived amino acid Pip in *A. thaliana* requires the aminotransferase ALD1 (Návarová et *al*., 2012; Zeier,

2013). The *ALD1* gene has 10 exons and encodes a 456–amino acid protein. ALD1 has a distinct enzymatic activity from the AGD2 enzyme, as it works in the opposite direction with Lys as its most preferable substrate (Song et *al.*, 2004a; Song et *al.*, 2004b). The structure of *A. thaliana* ALD1 (AtALD1; UniProt ID Q9ZQI7) was solved at a resolution of 2.3 A˚ (Sobolev et *al.*, 2013). ALD1 and AGD2 are both pyridoxal-50-phosphate (PLP) dependent enzymes and contain PLP in their cofactor-binding sites with very similar interaction modes. However, differences in the residues within the malate-binding site of AGD2 suggest different substrate interactions in AGD2 and ALD1 (Sobolev et *al.*, 2013).

AGD2 and ALD1 homologs are present in many plant species. The *Oryza sativa* (rice) genome for example has two genes, *OsAGD2* (GenBank accession number AY338235) and *OsALD1* (GenBank accession number AY338236), whose products had high similarities to both AGD2 and ALD1 (Song et *al.*, 2004a). *agd2-1* plants are resistant to *P. syringae* (Rate and Greenberg, 2001) and showed elevated *ALD1* expression. Upon pathogen infection, AGD2 mRNA levels were not significantly changed, whereas *ALD1* was induced in a similar manner like *PR-1*. Mutant plants deficient in ALD1 show reduced levels of pathogen triggered SA production and are high susceptibility against *P. syringae* (Song et al., 2004a; Song et *al.*, 2004b). *ALD1* is highly up-regulated in the *agd2-1* mutant. Both, the enhanced *P. syringae* resistance and dwarfism phenotypes of *agd2-1* were strongly dampened in an *agd2 ald1* double mutant. AGD2 was down-regulated after *Psm* treatment in local and systemic leaves of Col-0 (Song et *al.*, 2004a). The amino acid levels in *agd2-1* were measured by Parker and colleagues and a twofold increase in Thr content was detected which was claimed to contribute to *Hpa* resistance (Stuttmann et *al.*, 2011). *ALD1* transcripts strongly increased in local and systemic leaves of *Psm*-infected Col-0 plants (Song et *al.*, 2004a; Návarová et *al.*, 2012). The *ald1* mutant failed to express *ALD1* in local and distal tissues and was fully blocked in *Psm*-induced Pip biosynthesis in local and distal tissues and in the petiole exudates after pathogen inoculation (Návarová et *al.*, 2012). These results demonstrate that ALD1 is required for pathogen-induced Pip biosynthesis. On the other hand, ALD1 is not essential for Aad production, another Lys catabolite, but results of Zeier and colleagues indicate that the LKR/SDH and the saccharopine pathway are involved in pathogen-induced Aad biosynthesis (Návarová et *al.*, 2012). ALD1 was furthermore identified as an important regulator of *enhanced disease resistance2* (*edr2*)-mediated defense responses and senescence. In a supressor screen for the *edr2*-resistance phenotype, three *ALD1* alleles, *ald1-10*, *ald1-11* and *ald1-12,* were identified through map-based cloning. The *edr2*-mediated resistance phenotypes, like powdery mildew resistance, programmed cell death, hydrogen-peroxide production and ethylene-induced senescence were suppressed by mutations in *ALD1*. The *edr2* mutant exhibited induced expression of defense genes, which was absent in the *edr2 ald1* mutant (Nie et *al.*, 2011). Another supressor screen with the

syntaxin mutant *syp121 syp122* revealed that FMO1, ALD1, and PAD4 are important for lesion development. *syp121 syp122* mutants exhibit a constitutively activated (SA) signaling pathway, a dwarfed growth phenotype, develop severe necrosis and have a low penetration resistance to powdery mildew fungi. Multiple crosses between *syp121 syp122* and other signaling mutants, suggested that FMO1 and ALD1 contributed to lesion formation parallel to SA- and PAD4-dependent pathways, but also independent of EDS5 and SID2. Syntaxin mutants in combination with knockouts of *FMO1* and *NPR1* or *ALD1* and *NPR1*, respectively did not show an improved phenotype, suggesting that ALD1 and FMO1 mediated signals were fully dependent on NPR1 (Zhang et *al.*, 2008).

II.4.2.2. Pipecolic acid biosynthesis and metabolism

The exact biochemical pathway of Pip production via *ALD1* still needs to be uncovered, but the natural occurrence of L-pipecolic acid and the conversion from Lys to L-Pip was shown in *Lemna paucicostata* 151 (Fujioka and Sakurai, 1997).

Lys is catabolized to α-amino-adipidic acid (AAD) via saccharopine and α-aminoadipate semialdehyde (Galili, 1995). The formation of L-Pip from Lys independent of α-aminoadipidic acid has also been suggested by tracer studies in *Phaseolus vulgaris*, in a rat, a Lys auxotroph of *Neurospora crassa* and excised shoots of *Sedum acre* (Gupta and Spenser, 1969). It was concluded that the conversion of Lys into Pip proceeds in all cases by way of ε-amino-α-ketocaproic acid and Δ^1-piperideine-2-route, which involves loss of the α-amino nitrogen of lysine and leads to incorporation of the ε-nitrogen into pipecolic acid (Gupta and Spenser, 1969). ε-amino-α-ketocaproic acid and Δ^1-piperideine-2-carboxylic acid are possible ALD1 reaction products within the Lys catabolism pathway leading to Pip (Gupta and Spenser, 1969; Návarová et *al.*, 2012). It is proposed that Pip biosynthesis furthermore requires the reduction of Δ^1-piperideine-2-carboxylic acid to hydrogenate the C-N single bond via ORNCD1 (Fig. 2; Zeier, 2013).

ORNCD1 (AT5G52810) is the closest putative *Arabidopsis thaliana* homolog of a mammalian forebrain protein amino acid related μ-cristallin protein (CRYM) identified as ketamine reductase that reduces different imine substrates with either NADH or NADPH as cofactor (Hallen et *al.*, 2011). Willows and colleagues also included the previously characterized Δ^1-piperideine-2-carboxylate (P2C)/Δ^1-pyrroline-2-carboxylate (Pyr2C) reductase isolated from porcine kidney and *Pseudomonas putida* in the scheme (Petrakis and Greenberg 1965; Nardini et *al.* 1988a; Payton and Chang 1982; Hallen et *al.*, 2011). It was described, that P2C is a substrate for a ketimine reductase, derived from Lys catabolism within the Pip-pathway (Hallen et *al.*, 2011). In mammals it is known that Lys is metabolized

by two main pathways, the saccharopine pathway and the pipecolic acid pathway. CRYM is able to convert P2C to Pip and results of ATH microarray show that ORNCD1 was up-regulated after pathogen treatment locally but even more pronouncedly at the systemic level, which was synchronized with the transcriptional regulation of *ALD1* and Pip accumulation during defense (Hallen et *al.*, 2011; Návarová et *al.* 2012; Zeier pers. communication). In the Pip biosynthetic pathway, oxidation of L-Lys resulted in the formation of a α-keto acid that cyclized to P2C (Garweg et *al.*, 1980). L-Pip, derived from the reduction of P2C by ketamine reductase, had been shown to be a weak inhibitory neurotransmitter (Charles, 1986). Taking this into account ORNCD1 is a suitable candidate to catalyze the possible reduction step of Δ^1-piperideine-2-carboxylic acid to Pip.

Interestingly it was found that Pip can be converted via a sarcosine oxidase into Δ^1-piperideine-6-carboxylic acid, a precursor of Aad (Goyer et *al.*, 2004). The Arabidopsis candidate for this conversion step is the SARCOSINE OXIDASE/PIPECOLATE OXIDASE (SOX/PIPOX; At2g24580). The animal SARCOSINE OXIDASE (SOX) is localized in peroxisomes and oxidizes N-methylated amino acids such as sarcosine (N-methylglycine), a key metabolite of the mammalian liver functioning as PIPECOLATE OXIDASES (PIPOX; Reuber et *al.*, 1997). SOX/PIPOX encodes an amino-acid related putative sarcosine oxidase in Arabidopsis with high sequence similarity to SOX/PIPOX in rabbit, and was identified as PIPOX catalyzing the conversion of Pip to P6C/ Δ^1-piperideine-6-carboxylic acid *in vitro* (Goyer et *al.*, 2004). P6C can spontaneously add water to form non-cyclic α-aminoadipidic semialdehyde, the precursor of Aad (Fig. 2; Galili et *al.*, 2001; Zeier, 2013). Hanson and colleagues gave a strong evidence for the function of SOX/PIPOX *in planta* (Goyer et *al.*, 2004). Arabidopsis RNAi lines of AtSOX accumulated Pip up to six fold and reduction of Aad by 30-fold. ATH1 microarray results indicate that SOX/PIPOX is down-regulated after *Psm* treatment (Zeier, pers. communication).
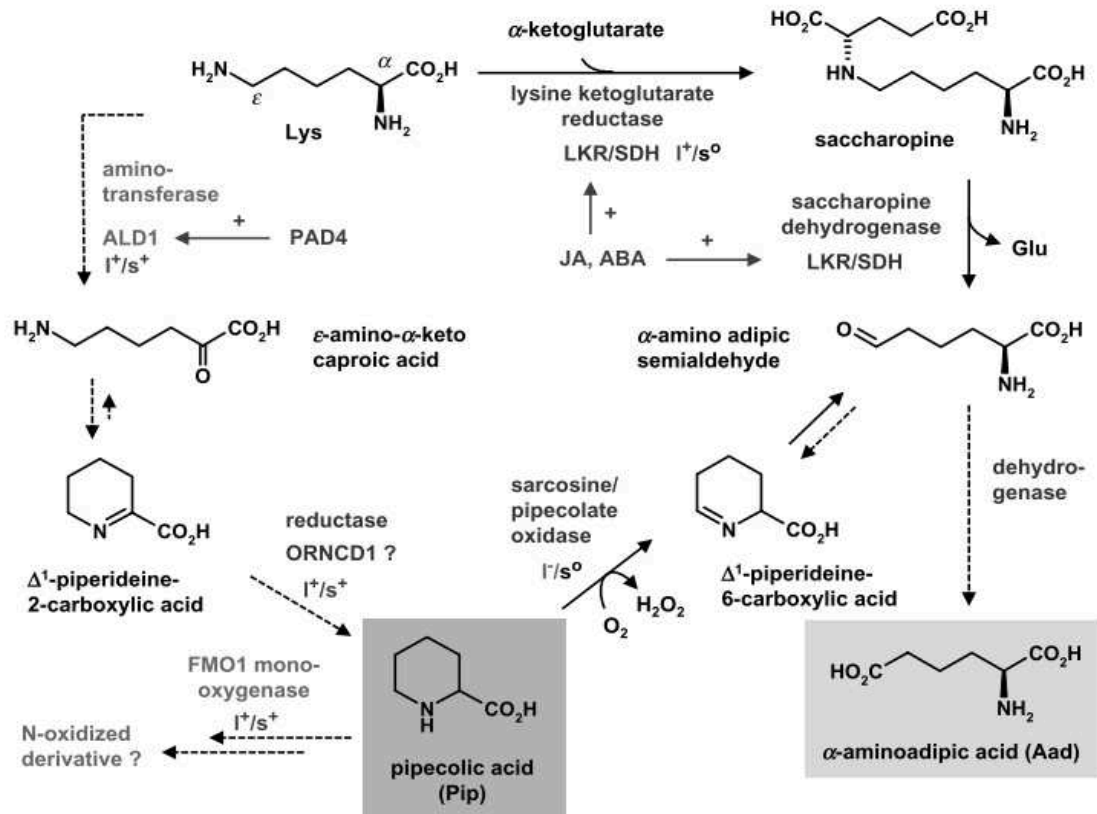
Figure 2. Possible scheme for the metabolism of the Lys catabolites Pip and Aad following pathogen attack. The Lys aminotransferase ALD1 mediates pathogen-induced pipecolic acid production but the exact biochemistry of Pip biosynthesis still needs to be clarified. ORNCD1 is the closest Arabidopsis homolog to mammalian CRYM which is capable to convert D1-piperideine-2-carboxylic acid to Pip. Arabidopsis pipecolate oxidase might mediate the conversion of Pip to Aad and contribute to modulate endogenous Pip levels. FMO1 might N-oxygenate Pip or a Pip derivative to transduce the Pip signal. Regulatory aspects of the expression of particular genes are indicated: I+/s+: genes up-regulated by *P. syringae* both in inoculated and in distal leaves, I+/s°: transcript levels increase in *P. syringae* inoculated, but are not altered in distal leaves, I-/s°: gene is down-regulated at inoculation sites (Zeier, 2013).

II.4.2.3. Function of pipecolic acid in plants

Pip accumulates in various plant species like rice (*Oryza sativa*), potato (*Solanum tuberosum*), tobacco (*Nicotiana tabacum*) and soybean (*Glycine max*), and is increasing after application of chemical or osmotic stresses (Pálfi and Dézsi, 1968; Yatsu and Boynton, 1959; Moulin et *al.*, 2006). Pálfi and Dézsi described Pip as an indicator of abnormal protein metabolism in diseased plants, as Pip accumulated in tobacco and potato plants after virus-infection and in fungus-infected rice (Pálfi and Dézsi, 1968). Pip was also identified as flower inducing factor together with benzoic acid, nicotinic acid and nicotine amide in the aquatic plant *Lemna gibba* (Fujioka et *al.*, 1987). Zeier and colleagues recently identified Pip as a critical regulator of basal immune responses, SAR and several other forms of inducible plant immunity in *Arabidopsis thaliana* (Návarová et *al.*, 2012). Elevated levels of Pip were found in

tobacco plants (*Nicotiana tabacum* cv Xanthi) infected with the compatible *P. syringae* pv. *tabaci* 6605 (Pstb). Pip enhanced resistance in tobacco to bacterial infection and primed salicylic acid and nicotine accumulation (Vogel-Adghough et *al.*, 2013).

Arabidopsis plants defective in ALD1 are unable to accumulate Pip and realize SAR (Návarová et *al.* 2012). Exogenous application of Pip to *ald1* plants show restored systemic SA accumulation and SAR establishment. Pip therefore has an important function in SAR activation upstream of SA biosynthesis. Exogenous Pip increased wild-type resistance to bacterial pathogens, which demonstrates that besides SAR, Pip has an important role in PAMP and ETI (Návarová et *al.* 2012). β-amino butyric acid (BABA)-induced resistance of Arabidopsis to *P. syringae* is mediated by Pip (Návarová et *al.* 2012). BABA is a non-protein amino acid that does not occur naturally in Arabidopsis, but promotes plants to a primed state when applied exogenously (Zimmerli et *al.* 2000). Taken together, bacterial pathogen infection triggers Pip-biosynthesis enables SAR establishment and mediates PTI, ETI and BABA-induced resistance (Návarová et *al.*, 2012).

Zeier and colleagues showed that Pip accumulates in Arabidopsis leaves local and distal to the infection site and in the petiole exudates of *P. syringae* inoculated leaves (Návarová et *al.*, 2012). Together with Pip, the precursor Lys and another Lys-catabolite, α-aminoadipic acid (Aad), aromatic and branched-chain amino acids accumulated in the local, infected leaves. However, Pip was the only amino acid that accumulated to high levels in the distal, untreated leaves of Arabidopsis and in the petiole exudates (Návarová et *al.*, 2012). This means that Pip is able to move from the inoculated tissue and possibly send throughout the plant vasculature to distal plant tissues (Návarová et *al.*, 2012). Zeier and colleagues proposed that a modest rise of Pip in distal leaves might initate elevated *ALD1* transcripts that further lead to *de novo* Pip biosynthesis in the distal leaf. Newly synthesized Pip, SA accumulation and *PR* gene expression then would lead to the full SAR response (Návarová et *al.* 2012).

Plants with activated SAR are strongly primed for Pip and camalexin biosynthesis and defense gene expression such as *ALD1*, *FMO1* and *PR1*. Defense priming contributes to increased resistance during SAR with enhanced SA biosynthesis and because of the preconditioned state plants can react faster and stronger to a subsequent pathogen encounter (Jung et *al.*, 2009; Návarová et *al.*, 2012; Conrath, 2011). Insect oviposition by the Large White butterfly *Pieris brassicae* or treatment with egg extract activates SAR in Arabidopsis and inhibits growth of different *Pseudomonas syringae* strains. This so-called egg-induced SAR involves an accumulation of Pip, is dependent on ALD1 and FMO1, and primes the expression of defense associated genes (Hilfiker et *al.*, 2014).

Priming is absent in *ald1* mutant plants, however it is restored upon exogenous Pip treatment. Therefore Pip is necessary for priming upon biological SAR activation. Taken

together Pip is an important mediator of SAR establishment and defense priming upon SAR activation (Návarová et *al*. 2012).

II.4.2.4. Function of pipecolic acid in other organisms

Pip has been recognized as weak inhibitory neurotransmitter and endogenous gamma-aminobutyric acid (GABA) agonist in animals that might bind to the same receptor complex (Charles, 1986). In mammals L-Pip was identified as the major Lys catabolite (Chang, 1976; Rothstein and Miller, 1954; Broquist, 1991).

In humans elevated pipecolic acid levels in urine and plasma are a characteristic of the hyperlysinemia/Zellweger syndrome (Hutzler and Dancis, 1983; Dancis and Cox, 1989). Furthermore Pip levels were found to be elevated in plasma and cerebrospinal fluid (CSF) of patients with pyridoxine-dependent epilepsy. Although not involved in mediating resistance to pyridoxine-dependent epilepsy, pipecolic acid levels were inversely correlated to the oral intake of pyridoxine and therefore it can be used as a diagnostic marker of pyridoxine-dependent epilepsy (Plecko et *al*., 2005).

The bacterium *Streptomyces hygroscopius* produces the antifungal compound rapapmycin that is of commercial interest because of its potent immunosuppressive and anticancer properties. During rapamycin biosynthesis, the amino acid L-pipecolic acid is incorporated into the rapamycin molecule prior to final ring closure (Ritacco et *al*., 2005).

II.4.3. AROMATIC AMINO ACIDS

The essential aromatic amino acids (AAAs) L-Tryptophan (Trp), L-phenylalanine (Phe), and L-tyrosine (Tyr) are required for protein biosynthesis in all living cells and are involved in processes like plant growth, development, reproduction, defense and environmental responses (Maeda and Dudareva, 2012). In plants Trp is precursor for the synthesis of the hormone auxin, phytoalexins, glucosinolates, and both indole- and anthranilate-derived alkaloids, whereas Tyr is a precursor of isoquinoline alkaloids, pigment betalains, and quinones (tocochromanols and plastoquinone; Radwanski and Last, 1995; Kutchan, 1995). The AAA with the highest carbon flux during biosynthesis is Phe, a common precursor of phenolic compounds, like flavonoids, condensed tannins, lignans, lignin, and phenylpropanoid/benzenoid volatiles (Vogt, 2010). The three AAAs are produced from chorismate, the final product of the shikimate pathway and individual postchorismate pathways that lead to the biosynthesis of Trp, Tyr and Phe. Chorismate is furthermore a precursor for the vitamins K1 and B9 and the plant defense hormone salicylic acid (Maeda

and Dudareva, 2012). The chorimate biosynthesis proceeds via seven enzymatic reactions starting with the conversion of phosphoenolpyruvate (PEP) and D-erythrose 4-phosphate (E4P) to 3-Deoxy-D-*arabino*-heptulosonate7-phosphate (DAHP), catalyzed by DAHP-synthase (DAHPS). Two DAHPS genes have been identified in Arabidopsis (*DAHPS1* and *DAHPS2*) that show differential expression. *DAHPS2* is constitutively expressed, whereas *DAHPS1* is strongly induced upon pathogen infection and wounding (Keith et *al.*, 1991). In a second reaction DAHP is converted to 3-dehydroquinate by 3-Dehydroquinate synthase (DHQS) using divalent cations (e.g. Co^{2+}) and NAD cofactors. In the third reaction the first double bond is introduced into the ring through dehydration of 3-dehydroquinate to 3-dehydroshikimate catalyzed by 3-Dehydroquinate dehydratase (DHD). This reaction is followed by the reversible reduction of 3-dehydroshikimate into shikimate by shikimate dehydrogenase (SDH) using NADPH. The fifth reaction is catalyzed by shikimate kinase that catalyzes the phosphorylation of the C3 hydroxyl group of shikimate using ATP as a cosubstrate to yield shikimate 3-phosphate. 3-phosphoshikimate1-carboxyvinyltranferase (EPSP) catalyzes the formation of EPSP in the sixth step of the shikimate pathway by transferring the enolpyruvyl moiety of PEP to the 5-hydroxyl position of shikimate 3-phosphate (Tzin and Galili, 2010). The activity of EPSP is induced upon infection with the necrotrophic fungal pathogen *Botrytis cinerea* together with two other genes of the shikimate pathway 2-dehydro-3-deoxyphosphoheptonate aldolase (DHS1) and chorismate synthase (CS; Ferrari et *al.*, 2007). Finally chorismate is produced via CS through introduction of the second double bond in the ring by chorismate synthase (Macheroux et *al.*, 1999).

II.4.3.1. Phenylalanine and Tyrosine

Chorismate mutase (CM) catalyses the first step in the Phe/Tyr biosynthesis and converts chorismate to prephenate. At least two isozymes of CMs, CM1 and CM2 are known in plants (Singh et *al.*, 1986). CM1 is localized in the plastids and is generally inhibited by Phe and Tyr and activated by Trp. Arabidopsis has an additional plastid localized gene encoding CM3 that is regulated in a similar manner (Mobley et *al.*, 1999). The activity of *CM3*, and to a lesser extent *CM1*, is elicitor and pathogen inducible (Eberhard et *al.*, 1996). The biosynthesis of Phe and Tyr proceeds via two separate pathways, the arogenate and the 4-hydroxyphenylpyruvate pathway (Siehl, 1999). In the Phe biosynthesis prephenate is further converted to phenylpyruvate through decarboxylation and dehydration of prephenate by prephenate dehydratases (PDT), also a spontaneous formation of phenylpyruvate from prephenate is possible. Arogenate dehydrogenase (ADT) converts arogenate to Phe in the final step of the arogenate route. PPA-Aminotransferase activity was shown to be 3-fold

higher compared to the ADT activity in petunia petals suggesting that ADT catalyzes a rate-limiting step within the arogenate pathway of the Phe biosynthesis (Maeda et *al.*, 2010). Prephenate is also a precursor for Phe, when converted by phenylpyruvate aminotransferase (PPY-AT) that catalyzes a reversible transamination between phenylpyruvate and Phe (Tzin and Galili, 2010). The last committing step in Phe and Tyr biosynthesis are the phenylpyruvate and 4-hydroxyphenylpyruvate transaminations, respectively (Maeda and Dudareva, 2012). Dudareva and colleagues identified a prephenate aminotransferase (PPA-AT) in Arabidopsis that drives the carbon flux from prephenate towards arogenate, indicating that Phe biosynthesis via arogenate is the predominant route in plants (Maeda et *al.*, 2011).

II.4.3.2. Tryptophan

The biosynthesis of Trp consists of six different enzymatic reactions that take place in the plastids (Radwanski and Last, 1995; Siehl, 1999). The first step on Trp biosynthesis is catalyzed by anthranilate synthase (AS), a chorismate-pyruvate lyase that accepts the amino acid Gln in the formation of anthranilate and pyruvate. AS consists of two subunits, a large α and a small β subunit (ASα and ASβ, respectively), which can form a α/β heterodimer or a α2/β2 tetramer (Romero et *al.*, 1995). In plants two genes encode for ASα and one gene encoding ASβ. Whereas one ASα is constitutively expressed, the other is regulated in developmental processes and induced upon pathogen infection and wounding (Niyogi and Fink, 1992). Phosphoribosylanthranilate transferase (PAT) transfers the phosphoribosyl moiety from phosphoribosylpyrophosphate to anthranilate and produces 5-phosphoribosylanthranilate. Phosphoribosylanthranilate isomerase (PAI) catalyzes the irreversible rearrangement of 5-phosphoribosylanthranilate to 1-(o-carboxy- phenylamino)-1-deoxy-ribulose 5-phosphate (CdRP). Indole-3-glycerol phosphate synthase (IGPS) catalyzes the irreversible conversion of CdRP to indole-3-glycerol phosphate. *trp2* and *trp3* Arabidopsis mutants defective in Trp synthase (see below) have less Trp but accumulate more auxin, suggesting that indole-3-glycerol phosphate serves as a key branch-point intermediate in Trp-independent auxin biosynthesis (Ouyang et *al.*, 2000). The final two reactions of the Trp pathway are catalyzed by the Trp synthase α-subunit (TSα) and β-subunit (TSβ), respectively. TSα catalyzes the reversible retro-aldol cleavage of indole-3-glycerol phosphate to indole and glyceraldehyde 3-phosphate (G3P), and TSβ subsequently condenses indole and serine to produce Trp using pyridoxal 5-phosphate (PLP) as a cofactor (Barends et *al.*, 2008). The expression of TSα and TSβ in Arabidopsis (as well as AS) is induced upon infection with bacterial pathogens like *Pseudomonas syringae* pv. *tomato*, *P. s.* pv. *maculicola or Xanthomonas campestris* pv. *campestris* infection, after abiotic elicitors like

silver nitrate (AgNO$_3$) and α-amino butyric acid (AABA), under amino acid starvation and under oxidative stress emphasizing the role of the Trp pathway and derived products in plant defense (Zhao et *al.*, 1998; Zhao and Last, 1996).

A Trp-derived metabolite with a major role in plant response to biotic and abiotic stresses is the indolic phytoalexin camalexin (3-thiazolylindole). Precursors of camalexin are cysteine and Trp which is converted to indole-3-acetaldoxime and subsequently dehydrated to indole-3-acetonitrile (Rauhut and Glawischnig, 2009). Arabidopsis phytoalexin deficient mutants, *pad1, pad2, pad3, pad4* and *pad5* show altered camalexin accumulation with effects on resistance to pathogen infections (Glazebrook et *al.*, 1996; Glazebrook et *al.*, 1997). *pad3* mutants are mutated in CYP71B15, the enzyme that commits the last step in camalexin biosynthesis, and show enhanced susceptibility to the fungal pathogens *Hyaloperonospora arabidopsidis* and *Alternaria brassicicola* (Schuhegger et *al.*, 2006; Glazebrook et *al.*, 1996). *pad4* mutants carry a recessive allele of a single gene that causes reduced camalexin synthesis (10-20% of the wild type levels) and strongly enhanced susceptibility to *Psm* ES4326 (Glazebrook et *al.*, 1996). Other mutants identified with reduced camalexin levels are the *boytritis-susceptible* mutants *bos2* and *bos4* that are susceptible to *Boytritis cinerea* and in case of *bos4* also to *Alternaria brassicicola*, another necrotrophic pathogen. The *bos2* and *bos4* mutants accumulate significantly less camalexin than the wild-type (Veronese et *al.*, 2004). The *ald1* mutant also was compromised in camalexin induction in response to both virulent and avirulent *P. syringae* strains and showed enhanced susceptibility and disease symptoms. The double mutant *pad4 ald1* even accumulated less camalexin upon pathogen infection than the single mutants, indicating that *PAD4* and *ALD1* contribute additively to the regulation of camalexin accumulation (Song et *al.*, 2004a). Camalexin accumulates in response to other bacterial strains like *P. syringae* pv. *tomato* and *Xanthomonas campestris* (Glazebrook and Ausubel, 1994), viruses, e.g. the cauliflower mosaic virus, turnip crinkle virus (Callaway et *al.*, 1996; Dempsey et *al.*, 1997) and oomycetes (Roetschi et *al.*, 2001). Abiotic stresses like amino acid starvation assays, as well as treatment with the ROS-inducing chemical acifluorfen and the abiotic elicitor AABA induce the accumulation of camalexin and Trp biosynthetic enzymes (Zhao et *al.*, 1998). Furthermore, AgNO$_3$ and UV-B radiation cause an accumulation of camalexin in plants (Zhao and Last, 1996, Schuhegger et *al.*, 2006).

II.4.5. BRANCHED-CHAIN AMINO ACIDS

The branched-chain amino acids (BCAAs) valine (Val), leucine (Leu) and isoleucine (Ile) are classified by the branched hydrocarbon residue and have an aliphatic character. BCAAs are

de novo synthesized in plants, but not in mammals that have to take up BCAAs with their diet or find another source like symbiotic bacteria (Binder, 2010; Akman Gunduz and Douglas, 2009). BCAAs carry out important functions in mammalian metabolism and levels need to be well balanced to avoid diseases like the Maple Syrup Urine Disease and neurological degeneration (Chuang et *al.*, 2006). Leu for example functions as a signaling molecule in mammals which regulates food intake, stimulates translation and triggers autophagy (Binder, 2010). In plants, the BCAAs Val and Ile are synthesized in the chloroplast via two parallel pathways with four enzymes; acetohydroxyacid synthase (AHAS), ketolacid reductoisomerase (KARI), dihydroxyacid dehydratase (DHAD) and branched-chain aminotransferase (BCAT) that catalyze the reactions (Diebold et *al.*, 2002; Binder, 2010; Singh and Shaner, 1995; Singh, 1999). The biosynthetic pathway of Ile requires a threonine deaminase (TD), which catalyzes the deamination and dehydration of Thr and yields pyruvate and 2-oxobutanoate (α-ketobutyrate). One of the initial substrates in BCAA biosynthesis is 2-oxobutanoate. 2-oxobutanoate can be synthesized from both methionine and threonine in *A. thaliana.* Acetolactate synthase catalyzes the first step in isoleucine biosynthesis from 2-oxobutanoate and also the first step in the parallel biosynthetic pathway leading from pyruvate to valine and leucine (Coruzzi and Last, 2000). Leu biosynthesis proceeds via 2-oxoisovalerate, the last intermediate that is transaminated to form Val (Binder, 2010). The last step in the biosynthesis of BCAA is the transamination of 4-Methyl-2-oxopentanoate and 3-Methyl-2-oxobutanoate into Leu and Val, respectively and 3-Methyl-2-oxopentanoate into Ile catalyzed by a branched-chain aminotransferase (BCAT) (Singh, 1999; Diebold et *al.*, 2002). Arabidopsis has six transcribed BCAT genes localized in the mitochondria, cytosol and the plastids (Diebold et *al.*, 2002). *AtBCAT2* (At1g10070), has a very low basal transcription, but is induced upon various stresses and hormone treatments like ABA and its expression is correlated with a rise in free BCAAs upon dehydration (Matsui et *al.*, 2008; Urano et *al.*, 2009. Abiotic stresses, like osmotic stress and temperature, seem to have an especially high impact on accumulation of BCAAs which might provide an alternative carbon source (Taylor et *al.*, 2004). A direct effect of BCAAs on plant resistance was not detected, but defects in Val and Ile metabolism do have an effect on plant defense. The glucosyltransferase UGT76B1 for example was identified as novel player in the SA-JA-crosstalk in Arabidopsis, as it showed attenuated SA-dependent defense responses and had a positive effect on JA-related processes. Mass spectrometric fragmentation identified Isoleucic acid (2-hydroxy-3-methyl-pentanoic acid; ILA), which is related to Ile, as an endogenous substrate of UGT76B1. ILA conferred resistance to bacterial pathogen *P. syringae*, and induced biosynthesis of SA and elevated levels of basal expression of SA-associated defense genes like *PR1* (von Saint Paul et *al.* 2011). Another role of Ile in JA-associated defense responses is the conjugation with JA which results in the biological active

form JA-Ile. JA-Ile binds to the SCF^{COI1} protein that binds the JAZ protein. This complex is then degraded through ubiquitination of the 26S proteasome and JA responsive genes and associated defense responses get activated (Yan et *al*., 2009).

II.4.5. PROLINE AND OTHER AMINO ACIDS

II.4.5.1. Proline

Proline is synthesized in the cytosol and in the plastids of plants via two different precursors, glutamate and ornithine. Glutamate is converted to Pro in two successive reduction steps catalyzed by pyrroline-5-carboxylate synthase (P5CS) and pyrroline-5-carboxylate reductase (P5CR), respectively. The Pro biosynthesis proceeds via transamination of ornithine to pyrroline-5-carboxylate (P5C) by Orn-δ-aminotransferase (OAT). Pro contents in the absence of stress are highest in flowers and pollen grains and seeds and lowest in roots. Pro contents are independent of the amino acid pool, but dependent on plant and leaf age and position or leaf part in the plant (Verbruggen et *al*. 1993). Pro is used for protein synthesis, has protective functions as an osmolyte, contributes to the maintenance of the redox balance, regulates developmental processes and is a component of metabolic signaling networks controlling mitochondrial functions and stress relief (Verbruggen et *al*. 1993). The antioxidant nature of Pro might be due to ROS scavenging activity and its functions as a singlet oxygen quencher (Smirnoff and Cumbes, 1989; Matysik et *al*. 2002). An alternative route could be the protection and stabilization of ROS scavenging enzymes and activate alternative detoxification pathways. During osmotic stress the glutamate pathway is the main pathway for Pro biosynthesis, although the ornithine pathway seems to play an important role in Pro biosynthesis in younger plants (Roosens et *al*. 1998). Pro catabolism takes place in the mitochondria and is catalyzed by Pro dehydrogenase (PDH) and P5C dehydrogenase (P5CDH; Elthon and Stewart 1981; Szoke et *al*. 1992). Pro biosynthesis in plants is controlled by two isoenzymes of *P5CS* and one *P5CR* gene. Only *P5CS1* is required for Pro accumulation during abiotic stress and expression is only induced upon salt stress, but not during drought indicating a regulation via different signaling pathways (Parre et *al*. 2007). During salt stress *P5CS1* accumulates in the chloroplasts, suggesting that under unfavorable conditions, glutamate-derived proline biosynthesis increases where photosynthesis takes place (Székely et *al*., 2008; Rayapati et *al*., 1989). Pro accumulation depends on ABA in a dose-dependent manner and the ability of the plant to respond to ABA (Verslues and Bray, 2006). Exogenous SA enhanced the Pro levels in lentils (*Lens esculenta*), on the other hand SA-deficient mutants *eds5* and *NahG* did not show enhanced P5CS transcript or Pro levels

in response to pathogen attack (Misra and Saxena, 2009; Fabro et *al*., 2004). The activity of the Pro catabolic enzyme proline dehydrogenase (PDH) was shown to be SA-dependent. PDH was also elevated in HR cells upon avirulent pathogen infection, whereas PDH-silenced plants exhibit less cell death and production of ROS, but increased susceptibility to avirulent pathogens (Cecchini et *al*., 2011).

II.4.5.2. Other Amino Acids

The role of other free amino acids during stress was suspect of temperature- and osmotic stress studies in *E.coli* and Arabidopsis (Shahjee et *al*., 2002; Kaplan et *al*., 2004). Under stress conditions, particularly osmotic dehydration, *E. coli* accumulates L-amino acids that play an important role as osmoprotectants (Shahjee et *al*., 2002). During a temperature stress metabolic profiling the levels of Ala, Asn, β-Ala, γ-aminobutyric acid (GABA) rise significantly in response to heat stress. Similar to the heat stress response, an increase during the development of acquired freezing tolerance at low temperature is observed for Ala, β-Ala, Gly, Pro, Ser, Orn Asn and GABA (Kaplan et *al*., 2004). Oxidative stress, induced by menadione (Vitamin K) treatment, severely compromises the tricarbocylic acid (TCA) cycle. Levels of amino acids whose synthesis and maintenance of amino acid pools depend on the TCA downstream glycolytic intermediates are significantly decreased, as well as amino acids in the Asp branch of linked to oxaloacetate (Asp, b-Ala, homoserine, Met, and Thr), and in the Glu branch linked to 2-oxoglutarate (Glu, Gln, and Pro). Oxidative stress also leads to decreases in amino acids such as Gly and Ser (linked to 3-phosphoglycerate), and Ala (linked to pyruvate) that are not directly connected to the TCA cycle (Baxter et *al*., 2007).

Although the non-proteinogenous amino acid β-amino-butyric acid (BABA) is not produced in the plant, it is a potent inducer of resistance in a wide range of monocot and dicot hosts against a wide range of pathogens including oomycetes, fungi, bacteria, tobacco mosaic virus (TMV) and nematodes (Cohen, 2002). The resistance inducing effect of BABA treatment was first observed in induced resistance to tomato late blight (Oort et *al*., 1960). BABA is also effective against the necotrophs *Plectosphaerella cucumerina* and *Alternania brassisicola* (Ton and Mauch-Mani, 2004), and *Botrytis cinerea* (Zimmerli et *al*., 2001) and (hemi-) biotrophs *Hyaloperonospora arabidopsidis* and *Pseudomonas syringae* pv. *tomato* (Zimmerli et *al*., 2000). BABA is rapidly taken up by the root system and accumulates mainly in the younger parts of the shoot, inducing resistance (Cohen et *al*., 1994; Jakab et *al*., 2001). Resistance induced by BABA protects mutants defective in the jasmonate and ethylene pathway, but not in SAR transduction pathway mutants and depends in the case of infection with against *P. syringae* pv. *tomato* on SA and *NPR1* (Zimmerli et *al*., 2000).

Furthermore, the SA-associated gene *PR-1*, but not the JA-responsive *PDF1.2* is highly induced upon BABA-treatment (Zimmerli et *al*., 2001). On the contrary, BABA induced resistance was blocked in the ABA-deficient mutant *aba1-5*, the ABA-insensitive *abi4-1* and the callose-deficient mutant *powdery mildew resistant4* (*pmr4-1)* upon infection with *P. cucurimerica*, but was unaffected in ethylene and SA-signaling mutants (Ton and Mauch-Mani, 2004). Zeier and colleagues found that exogenous BABA application induces a rise in Pip levels and enhanced resistance in the wild type, whereas this effect was absent in *ald1* mutants. This indicates that Pip regulates BABA-induced resistance against bacterial infection (Návarová et *al*., 2012). The mechanisms behind the BABA-induced resistance are connected to callose deposition and SA-dependent signaling, but also to SA-independent resistance and ABA-signaling. As a priming agent BABA provides broad-spectrum resistance, but also induces a dose-dependent growth reduction of the plants. Very recently IMPAIRED IN BABA-INDUCED IMMUNITY 1 (IBI1) was identified as a new master regulator of BABA-induced resistance. *IBI1* encodes an aspartyl-tRNA synthetase (AspRS) and binding of the R enantiomer of BABA to IBI1 primes the protein for non-canonical defense signaling in the cytoplasm after pathogen attack. IBI1 seems to control plant immunity and growth via separate pathways, giving rise to the opportunity to uncouple the growth inhibiting and resistance inducing effect of BABA treatment in the future (Luna et *al*., 2014).

II.5. THE PATHOSYSTEM ARABIDOPSIS THALIANA AND PSEUDOMONAS SYRINGAE

The thale cress *Arabidopsis thaliana* L. Heynh is an annual dicot that belongs to the family *Brassicaceae* and was established as a model organism in plant research. Arabidopsis has a short life cycle (6-8 weeks) and a number of different ecotypes, including Columbia (Col-0), Landsberg (Ler-0), Wassilewskija (Ws) and C24, with natural habitats distributed all over the northern hemisphere. Arabidopsis consists of approximately 30,000 genes that are located on 5 chromosomes. About 115.4 Mb of 125 Mb of the genome have been sequenced, which renders Arabidopsis as a suitable tool for forward and reverse genetic manipulation to identify genes and determining their functions (Arabidopsis Genome Initiative, 2000).

Pseudomonas syringae is a rod-shaped, gram negative bacterium, with polar flagella that consists of a large number of pathovars (pv.) infecting different host plants. *P. syringae* is named after the lilac tree (*Syringa vulgaris*), from which it was first isolated (Krieg and Holt, 1984). *P. syringae* pv. *tomato* DC3000 for example causes bacterial speck disease of tomato (*Solanum lycopersicum*) and has become a model for studying bacterium–plant interactions since it also attacks *Arabidopsis thaliana* and *Nicotiana benthamiana*. The (hemi-) biotrophic bacteria enter the plants through wounds or natural openings like stomata, to proliferate in the apoplast. Depending on the combination of *P. syringae* strain and Arabidopsis accessions, different defense responses, like non-host resistance, incompatible interaction due to recognition of an Avr-gene, and compatible interactions during basal resistance, are triggered. *P. syringae* strains are host-specific and assigned to more than 50 pathovars. *P. syringae* is in possession of a type 3 secretion system (T3SS) that enables the bacteria to shuttle toxins and a large repertoire of effector proteins into the plant (Göhre and Robatzek, 2008; Mota and Cornelis, 2005; Glazebrook, 2005). To study the compatible interaction that overcomes basal resistance, we used the virulent *P. syringae* pv. *maculicola* ES4326 (*Psm*) and for incompatible interaction during gene-for-gene resistance *Pseudomonas syringae* pv. *maculicola* ES4326 carrying the plasmid containing the avirulence gene *pLAFR3::avrRpm1* [*Psm(avrRpm1)*)] in our studies.

III. AIM OF THESIS

Detection of microbes by the plant innate immune system leads to both local and systemic responses. The identity of the molecules critical for the activation of these immune responses, as well as their inter-relationship, is however still unclear. A previous study by our group revealed changes in amino acids levels during pathogen attack, and emphasized the important role played by amino acids in plant defense (Návarová et *al*. 2012). Specifically, this study identified the Lys-derived non-proteinogenous amino acid pipecolic acid (Pip) as a novel important regulator of both local and systemic resistances, as well as priming in *Arabidopsis thaliana* (Návarová et *al.* 2012). The major aims of my thesis were to characterize in detail the regulation of free amino acids levels (including Pip) and to elucidate the interplay of Pip and salicylic acid (SA) during systemic acquired resistance (SAR) and defense priming in *Arabidopsis thaliana*.

We aimed to assess the differential accumulation of free amino acids by different branches of plant immunity during infection with virulent and avirulent strains of the bacterium *Pseudomonas syringae* pv. *maculicola*, as well as upon treatment with the bacterial pathogen-associated molecular pattern (PAMP) flg22. In order to understand the regulatory mechanisms underlying changes in free amino acids during immunity, we sought to analyse their levels in mutants deficient in biosynthesis and/or signaling of the defense-related hormone SA, ethylene and jasmonic acid. In addition, given the central role played by SA in SAR, we wanted to study the inter-relationship between Pip and SA during resistance development at the infection site and in the distal leaf. Notably, since our analysis of the SAR transcriptome in distal leaves suggested a down-regulation of photosynthesis-related genes, we further investigated the effect of SAR on photosynthesis rate.

The Lys aminotransferase ALD1 is required for Pip biosynthesis (Návarová et *al*. 2012), but it is still unclear which other enzymes are involved in this process. To this end, we selected candidate genes based on expression patterns and homology to known biosynthetic genes in other organisms to test their potential role upstream and downstream of Pip biosynthesis in *Arabidopsis thaliana*. In addition, we were curious to test what is the role of the close ALD1 homolog, AGD2; especially since its mutation leads to a constitutive resistance phenotype. These analyses were complemented by the study of the sub-cellular localization of ALD1 (as an important Pip biosynthetic enzyme) and FMO1 (as a critical regulator of Pip-mediated resistance) to obtain further insight into Pip biosynthesis and signaling processes.

IV. RESULTS

IV.1. DIFFERENTIAL REGULATION OF AMINO ACID SYNTHESIS DURING DEFENSE IN ARABIDOPSIS
(Part of the results presented here are published in Návarová et *al*. 2012)

IV.1.1. ACTIVATION OF SPECIFIC AMINO ACID BIOSYNTHETIC PATHWAYS AND PIP ACCUMULATION OCCUR IN RESPONSE TO BACTERIAL INFECTION AND PAMP PERCEPTION

Free amino acid accumulation is massively changed during *Psm*-induced SAR in the local, inoculated leaves of Col-0. Aliphatic amino acids like Val, Leu, Ile and β-Ala, as well as the aromatic amino acids Tyr, Trp, Phe and His are induced up to 5- to 20-fold. More moderately triggered is the accumulation of GABA, Cys, Asn, Ala, Orn, Ser and Gly. The biosynthesis of Lys-derived amino acids Aad and Pip is specifically triggered after *Psm* inoculation and levels in inoculated leaves increased up to 70-fold (Návarová et *al*. 2012). Levels of Asp are reduced upon pathogen challenge, while Lys, an Asp-derived amino acid (Galili et *al*., 2001; Návarová et *al*. 2012) accumulates up to 20-fold upon pathogen challenge, indicating that Lys biosynthesis and catabolism are pathogen inducible events (Návarová et *al*. 2012).

To better understand the defense components that are required for the accumulation of Pip, Pip downstream signaling and the regulatory principles of amino acids biosynthesis in plant tissues upon pathogen infection, we comparatively analyzed the levels of further free amino acids in response to an inoculation with compatible and incompatible *Pseudomonas syringae* strains and the PAMP flg22. Free amino acids were extracted from local leaves of Col-0 inoculated with the virulent *Psm*, the avirulent *Psm avrRpm1* and 100 nM flg22 to characterize potential differences in amino acid metabolism in leaves of Arabidopsis Col-0 one day after inoculation. The results showed that during the incompatible interaction between Arabidopsis and *Psm avrRpm1* the biosynthesis of a number of free amino acids was strongly induced one day after inoculation of the pathogen. Almost all amino acids analyzed were significantly changed in leaves inoculated with *Psm avrRpm1* compared to mock treated leaves, except for Ala, Glu, Gln and Orn (Tab. 1). Levels of Pip and Aad were strongly increased; up to 200- and 300-fold, respectively, followed by a more moderate increase of aromatic amino acids Phe, Tyr, Trp at around seven fold. Aliphatic amino acids like Val, Leu Ile and the Asp-derived Lys were as highly induced as the aromatic amino acids. Significantly decreased during the incompatible interaction are Pro, Asp and Asn (Tab. 1). During the compatible interaction the biosynthesis of the same free amino acids was

induced compared to the changes observed during the incompatible interaction. The strength of induction, observed during the compatible interaction upon *Psm* inoculation, was noticeable stronger compared to the incompatible interaction (Tab. 1). One day after inoculation of *Psm,* Pip and Aad levels were increased by a factor of 90- and 9-fold, respectively. The biosynthesis of aromatic-amino acids Phe and Tyr was increased significantly, as well as the aliphatic amino acids Val, Leu and Ile. Interestingly, the induction of branched-chain amino acids was overall stronger in the compatible, compared to the incompatible interaction, as levels of Leu were increased up to a 24-fold. Significantly decreased amino acids one day after *Psm* inoculation are Pro, Asp and Orn (Tab. 1). We then analyzed the changes in levels of free amino acids after PAMP treatment. A significant induction of biosynthesis was observed for the free amino acids Pip, Lys, Ala, Val, Leu and Ile one day after inoculation of 100 nM flg22. Pip accumulated by 13-fold upon PAMP-treatment which was, compared to the incompatible and compatible interaction, a weak response. Still, the biosynthesis of the branched-chain amino acid Leu was, like in the compatible interaction, with 23-fold strongly increased (Tab. 1). Even though not all free amino acids were changed significantly, the color code of the fold change *P*/M (Tab. 1) suggested that the regulatory principle behind the induction of biosynthesis was shared among the incompatible and compatible interaction and PAMP treatment and thus followed similar signaling pathways. Taken together one day after inoculation of the HR-inducing pathogen *Psm avrRpm1* the biosynthesis of Pip, Aad, aromatic and branched-chain amino acids was strongly induced, followed by the biosynthesis triggered by the virulent pathogen and PAMP treatment. However, the processes involved in PTI seemed to have a greater influence on the biosynthesis of aliphatic amino acids than ETI.

µg g^{-1} FW	incompatible interaction				ratio	compatible interaction				ratio	PAMP treatment				ratio
amino acid	MgCl$_2$	±	*Psm avr Rpm1*	±	P/M	MgCl$_2$	±	*Psm*	±	P/M	H$_2$O	±	flg22	±	flg22/ H$_2$O
Gly	11.5	2.5	18.3	0.7	1.6 **	21.6	3.6	43.9	11.5	2.0	20.1	10.7	38.2	12.5	1.9
Ala	28.0	37.5	37.5	2.8	1.3	55.2	16.9	111.4	34.9	2.0 **	55.2	4.8	111.4	14.3	2.0 **
Val	3.5	16.6	16.6	1.3	4.7 ***	5.9	1.0	36.3	1.4	6.1 ***	5.0	0.3	23.9	3.1	4.8 ***
Leu	1.1	0.2	8.5	1.2	7.6 ***	1.5	0.2	36.9	5.5	24.2 ***	0.9	0.0	21.5	9.5	23.3 **
Ile	1.3	0.2	7.3	0.8	5.4 ***	2.0	0.3	18.3	1.8	9.0 ***	1.6	0.1	11.1	3.7	6.8 **
GABA	2.1	0.0	5.3	0.2	2.6 ***	3.0	0.9	6.7	1.0	2.2 **	2.0	0.5	6.3	3.2	3.2
Thr	33.2	3.6	76.1	5.1	2.3 ***	93.7	6.7	100.8	70.6	1.1	69.1	8.8	114.4	22.3	1.7
Pro	14.5	1.4	7.4	0.3	0.5 ***	29.6	1.9	17.0	0.9	0.6 **	42.5	11.7	34.5	7.9	0.8
Pip	0.1	0.0	18.2	2.2	201.5 ***	0.3	0.1	25.8	4.1	93.6 ***	0.2	0.0	2.5	0.4	13.3 ***
Aad	0.0	0.0	10.1	1.3	311.7 ***	0.2	0.0	2.0	0.4	8.5 ***	0.2	0.0	0.9	0.4	5.8
Asp	433.7	57.0	267.8	10.3	0.6 **	1429.0	28.5	631.1	159.6	0.4 ***	937.8	83.8	1215.3	225.1	1.3
Glu	150.7	3.7	166.0	10.8	1.1	822.4	34.0	572.5	93.0	0.7 **	521.0	27.3	890.6	241.8	1.7
Asn	433.7	1.0	267.8	0.3	0.6 ***	53.1	1.7	48.4	10.2	0.9	37.5	12.7	54.4	8.8	1.5
Gln	58.8	12.0	43.0	7.0	0.7	272.7	18.5	233.6	48.5	0.9	185.4	55.2	306.3	88.8	1.7
Orn	0.6	0.1	0.4	0.1	0.6	1.5	0.2	0.4	0.2	0.3 **	1.4	0.6	0.7	0.1	0.5
Lys	1.8	0.2	11.5	1.0	6.5 ***	3.6	0.1	7.6	3.0	2.1	2.7	0.4	19.2	5.8	7.0 **
Phe	1.6	0.2	11.7	1.5	7.2 ***	7.7	0.2	36.1	9.2	4.7 **	7.2	1.6	25.3	10.7	3.5
Tyr	0.3	0.1	1.7	0.1	5.9 ***	0.6	0.1	10.5	1.8	18.0 ***	0.3	0.2	5.5	2.6	18.6
Trp	0.1	0.0	0.7	0.1	6.5 ***	0.6	0.1	2.4	1.0	4.0	0.4	0.1	3.6	2.0	8.9

> 20
5 - 20
3 - 5
1.6 - 3
0.5 – 0.8
< 0.5

Table 1. Changes in the levels of free amino acids in Arabidopsis Col-0 plants upon leaf inoculation with avirulent *P. syringae* pv. *maculicola* (*Psm*) *avrRpm1* (left column), virulent *Psm* (middle column), and 100 nM flg22 (right column) one day after inoculation. Mean values of amino acids for local leaf samples are given in µg g^{-1} fresh weight (FW) ± SD from at least three replicate samples. Mock-treatments were performed by infiltration of leaves with a 10 mM MgCl$_2$ solution or water. Asterisks denote statistically significant differences between *Psm* (P) and MgCl$_2$ (M) samples (***P < 0.001, **P < 0.01, and *P < 0.05; two- tailed *t* test).

The perception of PAMPs triggers local and systemic defense responses and activates distinct metabolic pathways in Arabidopsis (Mishina and Zeier, 2007; Griebel and Zeier, 2010). Like in *Psm*- or *Psm avrRpm1*-inoculated leaves, a treatment with 100 nM flg22 triggered the accumulation of Lys, Pip and Aad and aromatic as well as aliphatic amino acids (Tab. 1).

To investigate whether SA has an influence on PAMP-induced Pip-biosynthesis, 100 nM flg22 were infiltrated into leaves of Col-0 and *sid2-1* and samples of treated leaves taken one day later. The *sid2-1* mutant is defective in SA-biosynthesis and pathogen-induced production of SA (Nawrath and Metraux, 1999; Wildermuth et *al.*, 2001). Col-0 and *sid2-1* accumulated Pip to similar levels in the infiltrated leaves one day after infiltration of 100 nM flg22 (Fig. 3A). We also analyzed the levels of Aad in the local leaf after mock and flg22

treatment. Aad accumulated in Col-0 and *sid2-1* leaves after inoculation of 100 nM flg22. The Aad levels in Col-0 did not significantly increase upon flg22 treatment compared to the control situation, whereas in *sid2-1* a significant increase was detectable (Fig. 3B). However, Zeier and colleagues showed a significant accumulation of Aad after infiltration of 200 nM flg22 two days after treatment (Návarová et *al.* 2012). The Aad levels of flg22-treated leaves of Col-0 and *sid2-1* did not differ significantly (Fig. 3B). Thus, PAMP-induced Pip- and Aad-biosynthesis was an SA-independent process.

(A)   (B)
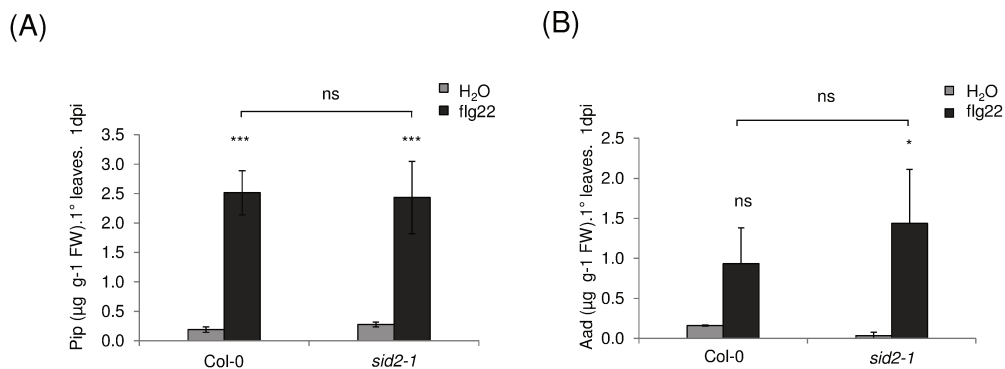
Figure 3. Metabolite levels in leaves following leaf infiltration with 100 nM flg22 or water one day after infiltration. Infiltration of 100 nM flg22 leads to an enhancement of Pip and Aad levels in Col-0 and *sid2-1* plants. Leaf contents of Pip **(A)** and Aad **(B)** in Col-0 and *sid2-1* plants one day after infiltration of 100 nM flg22 or water in infiltrated leaves. Mean values of amino acids for local leaf samples are given in µg g^{-1} fresh weight (FW) ± SD from at least three replicate samples. Asterisks denote statistically significant differences (***: P< 0.001; **: P < 0.01; *: P < 0.05; ns = not significant, two-tailed *t* test).

IV.1.2. AMINO ACID METABOLISM IN RESPONSE TO PSM IS REGULATED BY PAD4

To uncover the relationship between the Pip- and the SA-regulatory pathway and the regulatory principles of amino acid accumulation during defense we used a selection of mutants affected in SA-, JA- and ET- pathways including *phytoalexin deficient4 (pad4), non-expressor of pr genes1 (npr1), isochorismate synthase1 (sid2-1/ics1), flavin-dependent monooxygenase1 (fmo1), agd2-like defense response protein1 (ald1), non-race specific disease resistant1 (ndr1), constitutive expression of pr genes5 (cpr5), coronatine insensitive1 (coi1), delayed-dehiscence2 (dde2)* and *ethylene receptor1 (etr1)*. The mutant plants and Col-0 were inoculated with *Psm* (OD 0.005) or 10 mM MgCl$_2$ as mock treatment and samples for comparative amino acid analysis were taken one day after inoculation. The levels of Pip after *Psm* inoculation were strongly induced in the wild type as described before (Tab. 1).

Compared to the wild type, Pip accumulated to similar, not significantly changed levels in *fmo1* and *sid2-1*. In the mutants *npr1* and *pad4* Pip levels upon *Psm* inoculation were significantly reduced one day after inoculation compared to the wild type (Fig. 4A). These results indicated that Pip biosynthesis was proceeding independently of FMO1 and SA-biosynthesis, but dependent on a functional SA-signaling pathway and even more on the lipase-like defense regulator PAD4 one day after pathogen attack. Pip levels were also investigated in mutants defective in the JA or ethylene signaling pathway one day after inoculation with *Psm* (Fig. 4B). The mutant *dde2* is blocked in the synthesis of the active form of JA, JA-Ile and *coi1* is defective in JA-triggered responses. A mutation in ETR1, a membrane bound receptor protein, disables ET-triggered induction of defense signaling pathways. Ethylene and JA are two important plant hormones that regulate defense responses against necrotrophic pathogens (Wang et *al.*, 2002). Pip levels in *dde2, coi1* and *etr1* were not significantly changed after *Psm* inoculation, compared to the wild type, although the Pip level of *dde2* seems to be slightly reduced (Fig. 4B). Thus Pip accumulation seemed not to be dependent on the JA- or ET-signaling pathway. After the comparative analysis of free amino acid accumulation upon inoculation with the avirulent *Psm avrRpm1* in the local leaves of Col-0, we analyzed the levels of Pip accumulation in a set of defense related mutants. One day after inoculation of *Psm avrRpm1* Pip accumulated significantly in Col-0 and to wild type-like levels in *fmo1, sid2-1* and *npr1* (Fig. 4C). Pip biosynthesis was also significantly activated in *pad4*, but compared to the wild type strongly reduced, although not completely blocked. The *ald1* mutant was fully blocked in pathogen-induced Pip biosynthesis (Fig. 4C). The results indicated that Pip biosynthesis during PTI and ETI proceeded independently of FMO1 and SA. Interestingly, Pip biosynthesis after inoculation with *Psm avrRpm1* was independent of NPR1. The positive regulatory role of PAD4 on Pip biosynthesis seemed to be conserved between PTI and ETI.
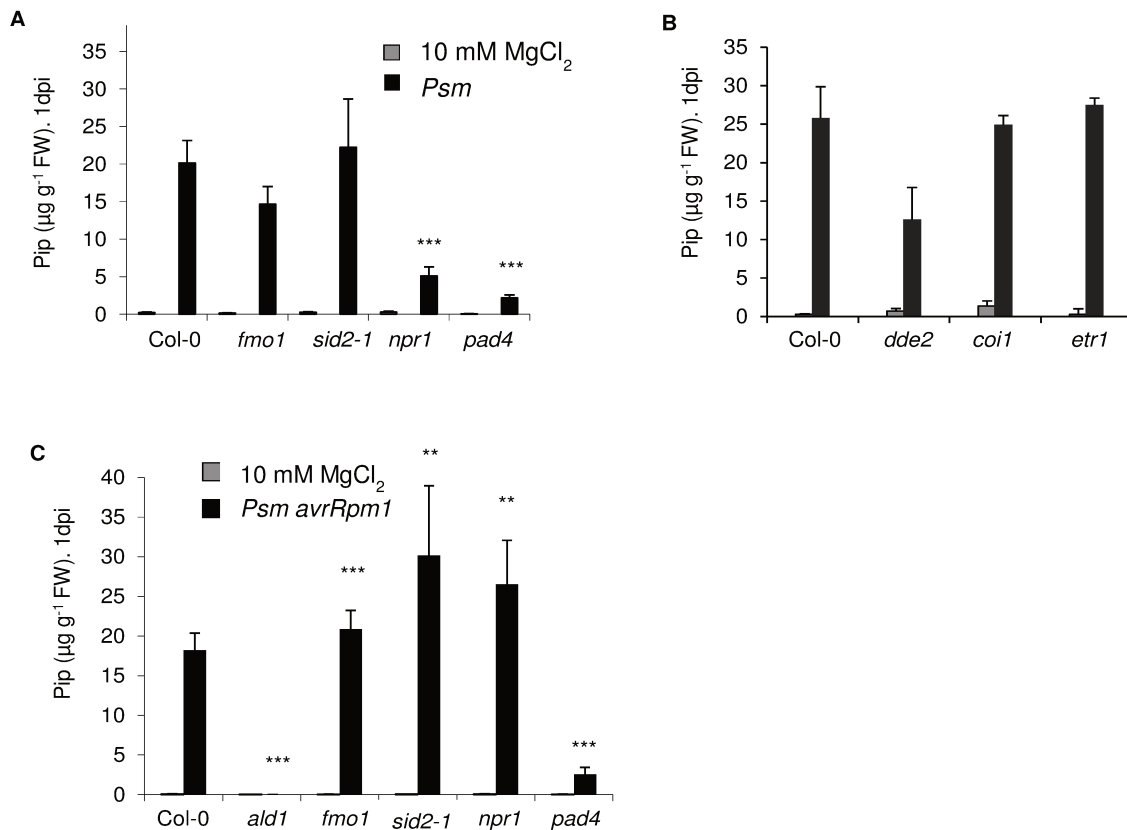
Figure 4. Pip accumulation in *P. syringae*-inoculated *Arabidopsis* leaves one day after inoculation. Accumulation of Pip in *Psm* inoculated leaves of wild type Col-0, *fmo1, sid2-1, npr1* and *pad4* **(A)** and accumulation of Pip in *Psm* inoculated leaves of wild type Col-0, *dde2, coi1* and *etr1* **(B)**. Accumulation of Pip in *Psm avrRpm1* inoculated leaves of wild type Col-0, *ald1, fmo1, sid2-1, npr1* and *pad4* **(C)**. Asterisks denote statistically significant differences between *Psm* mutant and the *Psm* Col-0 sample. (***: P< 0.001; **: P < 0.01; *: P < 0.05; two-tailed *t* test).

To get a better idea of the regulation of Pip- and Aad-biosynthesis at the later stages of defense, amino acid levels were comparatively analyzed in local leaves two days after inoculation with the virulent *Psm* strain. The selection of regulatory defense mutants that was used in the analysis of Pip levels during compatible and incompatible interaction one day after inoculation of the pathogen was complemented by *cpr5* and *ndr1*. CPR5 is a membrane protein of unknown function and *cpr5* mutants exhibit a dwarfed growth phenotype and constitutive disease resistance with elevated basal levels of SA and *PR* gene transcripts (Bowling et *al.*, 1997). NDR1 is required for the function of CC-NB-LRR resistance proteins like RPS2, RPS5 and RPM1 (Coppinger et *al.*, 2004). Pathogen-triggered Pip biosynthesis in *ald1* was completely blocked after two days of infection with *Psm* (Fig. 5A). The SA-deficient mutant *sid2-1* accumulated slightly, but yet significantly lower amounts of Pip compared to Col-0 two days after inoculation and thus showed a positive influence on Pip biosynthesis at the later stages of resistance (Fig. 5A). Interestingly, *fmo1* mutants almost doubled the amounts of Pip produced in the local leaves, compared to the wild type, which indicated a possible downstream role of the SAR-regulator FMO1 in the Pip biosynthesis pathway (Fig.

5A). *cpr5* accumulated up to 20 µg g^{-1} FW in the mock-treated local leaves, but did not increase these levels after pathogen attack. No influence on Pip biosynthesis, at later stages of infection with a virulent bacterial strain, had NDR1 and NPR1, as the levels were not significantly altered compared to wild type levels (Fig. 5A). The dependency of Pip biosynthesis on PAD4 however was confirmed, as Pip accumulated only up to a third in *pad4* compared of pathogen induced Pip levels in Col-0 (Fig. 5A). Pip biosynthesis was positively regulated by *PAD4* and, at earlier stages of compatible interactions, also by *NPR1*.
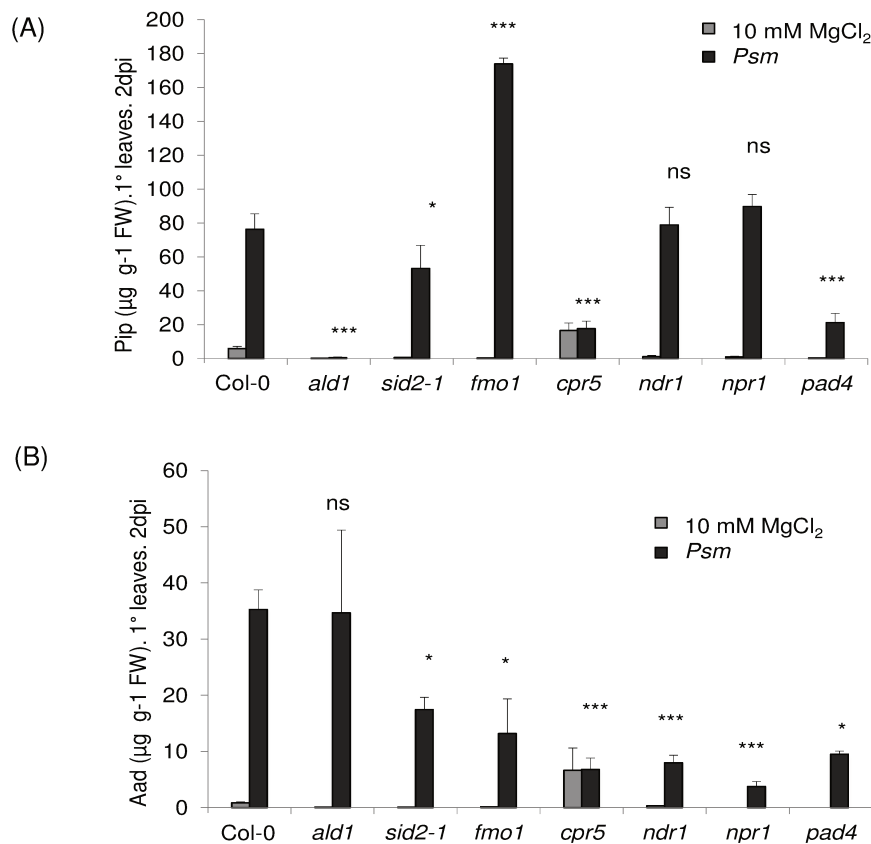
Figure 5. Accumulation of Pip **(A)** and Aad **(B)** in *Psm* inoculated and distal leaves of wild type Col-0 and *ald1, sid2-1, fmo1, cpr5, ndr1, npr1* and *pad4* mutants one day post inoculation. Grey bars represent leaves inoculated with 10 mM MgCl$_2$ as a control treatment, black bars represent *Psm* treated leaves. Asterisks denote statistically significant differences between *Psm* mutant and the *Psm* Col-0 sample (***: P< 0.001; **: P < 0.01; *: P < 0.05; ns = non-significant, two-tailed *t* test).

Aad is like Pip a Lys-derived amino acid, that was found to accumulate after pathogen inoculation in the local, but not in the distal leaves of Col-0 (Tab. 1; Návarová et *al.* 2012). We also analyzed the levels of *Psm*-inducible Aad two days after inoculation and found that Aad biosynthesis was completely independent of ALD1 (Fig. 5B). The levels of Aad produced in *sid2-1* and *fmo1* were significantly, although not very strong, reduced compared to Col-0 (Fig. 5B). Like Pip, the constitutive levels of Aad are highly elevated in *cpr5* mutants that give another hint for a potential role in local resistance (Fig. 5B; Návarová et *al.* 2012). However,

NDR1 and NPR1 had a positive influence on Aad-biosynthesis, demonstrating potentially different regulatory principles between Pip- and Aad-biosynthesis. PAD4 seemed to regulate both Lys catabolites, as Aad levels were significantly reduced in *pad4* (Fig. 5B). The Aad biosynthetic pathway however seemed to be stronger regulated in an NPR1-dependent manner.

As Pip is an important SAR regulatory metabolite and accumulated not only in the local, but also distal leaves and petiole exudates of Col-0, we wanted to know whether Pip does accumulate systemically in the different defense associated mutants two days after inoculation. In the systemic leaves of *Psm*-treated Col-0 Pip levels did increase strongly in the compared to the mock-treated leaves (Fig. 6). Interestingly Pip levels increased significantly in distal leaves of *sid2-1* and *fmo1 Psm*-treated plants, although compared to the increase in Col-0 not very high (Fig. 6). The low levels of Pip in distal leaves of mock-treated *sid2-1* and *fmo1* plants indicated that SA or FMO1 had an influence on basal Pip levels in the distal leaves. Pip did not accumulate systemically in distal leaves of *Psm*-treated *npr1* and *pad4* plants (Fig. 6).
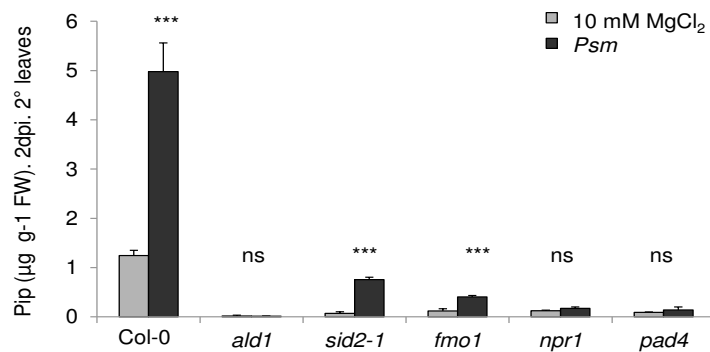
Figure 6. Accumulation of Pip in distal leaves of wild type Col-0 and selected mutant plants 2 days post *Psm* inoculation. Grey bars represent changes in distal leaves folowing inoculation with 10 mM MgCl$_2$ as a control treatment, black bars represent changes after *Psm* treatments. Asterisks denote statistically significant differences between 10 mM MgCl$_2$- and *Psm*-inoculation (***: $P < 0.001$; **: $P < 0.01$; *: $P < 0.05$; ns = non-significant, two-tailed t test).

In conclusion, local Pip biosynthesis during both the compatible and incompatible interactions was independent of the SA pathway and *FMO1*, but partially dependent on *PAD4*. The biosynthesis of Aad underlined different regulatory mechanisms than Pip biosynthesis, but basal levels of both amino acids were elevated in the constitutively resistant *cpr5* mutant. Interestingly, Pip accumulation in distal leaves of locally-inoculated plants was significantly increased compared to mock-treated plants in the SAR-deficient *sid2-1* and *fmo1,* but not in *npr1* and *pad4* mutants.

IV.1.3.   DIFFERENTIAL   REGULATION   OF   AMINO   ACIDS ACCUMULATION DURING DEFENSE

The regulatory principle of free amino acids was comparatively analyzed in Col-0 during a compatible and incompatible interaction and PAMP-treatment (Tab. 1). It revealed that amino acids were supposedly regulated via the same signaling pathways during PTI and ETI. To uncover the regulation of Pip and Aad biosynthesis at early and late stages of defense in interaction with virulent and avirulent bacteria, we used a set of mutants defective in defense associated signaling pathways. We found that Pip biosynthesis was positively regulated by the lipase-like defense regulator PAD4 and at earlier stages of defense also by NPR1. From the comparative amino acid analyses in Col-0 (Tab. 1) it became clear that members of the group of aromatic-amino acids and aliphatic amino acid are, like Pip, Aad and Lys strongly induced during defense.

To uncover the regulatory principle behind these biosynthetic patterns we performed comparative analysis of free amino acids with *fmo1, npr1, pad4, dde2, coi1* and *etr1* compared to Col-0 one day after inoculation with *Psm* or 10 mM $MgCl_2$ (Tab. 2 and 3). As described earlier, aromatic and aliphatic amino acids, as well as Pip and Aad accumulated significantly in the wild type, whereas Pro, Asp and Orn were decreasing upon pathogen attack (Tab. 2 and 3).

In *fmo1*, aromatic amino acids like Phe, Tyr, Trp, the aliphatic amino acids Val, Leu, Ile, as well as Lys and Glu and the Lys-derivatives Pip and Aad, significantly increased upon *Psm* inoculation compared to mock treatment, although to lower levels than in Col-0. Significantly decreases in *fmo1 P*/M were observed for Pro (Tab. 2). Amino acid accumulation compared between *fmo1* mock and Col-0 mock samples, showed that in *fmo1*, levels of Gly, Val, Ile, Pip, Asn, Gln and Orn were significantly reduced and Glu was the only amino acid that was significantly increased compared to the wild type (Tab. 2). In leaves inoculated with *Psm* no significant changes in amino acid levels were observed in *fmo1* compared to *Psm* inoculated wild type leaves, except for a decrease in Pip and Orn levels (Tab. 2). Pip biosynthesis was found to be independent of FMO1. Although at earlier stages of infection the Pip levels seemed to be reduced in the *fmo1* mutant (Fig. 4A), Pip over accumulated two days after inoculation of *Psm* in the local leaves (Fig. 5A).

Besides the regulation of Pip and Aad biosynthesis, NPR1 seemed not to have a major regulatory role in the metabolism of free amino acids one day upon pathogen infection as only Gly was significantly decreased compared to the wild type levels (Tab. 2). Comparing levels of amino acids in mock-treated leaves of *npr1* to mock Col-0 leaves, the only significant change was the decrease in Pro and Pip levels in *npr1*. Comparing amino acid

levels in *Psm* against mock-infiltrated leaves of *npr1*, significant induction after *Psm*-inoculation was observed in the aliphatic amino acids Val, Leu, Ile, in Ala, Pip, Aad and Lys and in the aromatic amino acid Phe and Tyr (Tab. 2).

The results of comparatively analyzed amino acids in *pad4* mutants showed a regulatory influence of PAD4. In leaves of *pad4* after inoculation with 10 mM $MgCl_2$ the levels of Gly, Val, Ile, Pip, Asn and Gln were decreased compared to levels measured in Col-0 mock leaves. Interestingly, Gly, Ala, aliphatic amino acids Val, Leu, Ile, as well as Pro and Pip in *Psm*-inoculated *pad4* plants were significantly decreased, compared to levels in Col-0 *Psm* inoculated leaves. On the other side a group of amino acids was significantly increased in the pathogen challenged leaf of *pad4* compared to wild type, consisting of Asp, Glu, Orn, Lys and Trp. The levels of free amino acids Gly, Leu, Ile, Thr, Pip, Aad, Gln, Lys, Phe, Tyr and Trp were increased in *Psm*-inoculated leaves compared to mock samples. Ala and Pro were decreasd comparing *Psm* against mock values in *pad4* plants.

μg g⁻¹ FW	Amino acid accumulation 24hpi in the local leaves																				
	Col-0					fmo1				npr1				pad4			
amino acid	MgCl₂	±	Psm	±	ratio P/M	MgCl₂	±	Psm	±	MgCl₂	±	Psm	±	MgCl₂	±	Psm	±
Gly	13.7	1.6	38.5	8.4	2.8 **	6.7	0.1	17.7	4.8	8.0	4.0	16.0	0.9	5.5	0.9	9.7	0.5
Ala	55.6	14.4	148.3	28.1	2.7 **	40.0	12.7	87.5	41.1	50.4	12.6	184.7	22.8	61.7	3.5	35.0	7.5
Val	6.7	0.9	31.9	7.1	4.8 ***	3.5	0.4	26.5	5.9	5.3	0.9	29.8	0.4	3.8	0.3	6.8	1.7
Leu	1.5	0.3	24.9	3.7	16.7 ***	1.2	0.1	22.0	3.5	2.2	1.2	26.4	2.9	0.9	0.2	9.6	0.7
Ile	1.7	0.1	14.3	1.9	8.4 ***	1.3	0.0	11.0	1.8	1.7	0.5	13.5	1.1	1.2	0.0	3.9	0.3
GABA	5.6	0.5	8.7	1.7	1.5	5.0	1.4	5.6	2.9	9.2	6.6	11.6	1.3	6.7	2.5	8.8	1.4
Thr	40.7	15.4	76.1	29.1	1.9	33.3	10.1	120.2	50.0	64.7	48.1	65.0	14.2	19.2	13.6	100.3	18.6
Pro	29.8	6.8	14.8	2.7	0.5 *	19.4	4.6	9.3	1.8	11.9	0.8	10.4	0.7	19.5	3.1	7.2	1.5
Pip	0.5	0.1	43.4	5.2	88.3 ***	0.3	0.1	26.4	4.3	0.9	0.1	8.0	1.1	0.1	0.0	3.6	0.8
Aad	0.1	0.1	1.7	0.4	20.4 ***	0.0	0.0	1.4	0.6	0.3	0.2	0.9	0.2	0.1	0.0	1.7	0.6
Asp	503.9	127.6	308.2	71.5	0.6	628.7	67.1	540.5	264.3	926.4	564.2	442.3	78.6	649.1	133.3	977.0	187.8
Glu	418.0	68.4	406.0	121.4	1.0	628.0	26.9	512.3	235.0	411.8	35.3	355.8	76.8	651.5	152.4	1260.8	303.3
Asn	90.9	13.6	63.6	15.7	0.7	38.2	7.9	52.8	26.1	61.9	34.8	55.3	7.8	18.3	4.0	31.0	7.5
Gln	210.1	56.1	101.6	27.7	0.5	39.0	11.7	50.1	11.3	97.0	69.4	58.7	10.7	18.1	4.4	78.2	15.2
Orn	0.8	0.2	0.2	0.0	0.2 **	0.1	0.0	0.1	0.0	0.2	0.0	0.3	0.2	0.3	0.0	0.8	0.3
Lys	0.9	0.4	2.0	0.6	2.1	0.5	0.1	1.3	0.3	0.5	0.0	1.9	0.4	0.9	0.3	6.9	1.4
Phe	6.4	1.3	27.0	7.3	4.2 **	5.3	0.3	20.8	0.9	4.6	0.3	27.7	4.2	4.0	1.1	25.5	7.2
Tyr	0.2	0.1	5.1	1.1	21.8 ***	0.2	0.1	4.6	1.8	0.2	0.0	6.6	1.5	0.2	0.0	4.2	1.1
Trp	0.1	0.0	0.4	0.1	3.9 *	0.1	0.0	0.4	0.1	0.1	0.0	0.2	0.1	0.0	0.0	0.7	0.0

Legend:
> 20
5 - 20
3 - 5
1.6 - 3
0.5 – 0.8
< 0.5

Table 2. Changes in the levels of free amino acids in Arabidopsis Col-0, *fmo1, npr1 and pad4* plants. Samples are given in μg g⁻¹ fresh weight (FW) ± SD from at least three replicate samples. Mock-treatments were performed by infiltration of leaves with a 10 mM MgCl₂ solution. Light blue and yellow colored boxes indicate mutant mock values that are significantly reduced or increased, respectively, compared to the Col-0 mock value. Dark blue and red colored boxes indicate mutant *Psm* values that are significantly reduced or increased, respectively, compared to the Col-0 *Psm* value. Numbers in italic indicate significant changes in MgCl₂ mutant and the *Psm* mutant sample (*P*/M) of the respective mutant. (***: P< 0.001; **: P < 0.01; *: P < 0.05; two-tailed *t* test).

Comparatively analysis of free amino acids was also performed in local leaves of *dde2, coi1* and *etr1* mutants one day after *Psm* inoculation.

Regulation of amino acid metabolism in *dde2* did not seem to differ greatly from the wild type, except a significant decrease in Pip produced in *Psm* inoculated leaves of *dde2* compared to *Psm*-inoculated wild type leaves. We previously described that *dde2* seemed to have no regulatory role in Pip-biosynthesis as the levels of *Psm*-induced Pip did not significantly differ from the wild type, still the Pip levels showed a minor reduction compared to wild type levels (Fig. 4B). Free amino acid levels in mock treated leaves of *dde2* were significantly reduced in Aad, Asp, Gln and Orn compared to Col-0 mock samples (Tab. 3).

Comparing *Psm* against mock samples in *dde2*, Val, Leu, Ile, GABA, Pip, Lys and the aromatic amino acids Phe, Tyr and Trp were significantly increased upon pathogen attack (Tab.3).

$\mu g\ g^{-1}$ FW amino acid	Amino acid accumulation 24hpi in the local leaves																			
	Col-0					dde2				coi1				etr1						
	MgCl₂	±	*Psm*	±	ratio P/M	MgCl₂	±	*Psm*	±	MgCl₂	±	*Psm*	±	MgCl₂	±	*Psm*	±			
Gly	21.6	3.6	43.9	11.5	2.0	35.2	12.3	34.0	4.3	24.6	8.9	59.5	7.0	33.7	8.7	44.2	5.4			
Ala	55.2	16.9	111.4	34.9	2.0 **	149.2	34.0	132.0	57.0	91.7	17.0	202.7	58.9	109.1	13.7	105.1	48.5			
Val	5.9	1.0	36.3	1.4	6.1 ***	8.1	1.4	26.6	6.3	5.6	2.1	37.7	4.0	6.8	1.0	26.3	7.7			
Leu	1.5	0.2	36.9	5.5	24.2 ***	1.7	0.3	30.8	5.8	1.9	1.3	40.3	3.9	2.0	0.3	49.2	6.5			
Ile	2.0	0.3	18.3	1.8	9.0 ***	2.4	0.1	15.6	2.3	1.9	0.9	21.0	0.5	2.5	0.2	20.5	3.1			
GABA	3.0	0.9	6.7	1.0	2.2 **	2.2	0.9	8.4	2.1	6.8	1.3	7.7	0.7	2.1	0.3	8.5	0.5			
Thr	93.7	6.7	100.8	70.6	1.1	80.3	30.4	187.7	57.0	33.9	4.6	96.2	66.1	102.4	16.3	260.3	10.3			
Pro	29.6	1.9	17.0	0.9	0.6 ***	28.7	6.1	16.8	5.6	21.8	7.4	26.2	4.1	31.1	3.9	15.8	2.4			
Pip	0.3	0.1	25.8	4.1	93.6 ***	0.7	0.3	12.6	4.2	1.4	0.7	25.0	1.2	0.3	0.1	33.5	8.4			
Aad	0.2	0.0	2.0	0.4	8.5 ***	0.2	0.0	2.0	0.8	0.2	0.0	1.7	0.2	0.3	0.0	5.3	0.1			
Asp	1429.0	28.5	631.1	159.6	0.4 ***	1022.6	158.3	759.7	319.9	552.4	47.1	522.8	33.8	1494.0	294.7	1000.1	173.1			
Glu	822.4	34.0	572.5	93.0	0.7 **	570.1	130.2	710.9	250.0	260.0	17.2	503.2	9.7	720.5	134.1	930.1	29.4			
Asn	53.1	1.7	48.4	10.2	0.9	45.4	13.0	52.3	11.5	17.2	1.1	48.6	8.1	61.1	14.5	71.7	8.2			
Gln	272.7	18.5	233.6	48.5	0.9	152.0	36.8	189.1	57.9	66.3	6.9	154.5	25.5	283.3	66.2	310.9	59.1			
Orn	1.5	0.2	0.4	0.2	0.3 **	1.0	0.1	0.9	0.5	0.4	0.0	0.5	0.2	1.8	0.5	3.5	0.9			
Lys	3.6	0.1	7.6	3.0	2.1	2.6	0.9	8.8	0.9	2.1	0.6	12.1	5.5	4.6	0.8	18.4	9.7			
Phe	7.7	0.2	36.1	9.2	4.7 **	9.2	3.0	47.4	12.4	5.4	0.8	45.5	8.0	11.2	2.6	69.7	12.5			
Tyr	0.6	0.1	10.5	1.8	18.0 ***	0.5	0.2	10.9	4.6	0.7	0.5	9.2	0.6	0.7	0.2	18.9	1.0			
Trp	0.6	0.1	2.4	1.0	4.0	0.5	0.2	2.9	0.8	0.2	0.1	2.6	0.8	0.8	0.2	6.9	1.9			

Legend:
> 20
5 - 20
3 - 5
1.6 - 3
0.5 – 0.8
< 0.5

Table 3. Changes in the levels of free amino acids in Arabidopsis Col-0, *dde2*, *coi1* and *etr1* plants Samples are given in µg g⁻¹ fresh weight (FW) ± SD from at least three replicate samples. Mock-treatments were performed by infiltration of leaves with a 10 mM MgCl₂ solution. Light blue and yellow colored boxes indicate mutant mock values that are significantly reduced or increased, respectively, compared to the Col-0 mock value. Dark blue and red colored boxes indicate mutant *Psm* values that are significantly reduced or increased, respectively, compared to the Col-0 *Psm* value. Numbers in italic indicate significant changes in MgCl₂ mutant and the *Psm* mutant sample (*P*/M) of the respective mutant. (***: P< 0.001; **: P < 0.01; *: P < 0.05; two-tailed *t* test).

Another mutant defective in JA-dependent defense is *coi1*. Regulation of amino acid metabolism after pathogen attack in a COI1-dependent manner was only observed in a significant increase in Pro and a decrease in Glu levels compared to Col-0 *Psm* samples. The levels of amino acids in the mock-treated leaves showed a significant reduction in Thr, Asp, Glu, Asn, Gln, Orn, Lys, Phe and Trp compared to Col-0 mock samples, whereas COI1 had a positive influence on GABA biosynthesis (Tab. 3). Significant increases in amino acid

levels during pathogen treatment compared to mock-treated leaves in *coi1* was observed for Gly, Ala, the aliphatic amino acids Val, Leu, Ile, as wells as GABA, the Lys-catabolites Pip and Aad, Glu, Asn, Gln, Orn and the aromatic amino acids Phe, Tyr and Trp. Significant decreases in *coi1* were observed for Asp in *coi1 Psm* vs. mock inoculated leaves (Tab. 3).

In the *etr1* mutant levels of free amino acids in mock-treated leaves were not significantly changed compared to levels in Col-0 mock leaves, except for a decrease in Glu (Tab. 3), while inoculation with *Psm* caused an increase in Aad, Glu, Orn and Tyr in *etr1* compared to Col-0 *Psm* samples. Induction of amino acid biosynthesis in *Psm* compared to mock-treated *etr1* plants was observed for the aliphatic amino acids Val, Leu, Ile, GABA, Thr, Pip, Aad and the aromatic amino acids Tyr and Trp. A significant decrease upon pathogen attack in *etr1* was observed for Pro (Tab. 3).

Taken together, the mutants tested, revealed that the regulatory principles of amino acid biosynthesis upon pathogen challenge were highly conserved and that the tendencies remained the same, independently of SA, JA or ET signaling. Biosynthesis of aliphatic and aromatic amino acids, as well as Pip and Aad was in almost all mutants induced upon pathogen attack, although in some cases to a lesser extent compared to Col-0. However, some interesting regulatory patterns were observed that are worth to follow up, as PAD4 positively regulated the biosynthesis of aliphatic amino acids and Pip and negatively regulated amino acids like Asp, Glu, Orn, Lys and Trp during defense. This revealed that particular defense components seemed to regulate distinct branches of amino acid metabolism.

IV.2. PIP REGULATES SAR VIA SA-DEPENDENT AND - INDEPENDENT PATHWAYS

IV.2.1. INTRODUCTION

In contrast to other amino acids and known defense metabolites, Pip accumulates markedly in distal leaves of *Psm*-treated leaves and petiole exudates of Arabidopsis Col-0 wild type (Návarová et *al.* 2012). The observation that Pip levels increased systemically after *Psm* inoculation in the distal leaf of *sid2-1*, led us to investigate the relationship and role of SA and Pip during SAR. To investigate the dependency of *ALD1* and *FMO1* expression on SA in the systemic leaves, we measured gene expression quantitatively in distal leaves of Col-0 and *sid2-1* mutants two days after inoculation with *Psm* and *Psm avrRpm1* (Fig. 7A+B). Systemic expression of *ALD1* and *FMO1* was induced strongly in Col-0. The increase in gene expression was much lower in *sid2-1*, but was still markedly enhanced compared to the mock-treatment. SA positively regulated *ALD1* and *FMO1* expression in the distal leaves, but also independent induced upon pathogen attack (Fig. 7A+B).
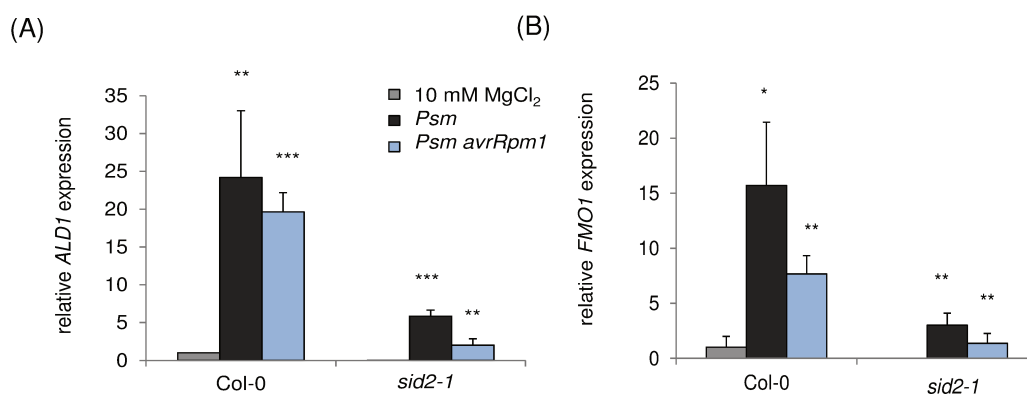
Figure 7. Relative *ALD1* and *FMO1* gene expression is induced in the distal leaves of Col-0 and *sid2-1* after inoculation with virulent and avirulent bacteria two days after inoculation.
Psm- and *Psm avrRpm1*-induced relative *ALD1* **(A)** and *FMO1* expression **(B)** in distal leaves of Col-0 and *sid2-1* plants. Transcript levels were assessed by quantitative real-time PCR analysis, are given as means ± SD of three replicate samples, and are expressed relative to the respective mock control value. Asterisks denote statistically significant differences between the mock sample and the *Psm/Psmavr* of Col-0 and *sid2-1* (***: P< 0.001; **: P < 0.01; *: P < 0.05; ns = non-significant, two-tailed *t* test; cDNA provided by K. Gruner).

IV.2.2. EXOGENOUS PIP REGULATES SEVERAL FORMS OF INDUCED RESISTANCE IN PLANTS

Exogenously applied Pip can override local resistance defects of *ald1* and reduces disease symptoms in Col-0 and *ald1* (Návarová et *al.* 2012).

When Arabidopsis plants were fed via the roots with 10 µmol Pip, a significant increase in Pip was measured in leaves of Col-0 and *ald1* plants one day after application to the soil (Fig. 8 A+B). Pip levels were similar to the local increase of Pip seen one day after *Psm* inoculation in Col-0. Upon exogenous Pip application to the roots Aad levels increased besides Pip significantly in the shoot in Col-0 and *ald1* (Fig. 8B), leading to the hypothesis that Pip induced Aad biosynthesis. Exogenous Aad application on the other hand did not cause an increase in Pip, but a slight reduction in susceptibility that was not comparable to the Pip mediated resistance effect (Návarová et *al.*, 2012).
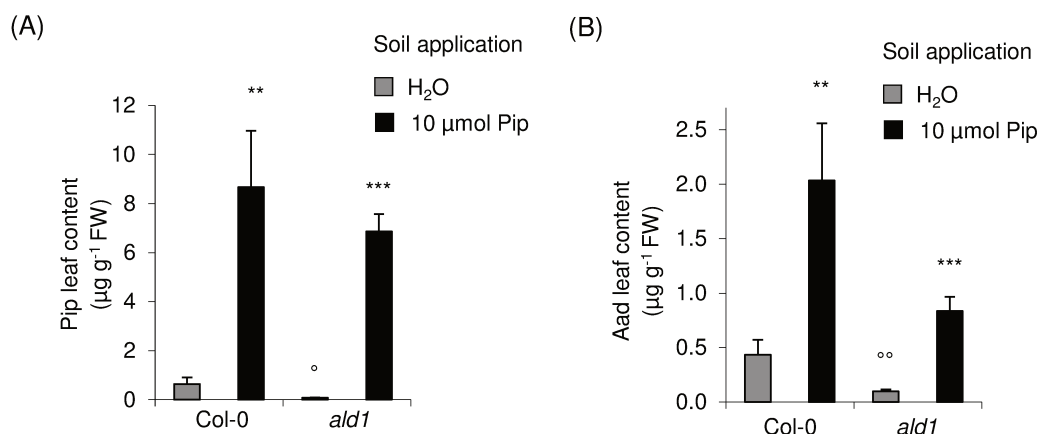
Figure 8. Exogenous Pip supplied via the root is transported to the shoot and leads to an enhancement of Aad levels. Leaf contents of Pip **(A)** and Aad **(B)** in Col-0 and *ald1* plants one day after supplying of 1 mM ($\equiv$ 10 µmol) Pip via the roots. Asterisks denote statistically significant differences between the water and the 10 µmol Pip sample. Open circles denote statistically differences between the water mutant and the water Col-0 sample (***: $P < 0.001$; **: $P < 0.01$; *: $P < 0.05$; ns = non-significant, two-tailed *t* test).

We wanted to identify potential downstream components in the Pip signaling pathway and test whether exogenous Pip induces resistance in other defense regulatory mutants. Therefore bacterial growth was measured after pre-treatment of Pip or water and inoculation of virulent *Psm* was measured three days later in a set of defense mutants, such as *ald1*, *sid2-1*, *npr1*, *pad4* and *fmo1* compared to Col-0. Pip-induced resistance strongly reduced bacterial growth in the wild type, emphasizing the importance of Pip in resistance against (hemi)-biotrophic bacteria (Fig. 9). Local resistance of *ald1* mutants is normally strongly

reduced compared to Col-0, but exogenous application of Pip restored resistance in *ald1*. Exogenous Pip reduced bacterial growth in *ald1* up to 24-fold and in the wild type up to 45-fold Pip vs. mock treatment (Fig. 9). Therefore, exogenous Pip was able to induce a growth reduction in *ald1* almost down to wild type level (Fig. 9).

Most interestingly, local resistance in *sid2-1* was even more impaired than in *ald1*, but exogenous Pip did induce SA-independent bacterial growth reduction up to 17-fold (Fig. 9). Local resistance of *npr1* and *pad4* was as impaired as in *sid2-1,* however; exogenous Pip treatment did only slightly reduce bacterial growth in *npr1* and *pad4.* In both cases resistance was induced only up to 2-fold and thus Pip only had a faint positive effect on resistance in *npr1* and *pad4* mutants. Local resistance in *fmo1* was, like in *ald1*, less severely affected compared to *sid2-1*, *npr1* and *pad4*. Interestingly, while exogenous Pip still had a minor effect on bacterial growth in *npr1* and *pad4*, it was not possible to induce a significant growth reduction in *fmo1* (Fig. 9). Together with the fact that Pip over accumulated in local leaves at later stages after pathogen inoculation in *fmo1* mutants (Fig. 5A) this led to the conclusion that FMO1 functions downstream of Pip-signaling pathway.
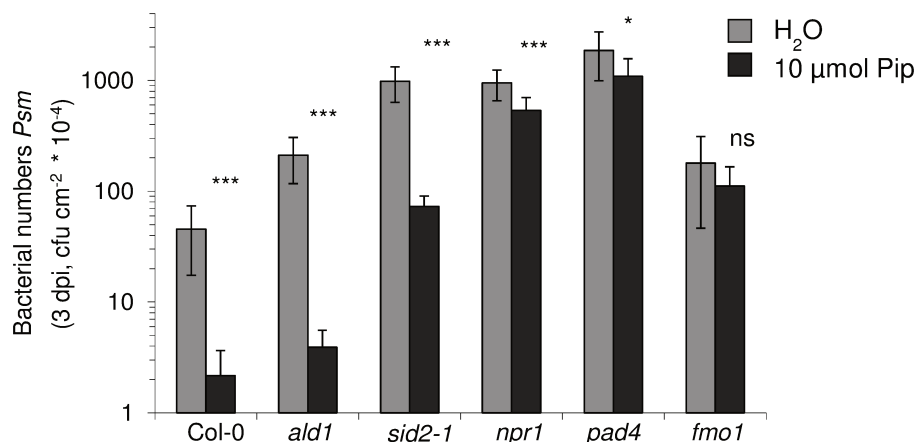
Figure 9. D/L-Pip-induced resistance in wild type Col-0 and defense mutants *ald1, ics1, npr1, pad4* and *fmo1* to *Psm* infection. Colony forming units of *Psm* (applied in titers of OD 0.001) at 3 dpi. Plant pots were supplied with 10 mL of H_2O or 10 mL of 1 mM ($\equiv$ 10 µmol) Pip one day prior to inoculation. Asterisks denote statistically significant differences between the water and the 10 µmol Pip sample. (***: P< 0.001; **: P < 0.01; *: P < 0.05; ns = non-significant, two-tailed *t* test).

IV.2.3. EXOGENOUS SA CAN INDUCE RESISTANCE INDEPENDENTLY OF THE PIP BIOSYNTHESIS PATHWAY

Exogenously applied Pip clearly had a positive effect on resistance establishment in Col-0, *ald1* and *sid2-1* plants, but bacterial growth in *sid2-1* was not fully reduced to wild type levels upon Pip treatment (Fig. 9).

To further uncover the relationship of SA and Pip in disease resistance, we also applied SA exogenously to the plant to measure its effect on expression levels of *ALD1* and *PR-1* as well as bacterial growth. Since we wanted to investigate the direct effect of SA and SA itself is not systemically moving through the plant (Vernooij et *al.*, 1994), 0.5 mM SA was infiltrated and gene expression was measured after 4 and 24 hours in the treated leaves. *ALD1* transcripts were significantly induced 4 hours after infiltration of SA and elevated after 24 hours, although not significantly different from the expression observed after infiltration of water (Fig. 10A). Thus, SA had no great impact on *ALD1* gene expression levels. The transcript level of the SA marker gene *PR-1* however, was over 3000-fold induced at 4 and 24 hours after infiltration of SA into leaves of Col-0 (Fig. 10B).
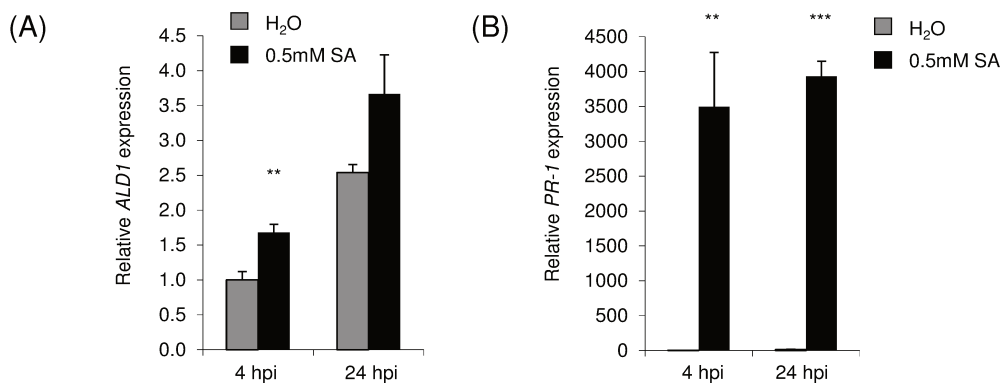
Figure 10. Effect of exogenous SA on *ALD1-* and *PR-1*-transcript levels in Col-0. Relative expression of *ALD1* (**A**) and *PR-1* (**B**) in Col-0 leaves at 4 and 24h after infiltration with water or 0.5 mM SA. Transcript levels were assessed by quantitative real-time PCR analysis, are given as means ± SD of three replicate samples, and are expressed relative to the respective mock control value. Asterisks denote statistically significant differences between the water and the SA sample. (***: P< 0.001; **: P < 0.01; *: P < 0.05; ns = non-significant, two-tailed *t* test).

Consequently, we next measured bacterial growth in leaves infiltrated with SA. When leaves were infiltrated with 0.5 mM SA (pH 7) twelve hours prior to a second inoculation with *Psm*, bacterial growth was significantly reduced in Col-0, *sid2-1*, *ald1* and *fmo1* (Fig. 11). Like in the Pip-induced bacterial growth assay, local growth in *sid2-1* mutants was much higher compared to *ald1*, *fmo1* and the wild type. While SA pre-infiltration reduced bacterial

growth in *ald1* and *fmo1* to the same levels measured in the wild type, the growth reduction in *sid2-1* was less pronounced (Fig. 11). This indicated that exogenous SA could not compensate completely for the reduced levels of endogenously produced SA in *sid2-1*. Pip- and SA-resistance pathways are operating in an independent manner, but SA might also function downstream of Pip-biosynthesis and signaling.
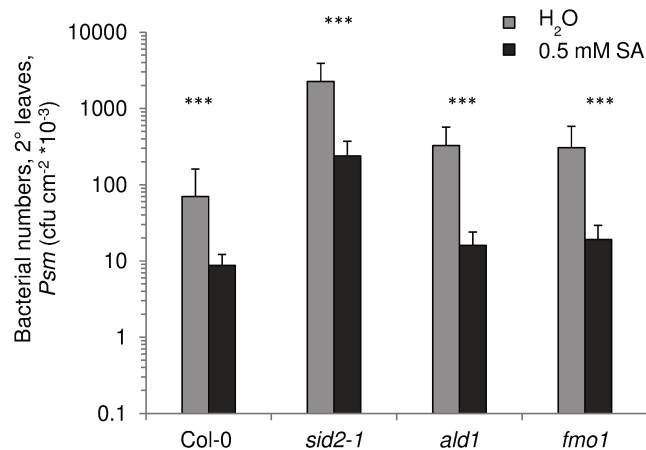
Figure 11. Effect of exogenous SA on bacterial growth. SA-induced resistance of wild type Col-0 and defense mutants *sid2-1, ald1* and *fmo1* to *Psm* infection. Colony forming units of *Psm* (applied in titers of OD 0.001) at 3 dpi. Leaves were infiltrated with 0.5mM SA (pH 7) or water 12 hours prior to inoculation. Asterisks denote statistically significant differences between the water and the SA sample (***: P< 0.001; **: P < 0.01; *: P < 0.05; two-tailed *t* test).

IV.2.4. CHARACTERIZATION OF THE DOUBLE MUTANT SID2-1 ALD1

To investigate the impact and interplay of both signaling pathways on basal resistance, SAR and defense priming the SA-deficient mutant *ics1/sid2-1* was crossed with the Pip-deficient mutant *ald1*. To characterize stable F2 *sid2-1 ald1* mutants we first performed a PCR with genomic DNA of Col-0 and *sid2-1 ald1* candidates and gene specific and T-DNA insertion primers for the *ald1* mutant (SALK_007673; Fig. 12A). The position of the T-DNA insertion in SALK_007673 alongside with a schematic overview of *ICS1* and *ALD1* is shown in figure 13. The loss of the isochorismate synthase 1 activity in *sid2-1* is due to a point mutation that changes a glycine into a stop codon (GAA to TAA; Wildermuth et *al.*, 2001, Fig. 13A). Site specific primer pairs were designed to identify the *sid2-1* specific point mutation in *sid2-1 ald1* (Fig. 12B). The specific annealing temperature to discriminate for the point mutation in *sid2-1* was determined by a gradient PCR (57 - 67°C). The annealing temperature of approximately 64°C gave a strong amplicon in Col-0, but did not amplify a product in *sid2-1*. Thus, an annealing temperature of 64°C was chosen for further screening

(Fig. 12A). About a 110 individual F2 *sid2-1 ald1* candidates were tested for the presence of the T-DNA insertion of the *ald1* mutant. The F2 candidates without a wild type band (a) #2, 4, 6, 13, 19 and 23 (Fig. 12A) were selected for PCR-based screening for *ICS1* with the point mutation specific *sid2-1* primer pair. The F2 candidate *sid2-1 ald1*#6 did not amplify any PCR product like the *sid2-1* single mutant and was therefore used for further characterization (Fig. 12C).
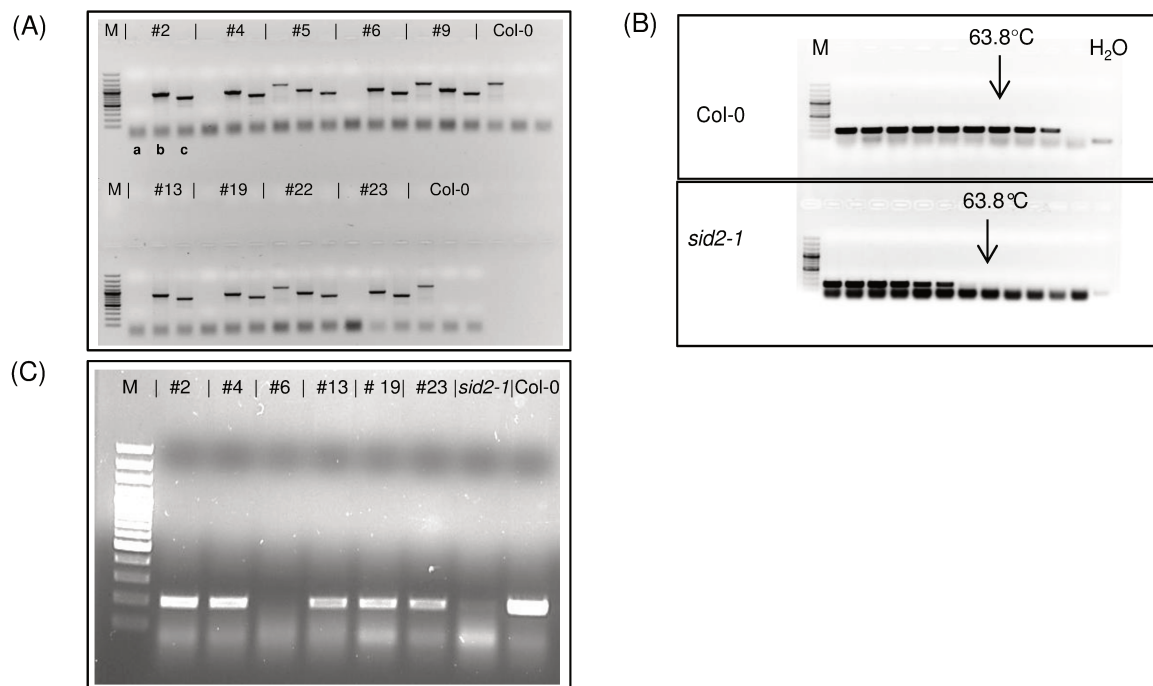
Figure 12. Molecular characterization of the *sid2-1 ald1* double mutant. PCR analysis of gDNA isolated from Col-0 and F2 *sid2-1 ald1* candidates to screen for *ALD1* T-DNA insertion a: Left genomic primer (LP) and right genomic primer (RP) primer, b: LP and left T-DNA insertion border primer (LB), c: RP and LB primer pair. M = 100bp marker **(A)**. Gradient PCR (57 - 67°C) using genomic DNA of Col-0 and *sid2-1* with *sid2-1* specific primer pair discriminating for the point mutation *(ICS1*-FV and *ICS1*- RV). 63.8 °C was identified as temperature specific to identify the *sid2-1* specific point mutation in *ICS1*. H_2O served as a negative control. M = 100bp marker **(B)**. PCR analysis of gDNA isolated from Col-0, *sid2-1* and preselected F2 *sid2-1 ald1* candidates. *sid2-1* specific primer *(ICS1*-FV and *ICS1*- RV) and annealing temperature of 64°C were used. M = 100bp marker **(C)**.
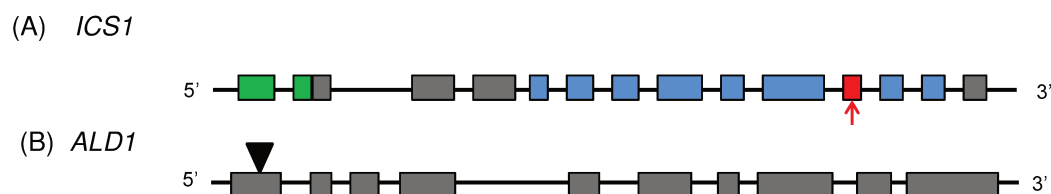
Figure 13. Schematic representation of *ICS1* and *ALD1* (5'→ 3'). *ICS1* (AT1G74710) consists of a putative plastid transit sequence (green) and a chorismate-binding domain (blue). The location of mutations in *sid2-2* and *sid2-1* are indicated by a red box and a red arrow, respectively (modified according to Wildermuth et *al.*, 2001) **(A)**. *ALD1* (AT2G13810) locus, showing the position of the T-DNA insertion (black triangle) in SALK_007673 **(B)**. Boxes represent exons and the spaces spliced introns.

The point mutation specific for the *sid2-1* mutation in *ICS1* was confirmed to be present in two *sid2-1 ald1* (#6 and #51) candidates by sequencing. As control, genomic DNA of Col-0 and *sid2-1* plants was used (Fig. 14B). The growth phenotype of *sid2-1 ald1* was not different from Col-0, *ald1, sid1* and *sid2-1*, respectively (Fig. 14C). Since isochorismate is a precursor of phylloquinone, which is a secondary electron acceptor from photosystem I (PSI), the *ics1 ics2* mutant exhibits a paler and smaller growth phenotype, compared to the wild type as it is completely devoid of phylloquinone (Fig. 14C; Gawroński et *al.*, 2013, Garcion et *al.*, 2008).

(A)

bp 2.731
|

TCTTATTATGCTTTCTTCTGCTTTGCAGG<u>GTATATGTGACAGAGTTGTTGTC</u>AAGCCTCAA
AAAACTGTGAGGAAGCTT*GCAAGAGTGCAACATCTATATTCTC*AATTGGCAGGGAGACTT
ACGAAGGAAGATGATGAGGTGAGATAATAGTATTGGAATAGTTTTTACATTTCCAAGCTCT
TCATTTCTTCGAATTAGCTTTAACCCTTTTTCTTTCTATCTGTCTATAGTATAAAATATTGGC
TGCTCTGCA*TCCAACTCCAGCTGTTTGTG*GGCTTC
|
bp 3.010

(B)

(C)
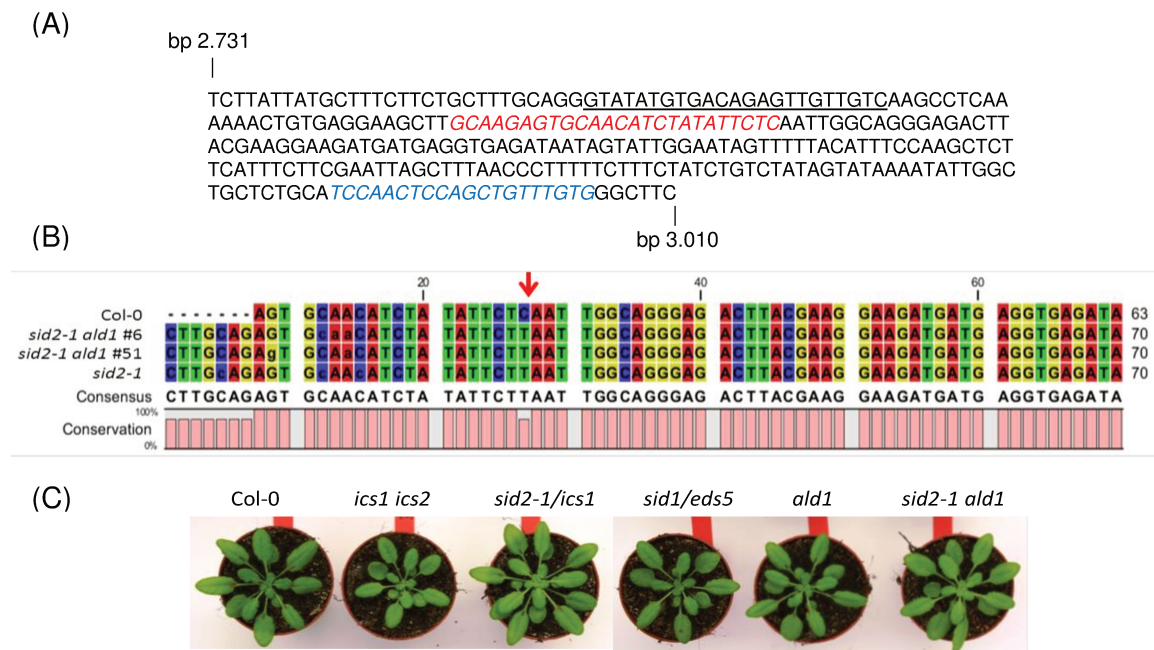
Figure 14. Characterization of *sid2-1 ald1* double mutant. Cutout (bp 2731–3010) of *Arabidopsis thaliana* chromosome 1, complete sequence *EDS16/SID2/ICS1* (NCBI Reference Sequence: NC_003070.9). Sequence of sequencing primer underlined, *sid2-1* specific fwd-primer in red and italics and *sid2-1* specific rev-primer in blue and italics (A). Multiple sequence alignment of Col-0, *sid2-1 ald1* candidates (#6 and #51) and *sid2-1*. The red arrow indicates the location of the *sid2-1* specific mutation (B). Growth phenotype of five week old *sid2-1 ald1* compared to SA-deficient *ics1 ics2*, *sid2-1/ics1* and *sid1/eds5* and Pip-deficient *ald1* mutants and Col-0 grown in short day conditions (9h day and 15h night) (C).

To confirm the successful generation of a Pip- and SA-deficient *sid2-1 ald1* mutant, the relative gene expression of *ALD1* and *ICS1* one day after *Psm* and *Psm avrRpm1* inoculation, compared to mock treatment was measured. *ALD1* expression was strongly induced after *Psm* inoculation in local leaves of the wild type and *sid2-1* (Fig. 15A). The induction of *ALD1* after *Psm avrRpm1* was much less pronounced, suggesting a different kinetic in defense gene activation during an ETI response, which is usually triggered within a few hours after the stimulus. *ALD1* was not expressed upon mock, *Psm* or *Psm avrRpm1* inoculation in the *ald1* mutant or in *sid2-1 ald1* (Fig 15A). *ICS1* expression was induced upon

virulent or avirulent *Psm* infection, but not as strong as *ALD1*. No *ICS1* gene expression was induced in *sid2-1* or *sid2-1 ald1* (Fig. 15B).

(A)   (B)
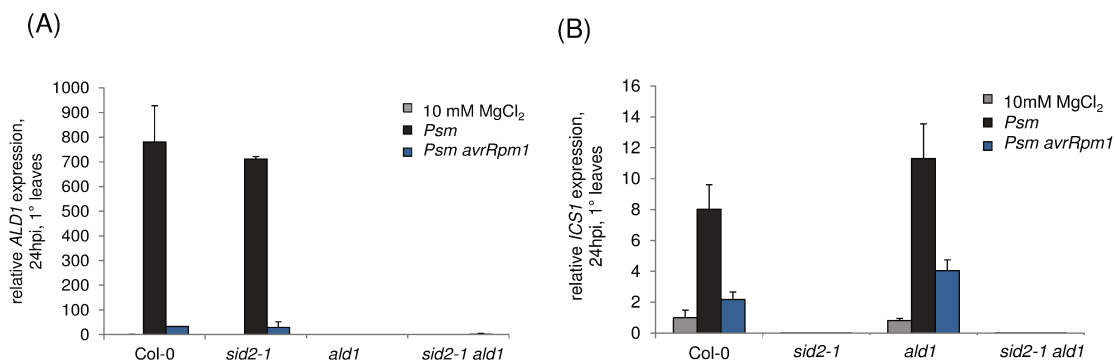
Figure 15. Relative *ALD1* **(A)** and *ICS1* **(B)** gene expression in local leaves of Col-0, *sid2-1*, *ald1* and *sid2-1 ald1* 24h after inoculation with 10mM MgCl$_2$, *Psm* and *Psm avrRpm*1. Transcript levels were assessed by quantitative real-time PCR analysis, are given as means ± SD of three replicate samples, and are expressed relative to the respective mock control value.

To uncover potential effects of the loss of SA, Pip or both metabolites on disease development and progression, we decided to measure the transcript accumulation of *PR-1* at different time points, during interaction with a virulent and an avirulent bacterial strain compared to the mock treatment in Col-0, *sid2-1*, *ald1* and *sid2-1 ald1*. The relative expression of *PR-1* following inoculation with *Psm* and *Psm avrRpm1* at 9, 16, 24hpi in the local and 24 and 48hpi in the distal leaves of Col-0, *sid2-1*, *ald1* and *sid2-1 ald1* illustrated the kinetics of defense gene expression after challenge with a virulent and an avirulent bacterial strain (Fig. 16). *PR-1* was strongly up-regulated in the early stages of defense against the avirulent HR-inducing pathogen *Psm avrRpm1* in Col-0 and *ald1*. The expression of *PR-1* was stronger between 16h and 24h post *Psm*-inoculation compared to *Psm avrRpm1* induced expression in Col-0 and *ald1*. While a systemic induction of *PR-1* expression was observed in Col-0 after 48h, it was completely absent in *ald1*.
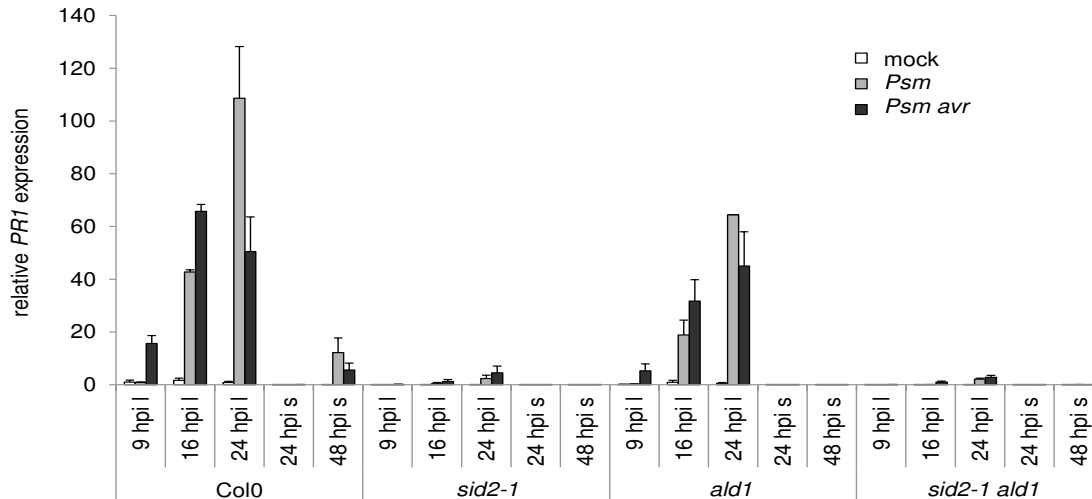
Figure 16. Relative *PR-1* gene expression in local (l) leaves after 9, 16, 24 h and in distal leaves (s) 24 and 48 h after inoculation with 10mM $MgCl_2$, *Psm* and *Psm avrRpm*1 (*Psm avr*) in Col-0, *sid2-1*, *ald1* and *sid2-1 ald1* plants. Transcript levels were assessed by quantitative real-time PCR analysis, are given as means ± SD of three replicate samples, and are expressed relative to the respective mock control value (in cooperation with A.-C. Döring).

This demonstrated that distal *PR-1* expression did also depend on Pip. *PR-1* expression was very low in the local leaves of *sid2-1* and no systemic induction was observed, as *PR-1* is a strongly SA-dependent defense gene. The *PR-1* expression level in *sid2-1 ald1* was similar to *sid2-1,* thus the *PR-1* expression was not suitable as indicator for altered disease kinetics due to the simultaneous loss of SA and Pip (Fig. 16).

To further characterize *sid2-1 ald1*, comparative amino acid and metabolite analysis were performed in Col-0, *ald1, sid2-1* and *sid2-1*. Leaves of Col-0, *sid2-1*, *ald1* and *sid2-1 ald1* were infiltrated with *Psm* or 10 mM $MgCl_2$ and levels of amino acids and SA measured two days after inoculation in the local and systemic leaves. In Col-0 Pip and SA accumulated strongly after pathogen attack, while pathogen induced SA or Pip accumulation was not observed in local and systemic leaves of *sid2-1 ald1*. This result confirmed the successful generation of a SA- and Pip- deficient double mutant (Fig. 17). Local accumulation of SA and Pip were not dependent on *ALD1* and *ICS1*, respectively (Fig. 17A+B). The basal levels of salicylic acid in *sid2-1* and *sid2-1 ald1* can be explained with a still functional *ICS2* gene in the mutants. However, since *ICS1* is the main contributor to pathogen induced SA accumulation, no accumulation was detected in *sid2-1 ald1* and *sid2-1* in local and systemic leaves two days after *Psm* inoculation (Fig 17A+C, Wildermuth et *al.*, 2001). Systemic accumulation of SA was only detectable in the wild type, emphasizing the importance of Pip-biosynthesis in the production of systemic SA (Fig. 17C). Pip accumulated significantly in the distal leaves of Col-0 and *sid2-1* plants two days after inoculation of *Psm* in the local leaves compared to the mock control (Fig. 17D). Hence, pathogen induced Pip accumulation in the

distal leaves was partially dependent on SA, as the reduced levels in *sid2-1* compared to the wild type show, but was still significantly elevated. This implied the existence of a SA-independent role of Pip in the distal leaf (Fig. 17D).
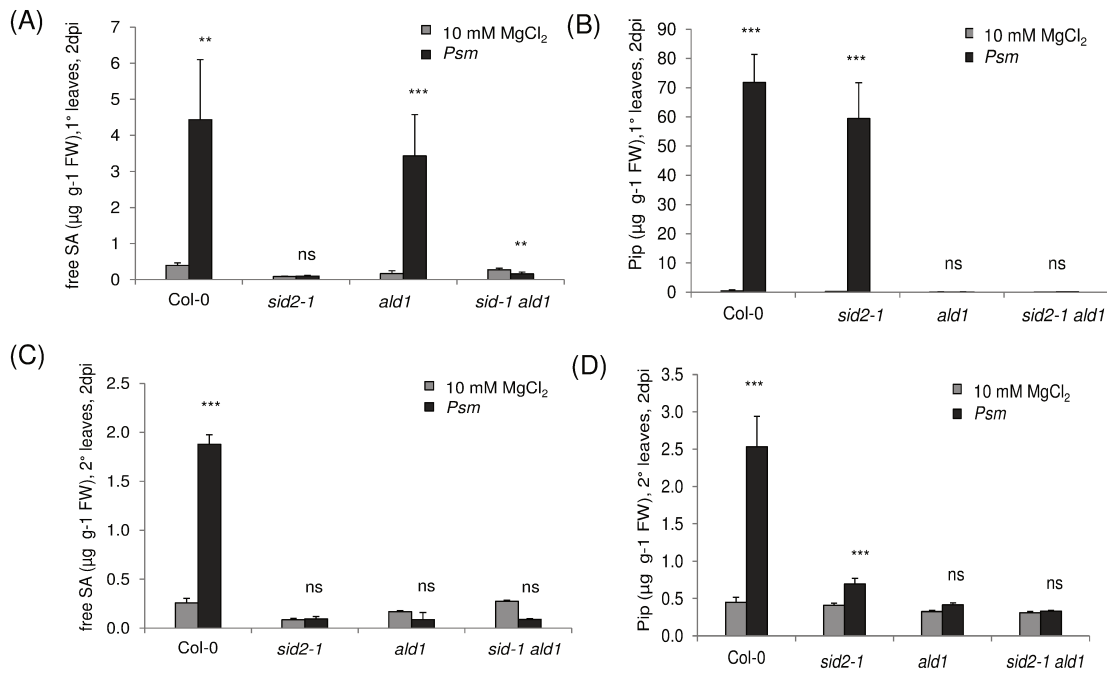
Figure 17. Local and systemic SA and Pip levels in local and systemic tissue. Accumulation of free SA **(A)** and Pip **(B)** in *Psm*-inoculated leaves and free SA **(C)** and Pip **(D)** in distal leaves of Col-0, *sid2-1 ald1* and *sid2-1 ald1* at two days after inoculation. Data represent the mean ± SD of three replicate samples. Asterisks denote statistically significant differences between MgCL$_2$ and *Psm* samples. (***: P< 0.001; **: P < 0.01; *: P < 0.05; ns = not significant; two-tailed *t* test). FW = fresh weight.

Other metabolites like the phytoalexin camalexin accumulated significantly higher in local leaves of *sid2-1, ald1 and sid2-1 ald1* compared to the wild type Col-0 upon pathogen attack. In *sid2-1,* camalexin showed the most prominent increase after pathogen attack compared to *ald1* and *sid2-1 ald1* (Fig. 18A). Local accumulation of camalexin was therefore independent of SA and Pip.
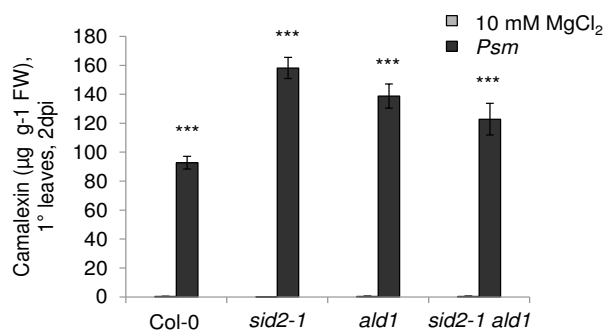
Figure 18: Accumulation of camalexin in *Psm*-inoculated leaves of Col-0, *sid2-1 ald1* and *sid2-1 ald1* two days after inoculation. Data represent the mean ± SD of three replicate samples. Asterisks denote statistically significant differences between MgCL$_2$ and *Psm* samples. (***: P< 0.001; **: P < 0.01; *: P < 0.05; ns = not significant; two-tailed *t* test). FW = fresh weight.

To further uncover regulatory principles of SA and Pip on the amino acid metabolism, we performed comparative amino acids analysis with Col-0, *sid2-1, ald1* and *sid2-1 ald1* one day after inoculation of *Psm* in the local leaves.

Like in the previously described experiments (Tab. 2+3), certain groups of amino acids were especially increased upon pathogen attack. In Col-0 aliphatic amino acids Val, Leu, Ile and aromatic amino acids Phe, Tyr and Trp alongside with Lys, Pip, Aad and Asn accumulated significantly after *Psm* inoculation (Tab. 4).

Levels of free amino acids after *Psm* inoculation in the local leaf were strongly affected in the SA-deficient mutant *sid2-1*. Aromatic amino acids Phe, Tyr, Trp, as well as Orn, Lys, Asn, Asp and Aad were significantly reduced while Ala was significantly increased in *sid2-1* compared to *Psm*-treated Col-0 leaves (Tab. 4). The absence of SA seemed to have not such a big impact on the metabolism of free amino acids in the local mock treated leaves, as only Lys and Tyr showed significantly reduced levels compared to Col-0. The loss of SA during pathogen attack had no effect on the accumulation of aliphatic amino acids Val, Leu, Ile, Pip, Pro, GABA, Gly, Glu and Gln. Comparing *Psm* against mock treated samples in *sid2-1* a significant increase of Ala, Leu, Ile, Aad, Phe and Tyr and a significant decrease of Asp, Glu and Orn was observed (Tab. 4).

Amino acid metabolism in the Pip-deficient *ald1* mutant showed a reduction during pathogen attack of the amino acids Asn, Orn and Tyr and an increase in Lys compared to levels in Col-0. The loss of Pip had no influence on basal amino acid levels in *ald1* compared to Col-0 mock samples. However, the amino acids Glu, Ala, Val, Leu, Ile, GABA, Glu, Asn, Lys, Phe, Tyr and Trp were significantly increased and Asp and Orn significantly decreased after *Psm* inoculation in *ald1* (Tab. 4).

μg g^{-1} FW	Amino acid accumulation 24hpi in the local leaves																		
	Col-0					sid2-1				ald1				sid2-1 ald1			
amino acid	MgCl₂	±	*Psm*	±	ratio P/M	MgCl₂	±	*Psm*	±	MgCl₂	±	*Psm*	±	MgCl₂	±	*Psm*	±
Gly	12.5	2.5	25.0	7.5	2.0	11.6	0.9	30.3	10.1	11.0	0.9	24.9	2.0	6.7	1.3	22.5	3.1
Ala	47.6	7.3	67.7	21.1	1.4	63.4	8.3	*151.2*	33.5	55.2	6.7	95.8	9.4	52.0	1.9	*148.1*	15.0
Val	3.4	0.3	23.0	5.6	6.7 ***	4.0	0.1	23.4	5.1	4.0	0.1	23.4	1.2	2.9	0.3	20.7	2.0
Leu	1.1	0.1	25.9	5.2	23.0 ***	0.9	0.2	17.5	4.5	1.0	0.1	19.7	0.6	0.6	0.1	*15.1*	1.3
Ile	1.2	0.1	13.47	2.4	11.9 ***	1.1	0.0	10.4	2.3	1.1	0.1	11.5	0.5	0.8	0.1	9.0	0.8
GABA	2.4	0.4	5.9	0.4	2.5 ***	2.2	0.1	5.0	1.8	1.9	0.1	*4.9*	0.5	1.2	0.4	*4.1*	0.4
Pro	13.4	3.0	10.0	3.5	0.8	17.9	1.5	11.2	2.5	16.1	2.1	11.8	1.0	15.0	0.6	13.5	2.9
Pip	0.6	0.1	13.6	2.9	23.4 ***	0.3	0.1	11.5	2.3	0.0	0.0	0.0	0.0	0.0	0.0	0.0	0.0
Aad	0.2	0.1	0.8	0.2	5.3 ***	0.1	0.0	*0.4*	0.1	0.0	0.0	0.4	0.2	0.0	0.0	*0.2*	0.0
Asp	425.4	91.9	293.4	46.8	0.7	273.4	18.1	*142.9*	23.2	372.1	15.3	209.3	21.5	361.1	45.5	*122.0*	6.4
Glu	216.4	46.4	246.8	52.3	1.1	153.1	13.3	*131.8*	34.4	168.6	14.4	199.5	6.1	164.8	18.0	*119.2*	4.0
Asn	13.3	2.6	30.5	3.8	2.3 ***	9.5	0.6	*15.2*	3.5	10.3	0.8	*20.6*	2.6	10.0	1.9	*12.4*	0.4
Gln	28.0	4.8	40.1	15.9	1.4	18.4	3.0	13.7	6.3	17.7	3.1	17.4	1.6	4.5	0.9	7.2	1.3
Orn	0.3	0.1	0.2	0.0	0.6	0.3	0.0	*0.1*	0.0	0.2	0.0	*0.1*	0.0	0.1	0.0	0.1	0.0
Lys	0.8	0.1	4.4	1.5	5.6 **	0.5	0.0	1.2	0.5	0.6	0.1	9.5	0.5	0.1	0.0	3.8	0.7
Phe	3.8	0.6	27.8	4.9	7.3 ***	3.0	0.0	*14.3*	3.4	3.1	0.1	19.3	1.0	2.4	0.4	*12.8*	0.7
Tyr	0.3	0.0	5.9	1.1	18.8 ***	0.2	0.0	*3.0*	0.8	0.2	0.0	*3.4*	0.3	0.1	0.0	*2.3*	0.1
Trp	0.1	0.0	0.4	0.1	6.3 ***	0.0	0.0	*0.1*	0.0	0.0	0.0	0.2	0.1	0.0	0.0	*0.1*	0.0

Legend:
- > 20
- 5 - 20
- 3 - 5
- 1.6 - 3
- 0.5 – 0.8
- < 0.5

Table 4. Changes in the levels of free amino acids in Arabidopsis Col-0, *sid2-1, ald1* and *sid2-1 ald1* Samples are given in μg g^{-1} fresh weight (FW) ± SD from at least three replicate samples. Mock-treatments were performed by infiltration of leaves with a 10 mM MgCl₂ solution. Light blue and yellow colored boxes indicate mutant mock values that are significantly reduced or increased, respectively, compared to the Col-0 mock value. Dark blue and red colored boxes indicate mutant *Psm* values that are significantly reduced or increased, respectively, compared to the Col-0 *Psm* value. Numbers in italic indicate significant changes in MgCl₂ mutant and the *Psm* mutant sample (P/M) of the respective mutant. (***: P< 0.001; **: P < 0.01; *: P < 0.05; two-tailed *t* test).

However, the simultaneous loss of SA and Pip had a massive impact on amino acid metabolism. Compared to amino acid levels in *Psm*-inoculated wild type leaves, a significant decrease was observed for almost all measured amino acids, except for Gly, Val, Ile, Pro and Lys that were not significantly changed. Like in *sid2-1* Ala levels were significantly higher in *sid2-1 ald1* compared to Col-0. In mock treated leaves of *sid2-1 ald1* levels of free amino acids like Gly, Leu, Ile, GABA and Aad, Gln, Orn, Lys, Tyr, Trp were as well significantly decreased. Although the levels of amino acids were in most cases strongly reduced compared to Col-0, there was still a significant increase of Gly, Ala, the aliphatic amino acids Val, Leu, Ile, GABA, Aad, Lys and the aromatic amino acids Phe, Tyr and Trp and significant decrease of Ala and Glu measured after *Psm*-inoculation compared to the mock treatment in

sid2-1 ald1 (Tab. 4). Lys, the possible precursor and substrate for *ALD1* over accumulated in *ald1*, but not in *sid2-1 ald1*. A possible reason could be a positive influence of SA on Lys biosynthesis, as Lys was significantly reduced in *sid2-1* after *Psm* inoculation compared with Col-0 (Tab. 4).

The results gave an impression about the impact of the loss of SA and Pip on the amino acid metabolism, but like in the other defense mutants we tested, the tendencies of amino acid metabolism that were observed after pathogen challenge compared to the mock-state, seemed to remain the same.

IV.2.5. SA AND PIP PROVIDE ADDITIVE CONTRIBUTIONS TO BASAL RESISTANCE

It is known that SA is crucial for the establishment of local resistance against *P. syringae*, as studies with SA-deficient mutants like *sid2-1/eds16* show severely enhanced basal susceptibility (Wildermuth et *al.*, 2001). Also many pathogen-responsive genes are regulated in an SA-dependent manner.

To test the impact of the simultaneous loss of SA and Pip on resistance, we conducted a local resistance assay measuring the bacterial growth two days after inoculation of *Psm* (OD 0.001). Basal bacterial growth was significantly higher in *sid2-1*, *ald1 and sid2-1 ald1* compared to Col-0. However, as observed in previous experiments, *sid2-1* was significantly more susceptible than Col-0 and *ald1* (Fig. 19). Interestingly the SA- and Pip-deficient mutant *sid2-1 ald1* showed a significant higher bacterial growth and overall increased basal susceptibility compared to Col-0, *ald1* and even *sid2-1* (Fig. 19).
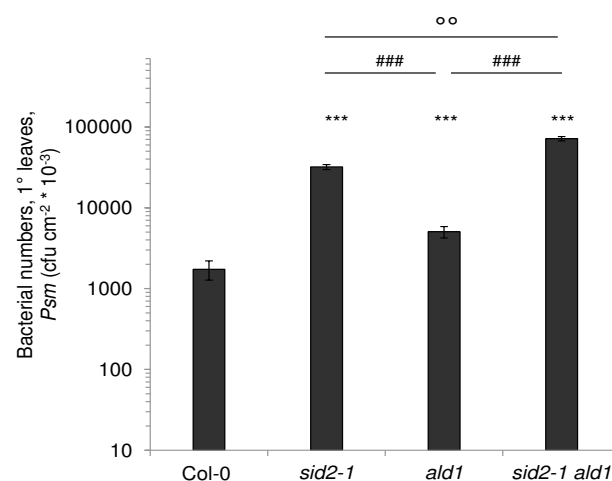
Figure 19. Additive contribution of SA and Pip to basal resistance against *Psm*. Local growth assay in Col-0, *sid2-1, ald1* and *sid2-1 ald1* mutants. Leaves were infiltrated *Psm* (OD 0.001) and bacterial growth in inoculated leaves was assessed three days after inoculation. Asterisks denote statistically significant differences to Col-0, hash keys and open circles denote statistically significant differences between indicated samples (***: P< 0.001; **: P < 0.01; *: P < 0.05; two-tailed *t* test).

From this result we concluded that SA plays an even more important role at the infection site and basal resistance than Pip and that Pip and SA have an additive effect on the establishment on basal resistance.

IV.2.6. PIP CONFERS SAR INDEPENDENTLY AND IN CONCERT WITH SA

SA is not only important for basal resistance, like Pip it is crucial for the establishment of systemic immunity in the plant (Vernooij et *al.*, 1994; Gaffney et *al.*, 1993).

We next tested whether the simultaneous loss of SA and Pip has an influence on the establishment of SAR. We conducted comparative systemic resistance assays with Col-0, *ald1*, *sid2-1, eds5 (ics2)*, *ics1 ics2* and *sid2-1 ald1*. For the SAR assays we first inoculated the local leaves with either 10 mM $MgCl_2$ or *Psm* (OD 0.005). The second inoculation of *Psm* (OD 0.001) followed two days later in the distal leaves and bacterial growth was measured after additional three days. Bacterial growth after pretreatment with *Psm* in distal leaves of Col-0 was reduced up to 12-fold, while *ald1* was fully attenuated in SAR (Fig. 20). In all SA-deficient mutants, *sid2-1*, *eds5*, *ics1 ics2* and *sid2-1 ald1*, a stronger bacterial growth in the $MgCl_2$-pretreated plants was observed compared to Col-0 and *ald1* (Fig. 20). Bacterial growth was significantly reduced in the distal leaves of *sid2-1* (1.5-fold growth reduction)*,* eds5 (2-fold growth reduction), *ics1 ics2 (*2-fold growth reduction) after pretreatment with *P. syringae* (Fig. 20). SA- and Pip deficient *sid2-1 ald1* was like *ald1* fully attenuated in SAR (Fig. 20).
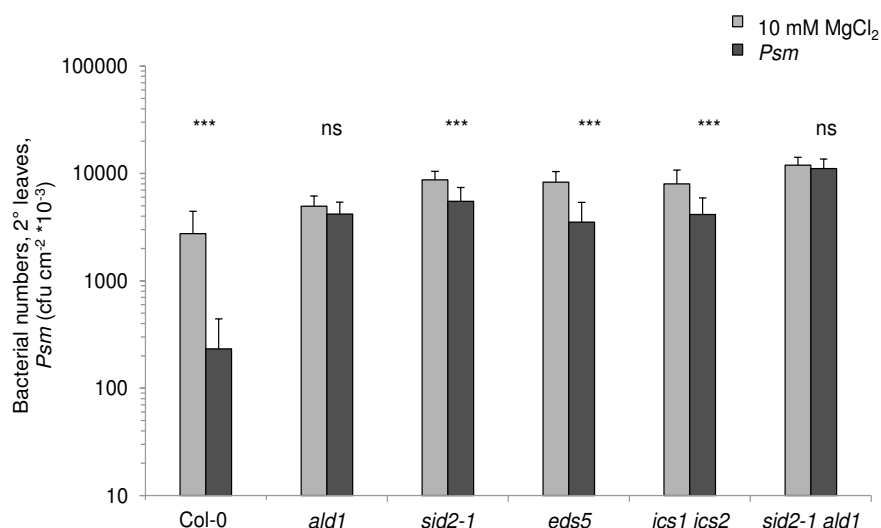
Figure 20. Pip confers partial SAR in the absence in SA. SAR assay in Col-0, *ald1*, *sid2-1*, *eds5*, *ics1 ics2* and *sid2-1 ald1* mutants. Lower (1°) leaves were infiltrated with either 10 mM MgCl$_2$ or *Psm* (OD 0.005), and two days later, three upper leaves (2°) were challenge infected with *Psm* (OD 0.001). Bacterial growth in upper leaves was assessed three days after 2° leaf inoculation. Asterisks denote statistically significant differences between MgCl$_2$ and *Psm* samples (***: P< 0.001; **: P < 0.01; *: P < 0.05; ns = not significant; two-tailed *t* test).

Pip was crucial for SAR establishment while SA was determining the strength of defense induction and was needed for a full SAR response (Fig. 20). SA-deficient mutants are able to establish a moderate, but significant SAR response and Pip and *ALD1* and *FMO1* transcripts accumulate significantly in the distal untreated leaves upon pathogen inoculation (Fig. 20).

IV.2.7. IDENTIFICATION OF THE SAR TRANSCRIPTOME REVEALS MECHANISMS AND DEFENSE STRATEGIES OF ARABIDOPSIS THALIANA AND THE ROLE OF SA AND PIP DURING SAR

The previously described results already indicated a shared role of SA- and Pip in the establishment of local defense and SAR.

To identify the reason for the SA-independent SAR, we performed two independent RNA-seq experiments. In RNA-seq experiment 1 including Col-0 and *sid2-1* (further referred to as SAR (1)) and RNA-experiment 2 including Col-0 and *ald1* (further referred to as SAR (2)) local leaves were inoculated either with 10 mM MgCl$_2$, or *Psm* with an OD of 0.005. After 48hpi the distal, non-treated leaves, were taken for RNA extraction. Samples were taken from three biological independent experiments and within each experiment three replicates were taken from 6 plants per treatment. The RNA was pooled afterwards and 2 µg were used for Illumina TruSeq™ RNA library preparation. Single end, 50 bp reads (SAR (1)) and 100 bp reads (SAR (2)), corrected according to Benjamini Hochberg for non-Gaussian distributed samples. A q-value of 0.01 was assumed and the threshold for a significant response was set to a fold change (log2) of >2, <-2. Bacterial growth reduction and metabolite accumulation in the distal leaves during SAR was controlled in all experiments used for the RNA-seq experiments. The transcriptional response of the distal leaf of Col-0 upon treatment with *Psm* in SAR (1) yielded 7441 and in SAR (2) 4832 significantly changed genes. Comparing the transcripts of both experiments, 3925 genes are common to both datasets (Fig. 21A). These 3925 genes were considered to be the core SAR genes in the distal leaf of Col-0 with 2057 up-regulated and 1868 down-regulated genes (Fig. 21A). In *sid2-1* the transcriptional response in the distal leaf was reduced. 717 of the core SAR genes and 989 total genes were changed upon *Psm* inoculation in the distal leaf (Fig. 21B). In SAR (2) only

two genes were significantly changed in the distal leaf of *ald1* upon pathogen attack, emphasizing the importance of *ALD1* and Pip for systemic defense gene responses (Fig. 21C).
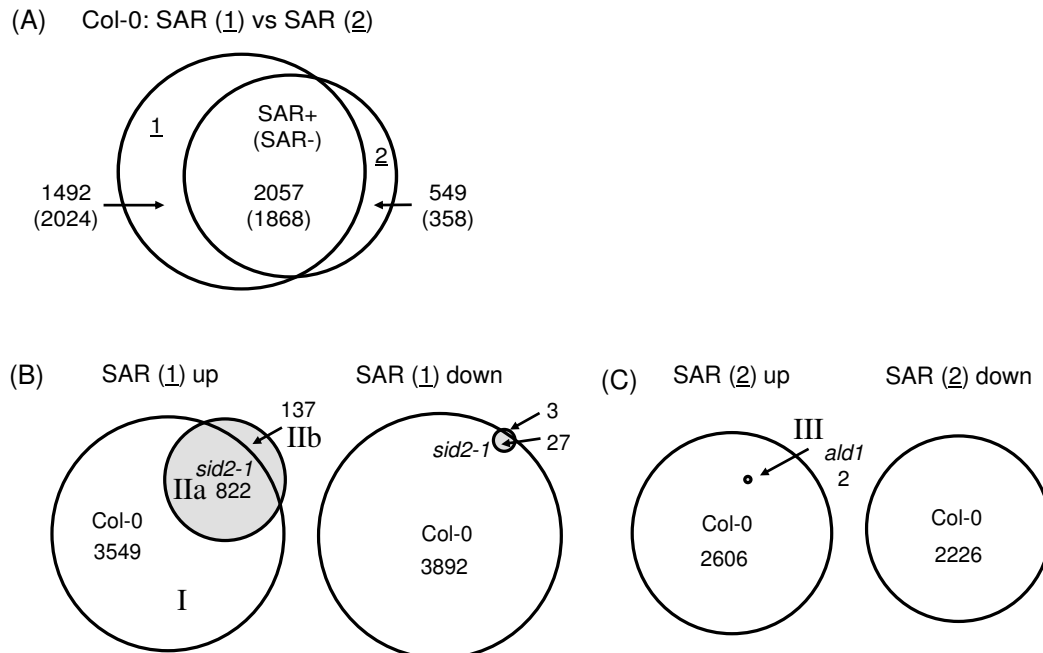
Figure 21. Venn diagram of differentially regulated genes in the distal leaf upon *Psm* challenge (FDR<0.01). **(A)** Genes in genes that are significantly up (SAR+) and down (SAR-) regulated in SAR (1) and (2) in Col-0. **(B)** Significantly regulated genes (up/down) in Col-0, *sid2-1* (SAR (1)) are grouped in three categories. Category Ⅰ includes all genes that are up-regulated in Col-0, category Ⅱa (grey) includes genes that are up-regulated in *sid2-1* and category Ⅱb (grey) includes genes that are in *sid2-1*, but not in Col-0 up-regulated. **(C)** Significantly regulated genes (up/down) of experiment SAR (2) in Col-0 and *ald1*. Significant regulated genes in *ald1* are grouped in category Ⅲ. (K. Gruner provided the RNA for experiment SAR (1) and the statistical analysis was done in cooperation with A. Bräutigam).

Comparing the distribution of SAR annotated transcripts of the two independent Col-0 experiments SAR (1) and (2) with the response in *sid2-1* and *ald1* it became clear, that the gene regulation was dependent on SA, but even stronger on Pip (Fig. 22A). Many genes still responded in *sid2-1*, but the magnitude of the response was smaller (Fig 22A). The response in *ald1* was very weak in up- and down-regulated genes, so we decided to compare the mean gene expression in *ald1* during SAR with randomly picked genes from the *ald1* P/M data set. A very faint response in expression of the up- and down-regulated SAR genes in *ald1* was still detectable (Fig. 22A+B).
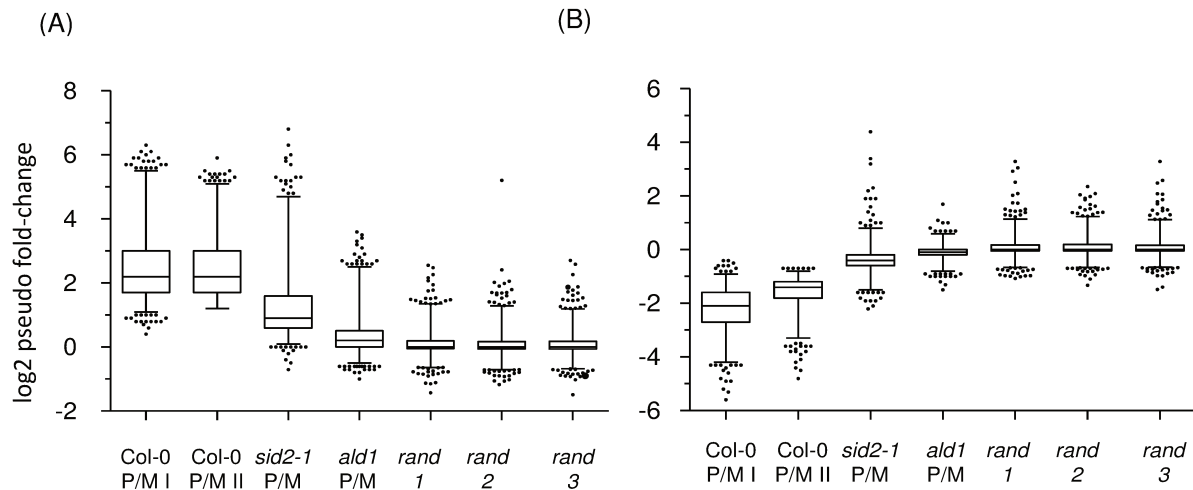
Figure 22. Distribution of SAR plus **(A)** and minus **(B)** annotated transcripts. Box plots show log2 normalized pseudo fold changes fold-changes of the SAR genes in the distal leaf of Col-0 (SAR (1) and (2), *sid2-1* and *ald1* two days after *Psm* inoculation compared to random sampling (rand 1, 2, 3) from the *ald1 Psm* against mock (*P*/M) data set (in cooperation with A. Bräutigam).

SA-dependent genes that were up-regulated during SAR in the distal leaf of Col-0 but not in *sid2-1* (Tab. 5, Fig. 21A) were grouped in category I. The mean expression values and fold change (log2) of genes in SAR (1) were sorted according to the highest fold change in Col-0 *P*/M. The fifteen genes with the highest fold-change in Col-0 in comparison with mean expression values and fold change of genes in *sid2-1* are displayed in table 5. Genes were up-regulated during SAR in Col-0 and *sid2-1*, but the basal level of gene expression was strongly dependent on SA, as the mean expression values were much lower in *sid2-1* mock (M) compared to Col-0 mock (M). The strength of expression upon pathogen attack strongly depended on SA (Tab. 5). The gene with the highest fold change in Col-0 *P*/M was the ACIDOREDUCTONE DIOXYGENASE 3 (*ARD3*). Moreover the list of SA-dependent SAR genes included e.g. the SA marker gene *PR-1*, *GRXS13*, *WRKY18* and a lysine/histidine transporter *LHT7*.

Category IIa genes consisted of genes that were up-regulated during SAR in the distal leaf in both, Col-0 and *sid2-1* and thus were considered to be SA-independent SAR genes. The mean expression values and fold change (log2) of genes in SAR (1) were sorted according to the highest fold change in *sid2-1 P*/M. The fifteen genes with the highest fold-change in *sid2-1*, in comparison with mean expression values and fold change of genes in Col-0, are displayed in table 6. The basal and pathogen-induced level of gene expression of category II genes was, like genes of category I, still dependent on SA, as the mean expression values were much lower in *sid2-1* compared to Col-0. Strikingly *ALD1* and *FMO1* were, together with the TYROSINE AMINOTRANSFERASE (*TAT3*), a marker for wounding

85

and JA (Yan et *al.*, 2007), among the most highly induced genes in the distal leaf of *sid2-1* *P*/M (Tab. 6).

				Mean Expression Value				Fold change* (log2)	
Pos.	AGI Code	Gene Name / Description	Abbrev.	Col-0 M	Col-0 *P*	*sid2-1* M	*sid2-1* *P*	Col-0 *P*/M	*sid2-1* *P*/M
1	At2g26400	ACIREDUCTONE DIOXYGENASE 3	ARD3	31.1	2604.8	2.2	2.7	6.3	0.2
2	At3g28510	AAA-type ATPase family protein	-	18.2	608.7	1.8	2.7	5.0	0.4
3	At1g66460	putative serine/threonine protein kinase	-	0.9	21.1	0.5	1.2	3.6	0.5
4	At3g53150	UDP-GLUCOSYL TRANSFERASE 73D1	UGT73D1	1.3	55.5	0.1	0.6	4.6	0.6
5	At3g22910	putative calcium-transporting ATPase 13	ACA13	8.3	442.8	1.6	3.1	5.6	0.6
6	At2g14610	PATHOGENESIS-RELATED PROTEIN 1	PR1	131.5	6808.3	6.0	10.3	5.7	0.7
7	At1g03850	GLUTAREDOXIN 13	GRXS13	7.8	175.8	2.7	5.2	4.3	0.7
8	At4g22592	conserved peptide upstream open reading frame 27	CPuORF27	4.4	62.3	2.9	5.5	3.6	0.7
9	At4g35180	LYS/HIS TRANSPORTER 7	LHT7	4.6	84.7	0.7	1.9	3.9	0.7
10	At2g32190	unknown protein	-	0.6	19.7	0.3	1.7	3.7	1.1
11	At3g14050	RELA-SPOT HOMOLOG 2	RSH2	20.5	283.7	16.0	36.6	3.7	1.1
12	At4g31800	WRKY DNA-BINDING PROTEIN 18	WRKY18	19.3	308.0	6.2	15.4	3.9	1.2
13	At1g64065	late embryogenesis abundant protein	-	4.2	71.9	3.2	10.0	3.8	1.4
14	At3g61190	BON ASSOCIATION PROTEIN 1	BAP1	3.6	87.2	1.2	5.8	4.3	1.6
15	At4g23190	RECEPTOR LIKE PROTEIN KINASE 3	RLK3	2.9	42.7	1.3	6.3	3.5	1.6

Table 5. Mean expression values and fold change (log2) of first 15 significantly up-regulated SA-dependent category I genes in the distal leaf upon *Psm* challenge in Col-0 and *sid2-1* in RNA-seq I sorted according to highest fold change in Col-0 *P*/M.

				Mean Expression Value				Fold change* (log2)	
Pos.	AGI Code	Gene Name / Description	Abbrev.	Col-0 M	Col-0 *P*	*sid2-1* M	*sid2-1* *P*	Col-0 *P*/M	*sid2-1* *P*/M
1	At2g24850	TYROSINE AMINOTRANSFERASE 3	TAT3	91.4	3554.9	11.1	1302.5	5.3	6.8
2	At2g13810	AGD2-LIKE DEFENSE RESPONSE PROTEIN 1	ALD1	18.3	523.7	0.8	140.2	4.8	6.3
3	At1g19250	FLAVIN-DEPENDENT MONOOXYGENASE 1	FMO1	3.7	201.6	0.4	84.3	5.4	6.0
4	At2g43570	putative chitinase	CHI	65.7	2496.7	3.7	286.4	5.2	5.9
5	At2g29460	GLUTATHIONE S-TRANSFERASE TAU 4	GSTU4	5.7	335.1	1.1	112.2	5.6	5.8
6	At3g09940	MONODEHYDROASCORBATE REDUCTASE 3	MDAR3	6.4	202.1	0.8	93.8	4.8	5.7
7	At1g54010	GDSL-LIKE LIPASE 23	GLL23	0.5	6.2	0.6	60.8	2.3	5.3
8	At1g02930	GLUTATHIONE S-TRANSFERASE 6	GSTF6	131.8	2278.8	14.7	596.6	4.1	5.3
9	At1g33960	AVRRPT2-INDUCED GENE 1	AIG1	84.4	3621.1	7.6	325.5	5.4	5.3
10	At3g57260	PATHOGENESIS-RELATED PROTEIN 2	PR2	191.2	3716.6	15.9	634.4	4.3	5.2
11	At3g22600	GPI-ANCHORED LIPID TRANSFER PROTEIN 5	LTPG5	16.4	945.8	1.2	81.1	5.8	5.2
12	At3g26830	PHYTOALEXIN DEFICIENT 3	PAD3	8.0	344.7	0.9	67.5	5.3	5.2
13	At2g38240	2–oxoglutarate-dependent dioxygenase superfamily	DOXC46	0.3	37.3	0.2	41.4	4.8	5.1
14	At2g29350	SENESCENCE-ASSOCIATED GENE 13	SAG13	33.6	1899.3	4.0	165.1	5.8	5.0
15	At1g57630	Toll-Interleukin-Resistance domain family protein	-	6.8	302.3	0.9	55.9	5.3	4.9

Table 6. Mean expression values and fold change (log2) of first 15 significantly up-regulated SA-independent genes in the distal leaf upon *Psm* challenge in Col-0 and *sid2-1* in RNA-seq I (category IIa) sorted according to highest fold change (log2) in *sid2-1* P/M.

Category IIb genes were defined as SA-independent genes that were up-regulated in *sid2-1*, but not up- or even down-regulated in Col-0 during SAR. Category IIb genes were sorted according to the highest fold change (log2) in *sid2-1* compared to Col-0 *P*/M (Tab. 7). Noteworthy was, that the basal level of gene expression was independent of SA, as the mean expression values for the mock samples were even higher in *sid2-1* compared to Col-0. Noticeably, the list contains genes that were clearly involved in JA biosynthesis like *ALLENE OXIDE SYNTHASE* (*AOS*) and *ALLENE OXIDE CYCLASE2* (*AOC2*) and signaling like *PLANT DEFENSIN1.2A/B* (*PDF1.2A/B*).

Pos.	AGI Code	Gene Name / Description	Abbrev.	Mean Expression Value				Fold change* (log2)	
				Col-0 M	Col-0 P	*sid2-1* M	*sid2-1* P	Col-0 P/M	*sid2-1* P/M
1	At2g43550	defensin-like protein 197	-	19.3	3.9	30.5	146.1	*-2.1*	*2.2*
2	At3g28220	TRAF-like family protein	-	26.4	7.2	31.2	686.5	*-1.7*	*4.4*
3	At2g26020	PLANT DEFENSIN 1.2B	PDF1.2B	6.6	1.6	2.6	15.9	-1.6	*2.2*
4	At1g52000	Mannose-binding lectin	-	16.9	5.0	33.4	306.8	*-1.6*	*3.2*
5	At5g02940	uncharacterized protein	-	107.8	36.3	148.3	464.3	*-1.5*	*1.6*
6	At4g18440	L-aspartase-like family protein	-	287.0	116.1	424.0	2972.3	-1.3	*2.8*
7	At4g13410	CELLULOSE SYNTHASE LIKE A15	CSLA15	4.1	1.4	2.6	95.5	-1.1	*4.7*
8	At4g24350	phosphorylase family protein	-	84.2	40.7	106.3	739.5	-1.0	*2.8*
9	At1g52040	MYROSINASE-BINDING PROTEIN 1	MBP1	4.4	1.7	6.0	71.4	-1.0	*3.4*
10	At5g42650	ALLENE OXIDE SYNTHASE	AOS	335.7	175.3	459.3	1684.3	-0.9	*1.9*
11	At5g44420	PLANT DEFENSIN 1.2A	PDF1.2	79.2	41.4	33.0	202.8	-0.9	*2.6*
12	At1g14250	GDA1/CD39 nucleoside phosphatase family protein	-	70.5	36.9	94.9	668.6	-0.9	*2.8*
13	At1g58270	TRAF-like family protein	ZW9	13.3	7.6	15.1	103.4	-0.7	*2.7*
14	At2g43530	defensin-like protein 194	-	23.9	14.3	28.6	293.5	-0.7	*3.3*
15	At3g25770	ALLENE OXIDE CYCLASE 2	AOC2	168.6	104.0	221.4	1201.9	-0.7	*2.4*

Table 7. Mean expression values and fold change (log2) of first 15 significantly up-regulated SA-independent genes in the distal leaf upon *Psm* challenge of *sid2-1*, but not in Col-0 in SAR (1) (category IIb) sorted according to highest fold change (log2) in *sid2-1* P/M.

We further checked for the percentage of JA responsive genes in the category IIb. A list of JA responsive genes was taken from NASCARRAYS-174 in which 7 day-old Col-0 seedlings grown in MS liquid medium under constant light at 22∘C were treated with 10 µM MeJA. The leaves were sampled 3 h after treatment (Goda et *al.*, 2008). After alignment of the 959 up-regulated genes in *sid2-1* with the list of JA responsive genes we could show that 12.5% of genes that were up-regulated in *sid2-1* were JA responsive (Tab. 8). Among the 959 up-regulated genes in *sid2-1*, 144 genes were down-regulated or not induced in Col-0. These genes up-regulated in *sid2-1*, but not up or even down-regulated in Col-0, consisted to 38.9% of JA responsive genes. The enrichment in JA responsive genes in the group of down-regulated genes in Col-0 during SAR was also shown by analyzing publicly available

microarray data. JA-responsive genes were down-regulated during SAR and up-regulated in the absence of SA (Gruner et *al.*, 2013).

category		# genes RNA-seq	% JA-inducible genes
whole genome		28496	2.0
Col-0 up	Fig. 21B (I)	3549	3.9
sid2-1 up	Fig. 21B (IIa)	959	12.5
sid2-1 up / Col-0 not up	Fig. 21B (IIb)	144	38.9

Table 8. Percentage of JA-regulated genes in SAR (1). Percentages were calculated among the whole genome, genes that are up-regulated during SAR in Col-0, genes that are up-regulated during SAR in *sid2-1* and genes that are up-regulated in *sid2-1*, but down-regulated during SAR in Col-0 (in cooperation with A. Bräutigam).

In experiment SAR (2) the mean expression values of significantly up-regulated genes in the distal leaf of *ald1* after pathogen challenge (P) were not higher compared to the expression of these genes in distal leaves of mock treated (M) wild type plants (Tab. 9). Although the transcriptional response in *ald1* during SAR was very weak; two genes, the *RECEPTOR-LIKE PROTEIN KINASE6* (*CRK6*) and *PLANT CADMIUM RESISTANCE1* (*PCR1*) were significantly up-regulated in SAR (2) and grouped in category III (Tab. 9 and Fig. 21C).

				Mean Expression Value				Fold change* (log2)	
Pos.	AGI Code	Gene Name / Description	Abbrev.	Col-0 M	Col-0 P	*ald1* M	*ald1* P	Col-0 P/M	*ald1* P/M
1	At4g23140	RECEPTOR-LIKE PROTEIN KINASE 6	CRK6	51	857	5	26	4.0	2.1
2	At1g14880	PLANT CADMIUM RESISTANCE 1	PCR1	84	2910	7	29	5.1	1.9

Table 9. Mean expression values and fold change (log2) of significantly up-regulated genes of category III in the distal leaf upon *Psm* challenge of Col-0 and *ald1* in RNA-seq II sorted according to highest fold change (log2) in *ald1* P/M.

To get an overview of affected metabolic pathways during SAR, the genes common to both datasets, significantly regulated in Col-0 were assigned to custom made MapMan categories (Fig. 23). The most obvious SAR response in the distal leaf was the down regulation of 77.5% of the genes that were involved in photosynthesis related processes. This included the Calvin Benson Bessham cycle, photosynthetic electron transfer chain and photorespiration. Furthermore, 43.5% of genes involved in tetrapyrrole synthesis, mainly

chlorophyll synthesis in leaf tissue, and in the major carbohydrate metabolism (-20.8%) were down-regulated. Anabolic pathways like N- (-16%) and S-metabolism (-16.7%) and synthesis of nucleotides (-15.6%), lipids (-14.3%) and secondary metabolites (-13.6%) were down-regulated to a lesser extent. Up-regulated categories included categories like redox (+12.6%), signaling (+15.8%), biotic stress (+12.8%), fermentation (+14.3%) and oxidative pentose phosphate (OPP) pathway (+15.4%; Fig. 23).
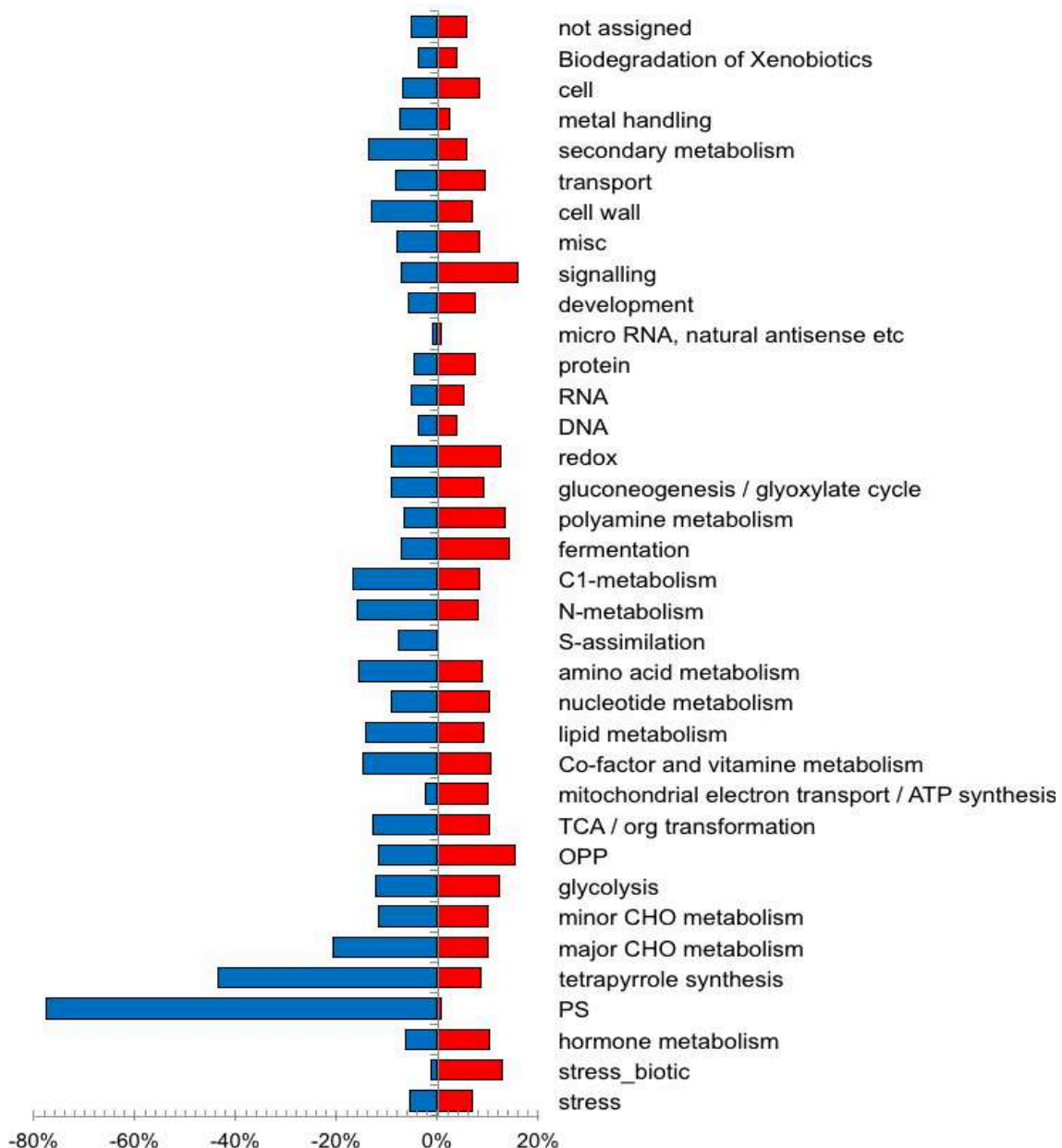
Figure 23. Relative expression changes of SAR genes in Col-0. Custom made MapMan bins (data set SAR 1+2) show relative changes of SAR genes to all genes in the respective category in the *Arabidopsis thaliana* genome (OPP= oxidative pentose phosphate pathway, PS= photosynthesis, CHO= carbohydrate, TCA= tricarboxylic acid cycle; in coorperation with A. Bräutigam).
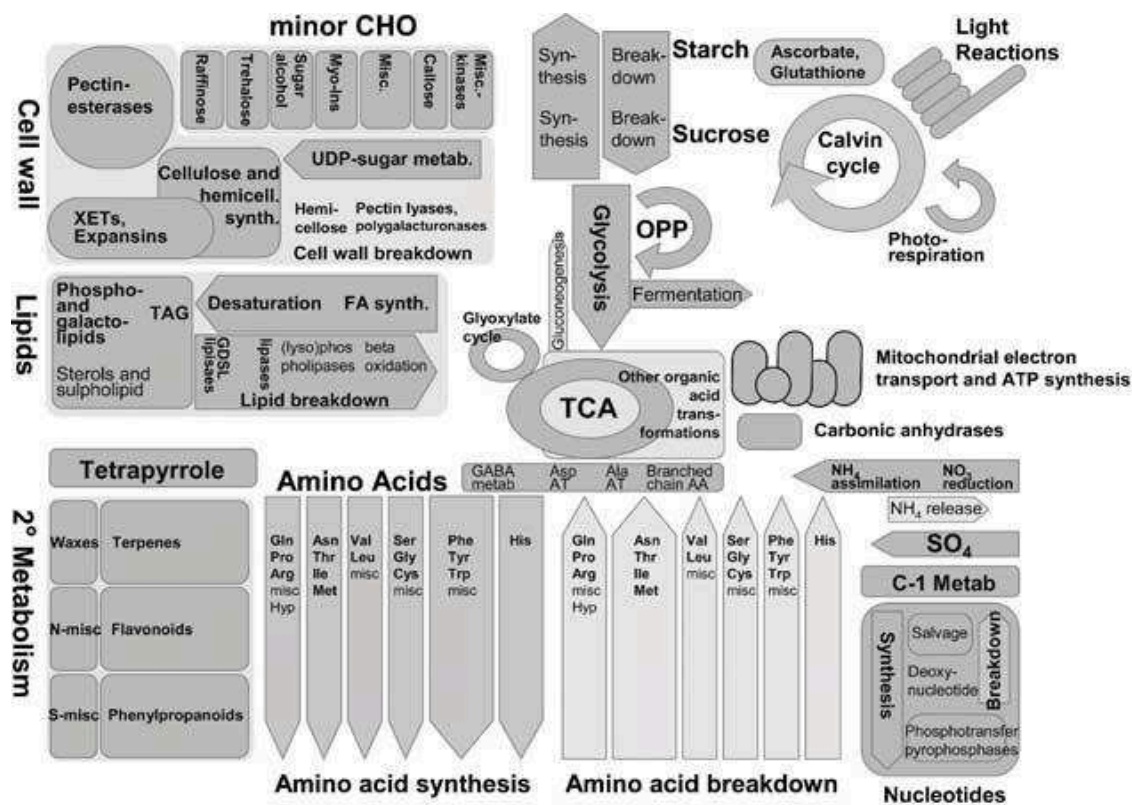
Figure 24. Overview display of genes assigned to metabolism. Explanation of the functional categories deposited at each location on the scheme (according to Thimm et *al.*, 2004).

For further visualization of gene expression patterns of the 3925 significantly regulated genes, common to both RNA-seq datasets, were assigned to MapMan (TAIR10) categories of central metabolic processes in the plant. An overview of MapMan functional categories (Fig. 24) visualized the changes in gene expression for every genotype and metabolic pathway. The photosynthesis apparatus was strongly down-regulated in Col-0 and was the most severely affected MapMan category during SAR in Col-0 SAR (1) and (2) (Fig. 25A + 26A). Comparing the expression patterns of all metabolic pathways in both Col-0 datasets SAR (1) and (2) the metabolic regulation during SAR seemed to be a highly robust and conserved mechanism, as the expression pattern was highly similar between the two RNA-seq experiments and MapMan categories (Fig. 25A + Fig. 26A). The response in *sid2-1* SAR (1) was reduced, but unlike *ald1* SAR (2) there was still some minor change in gene expression noticeable. The down regulation of photosynthesis and associated pathways was abolished in *sid2-1* and *ald1* (Fig. 25B + Fig 26B).
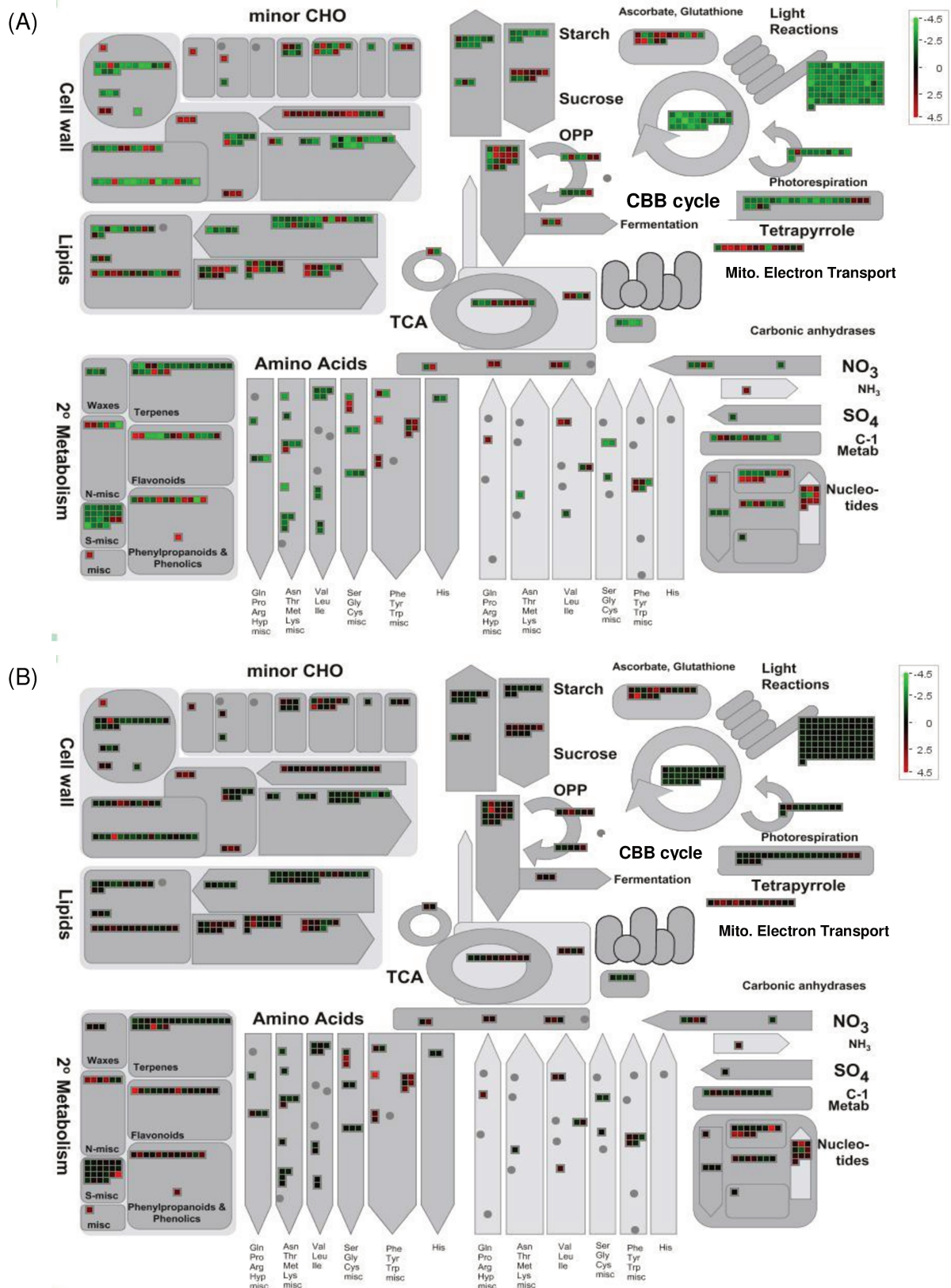
Figure 25. Overview of genes expression patterns as heatmaps in the central metabolism (Mapman, TAIR10) during SAR of the distal leaf. Heatmaps depict transcriptional fold changes (log2) during *Psm* versus mock conditions. Red (ratio>0) represent an increase and green (ratio<0) a decrease of transcript accumulation of Col-0 *P*/M (A) and *sid2-1 P*/M (B) in the SAR (1) data set.
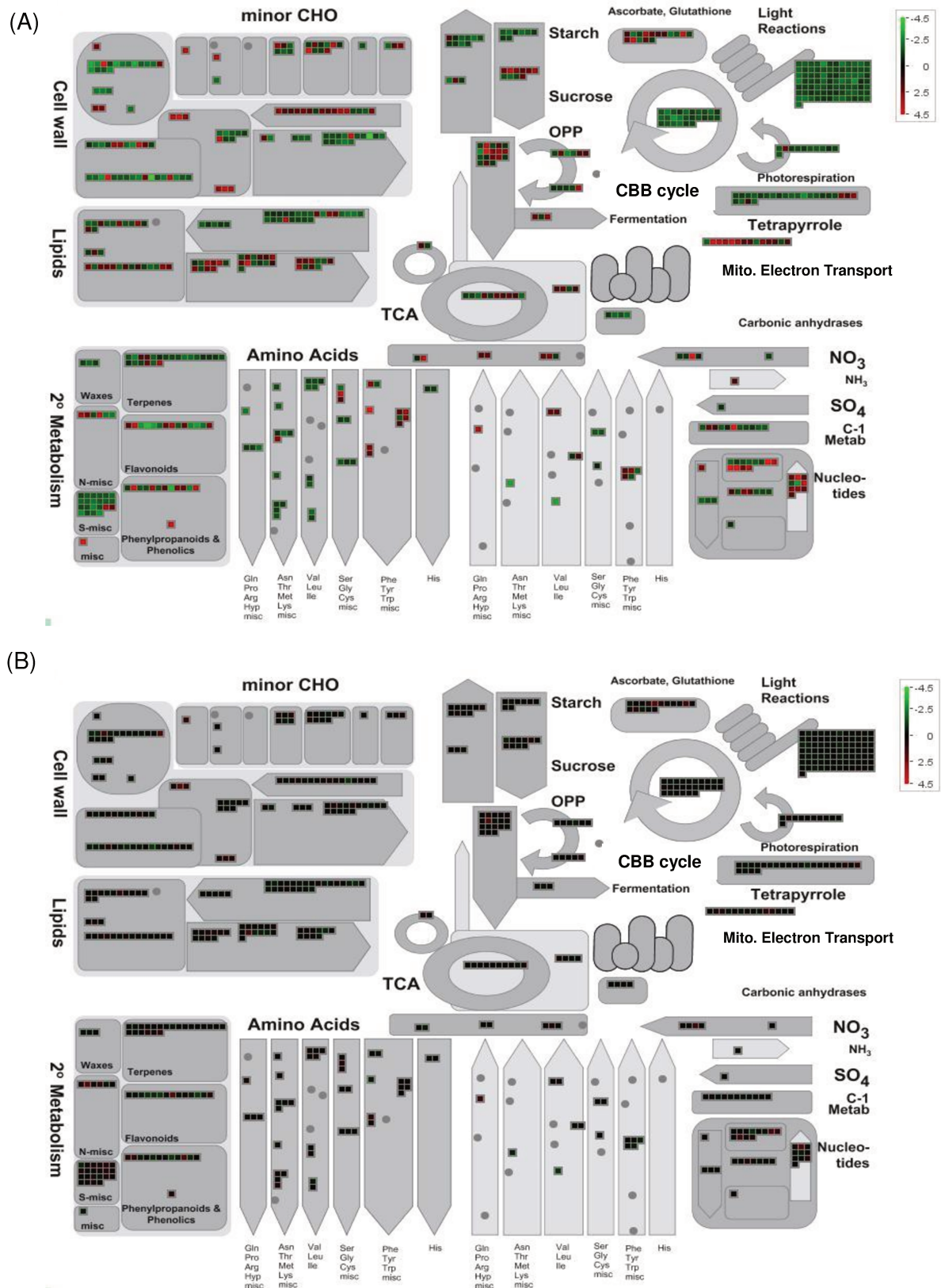
Figure 26. Overview of genes expression patterns as heatmaps in the central metabolism (Mapman, TAIR10) during SAR of the distal leaf. Heatmaps depict transcriptional fold changes (log2) during *Psm* versus mock conditions. Red (ratio>0) represent an increase and green (ratio<0) a decrease of transcript accumulation of Col-0 *P*/M (A) and *ald1 P*/M (B) in the SAR (2) data set.

The analysis of the SAR transcriptome revealed that compared to the unchallenged leaf, photosynthesis was the most severely changed process in Col-0. To investigate whether this was only a phenomenon on the transcript level, maximum photosynthesis by CO_2 uptake (CO_2 µmol m^{-2} s^{-1}) and transpiration rate (mmol H_2O m^{-2} s^{-1}) as measure for stomatal conductance was evaluated on intact leaves at 1000 µmol photons m^{-2} s^{-1} photosynthetic photon flux density (PPFD) using a LI-6400XT Portable Photosynthesis System. Arabidopsis Col-0, *sid2-1*, *ald1* and *sid2-1 ald1* plants were inoculated with *Psm* (OD 0.005) and two days later the photosynthetic and transpiration rate were measured in distal, untreated leaves. Photosynthetic and transpiration rate of distal leaves of pathogen challenged plants were compared to leaves of mock (10 mM MgCl₂) treated plants. A significant reduction in photosynthetic (Fig 27A) and transpiration rate (Fig. 27B) was observed in distal leaves of *Psm*-treated compared to mock-treated Col-0 plants. No significant difference could be observed between any of the treatments in *sid2-1*, *ald1* and *sid2-1 ald1* plants. This result was in line with the results of SAR (1) and SAR (2). The ability to reduce the photosynthesis and the transpiration rate during activated defense in the distal leaves was strongly SA- and Pip-dependent.
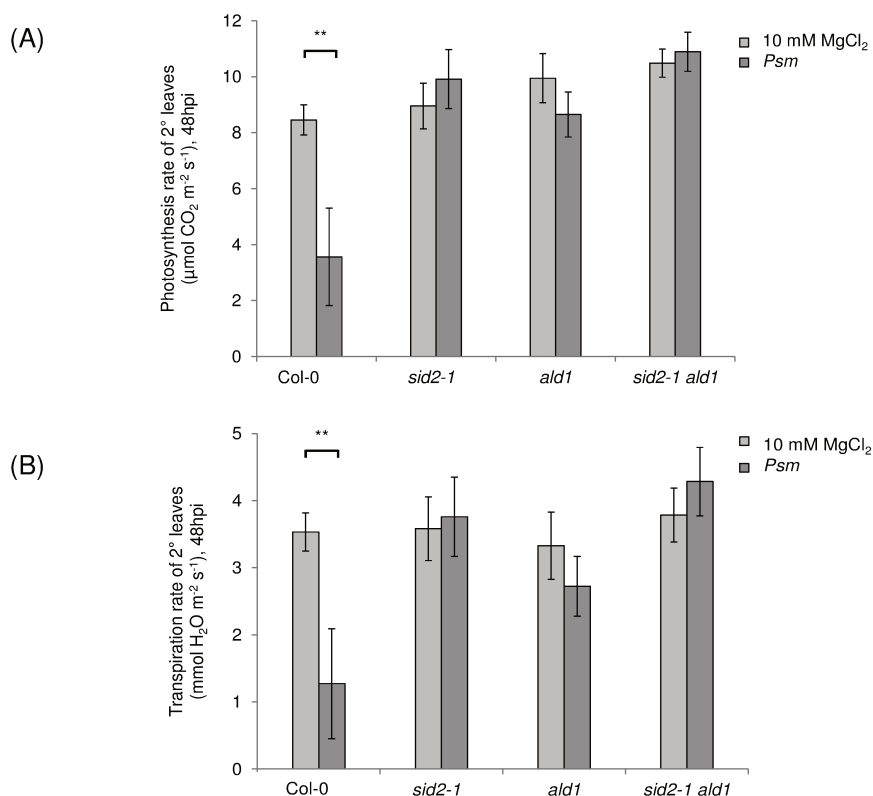
Figure 27. Maximum photosynthetic **(A)** and transpiration rate **(B)** 48h after *Psm* inoculation measured in the distal, untreated leaf of Col-0, *sid2-1*, *ald1* and *sid2-1 ald1* plants, compared to untreated and mock inoculated leaves measured with a LI-6400XT Portable Photosynthesis System. Asterisks denote statistically significant differences between MgCl₂ and *Psm* samples (***: P< 0.001; **: P < 0.01; *: P < 0.05; ns = not significant; two-tailed *t* test).

IV.2.8. BIOLOGICAL PRIMING OF CAMALEXIN ACCUMULATION DEPENDS ON SA AND PIP

Priming was defined as a long-lasting phenomenon of plant immunity that allows a quick and robust response of cells to very low levels of a stimulus, compared to non-primed cells. Local and systemic defense responses are faster and stronger activated in primed plants upon a subsequent pathogen challenge and plants are more tolerant towards infections (Jung et *al.*, 2009; Návarová et *al.*, 2012). It was shown that the production of camalexin is independent of SA and even higher in *sid* mutants compared to Col-0 after inoculation with virulent *Psm* and *P. s. tomato* DC3000 carrying *avrRpt2* (Fig. 17A; Nawrath et *al.*, 1999).

We conducted biological priming experiments to examine the impact of SA and Pip on the production of the phytoalexin camalexin, total levels of SA and defense gene expression during defense priming induced by biological SAR. In the experimental set-up a first inoculation of the local leaves (1°) was carried out with either 10 mM $MgCl_2$ or *Psm* (OD 0.005), followed by a second inoculation of 10 mM $MgCl_2$ or *Psm* (OD 0.005) in the distal leaves (2°) 48h later. 10 hours after the second treatment, distal leaves (2°) were harvested and metabolites analyzed to assay the early defense response. Four different regimes were analyzed: the control situation (1° $MgCl_2$/ 2° $MgCl_2$), the systemic response (1° *Psm* / 2° $MgCl_2$), the local response (1° $MgCl_2$/ 2° *Psm*) and the combined treatment (1° *Psm* / 2° *Psm*).

In our definition a primed state (P) existed when the response of gene expression, total SA or camalexin accumulation was stronger after the combined treatment (1° *Psm* / 2° *Psm*) as the sum of the local (1° $MgCl_2$/ 2° *Psm*) and the systemic response (1° *Psm* / 2° $MgCl_2$). In Col-0 the camalexin production was moderately increased after the local, compared to the systemic stimulus, but the production of camalexin was boosted upon a combination of a *Psm* inoculation in 1° and 2° leaves and thus strongly primed (Fig. 28A). In *sid2-1* the accumulation of camalexin during the systemic response was diminished and only increased after application of *Psm* in the treated leaves. As there was no further increase upon a combined *Psm* inoculation in the local and systemic leaves, camalexin was not primed in *sid2-1* (Fig. 28A). The Pip-deficient *ald1* mutant showed the same response in camalexin accumulation than *sid2-1*. Camalexin was only produced following a local stimulus and not further elevated upon a first *Psm* inoculation in lower leaves (Fig. 28A). This suggested that priming of camalexin was dependent on both, SA and Pip. Interestingly, camalexin production was completely absent in *sid2-1 ald1*, suggesting that with the loss of

SA and Pip camalexin production was fully inhibited and that SA and Pip was responsible for the local camalexin production observed in *ald1* and *sid2-1*, respectively.
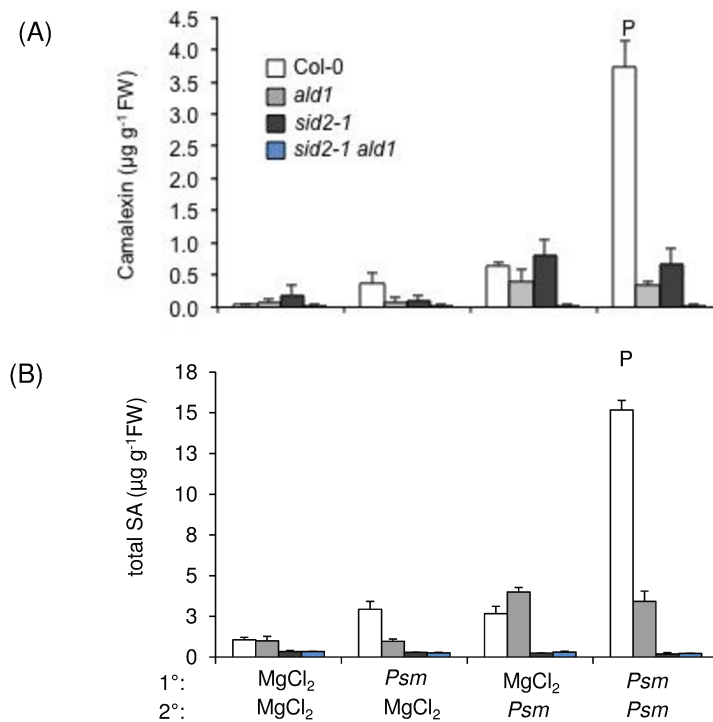
Figure 28. Biologically induced priming of defense metabolites depends on Pip and SA.
Double inoculation experiment to assess defense priming during SAR in Col-0, *ald, sid2-1, and sid2-1 ald1* plants were treated in lower (1°) leaves with 10 mM $MgCl_2$ or *Psm* (OD 0.005), and two days later, upper (2°) leaves were infiltrated with 10 mM $MgCl_2$ or *Psm*. Upper leaves were then scored for defense metabolite accumulation or defense gene expression at 10 h after inoculation. Four different regimes were analyzed corresponding to a control situation (1° $MgCl_2$/2° $MgCl_2$), a systemic pathogen stimulus (1° *Psm* /2° $MgCl_2$), a local pathogen stimulus (1° $MgCl_2$/2° *Psm*), and a combination of both the systemic and the local stimuli (1° *Psm* /2° *Psm*).
SAR priming (P) of defense metabolite accumulation. Camalexin **(A)** and total SA **(B)** accumulation at 10 h after 2° treatment. Bars represent the mean ± SD of at least three replicate samples. FW, fresh weight. (P < 0.05, two-tailed *t* test).

In Col-0 the production of total SA, the sum of free SA and glycosidic bound SA, was locally and systemically increased to similar levels during biological priming compared to the control situation. The combination of a local and systemic *Psm* inoculation triggered an SA production that exceeded the sum of SA, produced after a local and a systemic stimulus and thus was primed in Col-0 (Fig. 28B). The production of free and bound SA in SA-deficient *sid2-1* and *sid2-1 ald1* was very low and not induced upon pathogen attack in the local or the systemic leaves (Fig. 28B). Measuring the amount of total SA in *ald1* revealed that SA did not accumulate upon a systemic response compared to the control situation. The levels of total SA increased upon a local stimulus, but did not increase further upon a combined inoculation of *Psm* in the local and the systemic leaves of *ald1* (Fig. 28B).

This demonstrated that *ald1* was not able to establish, as observed for camalexin, a priming of SA. This result highlighted the importance of Pip for the establishment of systemic accumulation and priming of SA during SAR.

To test whether other defense related genes involved in basal and systemic defense against bacterial pathogens also play a role in biological priming, we used *eds1-2*, *fmo1* and *pad4* mutants together with Col-0 in the described double inoculation experiment. Lipase-like proteins EDS1 and its interaction partner PAD4 are both required for the interaction with TIR-NB-LRR *R*-genes. EDS1 is required to regulate RPP1-, RPP4-, RPP5, RPP21 and RPS4-mediated resistance to the biotrophic oomycete *Peronospora parasitica*, and to *Pseudomonas* bacteria expressing the avirulence gene *avrRps4* (Aarts et *al.*, 1998; Coppinger et *al.*, 2004). Biological priming of camalexin was not as prominent in Col-0 as observed in the previous experiment (Fig. 29). The local camalexin production in Col-0 was much stronger and the sum of the local and systemic trigger did not differ significantly from the production after a combination of local and systemic trigger (Fig. 29). However, priming of camalexin and production in the local and systemic leaves after inoculation of *Psm*, was strongly dependent on EDS1, FMO1 and PAD4. Like in the *ald1* mutant, priming of camalexin production was absent in *eds1-2*, *fmo1* and *pad4* mutants (Fig. 29).
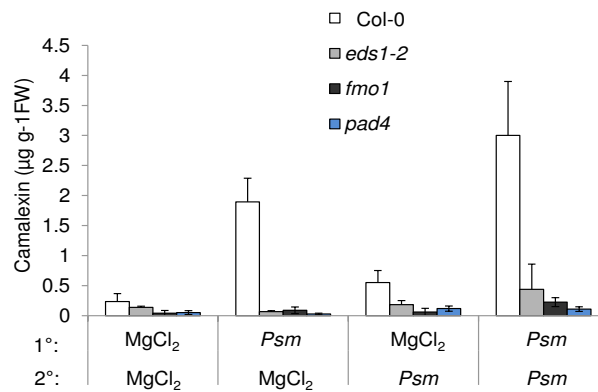
Figure 29. Biological SAR primes plants for camalexin accumulation in an *EDS1-*, *NPR1-* and *PAD4-*dependent manner. Double inoculation experiment to assess defense priming during SAR in Col-0, *eds1-2, fmo1* and *pad4*. SAR priming (P) of defense metabolite Camalexin at 10 h after 2° treatment: Plants were treated in lower (1°) leaves with 10 mM $MgCl_2$ or *Psm* (OD 0.005), and 2 d later, upper (2°) leaves were infiltrated with 10 mM $MgCl_2$ or *Psm*. Upper leaves were then scored for defense metabolite accumulation or defense gene expression at 10h after inoculation. Four different regimes were analyzed corresponding to a control situation (1° $MgCl_2$/2° $MgCl_2$), a systemic pathogen stimulus (1° *Psm* /2° $MgCl_2$), a local pathogen stimulus (1° $MgCl_2$/2° *Psm*), and a combination of both the systemic and the local stimuli (1° *Psm* /2° *Psm*). Bars represent the mean ± SD of at least three replicate samples. FW, fresh weight (P < 0.05, two-tailed *t* test).

In the SAR state, plants show elevated levels of *PR* gene expression and activated immune responses as direct protection against a possible second pathogen attack (Sticher et al. 1997). Biologically induced SAR primes the plants for systemic accumulation and biosynthesis of defense associated *PR* genes upon a subsequent pathogen attack (Jung et al. 2009). As published by Zeier and colleagues defense genes involved in SAR can be grouped into SA-dependent, SA-independent genes and partially SA-dependent genes (Gruner et al., 2013).

To study the regulation of defense priming of SAR-genes, genes of SA-dependent, SA-independent and partially SA-dependent categories were selected. To test whether the selected representatives of these groups were involved in biological priming of defense gene expression, transcript accumulation was measured in Col-0, *ald1, sid2-1* and *sid2-1 ald1*. Zeier and colleagues defined SA-dependent genes as genes up-regulated by SA whose local expression upon *Psm*-treatment were severely compromised in *sid2-1* and thus dependent on endogenous SA (Gruner et al., 2013). Genes of this category are for example *ARD3* and *PR-1* and selected for defense gene priming. SA-independent SAR genes are independently expressed from SA that showed a strong up-regulation upon *Psm* inoculation. Genes selected from this category are *FMO1*, *ALD1* and *SAG13*. Partially SA-dependent genes, like *GRXS13* that we used for defense priming studies, are grouped into a third category that mainly consisted of genes partly requiring *SID2/ICS1* for *Psm*-induced expression or of genes not locally up-regulated by *Psm* at 24 hpi (Gruner et al., 2013). The experimental set up was the same described for biological priming of total SA and camalexin (Fig. 28).

SA-independent genes *FMO1, ALD1* and *SAG13* were primed during biologically activated SAR in Col-0 (Fig. 30A, B and C). In *sid2-1 FMO1* priming was even more pronounced (Fig. 30A), whereas *ALD1* was equally (Fig. 30B) and *SAG13* weaker (Fig. 30C) primed compared to Col-0. The systemic (1° *Psm* / 2° $MgCl_2$) induction of *FMO1* and *ALD1* gene expression was, however, weaker or absent in *sid2-1* mutants compared to Col-0 (Fig. 30A and B). Naturally no expression of *ALD1* was observed in the Pip-deficient mutant *ald1* and *sid2-1 ald1* (Fig. 30B). Priming of *FMO1* and *SAG13* was strongly dependent on Pip in the systemic leaves, as expression levels were only elevated after a local (1° $MgCl_2$/ 2° *Psm*) response in *ald1* mutants. The partially SA-dependent gene *GRXS13* was strongly primed during biological SAR in Col-0 and also in *sid2-1*, but noticeable weaker (Fig. 30D). Priming of *GRXS13* was not only dependent on SA, but also on Pip in the systemic leaves, as *GRXS13* expression was only induced after a local *Psm* inoculation and not after a systemic trigger in *ald1* (Fig. 30D). *GRXS13* was not expressed at all in *sid2-1 ald1*, which indicated the importance and interplay of Pip and SA for induction and priming of defense gene expression. The SA-dependent defense genes *ARD3* and *PR-1* were both primed upon

biologically activated SAR in Col-0 (Fig. 30E+F). Noteworthy was that the systemic response of the *PR-1* expression was much stronger compared to the local stimulus in Col-0 10 hours upon pathogen challenge. As expected, *ARD3* and *PR-1* were not expressed in SA-deficient mutants and priming was dependent on a functional Pip-biosynthesis, since gene expression in *ald1* was only observed after a local stimulus (Fig. 30E+F).
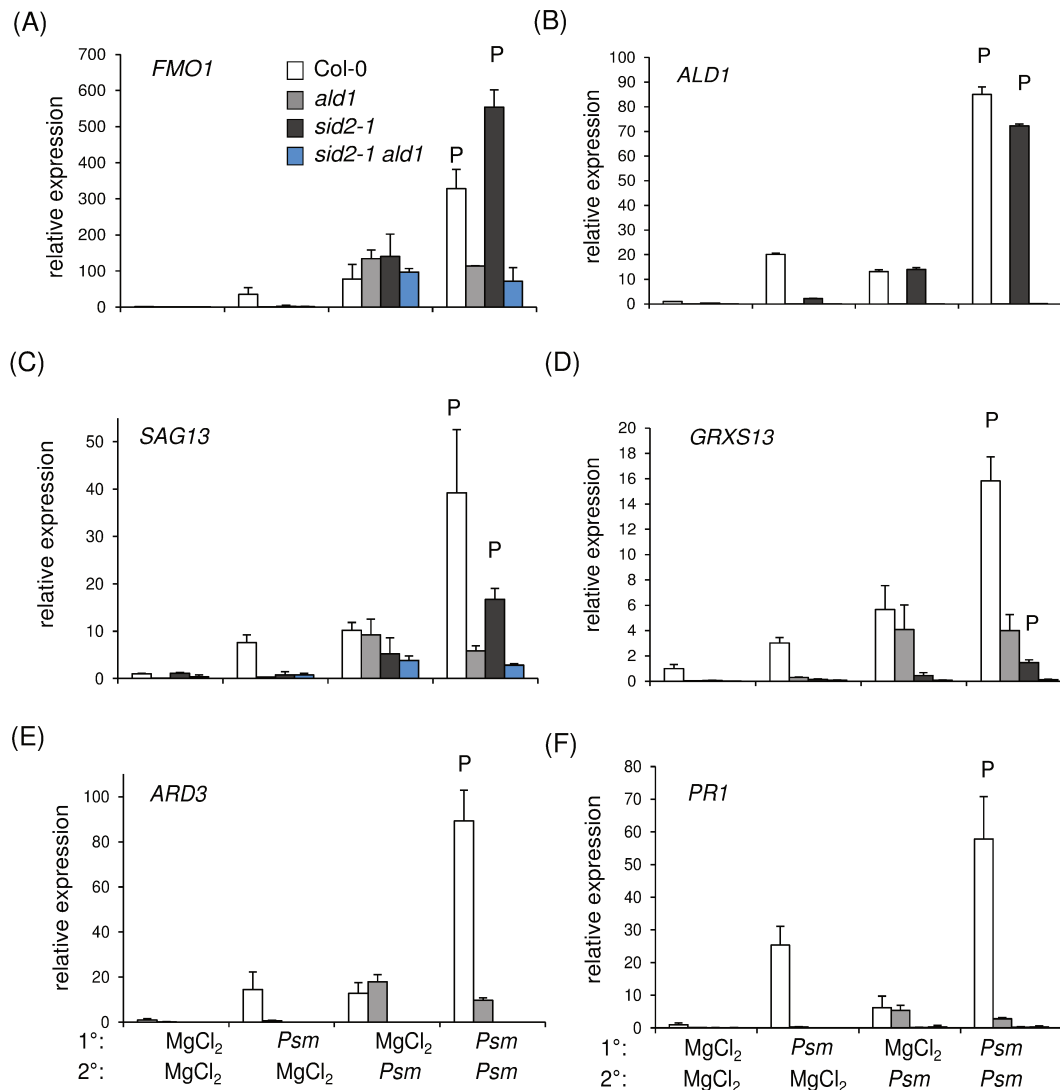
Figure 30. Biological SAR confers defense priming on the gene expression level in a Pip- dependent manner.

Double inoculation experiment to assess defense priming during SAR in Col-0, *sid2-1, ald1 and sid2-1 ald1* Plants were treated in lower (1°) leaves with $MgCl_2$ or *Psm* (OD 0.005), and 2 d later, upper (2°) leaves were infiltrated with $MgCl_2$ or *Psm*. Upper leaves were then scored for defense metabolite accumulation or defense gene expression at 10h after inoculation. Four different regimes of Pip-induced resistance were analyzed: the control situation (1° $MgCl_2$/2° $MgCl_2$), a systemic pathogen stimulus (1° *Psm* /2° $MgCl_2$), a local pathogen stimulus (1° $MgCl_2$/2° *Psm*), and a combination of both the systemic and the local stimuli (1° *Psm* /2° *Psm*).

SAR priming (P) of gene expression of SA-independent defense genes *FMO1* **(A)**, *ALD1* **(B)** and *SAG13* **(C)** and SA-dependent defense genes *GRXS13* **(D)**, *ARD3* **(E)** and *PR-1* **(F)** 10 h after 2° treatment. Bars represent the mean ± SD of at least three replicate samples (P < 0.05, two-tailed *t* test; in coorperation with A.-C. Döring).

Taken together the biological activated priming during SAR was dependent on SA and Pip. Whereas SA seemed to have an important role for the gene expression in the local leaf, priming was only conferred in the presence of Pip, as Pip deficient mutants did not show any defense gene priming. Therefore, endogenous Pip was crucial for induced resistance and priming of defense genes during SAR.

IV.2.9. EXOGENOUS PIP RESTORES PRIMING OF CAMALEXIN PRODUCTION AND DEFENSE GENE EXPRESSION IN PIP AND SA DEFICIENT MUTANTS

Endogenous Pip is crucial for the establishment of metabolite and defense gene priming. As described by Zeier and colleagues, exogenous Pip induces SA biosynthesis and strongly potentiates *Psm*-triggered camalexin production in *ald1* (Návarová et *al.* 2012).

To test whether exogenous Pip treatment would increase *Psm*-triggered defense responses in SA- and Pip-deficient mutants and induce priming, Pip was applied exogenously to Col-0, *ald1*, *sid2-1* and *sid2-1 ald1*. The experimental set-up differed from the biological priming experiment, as Pip, or water as a control, were applied exogenously to the soil one day before the inoculation of *Psm* or 10 mM $MgCl_2$ in leaves of Col-0, *ald1*, *sid2-1* and *sid2-1 ald1*. Samples for metabolite analysis or gene expression analysis were taken ten hours after leaf inoculation. Four different regimes of Pip-induced resistance were analyzed compared to the control situation wM (1° water / 2° $MgCl_2$): wP (1° water / 2° *Psm*) = *Psm*-induced responses, PM (1° Pip / 2° $MgCl_2$) = Pip-induced responses and PP (1° Pip / 2° *Psm)* = *Psm*-induced responses. According to our definition of priming, Pip-induced priming (P) existed, when the response of gene expression and camalexin accumulation was stronger after the combined treatment (PP), as the sum of the *Psm*-induced resistance (wP) and Pip-induced resistance (PM).

In Col-0 the production of camalexin was primed upon Pip- and *Psm*- induced resistance. The accumulation of camalexin in the wild type was stronger after *Psm*-inoculation in the leaf than Pip-application to the soil. Interestingly priming of camalexin was restored in *ald1*, *sid2-1* and *sid2-1 ald1* (Fig. 31), but the levels of camalexin were lower compared to camalexin accumulation in Col-0. *Psm*-induced camalexin production was stronger in *sid2-1* compared to Col-0, *ald1* and *sid2-1 ald1* (Fig. 31). During biological priming *sid2-1 ald1* completely lacked the ability to induce production and priming of camalexin upon a biological stimulus, but exogenous Pip restored the ability of camalexin production in SA- and Pip-deficient mutants (Fig. 31).
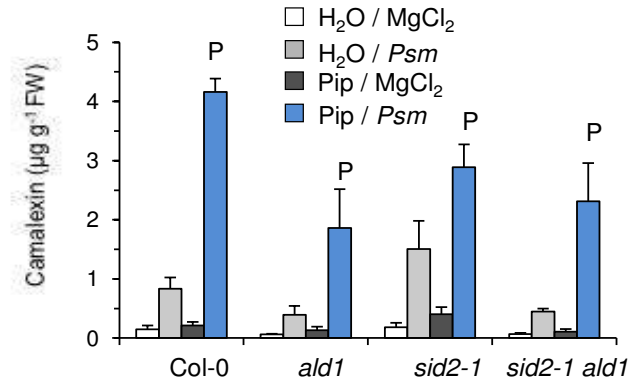
Figure 31. Exogenous Pip induces priming (P) of camalexin production.
Exogenous application of 10 mL of 1 mM ($\equiv$ 10 µmol) Pip or water one day prior to infiltration of *Psm* (OD 0.005). Samples of inoculated leaves for metabolite analysis were taken ten hours after inoculation from Col-0, *sid2-1, ald1 and sid2-1 ald1* plants. Four different regimes of Pip-induced resistance were analyzed: the control situation (1° water/ 2° $MgCl_2$), *Psm*-induced resistance (1° water / 2° *Psm*), Pip-induced resistance (1° Pip / 2° $MgCl_2$) and Pip- and *Psm*-induced resistance (1° Pip / 2° *Psm*). Bars represent the mean ± SD of at least three replicate samples. FW, fresh weight ($P < 0.05$, two-tailed *t* test).

We further analysed the Pip induced priming of defense gene expression. Pip promotes *ALD1* and *FMO1* expression in Col-0 and was responsible for establishment of *ALD1* and *FMO1* priming (Fig. 30A+B). We tested *FMO1, ALD1* and *PR-1* gene expression in Col-0, *ald1, sid2-1* and *sid2-1 ald1* in a Pip-induced priming experiment.

Upon exogenous Pip application and *Psm*-inoculation expression of *FMO1* was primed in Col-0, but also in *ald1, sid2-1* and *sid2-1 ald1* (Fig. 32A). While priming in *ald1* and *sid2-1 ald1* was strongly reduced, the expression of *FMO1* after Pip- and *Psm*-treatment exceeded the expression observed in Col-0 (Fig. 32A). Therefore, *FMO1* priming depended strongly on endogenously produced Pip and a functional *ALD1* gene (Fig. 32A). Like in the biological priming experiment *ALD1* expression was primed in Col-0 and *sid2-1* plants (Fig. 32B). *Psm*-induced (1° water / 2° *Psm*) *ALD1* expression was stronger compared to the Pip-induced (1° Pip / 2° $MgCl_2$) *ALD1* expression in *sid2-1* (Fig. 32B). Priming of *PR-1* was restored with exogenous application of Pip in Col-0 and *ald1*, but strongly dependent on SA (Fig. 32C). Taking a closer look, however revealed that Pip did induce a small priming response of the SA-dependent marker gene *PR-1* in *sid2-1* and *sid2-1 ald1*, however the expression level was very low (Fig. 32D).
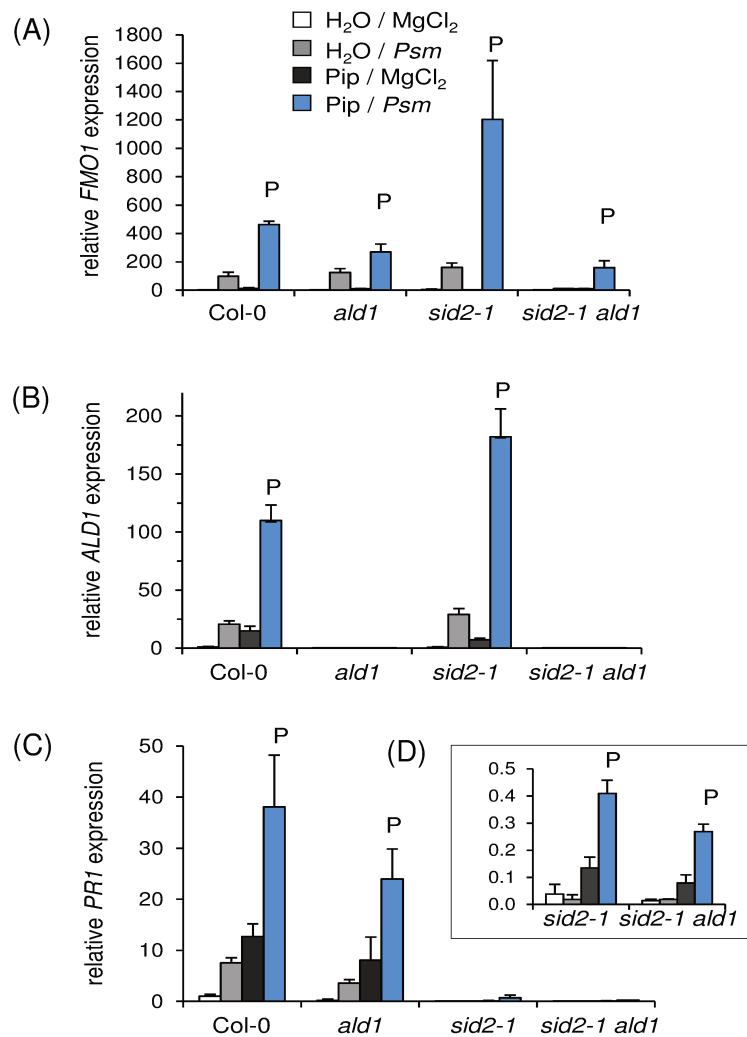
Figure 32. Pip- and *Psm*-induced priming (P) of defense gene expression. Exogenous application of 10 mL of 1 mM ($\equiv$ 10 µmol) Pip or water to Col-0, *sid2-1*, *ald1* and *sid2-1 ald1* plants one day prior to infiltration with either *Psm* or 10 mM $MgCl_2$. Relative *FMO1* **(A)**, *ALD1* **(B)** and *PR-1* **(C+D)** expression at 10 hpi after the 2° infiltration. Transcript levels were assessed by quantitative real-time PCR analysis, are given as means ± SD as the three replicates, and are expressed relative to the respective mock control value. Four different regimes of Pip-induced resistance were analyzed: the control situation (1° water/ 2° $MgCl_2$), *Psm*-induced resistance (1° water / 2° *Psm*), Pip-induced resistance (1° Pip / 2° $MgCl_2$) and Pip- and *Psm*-induced resistance (1° Pip / 2° *Psm*). (P < 0.05, two-tailed *t* test, in coorperation with A.-C. Döring).

FMO1 is an important SA-independent SAR regulator located downstream of Pip biosynthesis. Pip over accumulated in *fmo1* mutants and SAR was not restored upon exogenous Pip application (Fig. 5A + Fig. 7). Exogenous Pip restored priming of *FMO1* and *PR-1* expression, camalexin and SA production in Col-0 and *ald1* and the capacity to systemically enhance SA levels upon localized pathogen inoculation (Návarová et *al.* 2012). Furthermore, exogenous Pip treatment led to an accumulation of SA in local and systemic leaves of 10 mM $MgCl_2$ infiltrated plants, suggesting that Pip alone was not sufficient to activate, but that it positively regulated SA biosynthesis.

We wanted to investigate the effect of exogenous Pip on *ALD1* and *PR-1* gene expression, camalexin and total SA production in *fmo1* mutants. Upon exogenous Pip treatment, *ALD1* and *PR-1* were primed in Col-0 plants (Fig. 33A and B), but *ALD1* expression was only triggered after *Psm*-inoculation in *fmo1* and Pip was not able to establish priming of *ALD1* expression in *fmo1* (Fig. 33A). Expression of *PR-1* was triggered neither after Pip application, nor after *Psm* inoculation, indicating that *fmo1* plants lack the systemic stimulus that triggers *PR-1* expression and priming (Fig. 33B). *FMO1* was responsible for the induction of the SA-marker gene *PR-1* and camalexin biosynthesis (Fig. 33B and C). Camalexin accumulation and priming after exogenous Pip application was almost absent in *fmo1*, compared to the strong priming in Col-0, which emphasized the importance of *FMO1* for a functional Pip-signaling pathway and Pip-induced defense priming (Fig. 33C).
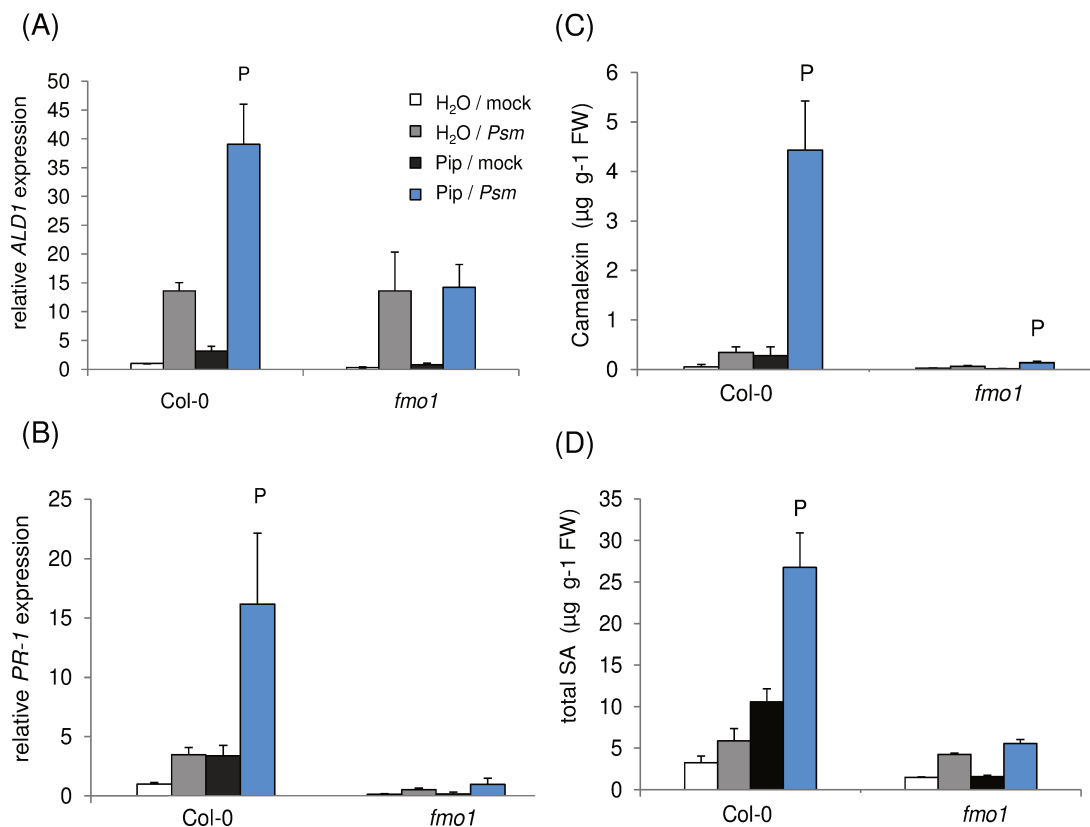
Figure 33. Pip- and *Psm*-induced priming (P) of defense gene expression, camalexin and total SA production depends on *FMO1*. Exogenous application of 10 mL of 1 mM ($\equiv$ 10 μmol) Pip or water to Col-0 and *fmo1* plants one day prior to infiltration with either *Psm* or 10 mM MgCl$_2$. Relative *ALD1* **(A)**, *PR-1* **(B)** expression, camalexin **(C)** and total SA **(D)** accumulation at 10 hpi after the 2° infiltration. Transcript levels were assessed by quantitative real-time PCR analysis, are given as means ± SD as the three replicates, and are expressed relative to the respective mock control value. Four different regimes of Pip-induced resistance were analyzed: the control situation (1° water/ 2° MgCl$_2$), *Psm*-induced resistance (1° water / 2° *Psm*), Pip-induced resistance (1° Pip / 2° MgCl$_2$) and Pip- and *Psm*-induced resistance (1° Pip / 2° *Psm*). (FW = fresh weight; P < 0.05, two-tailed *t* test; in coorperation with A.-C. Döring).

IV.2.10. *COMBINED TREATMENT OF EXOGENOUS SA AND PIP PRIMES DEFENSE GENE EXPRESSION*

To further uncover the relationship and action mode of SA- and Pip- induced defense, *PR-1* gene expression was monitored after simultaneous treatment of Pip and SA, compared to the single treatments of either exogenous Pip, or SA-treatment and the control situation. *PR-1* is a marker gene for SA accumulation (Wildermuth et *al.*, 2001) and is primed after biological induced SAR (Fig. 30F). Pip, or water as a control were applied exogenously one day before the 0.5 mM SA or water treatment of leaves of Col-0, *ald1*, *sid2-1*, *sid2-1 ald1*, *pad4, fmo1 and npr1*. Samples of leaves were taken for gene expression analysis four hours after SA/water treatment. Four different regimes of Pip- and SA-induced responses were analyzed: the control situation (1° water/ 2° water), SA-induced responses (1° water / 2° SA), Pip-induced responses (1° Pip / 2° water) and responses triggered by the simultaneous elevation of both Pip and SA (1° Pip / 2° SA).

In Col-0, *PR-1* gene expression was stronger induced upon SA-infiltration in the leaf compared to Pip application (Fig. 34A). Pip application alone did not trigger such a strong induction of *PR-1* expression, but after a combination of Pip and SA, *PR-1* expression was primed in Col-0 (Fig. 34A). In *ald1, PR-1* priming was established upon Pip application and SA-infiltration. Exclusive SA-infiltration did not induce *PR-1* expression as strongly in *ald1* as in Col-0, suggesting that a functional Pip biosynthesis was required for full expression (Fig. 34A). In *sid2-1* and *sid2-1 ald1 PR-1* expression was triggered after SA-infiltration and priming of *PR-1* was restored upon Pip-treatment and SA-infiltration, but exogenous Pip alone did not induce expression (Fig. 34A). The increase in *PR-1* transcript levels after SA-infiltration was, like in *ald1*, not as strong as in the wild type (Fig. 34A). SA-infiltration, but not exogenous Pip induced *PR-1* expression in *fmo1* mutants (Fig. 34B). Priming of *PR-1* expression depends on a functional *FMO1*/Pip-signaling pathway to let the systemic signal go through to the primed leaves. *PR-1* priming was also tested in *pad4* mutants that exhibited a priming response upon Pip- and SA-treatment, but no induction of *PR-1* gene expression after sole Pip-application (Fig. 34B). *NPR1* is functioning upstream of *PR-1* in the SA-signaling pathway and without a functional *NPR1* gene, no SA- or Pip-derived signal was going through to activate *PR-1* expression, showing that *NPR1* acts downstream of Pip, too (Fig. 34B).
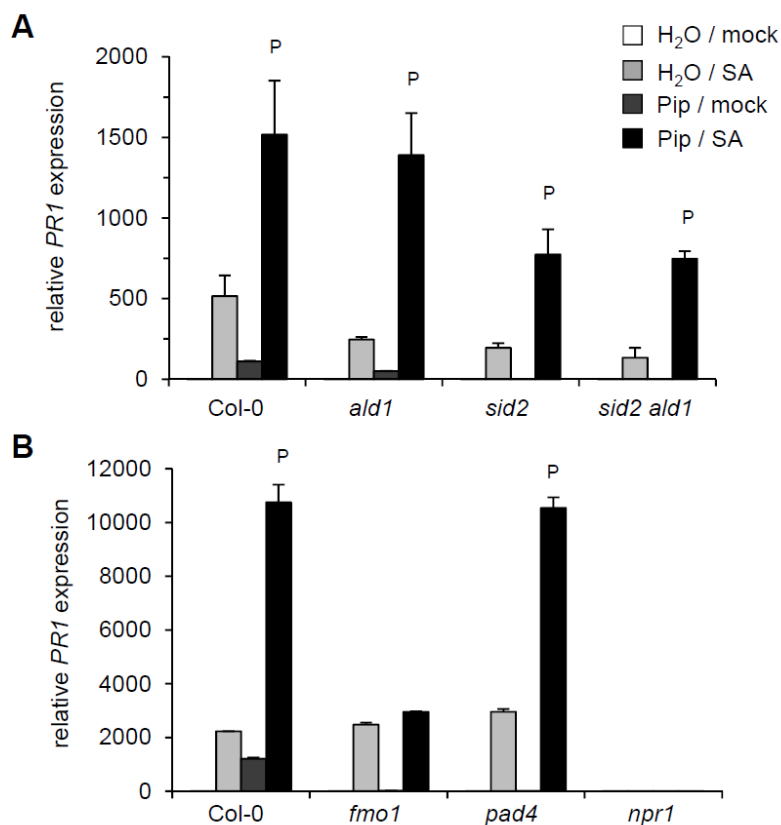
Figure 34. Pip- and SA-induced priming (P) of *PR-1* expression depends on *FMO1* and *NPR1*. *PR-1* expression was measured in Col-0, *ald1*, *sid2* and *sid2-1 ald1* **(A)** and Col-0, *pad4*, *fmo1* and *npr1* **(B)** plants that were supplied with 10 mL of 1 mM ($\equiv$ 10 µmol) Pip or water one day prior to infiltration with either 0.5 mM SA (pH 7) or water. Relative *PR-1 expression* was measured at 4 hpi after infiltration. Transcript levels were assessed by quantitative real-time PCR analysis, are given as means ± SD as the three replicates, and are expressed relative to the respective mock control value. Four different regimes of Pip-induced resistance were analyzed: the control situation (1° water/ 2° water), *Psm*-induced resistance (1° water / 2° SA), Pip-induced resistance (1° Pip / 2° water) and Pip- and *Psm*-induced resistance (1° Pip / 2° SA). (P < 0.05, two-tailed *t* test).

To conclude the results presented in this chapter, we have strong evidence for a scenario in SAR establishment, in which Pip and *FMO1* were needed in the distal leaf to establish SAR in the first place.

IV.3. FURTHER CHARACTERIZATION OF THE PIP-BIOSYNTHESIS AND -SIGNALING PATHWAY AND AMINO ACID HOMEOSTASIS DURING DEFENSE IN ARABIDOPSIS THALIANA

IV.3.1. SUBCELLULAR LOCALIZATION OF ALD1 AND FMO1

IV.3.1.1. Introduction

Upon bacterial pathogen recognition, Pip is produced via the Lys aminotransferase AGD2-LIKE DEFENSE RESPONSE PROTEIN1 (*ALD1*), and accumulates independently of SA in inoculated leaves as well as in leaves distal from the site of inoculation. Pip amplifies plant defense responses such as SA accumulation, camalexin production, defense gene expression and primes systemic defense responses in plants. Strikingly, a specific and strong enrichment of Pip in petiole exudates collected from pathogen-inoculated leaves was detected. This indicates specific transport of Pip out of inoculated leaves and, possibly, long-distance transport to distal leaves during SAR. The resistance enhancing ability of Pip requires the function of the downstream component FLAVIN-DEPENDENT MONOOXYGENASE1 (*FMO1*), which is also a critical SAR component. Recent metabolite analyses suggest that the *FMO1* monooxygenase converts Pip into an oxidized derivative and thereby transduces the Pip signal (Návarová et *al.*, 2012; Zeier, 2013).

The close homolog of *ALD1*, *AGD2* (ABERRANT GROWTH AND CELL DEATH 2) *AGD2* (At4g33680) encodes a LL-diaminopimelate aminotransferase (LL-DAP-AT) in plants that operates in the forward/biosynthetic direction towards Lys, directly converting THDPA into LL-DAP (Hudson et *al.*, 2006). *AGD2* was annotated as a 461-amino acid, class I/II family aminotransferase and the first 36 amino acids were predicted by TargetP to be a transit peptide for localization of the protein to plastids (Hudson et *al.*, 2006). The full-length protein of *AGD2* was fused to *gfp* under the control of the 35S promoter of *Cauliflower mosaic* virus (CaMV). This construct complemented the *agd2-1* mutant and the GFP fluorescence patterns in Arabidopsis protoplasts colocalized with the red autofluorescence patterns of the chloroplasts (Song et *al.*, 2004a). The chloroplast localization of *AGD2*-GFP is consistent with its role in amino acid synthesis, since many amino acids are synthesized in the chloroplasts (Bryan, 1990).

The main function of chloroplasts is to carry out photosynthesis, despite other roles such as biosynthesis of fatty acids, aromatic and several nonaromatic amino acids, isoprenoids, and tetrapyrroles. Plastids retain a functional genetic system, but their genome encodes only about 100 different proteins, meaning that most plastid localized proteins have

to be imported to be then assembled into active metabolic complexes (Jarvis, 2004; Froehlich, 2011). Chloroplasts consist in total of six distinct suborganellar compartments including two envelope membranes, the internal thylakoid membrane and three aqueous compartments: the intermembrane space of the envelope, the stroma and the thylakoid lumen (Jarvis, 2004). Approximately 3,000 proteins are estimated to be targeted to the chloroplasts with the help of an amino-terminal targeting signal, or transit peptide (Froehlich 2011; Bruce et *al.*, 2001). Mis-targeting of chloroplast precursor proteins might be cytotoxic, so it is indispensable to sort the proteins specifically to avoid transport into other organelles like mitochondria, peroxisomes and the endoplasmic reticulum (ER). It could be expected that the secondary structural motif of chloroplast transit peptides is highly conserved, but on the contrary it is highly heterogenic and the shares almost no sequence similarity among peptides. This is the reason why so far no consensus targeting sequence or secondary structure has been identified (Bruce et *al.*, 2001, Jarvis, 2004). Stromal-targeting domains may vary in length from 30 to 100 amino acids and are rich in serine and threonine but deficient in acidic amino acids (Keegstra et *al.*, 1989). Complete translocation of proteins into the stroma requires the oligomeric Toc (Translocon at the outer envelope membrane of chloroplasts) protein complex and the inner envelope membrane (IEM) via the oligomeric Tic protein complex (Translocon at the inner envelope membrane of chloroplasts; Kovács-Bogdán et *al.*, 2010; Froehlich, 2011).

IV.3.1.2. Subcellular localization of ALD1

To identify the subcellular sites of Pip production and catabolism was of special interest to contribute to a better understanding of Pip transport at the cellular and whole plant level. The TargetP1.1 algorithm predicted the presence of an N-terminal chloroplast transit peptide for *ALD1* and a localization of *FMO1* in the secretory pathway. Lys biosynthesis is thought to take place in the chloroplast, since a compartmentalization of dihydrodipicolinate synthase (DHPS) within the chloroplast is essential for it (Perl et *al.*, 1992). As Pip is a Lys derived amino acid, it is likely that also the Lys catabolism leading to Pip-biosynthesis can take place in the chloroplast.

For subcellular localization of ALD1, we used the GATEWAY® cloning system and fused ALD1 full-length protein to *yfp* under the control of the 35S promoter of *Cauliflower mosaic* virus (*CaMV*). *ALD1* cDNA was amplified with primer sets containing the attB1 (Michigan State University (MSU 1) and attB2 site. Primers for the attB2 site were designed without a STOP codon (MSU 2) for C-terminal YFP fusion and with a STOP-codon (MSU 6) for N-terminal YFP fusion. The PCR products, generated in a Phu-PCR, were extracted from the gel and purified, before cloned into the pDONR207 vector and transformed into chemical

competent DH5α *Escherichia coli* cells. Plasmids of colonies were sent for sequencing and confirmed constructs for N-terminal YFP (BP 14-2) and C-terminal YFP (BP 11-1), were used in a LR-reaction to clone *ALD1* into pEarleyGate104 (N-terminal YFP-tag) and pGW2YFP (C-terminal YFP-tag; Reumann et *al.*, 2009), respectively. The confirmed DH5α *E. coli* clones 35S::YFP-*ALD1* (LR 14-2-1) and 35S::*ALD1*-YFP (LR 11-1-1) were used for transformation into *Agrobacterium tumefaciens* GV3101. *A. tumefaciens* carrying the binary vector constructs were infiltrated into *Nicotiana tobacco* leaves. The YFP fluorescence patterns were observed two days later with a Zeiss LSM 510 Meta fluorescence microscope. The *ALD1* construct with the C-terminal YFP fusion co-localized with the auto fluorescence patterns of the chloroplasts (Fig. 35A-C). *ALD1* constructs, carrying an N-terminal YFP fusion localized to the plasma membrane and the nucleus (Fig 35D-F). This divergent results indicated, that the target signal in *ALD1* was masked by the N-terminal YFP fusion and therefore mis-localized.
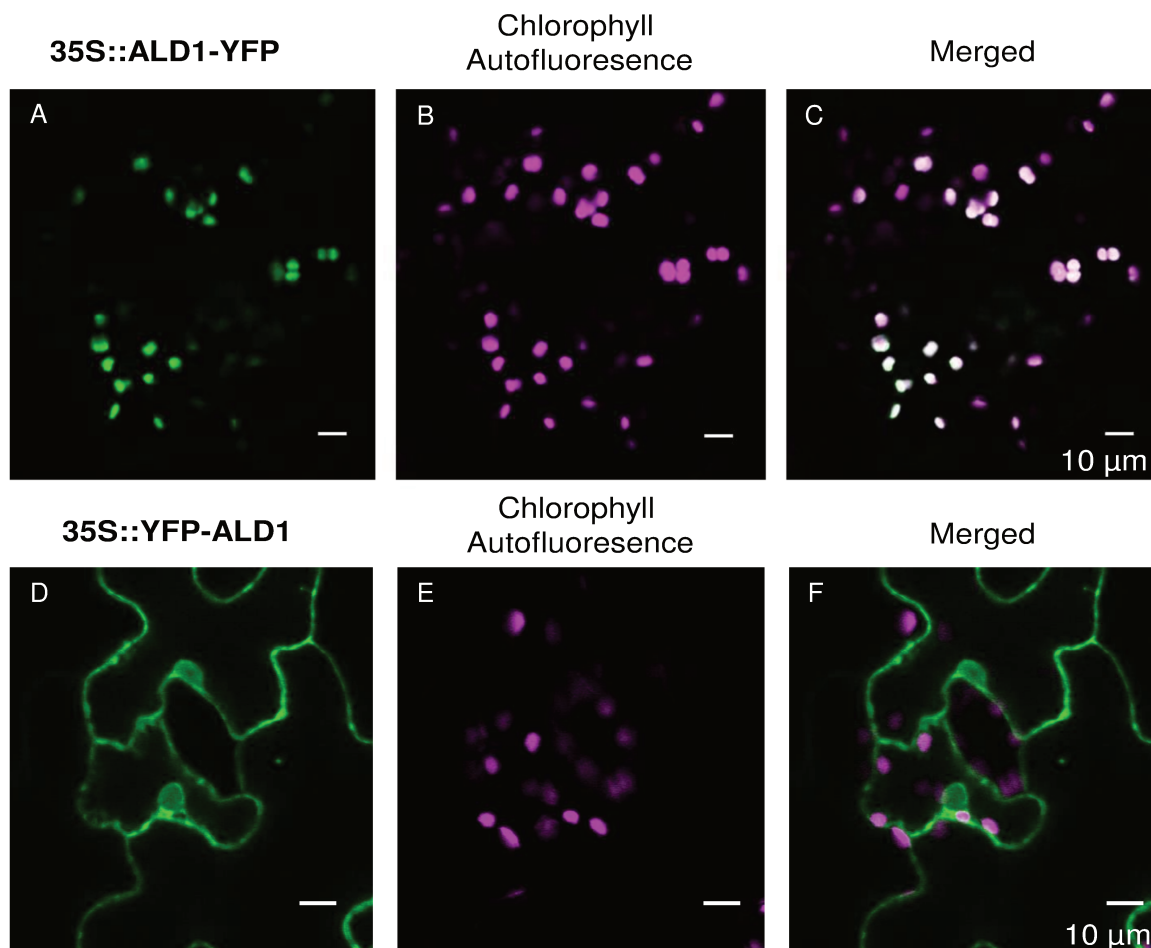
Figure 35. Transient Subcellular Localization of *ALD1* in *Nicotiana tobacco*. (A) 35S::*ALD1*-YFP and (D) 35S::YFP-*ALD1* were transformed into *Agrobacterium tumefaciens* GV3101 and inoculated into *N. tobacco* leaves. Chlorophyll autofluorescence (B + E) and merged images (C+F) YFP fluorescence was observed using a fluorescence microscope

To confirm the localization of *ALD1* we performed chloroplast uptake experiments using the "protease" protection assay (Fig. 36; Froehlich, 2011). Protein has been imported into intact, freshly purified pea chloroplasts. The import reaction was split in two, one set of the import reaction received no protease treatment (-), whereas the second set was treated with the protease (+) trypsin. After termination of the protease treatment, the chloroplasts were recovered, lysed and then fractionated into a pellet (P; essentially total membranes both envelope and thylakoids) and soluble (S; essentially stroma) fraction. Samples were analyzed by SDS-PAGE and radiolabeled imported products were visualized after fluorography treatment and exposure to X-ray film (Fig. 36 + 37B).
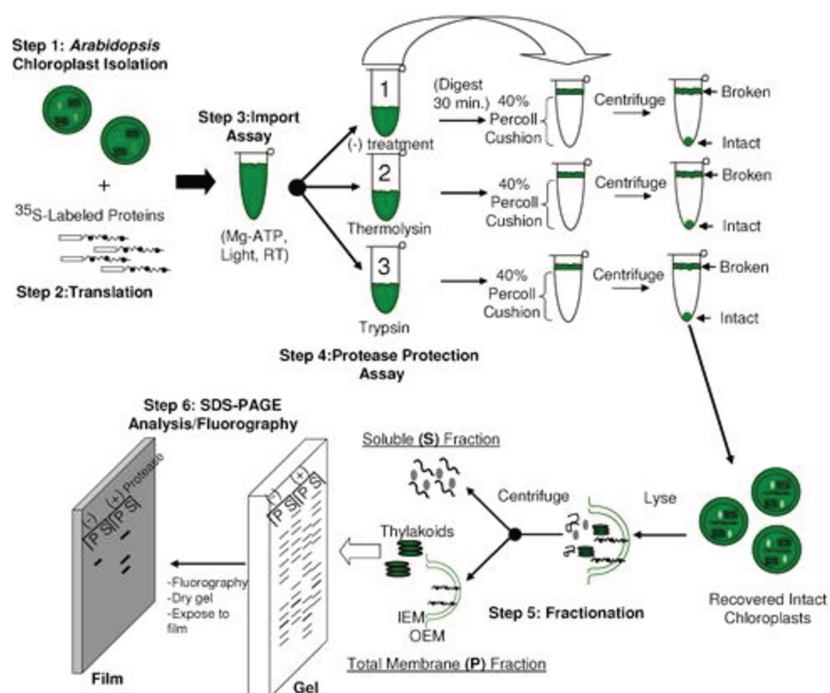
Figure 36. Schematic outline of the overall flow of a "dual protease" protection assay. (1) Arabidopsis chloroplasts isolation, (2) translation reaction, (3) import assay, (4) "dual protease" protection assay, (5) fractionation, and (6) SDS-PAGE and fluorography. OEM, outer envelope membrane; IMS, Intermembrane space; IEM, inner envelope membrane (Froehlich, 2011).

Trypsin, which is a member of the serine protease S1 family and 23.5 kDa small, cleaves peptide chains mainly at the carboxyl side of the amino acids Lys or arginine, except when either is followed by proline. The protease trypsin can partially disrupt the integrity of the OEM and thus proceed to the intermembrane space (IMS) where it can digest regions of OEM proteins or IEM proteins that extend to the IMS (Fig. 37A; Froehlich *et al.*, 2011). Thermolysin, another protease, for example specifically digests OEM proteins that are exposed towards the cytosol without causing any major damage to the integrity of

chloroplasts (Fig. 37A). The results of the trypsin protection assay confirmed that *ALD1* was processed to its correct mature form into the cholorplasts (Fig. 37B). *ALD1* was insensitive to trypsin treatment and was exclusively localized to the stroma (Fig. 37B). *FtsH8* served as a control gene, as it was targeted to the thylakoid membrane (Fig. 37B; Froehlich and Keegstra, 2011).
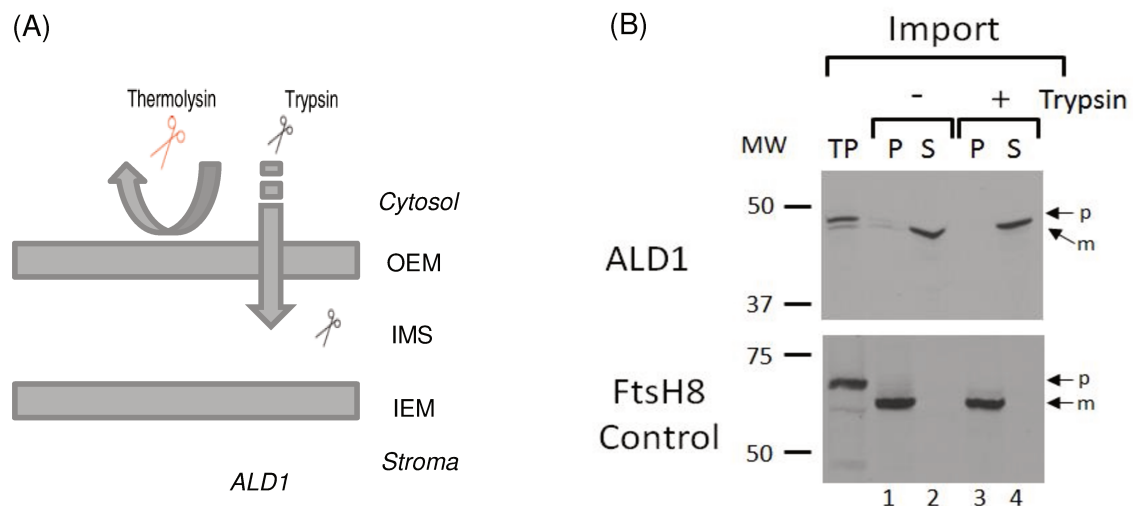
Figure 37. Principle of the protease protection assay in chloroplast uptake studies. **(A)** 'Dual protease' protection assay using thermolysin and trypsin. The protease thermolysin is represented by large scissors icon, while trypsin is represented by smaller black scissor icon. The hashed lines at the OEM represent regions of the outer envelope membrane that have been partially disrupted by trypsin, resulting in trypsin gaining access to the IMS. OEM, outer envelope membrane; IMS, Intermembrane space; IEM, inner envelope membrane (modified according to Froehlich, 2011). **(B)** Radiolabeled [35S]ALD1 or [35S]FtsH8 were imported into isolated pea chloroplasts for 30 minutes. After import, reaction were either treated without (-) or with(+) Trypsin for 30 minutes on ice. Protease reactions were quenched with Trypsin Inhibitor and then fractionated into total membrane (P) or soluble (S) fractions. All samples were analyzed by SDS-PAGE and fluorography. TP, 10% of Translation Product; p, precursor protein; m, mature protein; MW, Molecular Weight Standards (Import assay done in coorperation with J. Froehlich at the DOE-PRL, MSU).

To obtain stable transgenic lines the binary vector construct 35S::*ALD1*-YFP had been transformed into *A. tumefaciens* GV3101 and floral dip transformations with Col-0 and *ald1* Arabidopsis plants were conducted. Due to time restrictions the screening of candidates has not been completed and will be a task for the future.

IV.3.1.3. Isolation of the native ALD1 promoter

We further wanted to isolate the native promoter of *ALD1* and generate a stable Arabidopsis line, expressing *ALD1* under the control of the endogenous *ALD1* promoter. The aim was to test whether the *ald1* mutant can be complemented in terms of resistance

phenotype and Pip production and whether the subcellular localization was reproducible to be in the chloroplasts. A *pALD1::ALD1* construct with a C-terminal YFP tag would furthermore allow localization studies in transformed *ald1* mutants and time dependent studies of *ALD1* activation and signal progression throughout the plant after pathogen attack.

A PCR-based GATEWAY® cloning strategy was chosen to clone the constructs directly into the expression vector pGWB540 that carries a C-terminal YFP tag. Primer pairs were designed carrying the 5'-attB1 site, MSU 48b and MSU 49b, for 1.5 kb and 1 kb sized promoter fragments, respectively and 3'-attB2 (MSU 52) sites. Reverse (MSU 50) and forward (MSU 51) primer pairs overlapping the predicted genomic promoter region upstream of the 5' UTR of *ALD1* and the cDNA sequence of *ALD1* (Fig. 38). The first Phu PCRs amplified the promoter region (1,5 kb and 1 kb) from genomic DNA of Col-0 and the full-length *ALD1* (1,371 kb) from cDNA of *Psm* treated Col-0 leaves. Primer combinations for the predicted *ALD1* promoter region were MSU 48b/49b + MSU 50 and for the *ALD1* fragment MSU 51 + MSU 52.
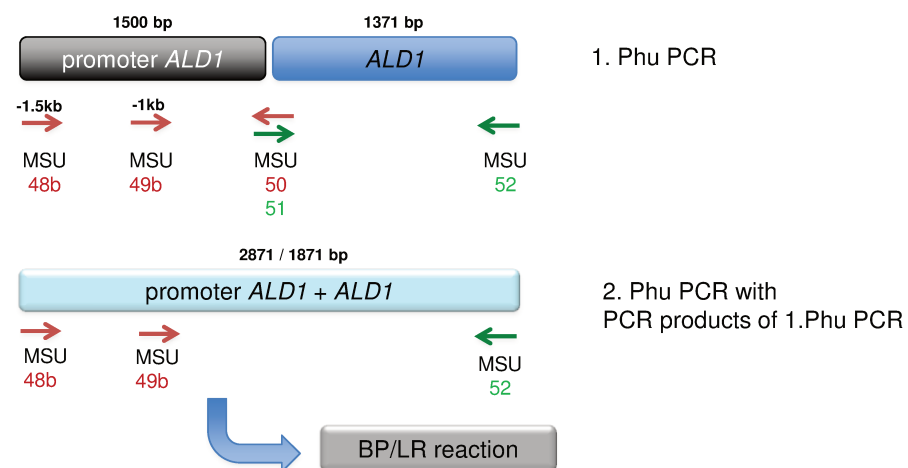
Figure 38. Two-step PCR–based GATEWAY® cloning strategy to generate a construct consisting of the native promoter of *ALD1* and *ALD1* cDNA.

After confirming the right size of the PCR products for the predicted *ALD1* promoter regions (1,5 kb and 1,0 kb, respectively) and for the *ALD1* fragment (1,371 kb) in a 1% agarose gel, the gel purified PCR products of the initial PCRs were used in equal parts as a template for the second Phu-PCR (Fig. 39A). The primer pairs carrying the recognition sites for the GATEWAY® cloning system (forward MSU 48b and reverse MSU 52) were used to generate an amplicon that covered the full-length of the predicted *ALD1* promoter region fused to *ALD1* cDNA (2,871 kb). The size of the construct was confirmed in a 1% agarose gel (Fig. 39B), gel purified and used in a BP reaction (named BP-4) to be integrated in the

pDONOR207. A colony PCR with BP clones (BP-4 #1,2,3) carrying the p*ALD1*::*ALD1* construct, confirmed the correct size and the integration into the vector (Fig. 39C).
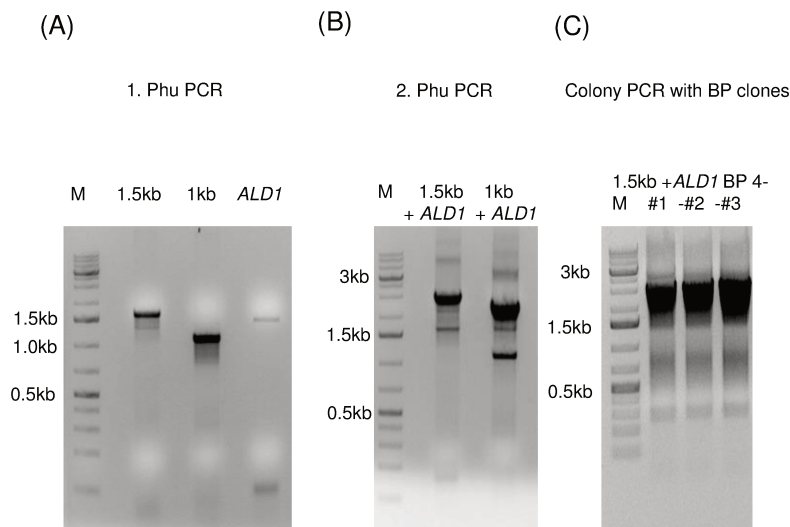
Figure 39. PCR-based cloning strategy to isolate native promoter of *ALD1* and generate a construct together with *ALD1* cDNA. **(A)** 1st Phu-PCR to generate first PCR products of 1.5 kb promoter region, 1 kb promoter region and *ALD1* cDNA (1,371 kb) **(B)** 2nd Phu PCR using the PCR product of 1st Phu PCR as a template generating 1.5 kb promoter plus *ALD1* cDNA constructs (2,871 kb and 1,872 kb) and 1 kb promoter plus *ALD1* cDNA constructs. **(C)** Colony PCR as control for BP reaction into pDONOR207 of 1.5 kb promoter plus *ALD1* with three colonies (#1,2,3).

BP-4 clones were furthermore sent for sequencing to confirm the presence of the predicted promoter region, the correct overlap and the *ALD1* cDNA sequence. After confirmation, the BP-4 clone number #1 was used for the LR-reaction (named LR-4-1) with the expression vector pGWB540. The LR clone (LR-4-1-1) was sequenced and transformed into *Agrobacterium tumefaciens* GV3101. The pGWB540 vector carries a hygromycin marker for selection *in planta*. The Agrobacterium transformation experiments of *ald1* plants have been conducted, but due to time restrictions, the selection and screening of candidates has not been completed and will be a task for the future, as well as the isolation of the native *FMO1* promoter and transformation of *fmo1* mutants.

III. 1.3. SUBCELLULAR LOCALIZATION OF FMO1

Since *ALD1* was localized to the chloroplast, we wanted to know whether *ALD1* and *FMO1* were indeed separated on the cellular level. We used the GATEWAY® cloning system to localize *FMO1* full-length protein fused to *yfp* under the control of the 35S promoter of *Cauliflower mosaic* virus (*CaMV*). *FMO1* cDNA was amplified with primers containing the attB1 (MSU 3) and attB2 site without a STOP codon (MSU 4) for C-terminal YFP fusion. The

111

PCR product, generated in a Phu-PCR, was extracted from the gel and purified, before cloned into the pDONR207 vector and transformed into DH5α *Escherichia coli* cells. Plasmids of colonies were sent for sequencing and the confirmed construct *(FMO1_*nostop-1) was used in a LR-reaction to clone *FMO1* into pGW2YFP (C-terminal YFP-tag; Reumann et al., 2009). The confirmed DH5α *E. coli* clone 35S::*FMO1*-YFP (*FMO1_*nostop-1-5) was used for transformation into *Agrobacterium tumefaciens* GV3101. Transformed *A. tumefaciens* carrying the binary vector constructs were infiltrated into *Nicotiana tobacco* leaves. The YFP fluorescence patterns were observed two days later with a Zeiss LSM 510 Meta fluorescence microscope. The *FMO1* construct colocalized with the CFP fluorescence pattern of the ER-marker (ER-ck/CD3-953; Nelson et al., 2007) and not with the CFP-fluorescence pattern of the Golgi marker (Fig. 40A-F; G-ck CD3-961; Nelson et al., 2007).
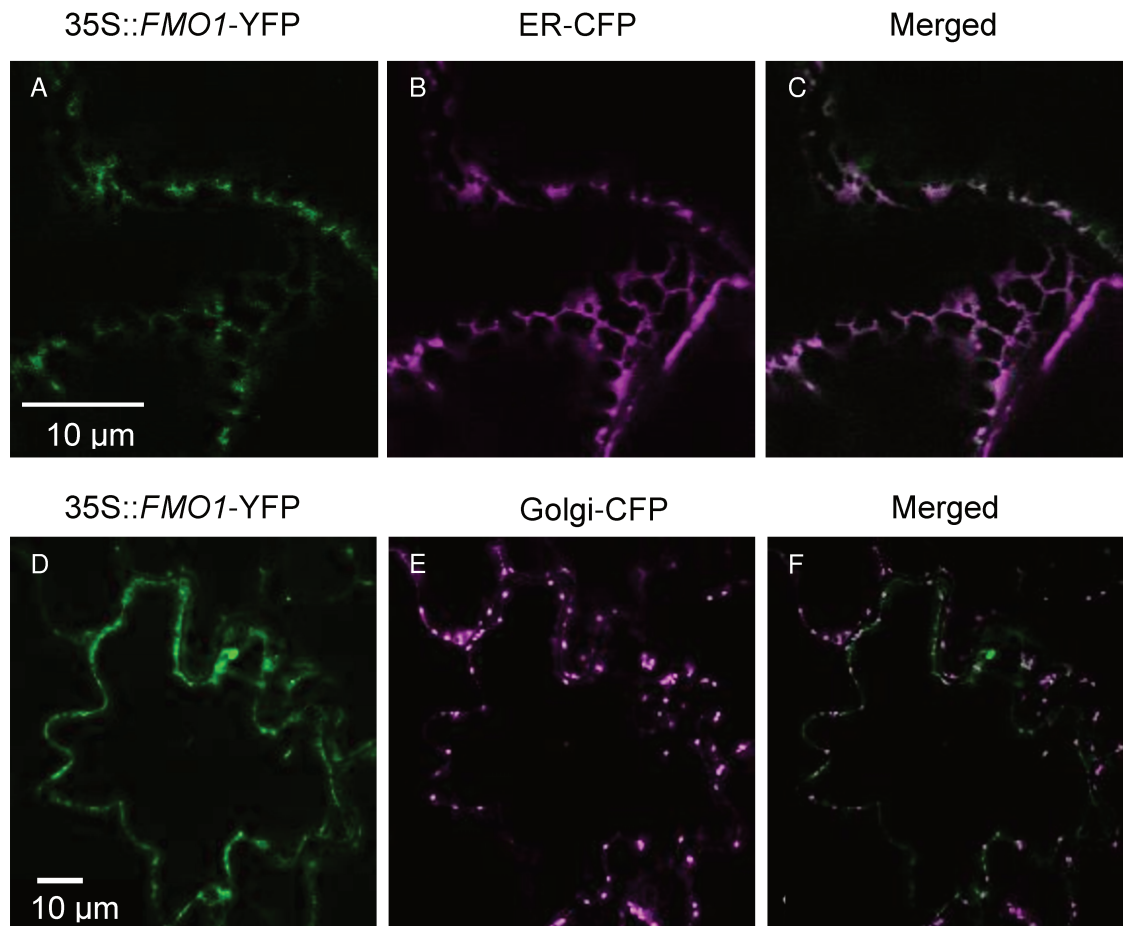
Figure 40. Transient Subcellular Localization of *FMO1* in *Nicotiana tobacco*. **(A+D)** 35S::*FMO1*-YFP was transformed into *Agrobacterium tumefaciens* GV3101 and coinfiltrated with either with Agrobacterium GV3101 carrying the ER-marker ER-ck CD3-953 **(B)** or with At GV3101 carrying the golgi marker G-ck CD3-961 **(E)** into *N. tobacco* leaves. YFP fluorescence was observed using a fluorescence microscope

The full-length of *ALD1* (50.5 kDa) and *FMO1* (60.4 kDa) protein plus YFP-tag (27 kDa) was confirmed by Western blot analysis, using the α-GFP antibody (Fig. 41).
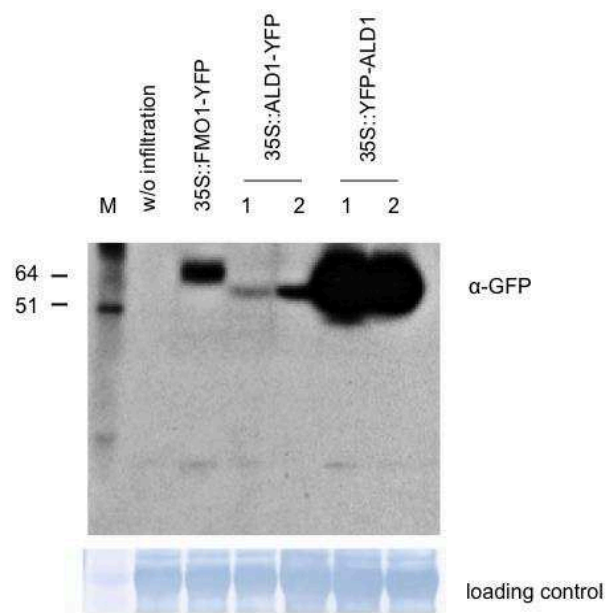
Figure 41. Confirmation of the full-length of protein fusion constructs. Western blot with α-GFP antibody shows negative control (crude protein without infiltration), full length of *FMO1* construct (35S-FMO1-YFP), the C-terminal *ALD1* construct 35S-*ALD1*-YFP #1 and #2 and the N-terminal *ALD1* construct 35S- YFP-*ALD1* #1 and #2, respectively. Loading control indicates equal amount of protein loaded to the SDS-PAGE gel. MW, Molecular Weight Standards.

IV.3.2. ALTERATIONS IN AMINO ACID HOMEOSTASIS DURING PLANT PATHOGEN RESISTANCE

IV.3.2.2. Characterization of altered amino acid homeostasis in the Lys metabolic pathway

With the objective to characterize the Asp- and Lys-pathway further and the amino acid accumulation pattern of *AGD2,* in particular, free amino acids of *agd2-1, rsp2* and *dmr1-4* were comparatively analyzed together with their respective ecotypes Col-0 and Ler. Since it was concluded that *AGD2* catalyzes the forward step leading to Lys production in plants (Hudson et *al.* 2006), we wanted to investigate the levels of Lys and Lys-derived amino acids, Aad and Pip in *agd2-1*. Furthermore, we analyzed production of free amino acids that were known to be affected in *rsp2* and *dmr1-4* mutants, like Thr and Ile and homoserine, respectively (van Damme et *al.* 2009; Stuttmann et *al.*, 2011). As part of the metabolite profiling, we also looked for peaks within the ion chromatograms with differential accumulation patterns between the mutants.

Free amino acids were comparatively analyzed one day after inoculation of 10 mM MgCl$_2$ in the local leaves (Fig. 42). In comparison to Col-0 basal levels of Pip, Aad and Lys were significantly higher in *agd2-1* and over accumulated two days after mock treatment (Fig. 42A, B and C). Pip accumulation in Ler did not differ significantly from Col-0, but from *rsp2* (Ler) and *dmr1-4* (Ler) showed a significant reduction compared to Ler wild type plants (Fig. 40A). Aad was not significantly changed in the Ler, *rsp2* and *dmr1-4* (Fig. 42B) and Lys accumulated significantly less in *rsp2* compared to Ler (Fig. 42C). We further checked for the amino acids that would be affected by the mutations in the different mutants. The homoserine kinase deficient mutant *dmr1-4* over accumulated homoserine as expected, whereas no other mutant tested showed elevated levels of homoserine (Fig. 42E). Ile was significantly increased in *agd2-1* and Ler compared to Col-0, whereas the levels in *rsp2* and *dmr1-4* did not differ from Ler (Fig. 42F). The level of Thr in *dmr1-4* did not show significant higher levels compared to the wild type, but it was over accumulating in *rsp2* compared to Ler (Fig. 42G). A so far unidentified peak of m/z 256 with an approximate retention time of 15.9 min was found exclusively in *agd2-1* (Fig. 42D).
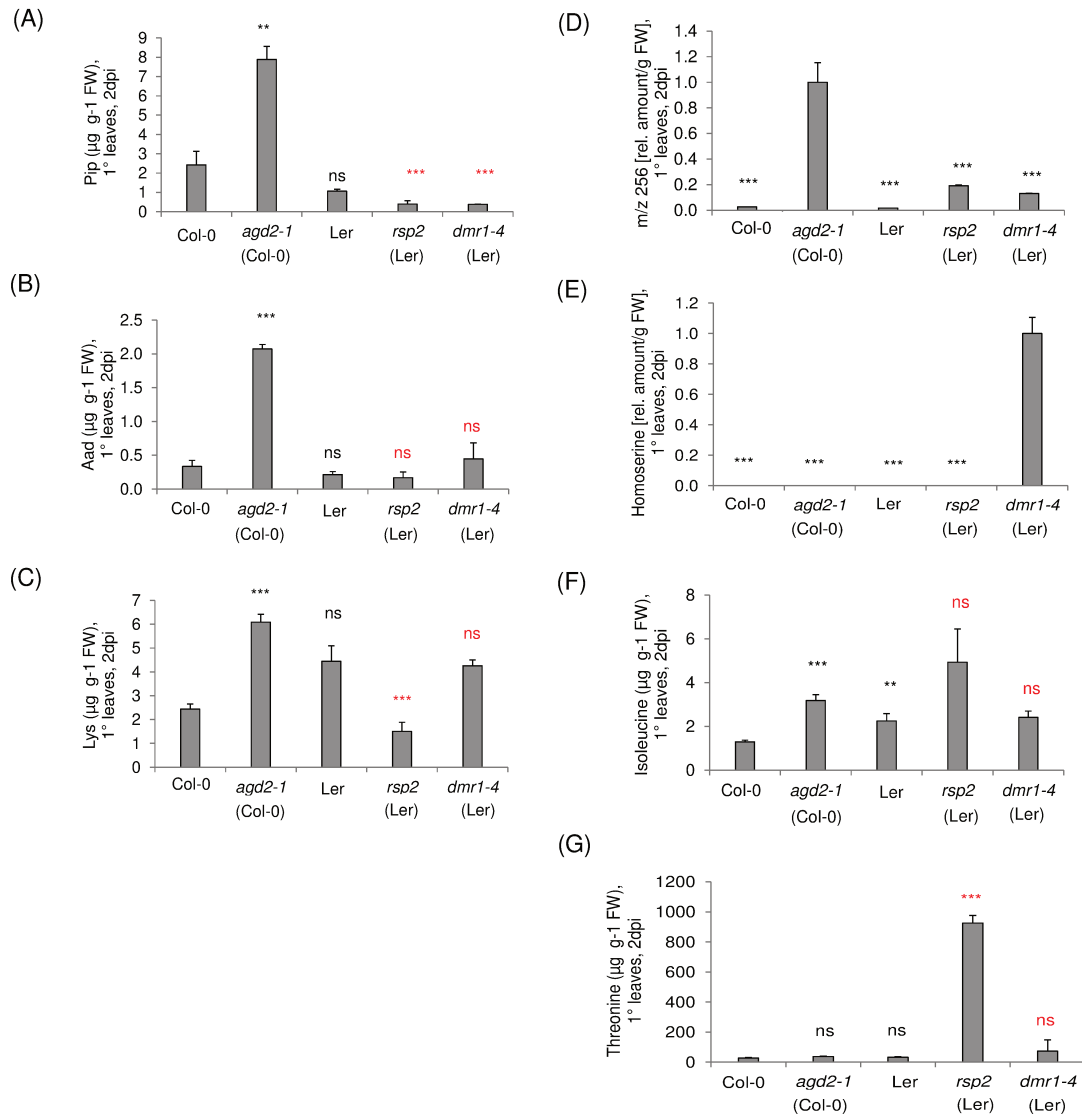
Figure 42. Basal levels of **(A)** Pip, **(B)** Aad, **(C)** Lys **(D)** m/z 256 RT (RT = retention time), **(E)** homoserine **(F)** Ile and **(G)** Thr two days after inoculation with 10 mM $MgCl_2$ in Col-0, *agd2-1*, Ler, *rsp2* (Ler) and *dmr1-4* (Ler) local leaves. Data represent the mean ± SD of three replicate samples. FW, fresh weight. For m/z 256 the amount g FW^{-1} relative to *agd2-1* and for homoserine the amount g FW^{-1} relative to *dmr4-1* is indicated, since no correction factor for the substance was determinded. Asterisks denote statistically different samples compared with Col-0 (black) or Ler (red) wild type plants (ns = non-significant, * = P < 0.05, ** = P 0.04-0.01, *** = P < 0.01, two-tailed *t* test compared).

To investigate the relationship of *AGD2-1* and *ALD1* in the Lys biosynthetic or catabolic pathway during activated defense responses, we performed comparative amino acid analysis with Col-0, *ald1*, *agd2-1* and *agd2-1 ald1* mutants two days after Psm inoculation compared to the mock treatment. Two days after inoculation with *Psm,* samples were harvested from local tissue, as well as from untreated and mock (10 mM $MgCl_2$) plants and the accumulation of Pip, Aad, Lys and the unidentified peak with m/z 256 was analyzed (Fig. 43). Pip accumulated strongly in Col-0 after 48 hours, but also the levels in mock treated leaves rose above the levels in the untreated tissue, implying an effect on Pip

production of the infiltration itself (Fig. 43A). No *Psm*-, or infiltration-induced accumulation of Pip was observed in *ald1* and *agd2-1 ald1*. The constitutive resistant *agd2-1* showed significant higher Pip levels in untreated leaves and a significant accumulation of Pip in *Psm*-treated leaves of 50 µg/g FW (Fig. 43A). Compared to Col-0, Aad accumulated in *ald1* to significant higher levels in the *Psm* treated tissue. *agd2-1* also showed significantly increased levels of Aad in mock–treated tissue (Fig. 43B). *ALD1* and *AGD2-1* seemed to negatively regulate the production of Aad, as the loss of both genes clearly had positive effects on the Aad biosynthesis upon *Psm* inoculation (Fig. 43B). In *agd2-1* Lys accumulated in *Psm*-treated tissue to a similar amount like the wild type, but to significant higher level in mock-treated tissue (Fig. 43C). The constitutive accumulation of Pip and Aad, and their precursor Lys suggested that this contributed to the constitutive resistance phenotype observed in *agd2-1*.
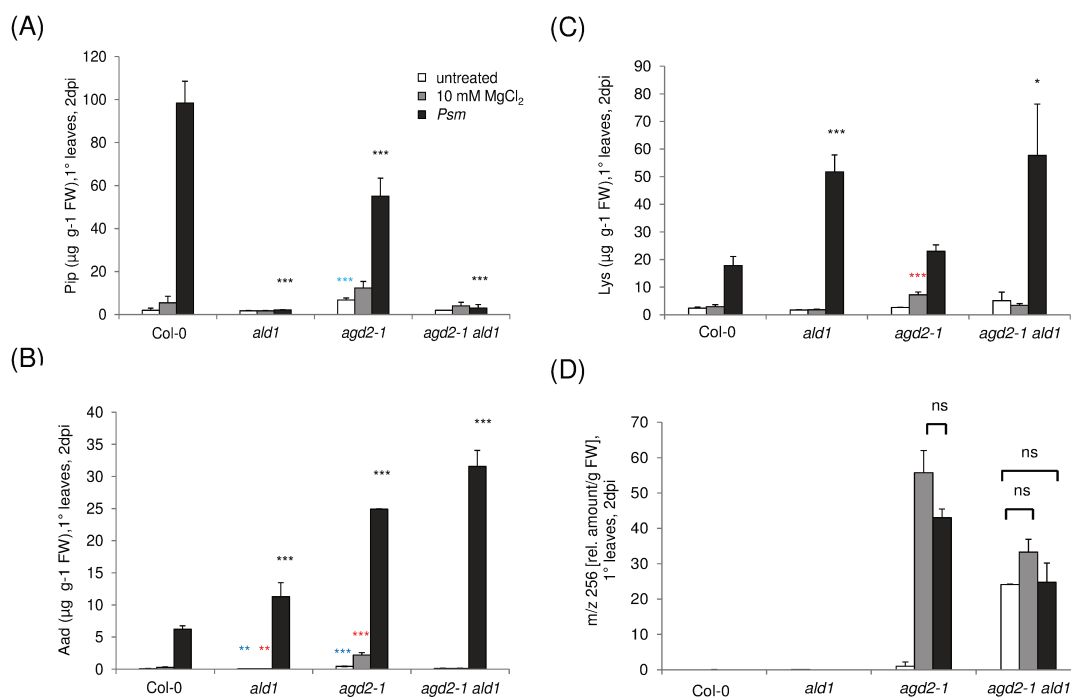
Figure 43. Accumulation of **(A)** Pip, **(B)** Aad, **(C)** Lys, **(D)** and m/z 256 RT 15.9 min in untreated (white), mock = 10 mM MgCl$_2$ (grey) and *Psm* OD 0.005 (black) treated local leaves of Col-0, *ald1*, *agd2-1* and *agd2-1 ald1* plants 2 days after inoculation. Data represent the mean ± SD of three replicate samples. FW, fresh weight. For m/z 256 the amount g FW^{-1} relative to the *agd2-1* untreated sample is indicated since no correction factor was determinded for the substance. Asterisks denote statistically differences of untreated, mock and *Psm* mutants samples compared to Col-0 *Psm* (black), Col-0 mock (red) and Col-0 untreated (blue) samples, respectively (* = P < 0.05, ** = P 0.04-0.01, *** = P < 0.01, two-tailed *t* test).

The unidentified compound with an m/z of 256 and a retention time of approximately 15.9 min exclusively accumulated in *agd2-1* but also in *agd2-1 ald1* and did not further increase upon pathogen treatment (Fig. 43D). The EZ faast Phenomenex database identified the peak as diaminopimelate. Two isoforms of diaminopimelate exist, L,L-2,6-diaminopimelic acid and *meso*-2,6-diaminopimelic acid. To identify the peak and assign it to the correct isoform, authentic substances of L,L-2,6-diaminopimelic acid (CAS number 14289-34-0; Sigma) and *meso*-2,6-diaminopimelic acid (CAS number 922-54-3; Sigma) were ordered. Amino acids extracted from *agd2-1* and *agd2-1 ald1* mutants and 2 µg of each pure substance were analyzed following propyl chloroformate derivatization via gas chromatography–mass spectrometry (GC-MS; Fig. 44A-H; Kugler et *al*., 2006). The mass spectra of L,L-2,6-diaminopimelate (Fig. 44E) and *meso*-2,6-diaminopimelate (Fig. 44G) had similar fragmentation patterns, but still differed to the mass spectra observed in m/z 256 peak in *agd2-1* (Fig. 44A) and *agd2-1 ald1* (Fig. 44C). The retention time of approximately 24 min completely differed from m/z 256 with 15.9 min (Fig. 45). The peak with the m/z 256 therefore could not be identified as either L,L-2,6-diaminopimelate or *meso*-2,6-diaminopimelate.
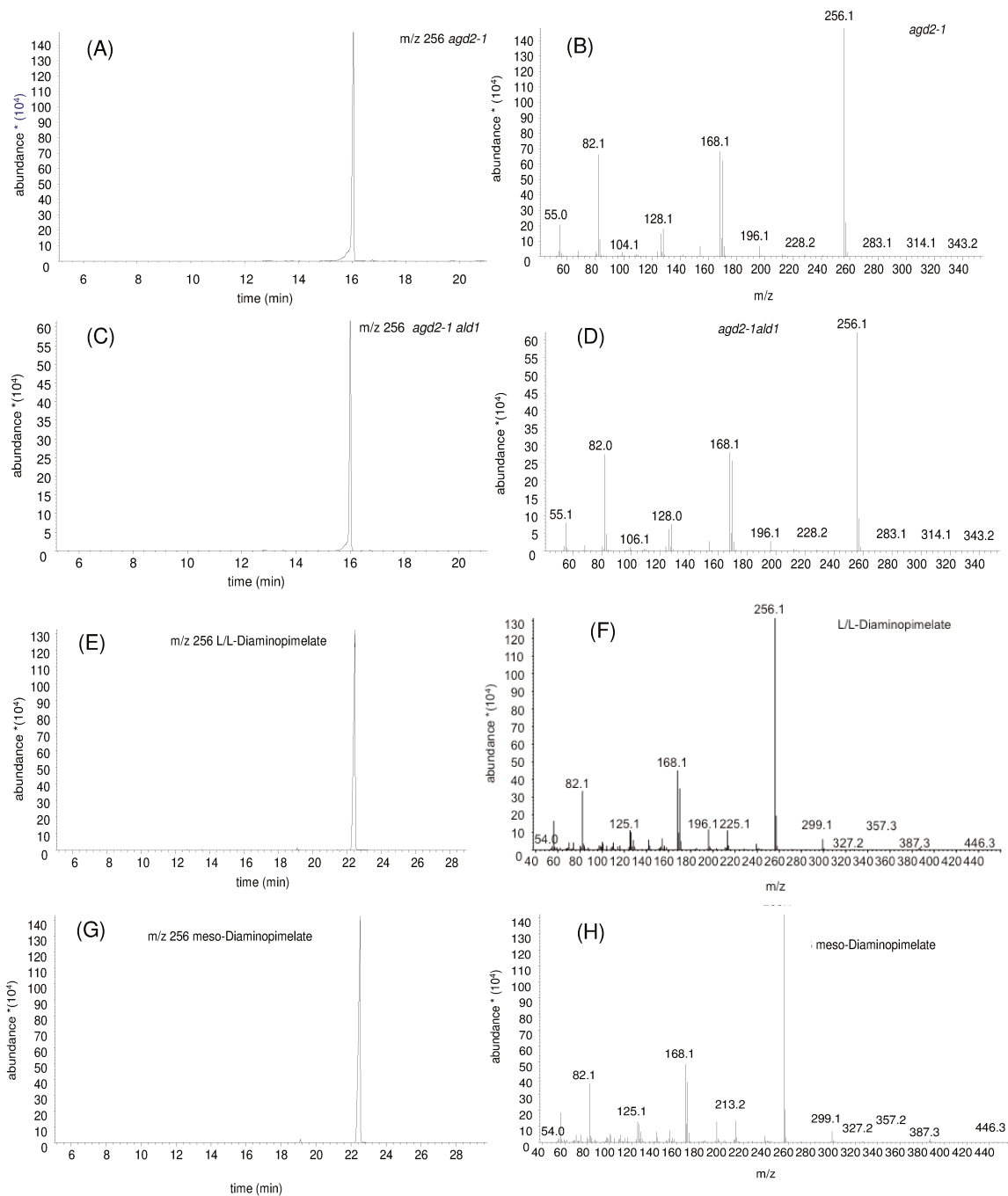
Figure 44. The plant-derived substance 'm/z 256' in *agd2-1* and *agd2-1 ald1* and authentic L/L-Diaminopimelate and meso-Diaminopimelate don't have identical GC retention times. **(A, C, E, G)** retention times and **(B, D, F, H)** mass spectra of m/z 256 in *agd2-1* and *agd2-1 ald1* and authentic L/L-2,6-Diaminopimelate and *meso*-2,6-Diaminopimelate, respectively, after derivatization with propyl chloroformate converting amino groups into propyl carbamate and carboxyl groups into propyl ester derivatives, of the unknown substance 'm/z 256' detected in extracts of *agd2-1* and *agd2-1 ald1* leaf tissue.
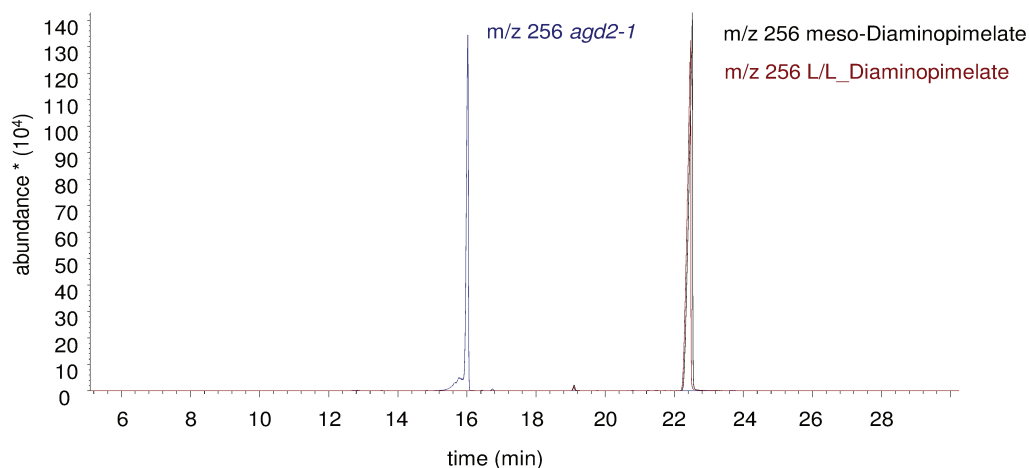
Figure 45. Overlay of GC ion chromatograms of m/z 256 derived from a pure *agd2-1* plant extract sample (blue) and 2 µg of authentic L,L-2,6-diaminopimelate (red) and *meso*-2,6-diaminopimelate (black).

To identify the structure of m/z 256 it was important to identify the masses true to the mass spectrum of the unknown substance. Therefore we compared potential M+ (molecular ion) peaks (marked in red in Fig. 46A) in *agd2-1* and Col-0.
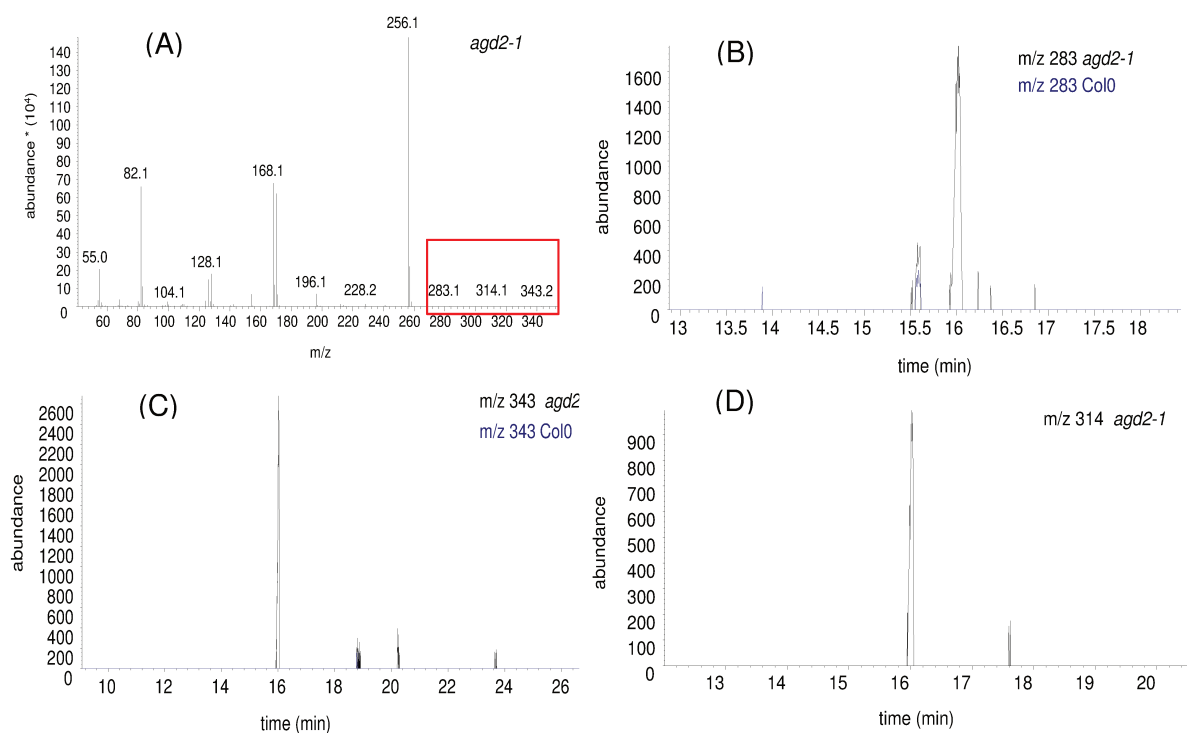
Figure 46. Identification of potential M+ of m/z 256 (red box) **(A)** via overlay of GC ion chromatograms of m/z 283 **(B)**, 343 **(C)** and 314 **(D)** derived from a pure *agd2-1* plant extract sample (black) and Col-0 (blue).

All potential M+ masses m/z 283, 343 and 314 exclusively accumulated in the *agd2-1* leaf extract with a retention time of 16 min and therefore could be considered as part of the true mass spectrum of m/z 256 (Fig. 46B, C + D).

IV.3.3. IDENTIFICATION OF CANDIDATE GENES PUTATIVELY INVOLVED IN PATHOGEN INDUCED PIP- AND AAD-METABOLISM

To characterize and uncover critical steps in Pip metabolism (Fig. 2), homozygous T-DNA lines in the Col-0 background for *ORNCD1* and *SOX/PIPOX* were identified and used for further molecular and metabolic characterization (Tab. 10). We expected that an *ORNCD1* mutant, defective in the reduction step of P2C to Pip, would theoretically over accumulate P2C, whereas Pip levels should be significantly reduced. Since Pip is a critical SAR regulatory compound the knockout mutant should have be severely impaired in local and systemic resistance.

Gene name	AGI	Name of mutant	SALK ID	Location of insert
SOX/PIPOX - Sarcosine oxidase	AT2G24580	*sox/pipox_1*	SALK_017108c	chr2 10446606
		sox/pipox_2	SALK_099135c	chr2 10446857
ORNCD1 reductase	AT5G52810	*orncd1_1*	SALK_131295 (BH) (BW)	chr5 21399378
		orncd1_2	gk-428e01.01	chr5 21400073

Table 10. T-DNA insertion lines used in studying candidate genes putatively involved in pathogen induced Pip and Aad-metabolism.

The knockout of *ORNCD1* relative gene expression was successfully confirmed in *orncd1-2* (gk-428e01; Fig. 47A). *SOX/PIPOX* was expressed in the mock-treated leaves and transcript levels were reduced upon *Psm*-inoculation in Col-0. The homozygous T-DNA line *sox/pipox_2* (SALK_099135c) showed reduced transcript levels in the mock samples comparable to *Psm*-inoculated samples in Col-0 (Fig. 47B). A down regulation of *SOX/PIPOX* would be necessary in case of defense to ensure Pip accumulation in the local leaf and development of SAR.
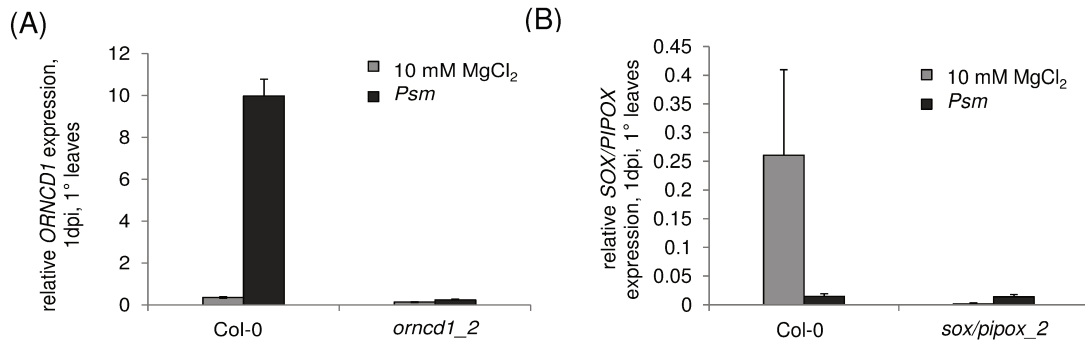
Figure 47. Relative gene expression of *ORNCD1* and *SOX/PIPOX* one day after infiltration of *Psm* (OD 0.005) and 10 mM MgCl$_2$. **(A)** *Psm*-induced *ORNCD1* expression in Col-0 and *orncd1-2*. **(B)** *Psm*-induced *SOX/PIPOX* expression in Col-0 and *sox/pipox_2*. Transcript levels were assessed by quantitative real-time PCR analysis, are given as means ± SD of three replicate samples, and are expressed to the respective mock control value.

In comparative analysis of free amino acids, Pip accumulated after *Psm* inoculation in the local leaf to significant higher amounts in *sox/pipox_2* and was significantly reduced in *orncd1_2* (Fig. 48A). The high accumulation of Pip could be caused by impaired functionality of *SOX/PIPOX*, so was the significant reduction of Pip in *orncd1_2* an indicator for a disruption in Pip biosynthesis. Since Pip was still induced upon pathogen attack, it could be speculated whether another gene acted in concert with *ORNCD1* in the pathway of Pip biosynthesis. Levels of Aad were not significantly changed in *orncd1_2* and *sox/pipox_2* compared to mock and *Psm*-treated leaves of Col-0 (Fig. 48B). Lys biosynthesis was induced in Col-0, *orncd1_2* and *sox/pipox_2* upon pathogen inoculation, but this accumulation was only in *orncd1_2* significantly different from Col-0 (Fig. 48C). In metabolite analysis, levels of free SA were significantly reduced in *sox/pipox_2*, but not changed in *orncd1_2* compared to Col-0 (Fig. 48D). The level of camalexin was significantly reduced compared to Col-0 in infected leaves of *sox/pipox_2* and *orncd1_2* (Fig. 48E).
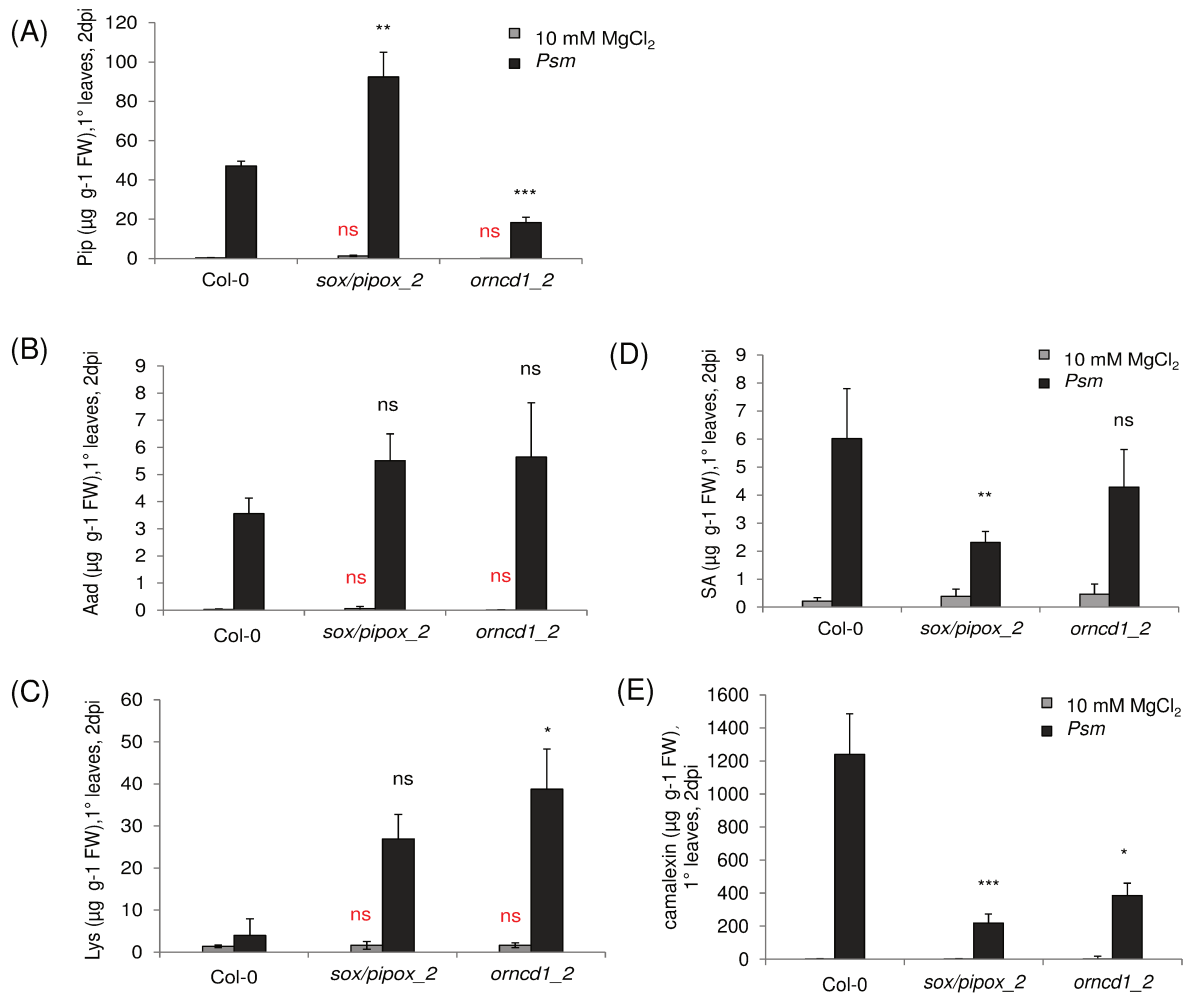
Figure 48. Accumulation of **(A)** pipecolic acid (Pip), **(B)** α-amino adipidic acid (Aad), **(C)** Lys and defense related metabolites SA **(D)** and camalexin **(E)** in local leaves of Col-0, *sox/pipox_2 and orncd1_2* plants 2 days after *Psm* or 10 mM MgCl₂ inoculation. Data represent the mean ± SD of three replicate samples. FW, fresh weight. Asterisks denote statistically different samples of *Psm* and mock mutant samples compared to Col-0 *Psm* (black) and Col-0 mock (red) samples, respectively. (* = P < 0.05, ** = P 0.04-0.01, *** = P < 0.01, two-tailed *t* test).

Other homozygous T-DNA lines of *SOX/PIPOX* and *ORNCD1* tested were *sox/pipox_1* and *orncd1_1* (Tab. 10). The T-DNA mutant *sox/pipox_1* still showed a wild type like accumulation of *SOX/PIPOX* transcript in the mock state, compared to the expression observed after infection with *Psm* (Fig. 49A) and thus was not sucessfully knocked out. Measuring the levels of Pip in *sox/pipox_1* after mock treatment and *Psm* infection in the local leaf did not result in a significant change compared to the wild type (Fig. 49B). The second T-DNA line tested for *ORNCD1* was *orncd1_1*. This mutant was devoid in transcript accumulation of *ORNCD1* after *Psm* inoculation (Fig. 49C), but did not show an altered Pip level compared to the wild type (Fig. 49D). The altered amino acid and metabolite levels had no influence on resistance, as *orncd1_2* and *sox/pipox_2* were able to develop a significant SAR response, as was *orncd1_1* that was not different than the SAR developed in Col-0 (Fig. 50A-C).
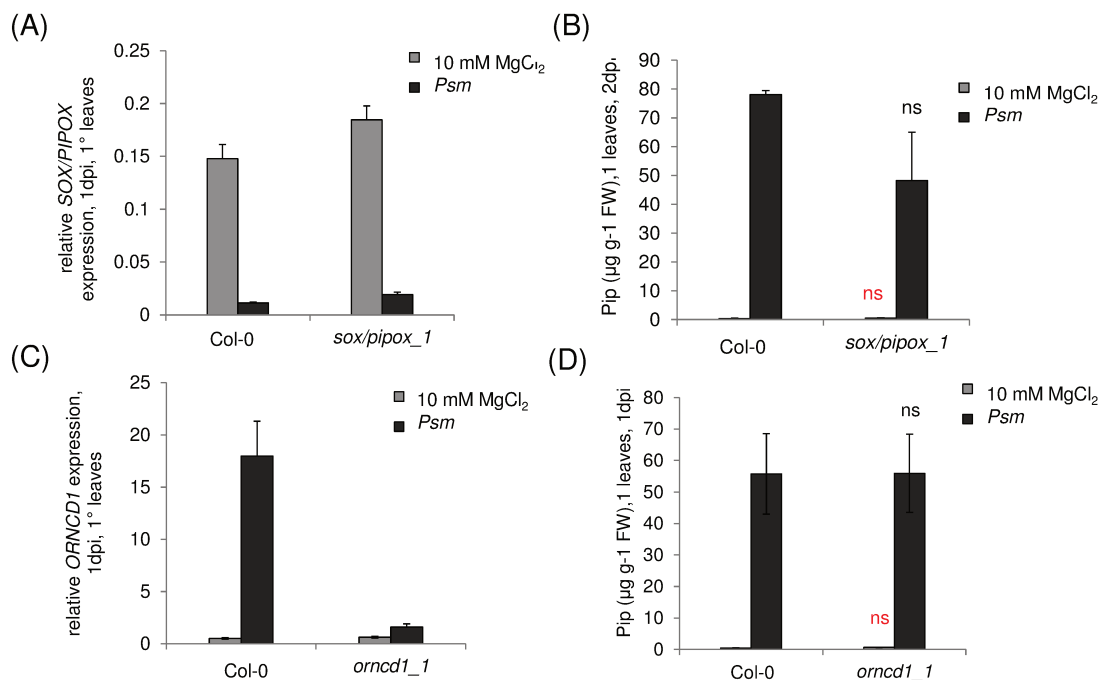
Figure 49. Characterization of T-DNA insertion lines *sox/pipox_1* and *orncd1_1*. Relative gene expression of *SOX/PIPOX* and *ORNCD1* in *sox/pipox_1* **(A)** and *orncd1_1* **(C)** respectively, one day after infiltration of *Psm* (OD 0.005) and 10 mM MgCl$_2$. Transcript levels were assessed by quantitative real-time PCR analysis, are given as means ± SD of three replicate samples, and are expressed to the respective mock control value. Accumulation of pipecolic acid (Pip) in local leaves of Col-0, *sox/pipox_1* **(B)** and *orncd1_1* **(D)** plants 2 days after *Psm* or 10 mM MgCl$_2$ inoculation. Data represent the mean ± SD of three replicate samples. FW, fresh weight. Asterisks denote statistically different samples of *Psm* and mock mutant samples compared to Col-0 *Psm* (black) and Col-0 mock (red) samples, respectively. (* = P < 0.05, ** = P 0.04-0.01, *** = P < 0.01, two-tailed *t* test).

SOX/PIPOX overexpressed under the control of the 35S promoter of *Cauliflower mosaic* virus (*CaMV*) in Arabidopsis could reveal whether the gene indeed acts in the reverse reaction and degrades Pip immediately. It was also expected that the resistance phenotype of the mutants would be severely impaired.

Full length *SOX/PIPOX* (1.395 bp linear mRNA) was therefore amplified from cDNA of *Psm* inoculated Col-0 leaves with the forward primer containing the attB1 site (MSU 13) and the reverse primer containing the attB2 site and a STOP codon (MSU 14) and cloned into the pDONR207 vector (BP 9-1-1). After sequencing the BP-clones, the LR reaction was conducted to transfer *SOX/PIPOX* into the pEarleyGate100 (LR 17-1-1) overexpression vector. Once the LR clone was confirmed via sequencing, it was transformed into competent *A. tumefaciens* GV3101 cells and stable Arabidopsis transformation was performed via floral dipping. Due to time restrictions, the screening for suitable candidates needs to be completed alongside with metabolite analysis and resistance assays.

(A) ... **(B)** ... **(C)**
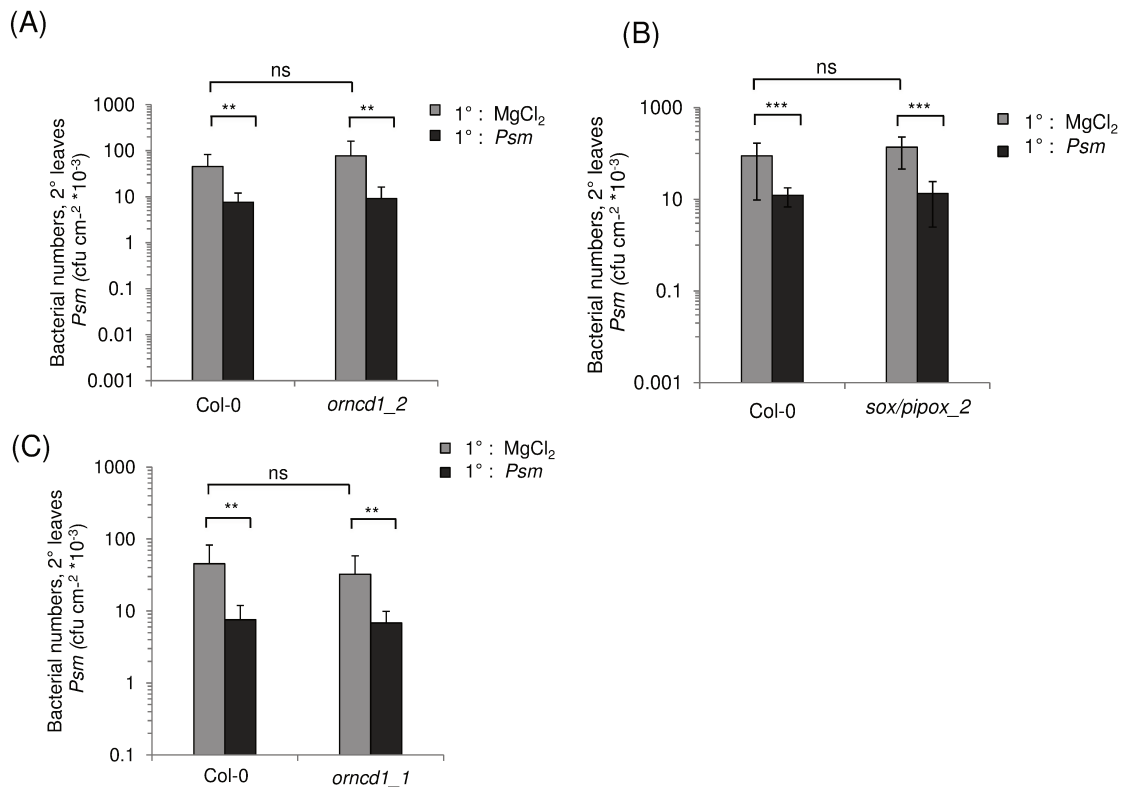
Figure 50. SAR assay with *orncd1_2* **(A)** *sox/pipox_2* **(B)** and *orncd1_1* **(C)** Lower (1°) leaves were infiltrated either with either 10 mM MgCl$_2$ or *Psm* (OD 0.005) and 2 d later. Three upper leaves (2°) were challenge infected with *Psm* (OD 0.001). Bacterial growth in upper leaves was assessed 3 d after 2° leaf inoculation. Asterisks denote statistically significant differences between indicated samples. (***: P< 0.001; **: P < 0.01; *: P < 0.05; two-tailed *t* test).

IV.3.4. BIOCHEMICAL CHARACTERIZATION OF ALD1 AND FMO1

To obtain insights in the enzymatic reactions and conversion products of the Lys aminotransferase ALD1 and flavin-dependent monooxygenase FMO1, we started to work on the biochemical characterization of both proteins. The goal was to uncover the biosynthetic reaction and pathway towards pipecolic acid and the ALD1 conversion products in the proposed pathway (Fig. 2). FMO1 is required for SAR and Pip-mediated resistance, which led to the conclusion that FMO1 acts downstream of Pip to realize SAR. Flavin-dependent monooxygenases in various organisms like plants, animals, or fungi oxidize either nitrogen- or sulfur-containing substrates (Schlaich, 2007). We therefore speculated that FMO1 could convert Pip or a Pip derivative into an oxidized form and thereby transduce the Pip signal. With the objective to use the cell free expression system (WGE – wheat germ expression), a full length Phu PCR product of *ALD1* (1371 bp linear mRNA; Fig. 51A) was sub-cloned into the pGEM®-T Easy vector and them cloned into the pIVEX1.4 expression vector used in the cell free translation reaction (Fig 51D). The 5 prime cell-free translation system RTS™ 100

Wheat Germ CECF allows a production of several hundred micrograms protein per milliliter (>400 µg/mL for GUS control protein, according to manufacturer). Substrates and energy components needed for a sustained reaction are continuously supplied via a semi-permeable membrane. Potentially inhibitory reaction byproducts are diluted as they diffuse from the 50 µl reaction compartment through the same membrane into the 1 ml feeding compartment (5 prime; RTS™ 100 Wheat Germ CECF Kit Manual). After conducting the translation reaction according to the manufacturer's instruction, obtained ALD1 protein was loaded to an SDS-PAGE gel. The coomassie staining showed no band specific for ALD1 protein (Fig. 51B), compared to the negative control (c-), but in a Western blot with His-antibody of the same gel, the band of ALD1 protein became very clear (Fig. 51C).
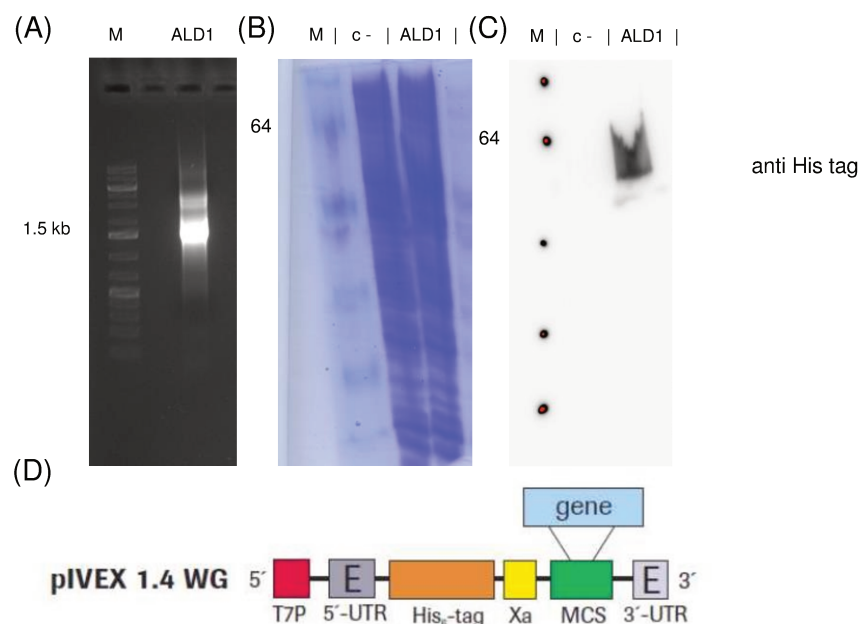
Figure 51. 5 prime-RTS™ 100 Wheat Germ CECF cell free expression with *ALD1*. Full-length *ALD1* Phu-PCR product **(A)**, SDS-PAGE of translated ALD1 protein stained with coomassie blue **(B)**, Western blot of ALD1 protein (50.5 kDa) and His-tag (17kDa) **(C)**, Functional elements of RTS Wheat Germ expression vector pIVEX1.4. T7P: T7 promoter; UTR: Untranslated regions (UTRs) containing optimized translation enhancer (E) elements; His6-tag: Tag sequence at C- or N-terminal position; Xa: Factor Xa restriction protease cleavage site; MCS: Multiple cloning site in three different reading frames for the insertion of the target gene **(D)**. (In coorperation with T. Pick)

We also wanted to produce FMO1 protein using the cell-free translation system RTS™ 100 Wheat Germ CECF. We generated two negative controls for *FMO1*, introducing mutations in the FAD- and NADPH-binding domain of FMO1, as described by Parker and colleagues (Fig. 52; Bartsch et *al.*, 2006). Intact FAD- and NADPH-binding sites in FMO1 are required for basal resistance to virulent strain *H. parasitica* (Bartsch et *al.*, 2006). Conserved Gly residues in the FAD and NADPH binding sites are important for cofactor binding and enzymatic activity and thus crucial for functionality of FMO1 (Bartsch et *al.*, 2006).

Besides cloning full-length FMO1 (1539 bp linear mRNA) into pGEM®-T Easy and pIVEX1.4, we introduced a single point mutation in the FAD- and NADPH-binding sites with a two-step PCR-based strategy in which the conserved Gly residues of these motifs were exchanged to Ala residues (Fig. 53A+B).
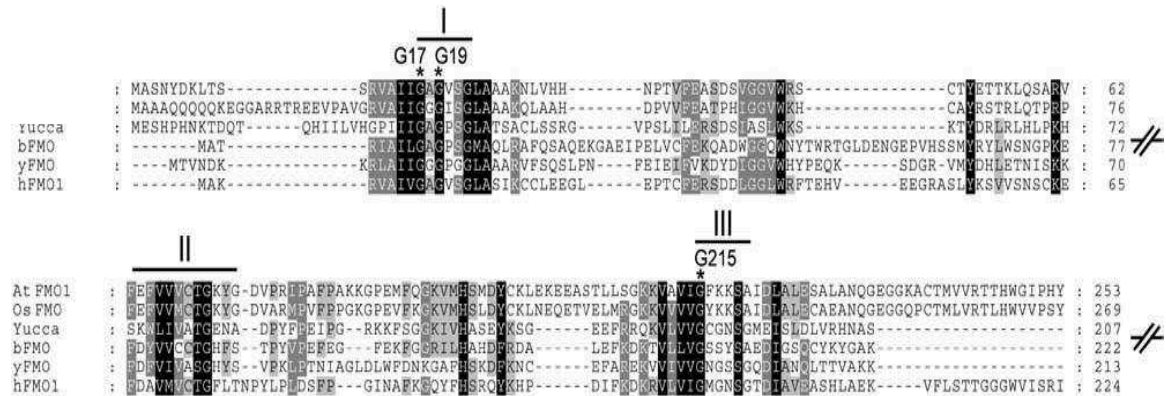
Figure 52. Alignment of amino acid sequences from Arabidopsis (At*FMO1* and YUCCA; Zhao et *al.*, 2001), rice (Os FMO), Methylophaga sp strain SK1 (bFMO; Choi et *al.*, 2003), yeast (yFMO; Zhang and Robertus, 2002), and human (hFMO1; Lawton et *al.*, 1994) was performed, and the N-terminal sequences are shown here. FMO-defining motifs and the conserved Gly residues exchanged by site-directed mutagenesis are indicated above the top line: I, FAD binding motif GXGXXG; II, FMO identifying sequence motif FXGXXXHXXX(Y/F); and III, NADPH binding domain GXGXX(G/A). Multiple alignments were visualized using GeneDoc (Nicholas et *al.*, 1997) with conserved residue shading mode set to level 4 using default settings and enabled similarity groups function. Amino acids with 100, 80, and 60% conservation are presented as white letters on black background, white letters on dark-gray background, and black letters on light-gray background, respectively (Bartsch et *al.*, 2006).

With two Phu-PCRs, overlapping primer pairs introduced the mutation by a change of one base pair in the FAD- (GGT to GCT) and in the NADPH-binding site (GGC to GCC) into *FMO1*. The first Phu-PCR generated the two single fragments that were fused in a second Phu-PCR to a full-length (1593 bp) fragment (Fig. 53A+B). FMO1 clones, mutated in G17 and G215 were sequenced and the exchange in the base pair confirmed (Fig. 54A+B). The names of all clones generated for the cell free expression using the 5 prime, RTS™ 100 Wheat Germ CECF system, are displayed in table 11.
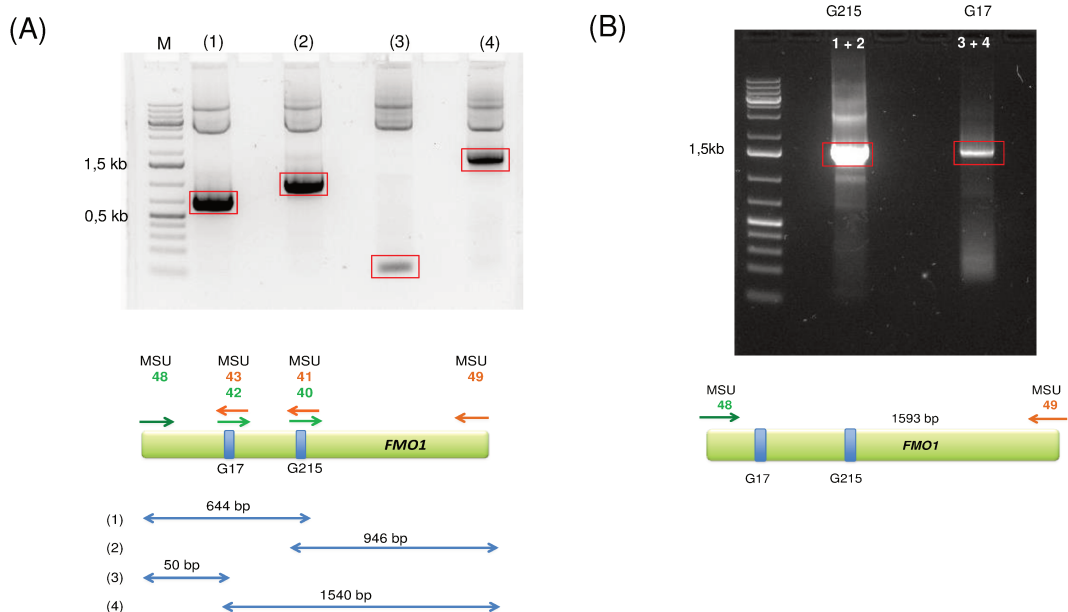
Figure 53. Two-step PCR–based cloning strategy to introduce single point mutation into the FAD (G17)- and NADPH (G215)- binding site of FMO. The first Phu PCR generated two constructs for each mutation introducing the point mutation via a primer overlap due to a change in base pair. For *fmo1-G215* two Phu PCRs (1) and (2) with the primer combination MSU3 + MSU41 and MSU40 + MSU4, respectively were carried out **(A)**. In the second Phu PCR for *fmo1-*G215 equal amounts of the purified PCR products (1) and (2) were used as template, to combine the two fragments to full length *FMO1* (1593 bp) with the primer pair MSU3 and MSU4 **(B)**. For *fmo1-*G17 Phu PCR (3) and (4) with the primer combination MSU3 + MSU43 and MSU42 + MSU4, respectively was carried out **(A)**. In the second Phu PCR equal amounts of the purified PCR products (3) and (4) were used as template, to combine the two fragments to full length *FMO1* (1593 bp) with the primer pair MSU3 and MSU4 **(B)**.

Gly (GGT) → Ala (GCT)

Gly (GGC) → Ala (GCC)

Figure 54. Multiple sequence alignment of *fmo1-*G17 **(A)** and *fmo1-*G215 **(B)** mutations with *FMO1* sequence. Introduced mutation of Gly to Ala are indicated in pink. List of constructs obtained for cell free expression of *ALD1* and *FMO1* in the pIVEX1.4 vector **(C)**.

127

Vector	Insert	Name of clone
pIVEX1.4	*ALD1*	*ALD1*+TS-1
pGEMTeasy	*fmo1*-G17	G50-1-6
pIVEX1.4	*fmo1*-G17	G50-1-6-4
pGEMTeasy	*fmo1*-G215	G644-2-6
pIVEX1.4	*fmo1*-G215	G644-2-6-8
pGEMTeasy	*FMO1*	*FMO1*stop-2-4
pIVEX1.4	*FMO1*	*FMO1*stop-2-4-7

Table 11. Constructs generated for the 5 prime, RTS™ 100 Wheat Germ CECF system.

The cell free translation with FMO1 still needs to be conducted and if protein is obtained from all reactions, enzymatic activity assay can be carried out with *ALD1* and *FMO1* constructs. In the case of ALD1 enzymatic acitivity assays feeding Lys as a substrate will be conducted and conversion products analyzed using GC/MS. FMOs bind the cofactor flavin adenine nucleotide (FAD) and catalyze oxygenation of substrates containing nucleophilic nitrogen, phosphorous, sulfur, or selenium at the expense of NADPH (Bartsch et *al.*, 2006). Thus, we think that FMO1 potentially takes Pip or a Pip-derivative as a substrate.

V. DISCUSSION

Systemic acquired resistance (SAR) is a broad-spectrum, long lasting immune response that develops after a localized primary infection and renders the whole plant more resistant to subsequent infection. To ensure development of enhanced disease resistance in the rest of the plant after infection, a signal must be generated that is sent throughout the plant to distal parts. The structure of this signal remains elusive, but a number of potential candidates and signaling mechanisms are currently discussed (Dempsey and Klessig, 2012; Shah and Zeier, 2013). A pathogen infection induces multiple defense related processes in the plant and metabolic and transcriptional changes. One metabolite most associated with SAR is the phenolic compound SA and a systemic accumulation of SA is crucial for SAR establishment in the distal leaf of cucumber, tobacco and Arabidopsis plants (Vernooij et *al.*, 1994; Gaffney et *al.*, 1993; Dong, 1998). It has been shown, that although indispensable for SAR, SA is not the long sought mobile SAR signal (Vernooij et *al.*, 1994). Other discussed compounds are the volatile methylated form of SA (MeSA), the diterpenoid dihydroabietinal (DA) and the glycerol-3-phosphate (G3P), both dependent on the lipid transfer protein DEFECTIVE IN INDUCED RESISTANCE 1 (DIR1), azelaic acid (AzA) and the non-proteinogenous amino acid pipecolic acid (Pip) (Park et *al.*, 2007; Chaturvedi et *al.*, 2012; Chanda et *al.*, 2011; Maldonado et *al.*, 2002; Champigny et *al.*, 2013; Jung et *al.*, 2009; Yu et *al.*, 2013; Návarová et *al.*, 2012).

Role of amino acids in plant defense

Here we provide evidence that the massive changes of free amino acids upon pathogen attack indicate an important role during plant stress resistance. An infection with a virulent or avirulent hemibiotrophic *Pseudomonas syringae* strain induced massive changes in amino acid metabolism of the plant (Tab. 1; Návarová et *al.*, 2012). We aimed to understand the regulation of amino acid metabolism during plant pathogen interaction and comparatively analyzed levels of free amino acids in leaves inoculated with virulent and avirulent *P. syringae* bacteria and PAMPs (flg22). The levels of free amino acid accumulation in the local leaf of Col-0 differ among treatments. The strongest response is observed during the interaction with the incompatible HR-inducing *Psm avrRpm1* strain one day after inoculation, followed by compatible interaction with virulent *Psm* E4326 and PAMP (100 nM flg22) treatment. The observed changes in amino acid metabolism follow a very similar pattern, comparing compatible and incompatible interaction, as well as the response to PAMP-treatment. Pip-, Aad- and Lys- levels increase, while Asp level decreases upon *P.*

syringae attack. This indicates that Lys biosynthesis and catabolism is a pathogen-triggered event. The aromatic amino acids Phe, Tyr, Trp, and His also show a strong increase during compatible and incompatible interaction and upon PAMP treatment (Tab.1). The change observed in amino acid levels upon pathogen attack is therefore a shared and conserved mechanism during interaction with virulent, avirulent hemi-biotrophic bacteria or PAMPs. It would be very interesting to test how amino acids accumulate upon an infection with necotrophic bacteria, fungi, oomycetes or insects.

It has already been described in previous studies, that free amino acids have a great impact either direct or indirect on resistance development against pathogens and pests in plants.

The aromatic amino acids (AAAs) Phe, Tyr and Trp are derived from the shikimate pathway and accumulate in response to various abiotic and biotic stresses. AAAs are common precursors for phytoalexins, glucosinolates, phenolic compounds involved in plant defense, including flavonoids, condensed tannins, lignans and lignin (Maeda and Dudareva, 2012; Vogt, 2010). The AAA Phe is a common precursor for diverse phenylpropanoids for example flavonoids, isoflavonoids, coumarins, stilbenes, lignans and lignins that are not only indicators of plant stress responses upon abiotic stresses, but are also key mediators of the plants resistance towards pests (Vogt, 2010; La Camera et *al*., 2004). Trp is a precursor for phytoalexins and indolic secondary metabolites, e.g. indole-glucosinolates that possess antimicrobial activity and play an important role in plant-pathogen interactions and defense against herbivores (Halkier and Gershenzon, 2006). The Trp-derived phytoalexin camalexin has been widely studied in its role as defense component in various Arabidopsis-pathogen interactions (Glazebrook and Ausubel, 1994; Thomma et *al*., 1999; Roetschi et *al*., 2001; Ferrari et *al*., 2003). Induction of camalexin biosynthesis is triggered by reactive oxygen species (ROS) and depends on SA signaling, the glutathione status and involves the cytochrome P450 enzymes CYP79B2 and CYP71B15 (PAD3; Glawischnig, 2007). To ensure camalexin production, it is conceivable that Trp biosynthesis is triggered during pathogen attack and has a positive effect on plant resistance. The fact that one of the most prominent phytoalexins camalexin is a Trp-derived metabolite also indicates that the accumulation of Trp is a pathogen-triggered event.

Another group of free amino acids that significantly accumulated upon pathogen inoculation and PAMP treatment are the branched-chain amino acids (BCAAs) Val, Leu and Ile (Tab. 1). BCAAs also have been reported to accumulate after dehydration during osmotic stress (Nambrara et *al*., 1998). When plant cells are sugar starved, BCAAs accumulate and promote their own catabolism to provide alternative sources of respiratory substrate for the TCA cycle during severe plant stress (Taylor et *al*., 2004). Catabolic products of Val, Leu and

Ile are acetoacetate, propionyl-CoA and acetyl-CoA that serve as energy source for the plant (Taylor et *al.*, 2004). High concentrations of BCAAs also have cytotoxic effects and have to be removed via respiratory oxidation to avoid damage to the cells. The plant needs to find a balance between maintenance of a pool of branched-chain amino acid for protein synthesis while preventing their build-up to toxic levels (Taylor et *al.*, 2004). BCAAs may serve as substrates for the synthesis of stress-induced proteins and signals to induce gene expression (Nambara et *al.*, 1998). A direct link to defense related processes and signaling provides the BCAA Ile that forms a complex with JA. The conjugation product JA-Ile is the functionally active compound in JA-induced resistance and defense signaling pathway against necotrophs and herbivores (Thines et *al.*, 2007). Another compound involved in JA related defense responses is isoleucic acid (2-hydroxy-3-methyl-pentanoic acid; ILA) which is related to Ile and an endogenous substrate of the glucosyltransferase UGT76B1. ILA accumulated together with valic acid in Arabidopsis mutants of UGT76B1 and conferred resistance to bacterial pathogens and promoted the activation of SA biosynthesis and signaling (von Saint Paul et *al.*, 2011). The role of Ile thus might not be directly linked to defense responses triggered by *P. syringae*, but to a promotion of JA-induced repression of SA-associated defense responses induced by the pathogen to facilitate infection.

Proline levels do not increase upon infection with virulent or avirulent *P. syringae* strains or PAMP treatment, but slightly decrease (Tab. 1). Nonetheless, Pro has an important function in the response to abiotic, mainly osmotic, stresses and its protective function as an osmolyte might be due to its ROS scavenging activity (Smirnoff and Cumbes, 1989; Matysik et *al.* 2002). It was furthermore reported that the Pro catabolic enzyme, proline dehydrogenase (PDH), was SA-dependent and levels of PDH were elevated in HR cells upon avirulent pathogen infection. PDH-silenced plants exhibited less cell death and production of ROS, but increased susceptibility to avirulent pathogens (Cecchini et *al.*, 2011). We can say that Pro has no direct function in plant-microbe interaction and resistance development, but might serve as a substrate precursor for defense components.

Lys is a precursor for the non-proteinogenous amino acids Pip and Aad and accumulates upon pathogen and PAMP stimuli. The simultaneous decrease in level of Asp indicates that the activation of the biosynthetic pathway towards Lys is a pathogen-triggered event. The transient flux of Lys catabolism is very efficient and catabolism via the LKR/SDH pathway not only yields Aad, but also Glu. Glu itself serves as a precursor for stress-related metabolites like Pro, γ-amino butyric acid (GABA) and Arg. GABA is a stress-related signaling molecule and Arg might serve as precursor of polyamines and NO (Galili et *al.*, 2001). In animals, glutamate may itself act as signaling molecule of brain signal transmission, interacting with glutamate receptors on the surfaces of nerve cells in animals.

Lys catabolism via LKR/SDH and Aad is indeed significantly up-regulated in animal brain tissue and it has been hypothesized that there might be a function of glutamate receptors against herbivores in plants (Brenner et *al.*, 2000; Lam et *al.*, 1998). The accumulation of GABA has been reported to have an effect on the inhibition of neurotransmission in herbivores (Huang et *al.*, 2011). Indeed, very recently, GLUTAMATE RECEPTOR-LIKE genes (GLRs 3.2, 3.3 and 3.6) have been identified to control the distal wound-stimulated expression of several key jasmonate-inducible regulators of jasmonate signaling (JAZ genes). GLRs are related to ionotropic glutamate receptors (iGluRs) that are important for fast excitatory synaptic transmission in the vertebrate nervous system (Mousavi et *al.*, 2013). In our comparative amino acid analysis no significant changes in Glu, Pro, Arg and only a small increase in GABA upon bacterial infection or PAMP treatment in wild type leaves were observed (Tab. 1). The strong increase in Lys levels does not account for an increase in Glu, Pro and GABA, but rather in the biosynthesis of Pip and Aad. Another reason might be that most of the free amino acids have a role in resistance to herbivores. Jasmonic acid inducible proteins (JIPs) have been reported to catabolize the essential amino acids Arg and Thr in the mid gut of *Manduca sexta,* which leads to significant growth reduction of the larvae. Thus, plant enzymes can exert anti-nutritional effects on herbivorous insects by perturbing amino acid homeostasis in the digestive tract (Chen et *al.*, 2005).

Here we present results that indicate another role of Lys biosynthetic pathway in plant resistance, besides its role as a Pip precursor. The close homolog of *ALD1, AGD2-1* encodes a L,L-diaminopimelate aminotransferase that functions in Lys biosynthesis catalyzing the forward step leading to Lys production in plants (Fig. 1; Hudson et *al.*, 2006). The *agd2-1/AGD2-1* knock-down mutant shows a constitutive resistance phenotype, with enhanced SA and Pip levels, as well as *PR-1* and *ALD1* expression (Fig. 42; Song et *al.*, 2004a). A complete knock-out of *AGD2-1* results in embryo lethality (Song et *al.*, 2004a). Interestingly, in comparative amino acid analysis Lys and the Lys-catabolites Aad and Pip accumulate consitutively in the *agd2-1* mutant, although we hypothesised that the levels of Lys and Aad and Pip would be significantly reduced. Besides a significant increase in Lys, Aad and Pip, we find a so far unidentified peak of m/z 256 exclusively accumulating consitutively in *AGD2-1* deficient mutants *agd2-1*, but also in *agd2-1 ald1* (Fig. 42D + Fig. 43D). The constitutive resistance observed in *agd2-1* is absent in *agd2-1 ald1* mutants, emphasizing the importance of *ALD1* for the observed phenotype in *agd2-1* (Song et *al.*, 2004a). A conclusion by analogy, taking the mass spectra of L-tetrahydro-dipicolinate and L,L-diaminopimelate into account, suggests the identity of the unknown compound to be 5-carboxy-picolinate (Fig. 55; J. Zeier pers. communication). A possible explanation could be that *AGD2-1* does catalyze Lys biosynthesis, but via a production of L-tetrahydro-dipicolinate that accumulates in the *agd2-1* mutant. L-tetrahydro-dipicolinate might be directly reduced to

the stable 5-carboxy-picolinate, which is accumulating exclusively in *agd2-1* and *agd2-1 ald1* mutants as the unidentified peak of m/z 256.

L-tetrahydro-dipicolinate
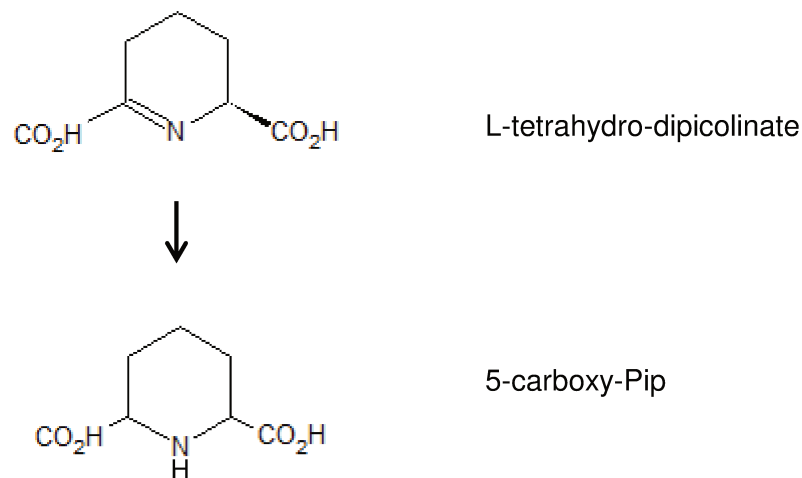
5-carboxy-Pip

Figure 55. Proposed chemical structure of 5-carboxy-Pip (m/z 256) accumulating in *agd2-1*. L-tetrahydro-dipicolinate will be reduced to the more stable form 5-carboxy-Pip and overaccumulates in *agd2-1* and *agd2-1 ald1* instead of being converted to L,L-diaminopimelate.

To confirm our hypothesis about the identity of m/z 256, authentic 5-carboxy-Pip would be needed as standard substance. Furthermore the question whether 5-carboxy-Pip itself is a signal that triggers the Lys catabolic pathway needs to be answered and might explain why Lys, AAD and Pip accumulate in *agd2-1* and *agd2-1 ald1*. The *agd2-1 ald1* double mutant had a lower basal level of total SA compared with the *agd2-1* single mutant, but still significantly more SA than the wild type. However, the disease susceptibility was equivalent in wild-type Col-0 (Song et *al.*, 2004a). It could be tested whether the accumulation of m/z 256 triggers SA-related defense responses. Further studies on the activity of AGD2 and ALD1 protein and their substrate specificity should be conducted to understand their role in Lys biosynthesis or catabolism and to place them at the right position in the Lys super pathway together with the correct conversion products that then can be identified using GC/MS.

Amino acid biosynthesis is regulated via PAD4

In comparative amino acid analysis of other free amino acids, we observe that PAD4 positively regulates the biosynthesis of aliphatic amino acids and Pip and negatively regulates the biosynthesis of amino acids like Asp, Glu, Orn, Lys and Trp during defense. In the wild type a decrease in Asp level and an increase in Lys is measured, while in the *pad4*

mutant Asp, Glu and Lys significantly increase upon pathogen attack compared to the wild type (Tab. 2). The negative regulation of Lys by PAD4 implies a control function in the defense associated biosynthesis and metabolism of Lys. Significantly increased levels of Glu in *pad4* mutants, compared to the wild type in pathogen inoculated leaves, indicate a possible function of PAD4 in repression of JA-related defense responses. As discussed before, Glu is involved in wound-induced JA signaling and JA biosynthesis might be controlled by PAD4 to ensure optimal SA-related defense responses. Interestingly in comparative amino acid analysis Trp levels are significantly higher induced in *pad4* mutants than Trp in Col-0 after pathogen attack. Due to the mutation in *pad4* that causes reduced camalexin levels and enhanced susceptibility of *pad4* mutants, we suppose that Trp is not further converted into camalexin and therefore accumulates upon pathogen attack in *pad4* (Tab. 2). Despite the function as regulator of ALD1 and Pip biosynthesis, the pathway of Asp-derived amino acid biosynthesis and Lys catabolism is controlled by PAD4. The positive regulatory role of PAD4 on Pip biosynthesis seems to be conserved among PTI and ETI and was the most prominent effect observed on the levels of free amino acids among the tested defense mutants. The biosynthesis of Aad underlies different regulatory mechanisms than Pip, but basal levels of both amino acids are elevated in the constitutively resistant *cpr5* mutant. The Aad biosynthesis is, unlike the Pip biosynthesis, dependent on SA-biosynthesis and FMO1, as well as SA-signaling. PAD4 seems to regulate Pip and Aad, as Aad levels are significantly reduced in *pad4* (Fig. 4A+B). The Aad biosynthetic pathway however, seems to be stronger regulated in an NPR1-dependent manner. Interestingly, distal Pip accumulation is significantly increased after *Psm* inoculation of the first leaves in the SAR-deficient *sid2-1* and *fmo1,* but not in *npr1* and *pad4* mutants (Fig. 5). A distal accumulation of Pip in *fmo1* and *sid2-1* mutants implies a remaining function of Pip in these mutants in the distal leaf. It remains unclear, whether the Pip measured is received from the vasculature produced in the local leaf, or whether it is *de novo* synthesized in the distal leaf. However, Pip measured in the distal leaf, depends on FMO1 and ICS1. Taken together an important question to be answered is whether the biosynthesis of all accumulating amino acids is regulated in a concerted manner, or whether particular defense components regulated distinct branches of amino acid metabolism. The role of branched-chain and aromatic amino acid accumulation in pathogen resistance is of special interest due to the accumulation patterns after pathogen attack. PAD4 seems to be specifically involved in the pathogen-induced biosynthesis of Pip and branched-chain amino acids but not in the production of aromatic amino acids (Fig. 56). The mutants tested, revealed that the regulatory principles of amino acid biosynthesis upon pathogen challenge are highly conserved and that the tendencies remain the same, independently of SA, JA or ET signaling pathways.
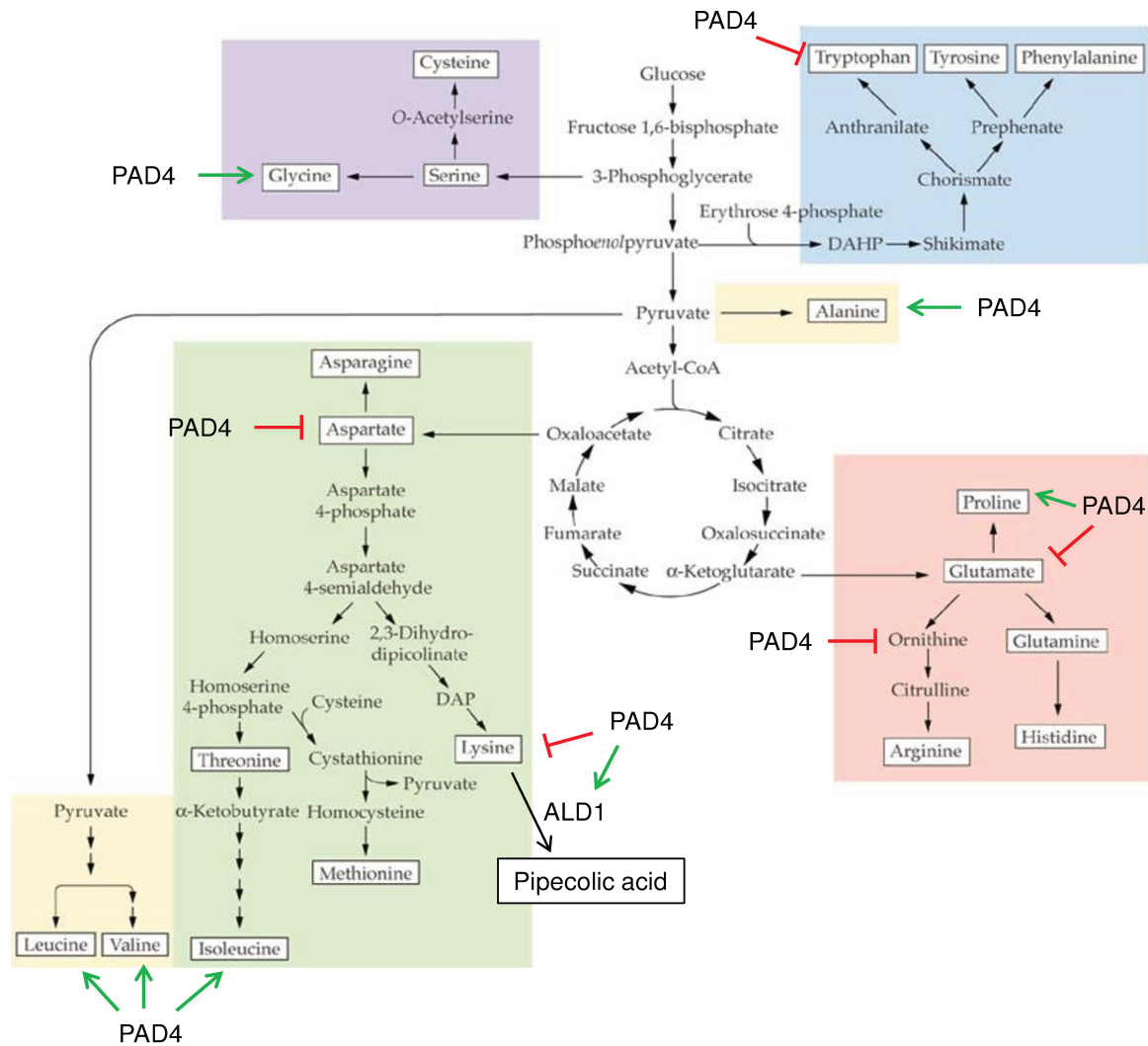
Figure 56. Scheme of amino acid biosynthesis in plants (http://www.uky.edu/~dhild/biochem/24/ASPP%208.2.jpg). Negative regulation via PAD4 is indicated with a red arrow and positive regulation is indicated with a green arrow.

For the future, we aim to better understand the role of branched-chain and aromatic amino acid accumulation in pathogen resistance. Therefore, pathogen-responsive candidate genes encoding aminotransferases and other enzymes with a predicted function in amino acid metabolism have been selected and corresponding Arabidopsis T-DNA lines and defects in those genes will be identified. Amino acid metabolism local and systemic resistance will be characterized in these lines to better understand the role of amino acid accumulation in plant-bacterial interactions. The identification of genes that are involved in pathogen-triggered accumulation of certain amino acids might reveal further significance of their role in plant pathogen resistance.

Pipecolic acid regulates SAR and defense priming via SA-dependent and SA-independent pathways

Our study reveals that Pip is an important regulator of defense priming and SAR, and that an SA-independent route to SAR establishment and priming via the Pip-biosynthetic and signaling pathway and FMO1 exists.

Pipecolic acid is an ubiquitous amino acid that is produced by various plant species, fungi, microorganisms and mammals (Morrison, 1953; Wickwire et *al.*, 1990; Zabriskie and Jackson, 2000; Fletcher et *al.*, 2001; Murthy and Janardanasarma, 1999). Lys-derived amino acid Pip accumulates after pathogen attack in the infected tissue, in the distal leaf and very interestingly in the phloem exudates of infected leaves (Návarová et *al.*, 2012). AGD2-like DEFENSE RESPONSE PROTEIN 1 (ALD1), a Lys aminotransferase is crucial for Pip biosynthesis and up-regulated during pathogen attack (Návarová et *al.*, 2012). The local resistance response is strongly attenuated in *ald1* and it is fully impaired in in systemic SA accumulation, β-aminobutyric acid (BABA)-induced resistance and SAR (Song et *al.*, 2004a; Návarová et *al.*, 2012). The metabolic changes during pathogen infection in the local and distal leaves as well as the petiole exudates, after infection with *P. syringae* have been studied, to investigate the effect of defense response on accumulation of free amino acids. Among the pathogen-inducible amino acids, Pip was the only one that accumulated in the distal leaf and the petiole exudates to a significant amount, indicating a possible movement throughout the plant vasculature in SAR long distance signaling (Návarová et *al.*, 2012).

To study the impact of SA-, JA and ET-biosynthetic and signaling pathways on the regulation of Pip and Aad biosynthesis, local leaves of defense mutants (*fmo1, pad4, npr1, sid2-1, coi1, dde2* and *etr1*) were inoculated with virulent and avirulent *P. syringae* strains. The results indicate that Pip biosynthesis one day after inoculation is independent of FMO1 and SA-biosynthesis (Fig. 4A-C). Furthermore, Pip biosynthesis seems to be dependent on a functional SA-signaling pathway in the early phase of defense during a compatible but not in an incompatible interaction (Fig. 4A+C). The JA- and ethylene signaling pathways have no impact on Pip biosynthesis (Fig. 4B). The lipase-like defense regulator PAD4 positively regulates Pip biosynthesis one and two days after inoculation in the local leaves (Fig. 4A+C) which is in line with the result of reduced expression levels of *ALD1* in *pad4* mutants after *P. syringae* infection (Song et *al.*, 2004a).

The Pip-deficient *ald1* mutant is severely compromised in SA accumulation, camalexin production and defense gene expression in the local leaf at the site of bacterial infection (Návarová et *al.*, 2012; Song et *al.*, 2004b). Endogenously produced Pip contributes to full PTI and ETI through amplification of defense responses and exogenously applied Pip

not only reduced disease symptoms in the wild type and *ald1* mutants, but also restored the ability of SA and camalexin biosynthesis (Fig. 9; Návarová et *al.*, 2012). Exogenous Pip has no positive influence on resistance induction in *fmo1* mutants, implying that FMO1 is required for SAR and Pip-induced resistance and acts downstream of Pip biosynthesis (Fig. 9; Návarová et *al.*, 2012). Exogenous Pip cannot enhance *P. syringae* resistance in *npr1*, but significantly increases bacterial resistance of the SA biosynthesis mutant *sid2/ics1* (Fig. 9). This indicates a function of *NPR1* downstream of Pip that is independent of its function in SA signal transduction. Thus, the regulation of *ALD1* expression and Pip biosynthesis via PAD4 and NPR1 seems to be more complex, as exogenous Pip does not induce a severe bacterial growth reduction that would induce an improved resistance phenotype. Therefore, PAD4 and NPR1 are required for Pip-induced resistance and SAR (Mishina & Zeier 2006; Jing et *al.* 2011; Návarová et *al.*, 2012). Furthermore, PAD4 positively regulates the transcription of *ALD1*, *FMO1* and *ICS1*, directly influences Pip and SA signaling pathways and is, like NPR1, required for Pip-induced resistance (Zhou et *al.* 1998; Jirage et *al.* 1999; Song et *al.* 2004a; Bartsch et *al.* 2006; Fig. 9). NPR1 functions, together with the orthologous proteins NPR3 and NPR4, as SA receptor (Fu et *al.* 2012) and as a downstream regulator of SA signaling triggering transcriptional activation of defense genes (Durrant & Dong 2004). Therefore we think that PAD4 and NPR1 also act downstream of Pip biosynthesis and signaling.

The systemic accumulation of Pip in SA-deficient *sid2-1* mutants (Fig. 5), the ability of Pip to induce resistance in an SA-independent manner (Fig. 9) and the accumulation of *ALD1* and *FMO1* transcripts in the distal leaves of *sid2-1* after inoculation with virulent and avirulent *P. syringae* (Fig. 7), points towards a SA-independent role of Pip in systemic defense responses. Exogenous SA induces resistance in *fmo1*, *ald1* and *sid2-1* mutants, indicating both that Pip and SA operate in separate pathways, or that SA functions downstream of Pip (Fig. 10). A role of Pip upstream of SA in SAR is conceivable since Pip accumulation precedes SA accumulation in the distal leaves (Návarová et *al.*, 2012). Pip is a water-soluble amino acid and would be suitable for long-distance transport to younger, distal parts of the plant via the plant vasculature. If Pip would be transported to the distal leaf, *ALD1* expression could be induced, or amplify *ALD1* expression that was already triggered by another SAR regulatory signal. Induced *ALD1* expression would induce Pip *de novo* synthesis in the distal leaf and lead to full Pip and SA accumulation and establishment of SAR (Návarová et *al.* 2012, Zeier, 2013).

To uncover the relationship between SA and Pip during ETI, PTI and SAR and the existence of a plant resistance pathway that is activated in an SA-independent manner in inoculated tissue, we crossed *sid2-1* and *ald1* mutants to generate a *sid2-1 ald1* double mutant deficient in pathogen inducible Pip and SA accumulation. In local resistance

experiments with Col-0, *sid2-1*, *ald1* and *sid2-1 ald1* it becomes clear that SA is most important for the establishment of basal resistance at the site of infection. SA-deficient *sid2-1* mutants exhibit a significant lower basal resistance, compared to *ald1* and the wild type. Interestingly the simultaneous loss of Pip and SA in the *sid2-1 ald1* double mutant contributes to an even higher degree of susceptibility, pointing to an additive effect of SA and Pip in local resistance (Fig. 19). However, local *PR-1* expression in *sid2-1 ald1* does not differ from expression observed in *sid2-1*, indicating that the SA-signaling pathway is affected in the same manner in *sid2-1* and *sid2-1 ald1* and cannot serve as an indicator of altered defense gene expression pattern due to the loss of Pip and SA (Fig. 16). All tested SA-deficient mutants, *sid2-1*, *eds5* and *ics1 ics2* show, besides the higher basal level of susceptibility, a modest, yet significant SAR response compared to Col-0 and *ald1* (Fig. 20). This reveals that indeed a Pip-dependent/SA-independent pathway in the establishment of SAR exists that is able to induce a partial and moderate bacterial growth reduction. The fact that all SA-deficient mutants show the same response proves the robustness of SA-independent resistance induction in the distal leaves. The Pip-deficient *ald1* mutant is fully compromised in SAR, but most interestingly *sid2-1 ald1* is also incapable of bacterial growth reduction during SAR (Fig. 20) We conclude from this that Pip is crucial for the establishment of SAR and that a SA-independent route via ALD1 and FMO1 towards SAR exists, but that SA is required for a full SAR response in the distal leaves.

We were interested to uncover the mechanisms behind the observed SA-independent SAR response and conducted two RNA-seq experiments with the objective to identify the SAR transcriptome in Col-0, the genes responsible for SAR establishment in SA-deficient *sid2-1* and genes differentially regulated genes in *ald1*. For the RNA-seq experiments, SAR (1) with Col-0 and *sid2-1* and SAR (2) with Col-0 and *ald1,* distal, untreated leaves were harvested two days after inoculation of *Psm* E4326 (OD 0.005). Comparing the transcripts of differentially expressed genes in Col-0, results in an overlap of 3925 genes that are common to both datasets and are considered to be the core SAR gene set (Fig. 21A). The transcriptional response in *sid2-1* is noticeable attenuated, as only 717 of the core SAR genes and 989 total genes are changed upon *Psm* inoculation in the distal leaf (Fig. 21B). This emphasized the impact of SA on defense triggered gene expression. Not only the pathogen triggered gene expression is affected, also the basal expression levels in mock treated *sid2-1* plants are markedly reduced compared to Col-0 (M) samples. The impact of Pip on gene expression during SAR is even greater, as only two genes from the whole dataset can be considered as significantly regulated during SAR (Tab. 9; Fig. 21C). However, the expression level in *ald1* after induction of SAR (P) is still lower than the basal expression level in the distal leaf of the mock treated Col-0 plant. An important role for this two candidate genes during SAR is therefore doubt worthy. Randomly picked genes from the

SAR (2) dataset confirm, that indeed a bit of a response is detectable in the *ald1* SAR leaf (Fig. 22A). This response is most probably not sufficient to gain a measurable outcome in resistance or defense reactions and explains why *ald1* plants were incapable to confer SAR.

In experiment SAR (1) we grouped the genes in three different categories. Category I includes SA-dependent genes that were up-regulated during SAR in the distal leaf of Col-0, but not in *sid2-1*. The mean expression values of the top 15 genes in category I are displayed in table 5 and sorted according to the highest fold change in Col-0 *P*/M. The first gene in the list is the *ACIDOREDUCTONE DIOXYGENASE3* (*ARD3*) that is part of the Yang cycle which is essential for ethylene production and polyamine and nicotianamine/phytosiderophore biosynthetic reactions (Pommerrenig et *al.*, 2011). Within the Yang cycle acidorecductone oxygenases (ARDs) convert 1,2-dihydro-3-keto-5-methylthiopentene (DHKMP) to 2-keto-4-methylthiobutyrate (KMTB) (Sauter et *al.*, 2005). Furthermore, the SA marker gene *PR-1* (position 6)*, GRXS13* (position 7), the lysine/histidine transporter *LHT7* (position 9) and *WRKY18* (position 12) are part of the SA-dependent SAR genes of Col-0 that were not expressed in *sid2-1*. The putative glutaredoxin GRXS13 increases susceptibility of Arabidopsis against the necotrophic fungus *B. cinerea*. Expression of *GRXS13* is negatively regulated by JA and positively by SA and limits basal and photooxidative stress-induced ROS production (La Camera et *al.*, 2011, Laporte et *al.*, 2012). The membrane-bound amino acid Lys/His transporter LHT7 is strongly flg22-responsive (Gruner et *al.*, 2013). WRKY transcription factor *WRKY18* is important for transcriptional regulation of biological SAR downstream of NPR1 and full SAR activation (Wang et *al.*, 2006). *WRKY18* forms a complex with two negative regulators of defense *WRKY40* and *WRKY60* that have partially redundant roles in response to different types of pathogens. Overexpression of *WRKY18* increases resistance to *P. syringae*, but simultaneous overexpression of *WRKY18* and *WRKY40* enhances susceptibility to *P. syringae* and *B. cinerea* (Xu et *al.*, 2006). The linkage between NPR1, WRKY transcription factors and transcript activation of SAR genes was earlier stated by Dietrich and colleagues who described the first map of a plant defense transcriptome during SAR (Maleck et *al.*, 2000). Gene-expression changes in *Arabidopsis thaliana* under 14 different either SAR-inducing or SAR-repressing conditions were monitored using a DNA microarray that represented approximately 25-30% of all *A. thaliana* genes. 413 ESTs (approximately 300 genes) were identified that were equally or greater than 2.5-fold expressed in at least two SAR-relevant samples. Conditions and treatments tested were either mutants with constitutive elevated SA-levels like *constitutive immunity* (*cim6/7/11*), a NPR1 overexpressor, *NahG* and *cim6 NahG* plants, BTH treatments (4 and 48h) or infections with virulent and avirulent pathogens *Peronospora parasitica* (Emwa1 and Noco2, respectively) and *Pst* DC3000 *avrRpt2* in Col-0 or Ws-0 genetic background. Based on regulation patterns, groups of genes or regulons

were defined. Since *PR-1* is a robust molecular marker for SAR, the regulon containing *PR-1* (45 ESTs, from a maximum of 31 different genes) was analysed more thoroughly, as it possibly contained genes with a function during SAR. The results indicated that several members of the *PR-1* regulon encoded proteins involved in redox regulation and were strongly activated in secondary SAR tissue. Members of the *PR-1* regulon were for example *PR-4*, *GST* (glutathione-S-transferase) and *PerC* (peroxidase C). Furthermore, it was found that expression changes during SAR were strictly dependent on *NIM1/NPR1*, suggesting a fundamental role in pathogen induced SAR gene activation. Notably, W-box motifs that clustered on *PR-1* regulon gene promoters were overrepresented, suggesting that WRKY factors (contain a cognate W-box) are crucial in coregulation of these genes (Maleck et *al.*, 2000).

Category IIa genes consist of SA-independent SAR genes, up-regulated during SAR in the distal leaf of Col-0 and *sid2-1*. The 15 most significantly up-regulated genes are sorted according to the highest fold change in *sid2-1* and therefore might uncover the genes that could be responsible for the SA-independent SAR response seen in the bacterial growth experiments. The gene on position number 1 is a TYROSINE AMINOTRANSFERASE (*TAT3*), a marker for wounding and JA (Yan et *al.*, 2007). The up regulation of genes involved in JA-biosynthesis and signaling might be a sign for an activated JA pathway in the absence of SA. Most strikingly, *ALD1* and *FMO1* are on position number 2 and 3, respectively. This emphasizes the importance of the Pip-biosynthetic and -signaling pathway in *sid2-1* during SAR (Tab. 6) and is in line with the result of the bacterial growth experiments and an involvement of Pip biosynthesis and FMO1 in SAR induction in SA-deficient *sid2-1* mutants. Furthermore, category IIa consists of other partially or completely SA-independent genes involved in defense for example a putative chitinase CHI (position 4), *PR2* (position 10)*, PAD3* (position 12) and *SAG13* (position 14). The SAR marker gene PATHOGENESIS-RELATED GENE 2 (*PR2*) encodes a β-1,3-glucanase and is partially SA-independent (Gruner et *al.*, 2013). Similar to *PR1, PR2* may have a direct impact on disease resistance, because the gene product has antimicrobial activity and can work synergistically with chitinases in the degradation of fungal cell walls (Mauch et *al.*, 1988). PHYTOALEXIN DEFICIENT 3 (*PAD3*), impaired in the production of camalexin, is defined as SA-independent, but still responds to exogenous SA (Gruner et *al.*, 2013; Zhou et *al.*, 1999). Other SA independent SAR-genes were the putative chitinase (*CHI*) and SENESCENCE-ASSOCIATED PROTEIN 13 (*SAG13*) that are also strongly inducible by ABA (Gruner et *al.*, 2013).

Category IIb genes consisted of SA-independent genes up-regulated in *sid2-1*, but not up or even down-regulated in Col-0. Genes of this category are not involved in the SAR

response of Col-0, but up-regulated in the absence of SA upon bacterial pathogen infection. Category IIb genes are sorted according to the highest fold change (log2) in *sid2-1* and compared to Col-0 *P*/M (Tab. 7). Unlike the genes in category I and IIa that are very severely affected in basal gene expression in the absence of SA, mean expression values of category IIb genes of the *sid2-1* mock (M) samples are even higher compared to Col-0 mock (M) (Tab. 7). Noticeably, the list contains genes that are clearly involved in JA biosynthesis like *ALLENE OXIDE SYTHASE* (*AOS*; position 10) and *ALLENE OXIDE CYCLASE2* (*AOC2*; position 15) and JA signaling like *PLANT DEFENSIN1.2A* (*PDF1.2A*; position 11) and *PDF1.2B* (position 3). We checked for the percentage of JA responsive genes in the RNA-seq dataset SAR (1). Interestingly, 38.9% of the genes up regulated in *sid2-1* and not up or even down-regulated in Col-0 are JA responsive. Up-regulated genes during SAR in Col-0 are to 3.9% JA responsive (Tab. 8). In the absence of SA during SAR, the usually repressed JA-responsive genes are induced upon pathogen infection in the distal leaf. The absence of SA and its negative regulatory effect on genes involved in JA biosynthesis and signaling is shown here. Due to the divergent role of SA and JA in resistance, the compromised basal resistance of *sid2-1* could be explained with the activation of the JA-defense pathway in the local leaf, facilitating bacterial infections. The enrichment in JA responsive genes in the group of down-regulated genes in Col-0 during SAR is also shown by comparing publicly available microarray data. JA-responsive genes are down-regulated during SAR and up-regulated in the absence of SA (Gruner et *al.*, 2013). Zeier and colleagues pointed out the difference between activation of JA responsive genes in local and distal leaves (Gruner et *al.*, 2013). Contrary to the distal leaf the JA pathway gets strongly activated at the inoculation site, leading to enhanced metabolite biosynthesis in the cause of gene activation, like for example the SA-methyltransferase *BSMT1*, the terpene synthase *TPS4*, cytochrome P450 monooxygenases (e.g. *CYP82G1, CYP94C1, CYP94B3, CYP79B2*), and UDP-dependent glycosyltransferases (*UGT76E12*, *UGT76E1*).

Category III genes are genes up-regulated in Col-0 and *ald1* during SAR and therefore Pip-independent SAR genes. This category only consists of two significantly expressed genes, *CRK6* and *PCR1* (Tab. 9). CYSTEINE-RICH RECEPTOR LIKE KINASES (CRKs) are one of the largest subgroups of receptor-like kinases in Arabidopsis. CRK6 is an active protein kinase involved in oxidative signaling induced by apoplastic ROS that is caused by O_3 and X + XO in *Arabidopsis thaliana* (Idänheimo et *al.*, 2014). PLANT CADMIUM RESISTANCE1 (AtPCR1) was identified in *Arabidopsis thaliana* as small plasma membrane protein with a Cys-rich domain, placenta-specific 8, involved in Cd resistance in plants because of its potential role in the efflux of heavy metals (Song et *al.* 2004). Arabidopsis plants and yeast overexpressing *PCR1* were more resistant to Cd (II) compared

to the corresponding wild type, whereas *PCR1* antisense plants were more sensitive (Song et *al.*, 2004).

We further wanted to check the effects of the SAR state on the metabolic processes in the distal leaf of Col-0. Differentially regulated genes were mapped to customized MapMan bins and changes were displayed as percentages of up- and down-regulated processes. Strikingly the effect of a primary infection in the distal leaf is strongest on genes involved in photosynthesis, including the Calvin-Benson-Bessham cycle, photorespiration, and the photosynthetic electron transfer, genes involved in tetrapyrrole synthesis, the major carbohydrate metabolism and anabolic pathways like N- and S-metabolism. Up-regulated MapMan categories include genes involved in redox processes, signaling, biotic stress, fermentation and the oxidative pentose phosphate (OPP) pathway (Fig. 23). While the photosynthetic apparatus and activity in Col-0 is shut down, only a minor response in the SAR leaf is observed in *sid2-1* and none at all in *ald1* (Fig. 25A+B; 26A+B). The loss of SA and Pip does not only have a direct impact on disease resistance, but also circumvent the reallocation of resources during defense. To check whether the transcriptional down regulation of genes involved in the photosynthesis also has an actual effect on photosynthesis, we measured the photosynthetic rate in Col-0, *sid2-1*, *ald1* and *sid2-1 ald1* in the distal leaf after a primary infection. Only in Col-0 the photosynthetic rate was significantly reduced after pathogen infection compared to the mock treated plant (Fig. 27A). SA- and Pip-deficient plants did not show a significant reduction in the photosynthetic rate during activated SAR (Fig. 27A). A reason for a reduced photosynthetic rate in Col-0 could be a closure of the stomata. We indirectly measured the stomatal closure by evaluation of the transpiration rate in the SAR leaf (Fig. 27B). Like the photosynthetic rate, the transpiration rate is significantly reduced in an SA- and Pip-dependent manner. A more direct approach would be to measure the stomatal opening after pathogen attack, after exogenous SA and Pip treatment, which might be a task for the future. Furthermore, the photosynthetic rate should be measured in a time course after pathogen infection, to investigate whether the observed reduction is a reversible process.

Defense priming is contributing to resistance during SAR as primed plants are able to react faster and stronger to a potential second threat (Conrath, 2011). Biologically-induced SAR priming is characterized by a strong potentiation of systemic accumulation and biosynthesis of the metabolites Pip, camalexin and expression of defense associated genes like *PR* genes, *ALD1* and *FMO1* upon a subsequent pathogen attack due to a potentiation of signaling events (Jung et *al*. 2009; Návarová et *al*. 2012). This puts the plant into an alarmed state for a faster response upon a pathogen threat to enable enhanced defense gene expression. This process is ALD1 dependent, as *ald1* mutants completely lack the systemic response and exhibit an attenuated local response and no increase of SA after a second

stimulus providing genetic evidence for a critical role of Pip in SAR priming (Návarová et *al.* 2012). It was observed that the priming of the phytoalexin camalexin and *PR* genes was completely absent in the Pip-deficient *ald1* mutant (Návarová et *al.*, 2012). Pip is a central regulator during SAR, because it is crucial for SAR establishment via a feedback amplification mechanism, triggering its own biosynthesis via enhanced *ALD1* expression, and endogenously mediating of defense priming (Návarová et *al.*, 2012).

Biological priming experiments were conducted to uncover the impact of SA and Pip on the production of the phytoalexin camalexin, total levels of SA and defense gene expression during defense priming induced by biological SAR. Priming of camalexin is dependent on both, SA and Pip, and an accumulation only occurs after a local *Psm* stimulus in the absence of Pip or SA (Fig. 28A). Because camalexin production is completely absent in *sid2-1 ald1*, we conclude that SA and Pip are both responsible for the local camalexin production observed in *ald1* and *sid2-1*, respectively. Furthermore, priming of camalexin and production in the local and systemic leaves after inoculation of *Psm* is strongly dependent on EDS1, FMO1 and PAD4 (Fig. 29). Total SA is primed in Col-0, but not in *ald1* (Fig. 28B). Like in the case of camalexin, free and bound SA does not accumulate upon a systemic stimulus. Priming of camalexin and SA is therefore fully dependent on Pip, FMO1 and the lipase-like defense regulators EDS1 and PAD4, emphasizing the importance of Pip and its signaling pathway for the establishment of systemic SA accumulation and priming during SAR in general. We conducted biological priming experiments of defense genes involved in SAR that were SA-dependent (*ARD3* and *PR1*), SA-independent (*FMO1*, *ALD1* and *SAG13*) or partially SA-dependent (*GRXS13*; Fig. 30). The results show that biological activated priming during SAR is dependent on SA and Pip. Whereas SA seems to have an important role for the gene expression in the local leaf, priming is only conferred in the presence of Pip, as Pip deficient mutants do not show any defense gene priming. The mechanisms of systemic gene expression, SA-dependent, or SA-independent are consistent with the phenomenon of priming. Endogenous Pip is crucial to induce resistance and defense gene priming during SAR.

Since exogenous Pip induces SA biosynthesis and strongly potentiates *Psm*-triggered camalexin production in *ald1* (Návarová et *al.* 2012), we wanted to test the impact of exogenous Pip treatment on *Psm*-triggered defense responses and priming in SA- and Pip-deficient mutants. Zeier and colleagues showed that exogenous Pip promotes a primed state similar to SAR and partially restores defense priming in *ald1* and thus is an endogenous mediator of defense priming (Návarová et *al.* 2012). We investigated the Pip- and *Psm*-induced resistance priming of camalexin production in Col-0, *ald1*, *sid2-1* and *sid2-1 ald1*. Priming of camalexin is induced in Col-0 upon exogenous Pip treatment, and partially

restored in all mutants tested (Fig. 31). Interestingly*, sid2-1 ald1* completely lacks the ability to induce production and priming of camalexin upon a biological stimulus, but exogenous Pip restores the ability of camalexin production in SA- and Pip-deficient mutants (Fig. 31). We furthermore investigated defense gene expression during Pip- and *Psm*-induced priming. Exogenous Pip triggers enhanced induction of *ALD1* to enforce its own biosynthesis and amplified expression of the downstream mediator *FMO1* (Návarová et *al.* 2012). Furthermore, exogenous Pip restores priming of camalexin in *sid2-1, ald1* and *sid2-1 ald1.* We also measured Pip-induced priming of the defense genes *FMO1*, *ALD1* and *PR-1* in Col-0, Pip- and SA-deficient mutants. Priming of *FMO1* is restored partially upon exogenous Pip-treatment. As proposed by Zeier and colleagues exogenous Pip might positively influence defense priming also because of the ability to endogenously trigger its own production (Návarová et *al.* 2012). A weaker priming response in *ald1* might hint to the impaired ability of self-amplification of *ALD1* and further Pip production. Priming of *FMO1* expression in *sid2-1* clearly is SA-independent and even stronger compared to the wild type, but dependent on a functional *ALD1* gene. This became more evident when *FMO1* priming in *sid2-1 ald1* was evaluated. Priming is restored in *sid2-1 ald1*, but due to a non-functional *ALD1* gene the expression of *FMO1* was not very strong. In Pip- and *Psm*-induced priming, the *Psm*-induced *FMO1* expression is much lower in *sid2-1 ald1*, compared to *sid2-1* and *ald1* (Fig. 32A). It is conceivable, that reduced expression of *FMO1* in the inoculated leaf might contribute to the enhanced susceptibility observed in *sid2-1 ald1* (Fig. 32A). Pip-induced priming of *ALD1* expression is independent of SA, emphasizing the impact of a functional *ALD1* gene and its self-amplification in the establishment of priming (Fig. 32B). The SA-dependent defense gene *PR-1* is primed upon exogenous Pip application in all mutants, but SA is needed for a full priming response (Fig. 32C).

FMO1 therefore is an important downstream mediator of priming and SAR. We wanted to investigate the effect of exogenous Pip on *ALD1* and *PR-1* gene expression, camalexin and total SA production in *fmo1* mutants. Pip-induced priming of *ALD1* and *PR-1* is absent in *fmo1* mutants and only expression in the local leaf is detectable (Fig. 33A+B). Camalexin accumulation and priming after exogenous Pip application is almost absent in *fmo1*, but still present compared to the strong priming in Col-0 (Fig. 33C). Also, priming of SA accumulation fully depends on a functional *FMO1* gene (Fig. 33D). This confirms that FMO1 is indispensable for the Pip-signaling pathway and Pip-induced defense priming. Furthermore, FMO1 is crucial for systemic induction of SA-related defense responses, including biosynthesis and signaling.

To further uncover the relationship and action mode between SA- and Pip- induced defense we combined the exogenous Pip treatment with SA-infiltration instead of *Psm*-

inoculation (Fig. 34A+B). *PR-1* gene expression was monitored in leaves of Col-0, *ald1*, *sid2-1, sid2-1 ald1, pad4, fmo1 and npr1*. Unlike in the Pip- and *Psm*-induced priming experiment the level of expression in SA-deficient mutants is now markedly enhanced. Thus, SA is indispensable for a wild type like *PR-1* expression and priming. Priming of *PR-1* expression is absent in *fmo1* mutants (Fig. 34B). This demonstrates that SA induced a local response, but *FMO1* is a central regulator of the priming response and priming of *PR-1* expression depends on a functional *FMO1*/Pip-signaling pathway to let the systemic signal go through to the primed leaves. Priming of *PR-1* is induced in *pad4* mutants upon Pip- and SA-treatment, but expression is not induced after sole Pip-application, whereas the SA-signaling mutant *npr1* is completely devoid in *PR-1* expression (Fig. 34B). *NPR1* is functioning upstream of *PR-1* in the SA-signaling pathway and without a functional *NPR1* gene no SA- or Pip-derived signal is going through to activate *PR-1* expression, showing that *NPR1* acts downstream of Pip, too. Lastly, the results showed that Pip-induced expression of *PR-1* is proceeding via *ICS1*, meaning endogenously produced SA, since there was no expression in *sid2-1* mutants observed.
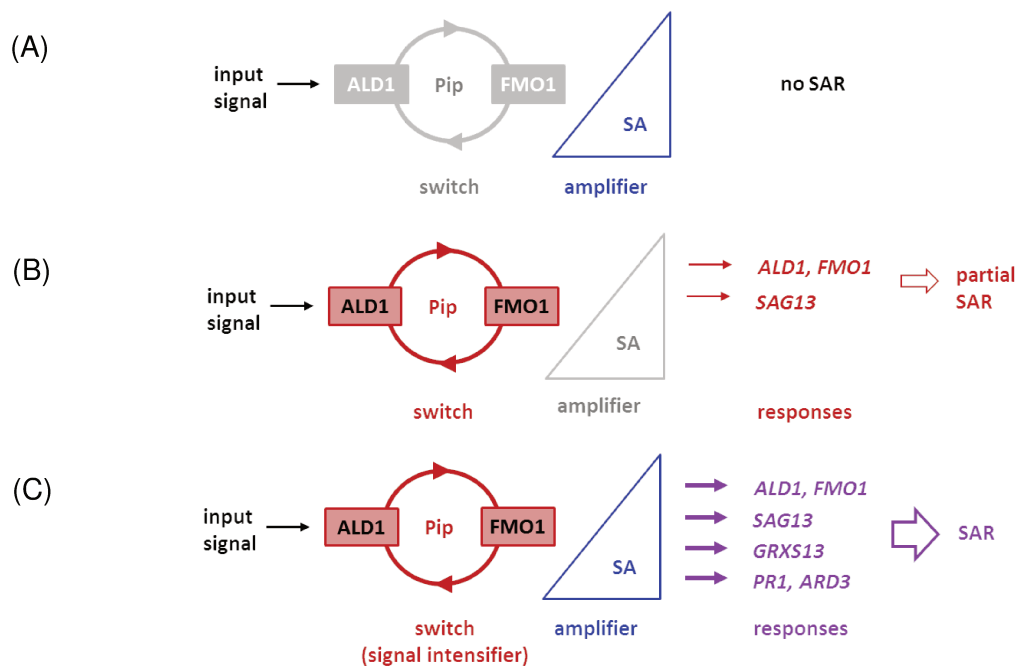
Figure 57. Hypothetical working model of SAR development. In the absence of Pip and SA no SAR will be established when the input signal reaches the distal leaf **(A)**. If the Pip/*FMO1* module is functional, *ALD1* expression will be triggered by the input signal in the distal leaf and a self-amplification loop leads to *de novo* Pip biosynthesis, *FMO1* expression and to partial SAR in the absence of SA **(B)**. A full SAR response is achieved with a functional Pip/*FMO1* module in combination with SA biosynthesis and signaling pathways. Pip and SA are both needed for defense responses like priming of SA-dependent defense genes **(C)**.

To conclude we have strong evidence for a scenario in SAR establishment, in which Pip is needed in the distal leaf to establish SAR in the first place (Fig. 57A). The input signal, the so far unidentified SAR-signal needs to be perceived in the distal leaf to trigger the *ALD1*, *FMO1* amplification loop leading to Pip production and accumulation. If SA is missing the SA-independent SAR machinery will be still working, leading to defense gene priming of *ALD1*, *FMO1* and *SAG13* and to partial SAR observed in SA-deficient mutants (Fig. 57B). The optimal defense situation for the plant however is the combination of an intensified Pip signal that leads to an enhanced *ICS1* expression and SA production, additional priming of SA-dependent genes like *PR-1*, *GRXS13* and *ARD3* and priming of camalexin (Fig. 57C). All this factors will finally lead to a full SAR response and bacterial growth inhibition. Due to the fact that Pip accumulated in the petiole exudates of *Psm*-infected leaves and is a watersoluble small molelcule, it is predestined to move throughout the plant vasculature. To prove our hypothesis that Pip itself, or a Pip-derivative could be the mobile SAR signal and is perceived in the distal leaf, where it would onset the Pip/FMO1 self amplification loop, grafting experiments with wild type, *ald1* and *fmo1* plants, tracer studies of radiolabeled Pip *in planta* and experiments to test the resistance inducing effect of wild type petiole exudates after pathogen infection, could be conducted.

ALD1 and FMO1 are separated at the subcellular level

To identify the subcellular sites of Pip production and catabolism was of special interest to contribute to a better understanding of Pip transport at the cellular and whole plant level. The results from the transient localization studies in *Nicotiana tobacco* show that *ALD1* and *FMO1* are located to the chloroplasts and the ER, respectively (Fig. 35; 37B; 40). Thus, ALD1 and FMO1 are separated at the subcellular level and Pip biosynthesis and catabolism therefore take place in distinct subcellular compartments. Subcellular or cell-to-cell transport of the immune regulator Pip will require specific membrane-bound transport proteins. Potential candidates are pathogen-inducible Pip transporter genes that are co-expressed with *ALD1* and *FMO1* in leaves inoculated with *Psm*, or systemic tissue. Taking this criteria into account, a list of candidate genes including candidates for putative Pip transporters was created from own and publicly available microarray data. In the future selected T-DNA lines of these transporters will be tested for the ability to enrich Pip in petiole exudates after leaf inoculation, for the level of Pip and *FMO1*-derived Pip oxidation products, and to develop SAR. To address the question whether Pip is moving throughout the plant vasculature, experiments with radiolabeled D9-Pip will be conducted and as well as grafting experiments.

Identification of candidates in the Pip metabolic pathway

We also wanted to uncover the complete Pip biosynthetic pathway including the intermediary steps (Fig. 2). We analyzed T-DNA knock-out lines of ORNCD1 (AT5G52810), one of our main candidates to commit the reduction step in the Pip biosynthetic pathway. One T-DNA line, *orncd1_2*, has significantly lower, but still considerable levels of Pip accumulating after pathogen attack, but it has no effect on resistance and SAR establishment (Fig. 48B; 50A). In the future, we will continue to test other T-DNA lines and will also consider the option that ORNCD1 might not work alone in this reaction. It is possible that another reductase, e.g. P5CR from the Pro biosynthetic pathway might compensate for ORNCD1. Stress induced Pro biosynthesis in the cytosol of Arabidopsis can be synthesized from Glu which is reduced to Glu semialdehyde by Δ^1-pyrolline-5-carboxylate (P5C) synthetase (P5CS). The resulting semialdehyde spontaneously cyclizes to P5C, the hydrogenation of the P5C imino bond is conducted by P5C reductase (P5CR) and results in Pro formation. Furthermore heterologous expression of *ORNCD1* in *E. coli* to produce protein for activity assays in combination with ALD1 would be interesting to identify the reaction product which is most likely Pip, when Lys is fed as a substrate.

Another candidate within the Pip metabolic pathway (Fig. 2) is the sarcosine oxidase/ pipecolate oxidase SOX/PIPOX (At2g24580), which was identified in rabbit as PIPOX catalyzing the conversion of Pip to P6C/Δ^1-piperideine-6-carboxylic acid *in vitro* (Goyer *et al.*, 2004). Hanson and colleagues showed that Arabidopsis RNAi lines of AtSOX accumulated Pip up to 6-fold and reduced Aad to 30-fold (Goyer et *al.*, 2004). In Pip feeding experiments we observed, besides a rise in Pip levels, also a rise of Aad in leaves of Col-0 and *ald1* (Fig. 8), indicating that Pip is converted to Aad. This might be a mechanism to regulate Pip levels. Arabidopsis SOX/PIPOX (At2g24580) knock-out line *sox/pipox_2* shows a significant increase in Pip levels after pathogen attack compared to Col-0 (Fig. 48A), suggesting that the conversion of Pip to Aad might be blocked in *soxpipox_2.* However, the mutant does not show an altered resistance phenotype (Fig. 50B). To uncover the role of SOX/PIPOX in Pip metabolism, we started to generate an overexpression line of *SOX/PIPOX*. Positive candidates that constitutively overexpress *SOX/PIPOX* are currently selected. Overexpression of *SOX/PIPOX* would prohibit the accumulation of Pip and affect resistance against pathogens. Furthermore it would allow insights into the role of Aad during pathogen attack in the local leaf.

VI. MATERIAL AND METHODS

VI.1. PLANT MATERIAL

Seeds of wild-type *Arabidopsis thaliana* (L. Heynth., Arabidopsis) ecotype Col-0 and Ler, mutants in Col-0 background *ald1* (SALK_007673), *orncd1_1* (SALK_131295)*, orncd1_2* (gk-428e01.01)*, sox/pipox_1* (SALK_017108c), *sox/pipox*_2 (SALK_099135c) from the SALK Institute collection (Alonso *et al.*, 2003) and *fmo1* (Mishina and Zeier, 2006), *npr1-2* (*npr1*, NASC ID: N3801), *pad4-1* (*pad4*, Glazebrook *et al.*, 1997), *cpr5* (Bowling *et al.*, 1997), *sid2-1* (*ics1*, Nawrath and Métraux, 1999), *ics1 ics2* (Garcion *et al.*, 2008), *eds5* (*sid1*, Nawrath and Métraux, 1999), *ndr1* (Century *et al.*, 1995), *agd2-1 (Song et al., 2004a),* Ler *rsp2/dhdps2-2* (Stuttmann *et al.*, 2011)*,* Ler *dmr4-1* (van Damme et al., 2009), *coi1-2* (Xu *et al.*, 2002), *dde2-2* (von Malek *et al.*, 2002), *etr1-1* (Bleecker *et al.*, 1988) and *sid2-1 ald1* were sown in soil. The 14-days-old seedlings were transferred into 120-ml pots containing a mixture of soil (Klasmann-Deilmann, Substrat BP3) vermiculite and sand (8:1:1). Plants were cultivated in a growth chamber at photoperiod 9 h day (110 µE m^{-2} s^{1}, 21 °C) and 15 h night (18 °C) cycle at 70% relative humidity. Plants were watered as needed. All experiments were done with 5-6-weeks old, naïve plants exhibiting a uniform appearance without any signs of stress.

Nicotiana tobacco (*Nicotiana tabacum* cv Samsun NN) plants were grown in 1.5 L pots with ready-mixed soil Growth conditions were 25/22 °C (night/day) under a 12-h photoperiod with full light intensity of 250 µE·m^{-2} s^{1}.

VI.1.1. CROSSING OF SID2-1 AND ALD1 TO GENERATE A DOUBLE MUTANT

For the generation of a *sid2-1 ald1* double mutant the respective single mutants *ald1* and *sid2-1* were used. To avoid the use of self-fertilized flowers, only closed flowers were used for crossing. For the male parent, open flowers that were visibly shedding pollen were selected. If the cross was successful, the silliques would have elongated after 3 days. All crosses were performed by emasculating the flowers of the recipient genotype and pollinating with the pollen from the donor. From every fertilized silique, the F1-seeds were collected individually and dried before planting. About 110 *sid2-1 ald1* plants were analyzed in the F2 generation. Two positive F2 candidates (*sid2-1 ald1* #6 and #51) were selfed and used for experiments. The position of the EMS-generated mutation in *sid2-1* results in a stop codon (TAA) at residue 449 instead of a glutamine (Wildermuth *et al.*, 2001). To discriminate for the EMS-generated mutation site specific primers were designed and the specific annealing temperature of 64 °C evaluated in a gradient PCR. To identify the homozygous T-DNA insertion of *ald1* by PCR, the method described by Alonso et al. (2003) was applied, using gene-specific primers (Návarová *et al.*, 2012). The primer pairs used to identify the single point mutation in *sid2-1* and the T-DNA insertion in *ald1* in the double mutant are shown in table 12. *sid2-1 ald1* did not show any detectable expression of *ICS1* and *ALD1*.

As control genomic DNA from Col-0 wild type and *sid2-1* was used, respectively. Positively identified double mutants were further checked for gene expression and content of salicylic acid and pipecolic acid.

Locus	Gene name	Primer ID	Primer sequence (5' to 3')
AT1G74710	*ICS1*	ICS1-fw	GCAAGAGTGCAACATCTATATTCTC
		ICS1-rev	CACAAACAGCTGGAGTTGGA
AT2G13810	*ALD*1	*ald1*-fw (LP)	TTACGATGCATTTGCTATGAC
		ald1-rev (RP)	TTTTAAATGGAACGCAAGGAG
		LB	TGGTTCACGTAGTGGGCCATC

Table 12. Primer sets used to identify *sid2-1 ald1* double mutant

VI.2. CULTIVATION OF PSEUDOMONAS SYRINGAE

The virulent pathogen *Pseudomonas syringae* pv. *maculicola* strain ES4326 (*Psm*) and the avirulent *Pseudomonas syringae* pv. *maculicola* ES4326 carrying the plasmid containing the avirulence gene pLAFR3::*avrRpm1* [*Psm(avrRpm1)*] were cultivated on King's medium B (King *et al.*, 1954) agar plates containing appropriate antibiotics. Agar plates for *Psm* were supplemented with 50 µg/L rifampicin (A2220, AppliChem), and for *Psm(avrRpm1)* with 50 µg/L rifampicin and 15 µg/L tetracycline (A2228, AppliChem).

VI.2.1. PSEUDOMONAS SYRINGAE RESISTANCE ASSAY AND INOCULATION PROCEDURES

P. syringae strains *Psm* ES4326 and *Psm (avrRpm1)* were cultured at 28°C (240 rpm) in King's medium B with appropriate antibiotics and used for inoculation at the following day. The bacteria were used in log growth phase and washed three times with 10 mM $MgCl_2$ (Acros Organics). *Psm* strain was inoculated with an optical density at 600 nm (OD600) of 0.005 for determination of local accumulation of metabolite and free amino acid levels, local gene expression, SAR induction and petiole exudates collection. For the second infiltration during a SAR assay in growth experiments *Psm* culture was diluted to OD600 0.001 and *Psm (avrRpm1)* to OD600 0.002. The bacterial solution was infiltrated with a needleless 1 mL syringe into the abaxial side. 10 mM $MgCl_2$ was infiltrated as mock treatment, if not indicated otherwise.

In a classical SAR experiment a plant was first inoculated with *P. syringae*, or 10 mM $MgCl_2$ in three lower (local) 1° leaves between 10-12 AM and two days later three distal leaves of a plant either were inoculated with *Psm*. Bacterial growth in the distal leaves during SAR was measured three days after the second treatment. For local growth assays plants were inoculated with virulent *Psm* (OD600 0.001) and levels of bacteria as well were assessed 3 days later. Three leaf discs of different infiltrated leaves were homogenized in 500 µL of 10 mM $MgCl_2$ and plated in appropriate dilutions on King's B medium containing 50 µg/L rifampicin. Colonies grown on agar plates were counted after 2 to 3 days

after incubation in 28 °C. For analysis of metabolite levels, and gene expression, local, treated leaves and distal, non-treated leaves were harvested. During biological defence priming, analysis of metabolite and gene expression was measured 10 hours after the second treatment in distal leaves inoculated with either 10 mM $MgCl_2$ or *Psm* (OD600 0.005).

VI.3. EXOGENOUS CHEMICAL TREATMENT

VI.3.1. PIPECOLIC ACID

One day prior to local inoculation or 1° treatments in case of a SAR experiment, 10 mL of 1 mM (10 µmol) D,L-pipecolic acid solution (S47167; Sigma-Aldrich) was pipetted onto the soil substrate of individually. Control plants were supplemented in the same manner with 10 mL of water only. 24 h post exogenous D,L-pipecolic acid/water treatment, leaves were inoculated with *Psm* (OD 0.005).

VI.3.2. SALICYLIC ACID

SA was infiltrated into leaves in a concentration of 0.5 mM SA (S5922; Sigma-Aldrich) with a pH of 7.0. Control infiltrations were performed with ddH_2O.

VI.3.3. FLAGELLIN EPITOPE FLG22

The *flg22* peptide from *P. aeruginosa* with the amino acid sequence QRLSTGSRINSAKDDAAGLQIA which represents the elicitor active domain of bacterial flagellin was ordered from EZBiolabs. *flg22* was diluted in 10 mM $MgCl_2$ to a final concentration of 100 nM (*flg22*) and infiltrated into leaves.

VI.4. DNA EXTRACTION

Genomic DNA (gDNA) was extracted from leaf of 5-week-old plants. Leaf material was homogenized with a tissuelyser (Qiagen, TissueLyser II) in Eppendorf tubes and resuspended in 800 µL of extraction buffer (1.5 M Tris-HCl pH 8.0; 1 M NaCl; 0.5 M EDTA; 10 % w/v SDS). The sample was heated for 5 min at 65°C and then 200 µL of chloroform was added. The plant material was pelleted by 5 min centrifugation at 14000 rpm. The supernatant (500 µL) was transferred to a new Eppendorf tube and precipitated with 2-propanol (1:1) for 10 min at -20 °C. The gDNA was pelleted by centrifugation 5 min, at 14000 rpm and the pellet was washed with 70% v/v ethanol, centrifuged and air-dried for 10 min. The dried pellet was dissolved in 30 µL of water (MolBio grade, AppliChem).

VI.4.1. CHARACTERIZATION OF T-DNA MUTANTS

The knock-out lines ordered were checked for insertion of the T-DNA fragment by three PCRs with gene-specific and T-DNA-specific primers. Genomic DNA of the respective T-DNA line was amplified in the first PCR with only gene-specific primers (RP+LP; Tab. 13) and another two samples were amplified with gene-specific primer RP or LP and LB primer specific for the T-DNA insertion (Tab. 13). Genomic DNA of Col-0 was amplified with all primer sets tested. The PCR was performed with 0.25

µM of each primer, 60 µM of each nucleotide, 0.25 U of Taq DNA polymerase (M0273; New England Biolabs) and 5X ThermoPol buffer in the final volume of 20 µL. PCR annealing temperature was 55 °C, polymerizing for 1 min for a total amount of 35 cycles. The PCR product was separated on a 1% w/v agarose gel with 0.5X TAE buffer [20 mM Tris; 10 mM boric acid; 0.5 mM EDTA] and 0.05 µg/mL ethidium bromide and visualized under UV light (GelDoc, INTAS). Based on the result of the three PCRs, seeds of plants homozygous in the T-DNA insertion were harvested and used for further experiments.

Gene name/ Locus	Mutant name	T-DNA line		Primer Sequence (5' to 3')
SOX/PIPOX/ AT2G24580	sox/pipox_1	SALK_017108c	LP	CACAACGGAGAGGAGACTCTG
			RP	TTGAAACTCCCATGCAACTTC
	sox/pipox_2	SALK_099135c	LP	AGTCTTCTGGCCTCTTTTTGC
			RP	CACAAATTCACGATCGCTATG
ORNCD1/ AT5G52810	orncd1_1	SALK_131295 (BH) (BW)	LP	AGCAATCATGGTACCATCTGC
			RP	AAGAAGGCATGAGGAGGAGAG
	orncd1_2	GK-428e01.01	LP	ATGATGACTGGTGGGTAGCAG
			RP	ATGTGAAATATTCGCAAACGC
			LBa	TGGTTCACGTAGTGGGCCATC
			GK: LBb1-3	ATTTTGCCGATTTCGGAAC

Table 13. List of primers used for characterization of T-DNA insertion lines.

VI.5. RNA EXTRACTION AND CDNA SYNTHESIS

Total RNA was isolated from frozen leaves using peqGOLD RNAPure reagent (PeqLab, Erlangen) following the manufacturer's instructions. RNA concentration was determined by absorption at 260 nm (BioPhotometer plus, Eppendorf) and 1 µg was treated with DNase I (EN0521; Fermentas) for 30 min at 37°C to remove genomic DNA. The DNase reaction was inactivated by incubation at 70°C for 10 min in the presence of 2.5 mM EDTA. The mRNA was converted to cDNA with the OligodT primers and the reverse transcriptase (205113; Omniscript RT Kit, Qiagen) according to the manufacturer's instructions. An equivalent of 11.3 ng of total RNA was amplified in the total 10 µL of reaction volume with 5 µL of SenziMix SYBR Green (SMP5-111C, Bioline) and 0.75 µM gene-specific primers (Table 14).

VI.5.1. QUANTITATIVE REALTIME PCR

The qPCR reaction was performed in triplicate in a Rotor-Gene Q apparatus (Qiagen) using the following cycling program: 95°C for 7 min, followed by 45 cycles at 95°C for 10s, 60°C for 30 s, and finally 72°C for 3 min. The gene encoding a polypyrimidine tract-binding (PTB) protein 1 (At3g01150) was used as a housekeeping gene. The data were analyzed using the Rotor-Gene Q 2.0.2 software, with a threshold of 0.1 of the normalized fluorescence. This corresponded to the exponential phase of the fluorescence signal. The resulting CT and E values were used to calculate the relative mRNA abundance according to the ΔΔCT method. The values of expression amplified with gene specific

151

primer were normalized to those of the reference gene and expressed relative to the MgCl$_2$-treated wild type control sample (Tab. 14).

Primer name	Primer sequence (5' to 3')	Usage
ALD1-FW	GTGCAAGATCCTACCTTCCCGGC	qRT-PCR
ALD1-RV	CGGTCCTTGGGGTCATAGCCAGA	qRT-PCR
ARD3-FW	CATGGACTTATGTGAGGTGTG	qRT-PCR
ARD3-RV	ACATCAAAGTATCCACTTCCTG	qRT-PCR
FMO1-FW	TCTTCTGCGTGCCGTAGTTTC	qRT-PCR
FMO1-RV	CGCCATTTGACAAGAAGCATAG	qRT-PCR
GRXS13-FV	GGTTGAGATTGGTGAAGAAGAC	qRT-PCR
GRXS13-RV	GCCATTAATATGAGCAGCCA	qRT-PCR
ICS1-FV	CTTCATTTGCTTCTCCAACAC	qRT-PCR
ICS1-RV	CACAAACAGCTGGAGTTGGA	qRT-PCR
ORNCD1-FV	CGATCACAAGCCCTGTCCGGC	qRT-PCR
ORNCD1-RV	GGTCACGAGCTTGACGCCCA	qRT-PCR
PR-1-FW	GTGCTCTTGTTCTTCCCTCG	qRT-PCR
PR-1-RV	GCCTGGTTGTGAACCCTTAG	qRT-PCR
SAG13-FV	GCGACAACATAAGGACGA	qRT-PCR
SAG13-RV	CTTCATTTGCTTCTCCAACAC	qRT-PCR
SOX/PIPOX-FV	AAGCTCCGCCGCGTATCAGC	qRT-PCR
SOX/PIPOX-RV	TGAGCCGCAGCCCATAACCG	qRT-PCR
PTB-FW	GATCTGAATGTTAAGGCTTTTAGCG	qRT-PCR; reference gene
PTB-RV	GGCTTAGATCAGGAAGTGTATAGTCTCTG	qRT-PCR; reference gene

Table 14. List of primers used for quantitative PCR.

VI.6. GAS CHROMATOGRAPHIC DETERMINATION OF DEFENSE METABOLITES

The determination of metabolites levels in leaves was performed by a modified vapor-phase extraction method (Schmelz *et al.*, 2004). Briefly, ca 150 mg frozen leaf tissue was homogenized with 600 µL of extraction buffer (H$_2$O : 1-propanol : HCl = 1 : 2 : 0.005). After addition of internal standards (D4-salicylic acid, dihydrojasmonic acid, indole-3-propionic acid; 100 ng each) and 1 mL of dichloromethane (KK47; GC ultra-grade, Roth), the mixture was vortexed thoroughly and phases separated at 14 000 rpm, for 1 min. The lower, organic phase was then removed, dried over Na$_2$SO$_4$. For methylation of the sample at room temperature, 2 µL of 2 M trimethylsilyldiazomethane (36,283-2, Sigma-Aldrich) in hexane were added to convert carboxylic acid groups into their corresponding methyl esters. The reaction was stopped after 5 min by adding 2 M acetic acid in hexane. Afterwards, the sample was subjected to a vapor phase extraction procedure (Schmelz *et al.*, 2004) using a volatile collector trap packed with Porapak-Q absorbent (VCT-1/4X3-POR-Q; Analytical Research Systems). The sample was completely evaporated under nitrogen stream at 70°C and final evaporation temperature was set to 200°C for 2 min. Samples were eluted from the collector trap with 1 mL dichloromethane. Finally, the sample volume was reduced to 30 µL in a stream of nitrogen, and then subjected to GC/MS analysis. To analyze the levels of glycosidically bound SA, the upper, aqueous phase was supplemented with 100 ng D4-salicylic acid for internal standardization and 1 mL of 0.1 M HCl and was heated to 100 °C for 30 min to convert the bounded SA to free SA. After cooling, the aqueous solution was extracted three times with 2 mL dichloromethane, and the combined organic

extracts were dried over Na_2SO_4. After removal of the organic solvent under a stream of nitrogen, the residue was dissolved in 400 mL of dichloromethane/methanol (3:1), methylated and subjected to vapor phase extraction as described previously. A volume of 4 µL of the sample mixture was separated on a gas chromatograph (GC 7890 A; Agilent Technologies) equipped with a fused silica capillary column (ZB-5MS 30m x 0.25mm, Zebron, Phenomenex) and combined with a 5975C (EI) mass spectrometric detector (Agilent Technologies). The initiation injection was at 250 °C and then the metabolites were separated by a temperature program: 50 °C/3min with 8 °C/min to 240 °C, with 20 °C/min to 320 °C/3 min, under constant flow of helium, 1.2 mL/min. For quantitative determination of metabolites, peaks originating from selected ion chromatograms were integrated. The area of a substance peak was related to the peak area of the corresponding internal standard [SA (m/z 120) – D4-salicylic acid (m/z 124) and camalexin (m/z 200)–indolepropionic acid (m/z 130)], and experimentally determined correction factors for each substance/standard pair were considered.

VI.7. GAS CHROMATOGRAPHIC DETERMINATION OF AMINO ACIDS

The amino acid levels were determined by the EZ:faast free amino acid analysis kit for GC-MS (Phenomenex), based on the separation and mass spectrometric identification of propyl chloroformate-derivatized amino acids (Kugler *et al.*, 2006). Homogenized leaf material (50 mg) was extracted with 200 µL of buffer (25% acetonitrile in 0,01 N HCl). The sample was shaken thoroughly for 15 min at room temperature and centrifuged at 14 000 rpm, for 4 min. Aliquot (100 µL) of supernatant was extracted following the EZ:faast user's manual (Phenomenex). The dry residue was then dissolved in 70 µL of dichloromethane and subjected to GC/MS analysis.

The sample mixture (3 µL) was separated on a silica capillary column (ZB-AAA 10m x 0.25mm, Zebron, Phenomenex). The initiation injection was at 250 °C and then the metabolites were separated by a temperature program: 70 °C/3min with 8 °C/min to 240 °C, with 20 °C/min to 320 °C/2 min, under constant flow of helium, 1.2 mL/min. For quantitative determination of individual amino acids, peaks originating from selected ion chromatograms were integrated: Gly (m/z 116), Ala (m/z 130), Val (m/z 158), β-Ala (m/z 116), Leu (m/z 172), Ile (m/z 172), GABA (m/z 130), Ser (m/z 146), Thr (m/z 101), Pro (m/z 156), Pip (m/z 170), Aad (m/z 244), Asp (m/z 216), Glu (m/z 84), Asn (m/z 69), Gln (m/z 84), Cys (m/z 248), Orn (m/z 156), Lys (m/z 170), His (m/z 282), Phe (m/z 148), Tyr (m/z 107), Trp (m/z 130), Homoserine (m/z 128) and m/z 256. The area of substance peak was related to the peak area of norvaline (m/z 158), which served as an internal standard or calculated as relative amount per g FW (Fresh weight) if no correction factor was determined. Experimentally determined correction factors for each amino acid were considered. Arg and Met could not be analyzed with the applied method.

VI.8. SUBCELLULAR LOCALIZATION OF ALD1 AND FMO1

For generation of a construct for subcellular localization of ALD1 and FMO1 the GATEWAY® system was used. Therefore primer pairs were generated that contained the attB1 and attB2 site, respectively.

Depending on the position of the yfp-fluorescence tag, either N- or C-terminal, the reverse primer either contained a STOP codon (stop) or not (nostop). Primer pairs used for localization are displayed in table 15, Fragments of *ALD1* and *FMO1* were generated by a Phusion PCR (Tab. 16A+B)

Primer name		Primer sequence (5' to 3')
attB1_*ALD1*	MSU 1	GGGGACAAGTTTGTACAAAAAAGCAGGCTTCATGGTCAGTCTAATGTTCTTTAG
attB2_*ALD1*_nostop	MSU 2	GGGGACCACTTTGTACAAGAAAGCTGGGTCATTGGTATTAGAAGTGGAA
attB2_*ALD1*_stop	MSU 6	GGGGACCACTTTGTACAAGAAAGCTGGGTCCTAATTGGTATTAGAAGTGG
attB1_*FMO1*	MSU 3	GGGGACAAGTTTGTACAAAAAAGCAGGCTTCATGGCTTCTAACTATGATAAGCTTACT
attB2_*FMO1*_nostop	MSU 4	GGGGACCACTTTGTACAAGAAAGCTGGGTCAGCAGTCATATCTTCTTTTTCTTC

Table 15. List of primers used for subcellular localization of *ALD1* and *FMO1*

(A)

Phusion® PCR	
Template	1 µL
5X buffer	10 µL
dNTP	1 µL
Forward primer	1 µL
Reverse primer	1 µL
Phusion® High-Fidelity DNA Polymerase	0.5 µL
ddH2O	35.5 µL

(B)

Phusion® thermocycler program		
Temperature	Time	Cycles
98°C	30 s	1
98°C	30 s	
50°C	15 s	35
72°C	20 sec/kb	
72°C	10 min	1
10°C	forever	1

Table 16. Master Mix and protocol **(A)** and thermocycler protocol **(B)** for Phusion PCR (Phu PCR) Phu-PCR products were extracted from the gel and purified according to the Qiagen QIAquick Gel Extraction Kit Protocol.

12.5 µL of 5 X loading dye were added to the PCR product, which was completely loaded on the gel (~60 µL) to two wells of a 1% agarose gel. The gel was running at 150 V for 50 minutes. The image was taken and the PCR band was excised from the gel and put into a 1.5 mL Eppendorf tube. 450 µL of QG buffer were added and the gel fragment melted in the buffer at 55°C for 10 min. 150 µL of Isopropanol were added and the mixture was added into the provided column of the kit. The columns were centrifuged at 13,000 xg for 1 min and the flow through discarded. 500 µL of QG buffer were added to the column to wash away last traces of gel on the membrane. Again the columns were centrifuged at 13,000 xg for 1 min. The flow through was discarded, 750 µL of PE buffer were added

to the column and centrifuged at 13.000 xg for 1 min. Afterwards the columns were transferred to a new tube. To dilute the PCR product, 10-50 µL of ddH2O were added, depending on the intensity of the PCR products in the agarose gel.

VI.8.1. GENE CLONING AND TRANSIENT EXPRESSION IN NICOTIANA TOBACCO

VI.8.1.1.Creating entry clones using the BP recombination reaction

For the BP reaction 0.5 µL of the clean PCR product, 0.5 µL of the pDONOR 207 (150 ng/µL), 3 µL of 1X TE buffer and 1 µL of BP clonase II were mixed in an 1.5 mL Eppendorf tube and incubated at 25°C for at least 2 hours. 1 µL of the Proteinase K solution was added to each reaction and incubated for 10 min. at 37°C.

Chemical competent DH5α *E. coli* cells were thawed on ice. 1 µL of the BP reaction was added to the cells and mixed gently. The *E. coli* cells were incubated on ice for 30 min. Afterwards the cells were heat-shocked for 30 seconds at 42°C without shaking and placed directly on ice for 2 minutes. 250 µL of room temperature LB medium (LB = Luria Bertani; 10 g tryptone, 5 g yeast extract, and 10 g NaCl in 950 mL deionized water, pH 7.0, no antibiotics added) were added to each vial and incubated at 37°C for 1 hour in a horizontal shaker (225 rpm). The transformation was diluted 1:10 in fresh LB medium before plating. 100 µL from each transformation was spread on a pre-warmed selective LB-plates and incubated overnight at 37°C.

VI.8.1.2. Creating expression clones using the LR recombination reaction

For the LR recombination 2 µL of the BP recombination were mixed with 0.5 µL of the respective pDEST vector (150 ng/ µL), 1.5 µL 1X TE buffer and 1µL of LR clonase II and incubated at 25°C overnight (Tab. 17). The transformation into DH5α *E. coli* was performed as described for the BP recombinant reaction.

Name of vector	Purpose	Features of vector	*E. coli* selection marker	Plant selection marker
pDONOR207	pENTR vector		Gentamycin	/
pEarleyGate 101	pDEST vector	5'-35S-Gateway-YFP-HAtag-OCS-3'	Kanamycin	BASTA
pEarleyGate 104	pDEST vector	5' 35S-YFP-Gateway- OCS-3'	Kanamycin	BASTA
pGW2YFP	pDEST vector	5' 35S-Gateway-YFP-3'	Spectinomycin	Kanamycin
pEarleyGate 100	pDEST vector	5' 35S-Gateway-3'	Kanamycin	BASTA
pGWB540	pDEST vector	5' Gateway-YFP-3'	Spectinomycin	Hygromycin

Table 17. List of pDEST vectors used for subcellular localization of *ALD1* and *FMO1*.

To analyze the transformants 10 colonies were picked with a toothpick and placed in 3-5 mL LB medium containing the appropriate antibiotics and incubated at 37°C overnight in a horizontal shaker. Plasmid DNA was isolated the next day using the Wizard® *PlusSV* Minipreps DNA Purification System.

To isolate plasmid DNA 5 mL of culture was spun down at 10,000 ×g for 10 min. The cell pellet was resuspended with 250 μL suspension solution. 250 μL cell lysis solution was added and the tube inverted for 4 times to mix. 10 μL of Alkaline Protease Solution was added to the solution and invert 4 times to mix. Incubate 5 minutes at room temperature. 350 μL of neutralization solution was added and inverted 4 times to mix. The lysate was centrifuged at top speed for 10 min at room temperature. The spin column was inserted into a collection tube and the cleared lysate decanted into the spin column. After centrifugation at top speed for 1 min at room temperature the flow through was discarded and the column reinserted into a collection tube. For the first wash step 750 μL of wash solution was added and centrifuged at top speed for 1 min. The flow through is discarded and 250 μL of wash solution added to the column and centrifuged at top speed for 2 min. After removal of the flow through, the spin column was centrifuged again to remove all traces of wash solution. The column was inserted into a new 1.5 mL microcentrifuge tube. 30 μL of nuclease free water was added to the spin column and centrifuged at top speed for 1 min at room temperature. The plasmid DNA was stored at -20°C.

VI.8.1.4. Agrobacterium transformation

For transient plant transformation, the binary vector constructs were transformed into the *Agrobacterium tumefaciens* strain GV3101:pMP90RK. 5 μL of LR plasmid DNA were added to 90 μL of 10% glycerol and 5 μL of GV3101 competent cells. The mixture was incubated on ice for 5 minutes and transferred to a cuvette (1mm). The electroporation machine was set to 130-200 Ω and a charging voltage of 1.44 kV. The cuvette was placed into the electroporation chamber and the pulse activated for approximately 5 ms. Immediately 1 mL of LB medium was added and the mixture transferred to an Eppendorf tube incubated at room temperature for 1 h without agitation. The cells were plated on selection plates containing the appropriate antibiotics and grown at 28°C overnight.

VI.8.1.5. Transient expression of cDNAs in Nicotiana tobacco

For transient plant transformation, the transformed GV3101:pMP90RK carrying the desired binary vector constructs were grown overnight in LB medium with appropriate concentration of antibiotics. The culture was incubates at 28°C for 24 h to an OD of 0.02 - 0.1 and 20 μL of the cultures are transferred to an 1.5 mL Eppendorf tube and spun down at 5000 xg for 5 min. After removal of the supernatant the pellet was suspended in 500 μL of ddH$_2$O. The solution was infiltrated with a needleless syringae into the fully expanded tobacco leaf as described by Witte et *al.* (2004). The tobacco plant was incubated for 48hours before observing the fluorescent signal using a confocal

microscope (LSM Meta 510). One day later the leaf tissue were mounted in water and viewed using a Laser Scanning Microscope LSM 510 (Carl Zeiss Microscopy, Germany). YFP, GFP and chlorophyll was visualized using a laser excitation wavelength of 514, 458 and 633 nm, respectively and a band pass of a 460- to 510-nm band pass for CFP, a 520- to 555-nm band pass for YFP, and a 650-nm long pass for chlorophyll.

VI.8.1.6. Detection of YFP-fusion in tobacco using western blot

VI.8.1.6.1. Isolation of total proteins

50 mg of fresh leaf tissue were collected and ground using liquid nitrogen. 500 μL of protein extraction buffer was added (Tab. 18). The tissue lysate was vortexed for 30seconds and incubated at 70°C for 10 minutes. The solution was centrifuged twice at 13.000 xg for 5 minutes at room temperature. The supernatant was transferred to a new tube.

Protein extraction buffer
60 mM Tris-HCl (pH 8.8)
2% SDS
2.5% Glycerol
0.13 mM EDTA (pH 8.0)
1X peroxidase inhibitor cocktail

Table 18. Protein extraction buffer

VI.8.1.6.2. SDS-PAGE electrophoresis and membrane blotting (NuPAGE gel system)

7.5 μL of total protein were plus 2.5 μL of 4x NuPAGE LDS sample buffer (Invitrogen) were loaded on a 4-12% NuPAGE (Invitrogen) gel together with 10 μL of protein marker. To separate the proteins the gel was running for 1 hour at 200 V and 120 mA. The proteins were transferred to a polyvinylidene fluoride (PVDF) membrane. First the membrane was activated by washing with 100% methanol. The transfer buffer contained 10% methanol and 10X transfer buffer (NuPAGE Invitrogen).

VI.8.1.6.3. Blocking and probing the YFP-fusion proteins

The membrane was removed from the blotting apparatus and blocked with 3% BSA in 1X TBST buffer at 4°C overnight. The next day the membrane was incubated with the Anti-GFP antibody in 3% BSA in 1X TBST buffer at room temperature for an hour. The membrane was washed with 1X TBST buffer three times for 5 min. After washing the membrane it was incubated with the second Antibody (Goat Anti-Rabbit IgH (H+L), Peroxidase Conjugated) in 3% BSA in 1X TBST buffer at room temperature for 1 hour. The membrane was washed with 1X TBST buffer four times for 10 min.

The blot was incubated with either 0.5X or 1X of Super Signal West Dura Substrate Working Solution for 5 minutes and afterwards exposed to an x-ray film for a 1 min or less.

VI.9. ISOLATION OF THE NATIVE PROMOTER OF ALD1

We isolated the predicted native promoter of *ALD1* (1.5 kb) with a two-step PCR protocol to generate a construct containing the promoter sequence and the ALD1 full-length protein. The principle of the two-step-PCR is that the PCR product of the first PCR is used as template in the second PCR. For the isolation of the native promoter of *ALD1* a region of approximately 1.5 kb upstream of the START codon on the chromosome was chosen. Primer pairs were designed with the purpose to later clone the fused fragment into the pDEST vector pGWB540 using the GATEWAY® system (Tab. 19).

Primer name		Primer sequence (5' to 3')	Fragment
attB1_pALD1 (-1.5kb)	MSU 48b	GGGGACAAGTTTGTACAAAAAAGCAGGCTTCCGAATTATTCTC TTTGGAAATATTTCTCC	-1588 to 0
attB1_pALD1 (-1kb)	MSU 49b	GGGGACAAGTTTGTACAAAAAAGCAGGCTTCTACTAGTGATGAC ATGCTATAAAAGTC	-1088 to 0
pALD1+ALD1-FW	MSU 50	CAAGTAAAGAATGGTCAGTCTAATG	overlap
ALD1+pALD1-RV	MSU 51	CATTAGACTGACCATTCTTTACTTG	overlap
attB2_ALD1 NO STOP	MSU 52	GGGGACCACTTTGTACAAGAAAGCTGGGTCATTGGTATTAGAA GTGGAA	+1371 to 0

Table 19. List of primers used for isolation of the native *ALD1* promoter and full-length ALD1 protein
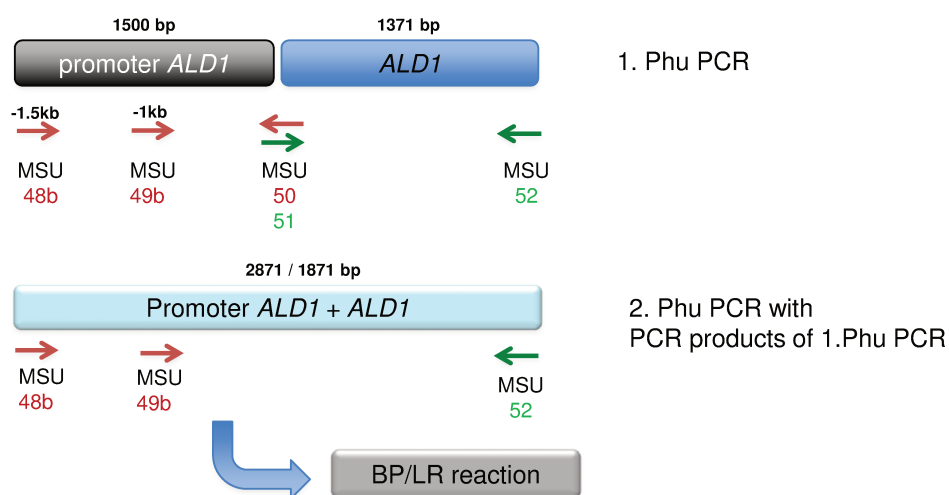
Figure 58. Two-step PCR strategy to isolate the native promoter of ALD1 and full-length ALD1 protein

Two first Phu PCRs were performed to obtain the fragment of the predicted promoter region upstream of the START codon of *ALD1*, amplified from genomic DNA of Col-0 with the primer set MSU 48b/49b

+ 50. And secondly the ALD1 full-length protein was amplified from Col-0 cDNA with the primer set MSU 51 + 52. The forward primer MSU 48b/49b contained the attB1 sites to later clone it into the pENTR and the pDEST vectors. The reverse primer MSU 50 was overlapping the genomic and the cDNA sequence. The reverse primer MSU 52 contained the attB2 site to later clone it into the pENTR and the pDEST vectors. The forward primer MSU 51 was overlapping the genomic and the cDNA sequence. The PCR products of both PCRs were loaded to a 1% agarose gel, excised and purified using a Qiagen QIAquick Gel Extraction Kit Protocol. The purified PCR products were used in equal amounts as templates for a second Phu PCR that should combine both fragments to one long construct containing the predicted promoter region of *ALD1* and *ALD1* full-length mRNA sequence (Fig. 58). This fragment was then cloned with GATEWAY® based system into the pDONR207 and in an LR reaction into the pDEST vector pGWB540. Transformation of *A. tumefaciens* GV3101 was carried out and floral dipping Arabidopsis transformation of *ald1* mutant plants and Col-0 wild type was conducted. Selection of positive transformants needs to be continued in the future.

VI.10. GENERATING AN SOX/PIPOX OVEREXPRESSION LINE

Full-length *SOX/PIPOX* was amplified with primer pairs MSU 13 and MSU 14 in a Phusion PCR (Tab. 20). The PCR product was loaded to a 1% agarose gel, excised and purified using a Qiagen QIAquick Gel Extraction Kit Protocol. The purified PCR product was cloned in a GATEWAY® clonase reaction into the pDONR207 and pEARLEYGate100 as described in *VI.8.1.1+2*. Sequenced constructs were transformed in *A. tumefaciens* GV3101. GV3101 carrying the binary vector construct p35S::*SOX/PIPOX*-YFP were transformed with the floral dip protocol into *Arabidopsis thaliana* Col-0 plants. Positive transformants were selected with BASTA on soil. Selected seedlings were transferred to single pots and seeds harvested. Due to time restrictions further selection should be carried out to identify over expression SOX/PIPOX lines.

Primer name		Primer sequence (5' to 3')
attB1_*SOXP*	MSU 13	GGGGACAAGTTTGTACAAAAAAGCAGGCTTCATGGAATATTCCGACGACG
attB2_*SOXP*_stop	MSU 14	GGGGACCACTTTGTACAAGAAAGCTGGGTCTTAATGTTTCAATGGGACATCAAG

Table. 20. List of primers used for generation of a *SOX/PIPOX* overexpression line.

VI.11. FLORAL DIP - STABLE TRANSFORMATION OF ARABIDOPSIS THALIANA

Healthy Arabidopsis plants were grown until they were flowering under long day conditions. The first bolts were clipped to encourage proliferation of many secondary bolts. Approximately 4-6 days after clipping plants were ready for transformation. GV3101 *Agrobacterium tumefaciens* strain carrying the gene of interest on a binary vector was grown in a large liquid culture at 28°C in LB with antibiotics to

select for the binary plasmid, overnight in a horizontal shaker (240 rpm). Mid-log cells or a recently stationary culture were used for transformation. The culture was spun down and resuspended to OD600 = 0.8 in 5% sucrose solution. 400-500 mL of culture/sucrose mixture was prepared for each two or three 3.5" (9cm) pots. Before dipping, Silwet L-77 was added to a concentration of 0.05% (500 µL/L) and well mixed. Above ground parts were dipped in Agrobacterium solution for 2 to 3 seconds, with gentle agitation. Dipped plants were placed under a cover in the dark for 16 to 24 hours to maintain high humidity. Afterwards, plants were grown und watered normally under long day conditions. Seeds were harvested and dried before used for selection of transformants using the appropriate antibiotic or herbicide marker. Sterilized seeds were plated on 0.5X MS/0.8% tissue culture agar plates with 50 µg/mL kanamycin, cold treat for 2 days, and grow under continuous light (50-100 µE) for 7-10 days (Bechthold et *al.*, 1993 and Clough and Bent, 1998).

VI.12. CELL FREE EXPRESSION SYSTEM (5 PRIME)

To obtain *ALD1* and *FMO1* protein for enzyme activity assays we used the RTS™ 100 Wheat Germ CECF Kit according to the manual for eukaryotic cell-free protein synthesis based on wheat germ lysate. Full-length *ALD1* was amplified in a Phu PCR using the primer set pIVEX1.4_*ALD1*_fwd and pIVEX1.4_*ALD1*_rev. Full-length *FMO1* was amplified in a Phu PCR using the primer set *FMO1*_EcoRI_fwd and *FMO1*_Xbal_rev. Purified PCR fragments were sub cloned into the pGemTeasy before cloned into the translation vector pIVEX1.4. For *ALD1* restriction sites NotI/NcoI and for *FMO1* restriction sites EcoRI/XbaI were introduced. The cell free expression was performed according to manufacturer's instructions for the 5 Prime RTS™ 100 Wheat Germ CECF Kit. ALD1 protein was checked in a SDS-PAGE gel and western blot using anti His-tag antibody (ab18184; abcam, Cambridge).

Primer name		Primer sequence (5′ to 3′)
pIVEX1.4_*ALD1*_fwd	HHU 129	GCGGCCGCATGGTCAGTCTAATGTTCTTTAGTTCG
pIVEX1.4_*ALD1*_stop_rev	HHU 130	GGTACCATTGGTATTAGAAGTGGAAGAGAGATAAG
*FMO1*_EcoRI_fwd	MSU 48	CACACGAATTCATGGCTTCTAACTATGATAAGCTTACT
*FMO1*_Xbal_rev	MSU 49	CACACTCTAGATTACTAAGCAGTCATATCTTCTTTTTCTTC
*FMO1*_G644_fwd	MSU 40	GTCATCGCCTTCAAGAAATCC
*FMO1*_G644_rev	MSU 41	GGATTTCTTGAAGGCGATGAC
*FMO1*_G50_fwd	MSU 42	CATCATCGCTGCTGGTGT
*FMO1*_G50_rev	MSU 43	ACACCAGCAGCGATGATG

Table 21. List of primers used for cell free expression of *ALD1* and *FMO1* in pIVEX1.4

Mutations in the FAD- and NADPH-binding sites of *FMO1* were introduced via a two-step PCR (Fig. 59A+B) using the primer sets displayed in table 21.
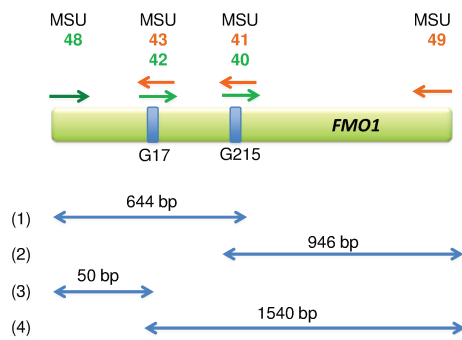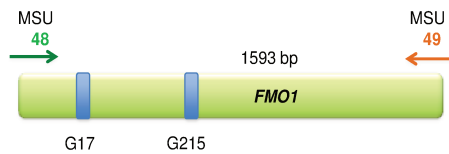
Figure 59. Two-step PCR strategy to introduce single point mutations in the FAD- (G17) and the NADPH- (G215) binding site of *FMO1*.

VI.13. RNA-SEQ: RNA EXTRACTION, LIBRARY CONSTRUCTION AND SEQUENCING

Plant material was extracted with the Plant RNeasy extraction kit (Qiagen, Germany). RNA was treated on-column (Qiagen, Germany) and in solution with RNA-free DNAse (New England Biolabs, MA, USA). RNA integrity, sequencing library quality and fragment size were checked on a 2100 Bioanalyzer (Agilent, CA, USA) and used if the RIN was above 6. Libraries were prepared using the TruSeq RNA Sample Prep Kit v2 (Illumina, San Diego, CA) and library quantification was performed with a Qubit 2.0 (Invitrogen, Germany). Illumina libraries were prepared according to the Illumina TruSeq protocol, sequenced on the HISEQ2500 Illumina platform (San Diego, CA) in the single end mode (SE) with lengths for RNA-seq experiment I (Col-0 and *sid2-1*) of 50 nucleotides and for RNA-seq experiment II (Col-0 and *ald1*) of 80 – 100 nucleotides. Single end sequenced leaf samples were multiplexed 12 libraries per lane with approximately 150 million reads per library. Results were demultiplexed and mapped to the *Arabidopsis thaliana* genome by CLC bio genomics workbench© with default parameters (alignment over at least 80% of the length of the read, up to three mismatches allowed) without alternative transcript detection. Differential expression was calculated using edgeR on raw read counts as implemented in Bioconductor (Robinson et *al.*, 2010). Genes are called significantly differentially expressed if the FDR is at or below 1% (Benjamini and Hochberg, 1995). Reads per million (rpm) are reported for all transcripts. Rpm were averaged for the three replicates of each condition and the log2 of pseudo fold-changes were calculated by adding one read to all rpm values (to account for transcripts with no expression detected in one or more samples) before fold-

change calculation and logarithmic transformation (Bräutigam et *al.*, 2011). Arabidopsis transcripts are annotated with descriptions from TAIR10 (Swarbreck et *al.*, 2008) and functional annotations from Mapman (Thimm et *al.*, 2004). Overlapping and exclusive membership in the significantly changed genes were calculated with Linux functions.

VI.14. GAS EXCHANGE MEASUREMENTS

Maximum photosynthesis was characterized by CO_2 uptake (CO_2 µmol m^{-2} s^{-1}) and stomatal conductance (mmol H_2O m^{-2} s^{-1}) measured on intact leaves at 1000 µmol photons m^{-2} s^{-1} photosynthetic photon flux density (PPFD) using a LI-6400XT Portable Photosynthesis System (LI-COR Environmental, Lincoln, Nebraska, USA). The temperature in the measuring cell was not controlled, but was monitored and it was 22–23°C throughout the measurement. Humidity was controlled and kept at a constant 40% during the measurement.

VI.15. CHLOROPLAST UPTAKE ASSAY

VI.15.1. CLONING OF ALD1

An *ALD1* cDNA PCR fragment was generated using the following PCR protocol (Tab. 22) using the primer set F-*ALD1* and R-*ALD1* (Table. 23). The resulting PCR fragment was resolved by 0.8% Agarose gel, purified using an EZNA® Gel Extraction Kit (Omega BioTek) and cloned into pENTR/SD/DTOPO vector (Invitrogen®; Tab. 24).

PCR reaction:		PCR cycle conditions:		
		Temperature	Cycle	Time
10X buffer	5 µL	94 °C	1	2 min
10mM dNTPs	1.5 µL	94 °C		30 sec
50mM MgSO$_4$	1.0 µL	55 °C	20X	30 sec
PlatPfx DNA Polymerase	0.5 µL	68 °C		2 min
ALD1 Template	1.0 µL	68 °C	1 X	10 min
F-*ALD1*	1.5 µL	4 °C		forever
R-*ALD1*	1.5 µL			
water	38 µL			
	50 µL			

Table 22. PCR master mix and protocol for amplification of *ALD1* for cloning into pENTR/SD/DTOPO

Primer name	Primer sequence (5' to 3')
F-*ALD1*	CACCATGGTCAGTCTAATGTTCTTTAGT
R-*ALD1*	CTAATTGGTATTAGAAGTGGAAGA

Table 23. List of primers used for *ALD1* amplification for pENTR/SD/DTOPO

Cloning into pENTR/SD/DTOPO vector	
ALD1 purified PCR fragment	1.0 μL
pENTR/SD/DTOPO vector	1.0 μL
Salt solution	1.0 μL
water	1.0 μL
	4.0 μL

Table 24. Protocol of cloning reaction of *ALD1* into pENTR/SD/DTOPO

The reaction was incubated for 15 minutes at room temperature. The entire reaction was transformed into TOP-10 *E. coli* cells using a standard transformation protocol. A portion of the transformation reaction was plated out onto LB/Kan plates. Positive clones were isolated, the plasmid was purified and all *ALD1*/pENTR/SD/DTOPO transformants were confirmed by PCR and sequencing. A confirmed *ALD1*/pENTR/SD/DTOPO vector construct was used for clonase reaction (Tab. 25). The entire reaction (i.e. all 6 μL) was transformed into TOP10 *E. coli* cells using a standard transformation protocol. A portion of the transformation reaction was plated out onto LB/Amp plates and incubated overnight at 37°C. Positive clones were picked, plasmid was isolated and all ALD1/pDEST14 transformants were confirmed by PCR and sequencing. A confirmed ALD1/pDEST14 clone was subsequently used for *in vitro* transcription/translation using Promega's TNT® Coupled Reticulocyte Lysate System according to the manufacturer's protocol.

Clonase Reaction: Cloning ALD1 into pDEST14 vector	
ALD1/pENTR/SD/DTOPO	1.0 μL
pDEST14®	1.0 μL
TE Buffer, pH8.0	2.0 μL
Clonase II® mix	1.0 μL
	5.0 μL
Incubate at room temperature	20 min
add Proteinase K	1.0 μL
	6.0 μL
Incubate for 10 minute at 37°C	

Table 25. Protocol of clonase reaction to generate ALD1/pDEST14

For chloroplast uptake assays *ALD1/*pDEST14 (Invitrogen®) was used together with the control AtFtsH8 (C104937). The cDNA encoding AtFtsH8 (C104937) was obtained from the Arabidopsis Biological Resource Center (ABRC) (Yamada et *al.*, 2003) and was likewise cloned into pDEST14 (Invitrogen®) according to the manufacture's protocol.

VI.15.2. IN VITRO TRANSLATION OF PRECURSOR PROTEIN

Both FtsH8 and ALD1 were radiolabeled using [^{35}S]-methionine and translated using Promega's TNT® Coupled Reticulocyte Lysate System according to the manufacturer's protocol. After translation, the labeled precursor proteins were diluted with an equal volume of 'cold' 50 mM L-methionine in Import Buffer (50 mM Hepes/KOH; 330 mM sorbitol; pH 8.0).

VI.15.3. ISOLATION OF PEA CHLOROPLASTS

Intact chloroplasts were isolated from 8- to 12-day-old pea seedlings (*Little Marvel* (Dwarf Variety), Livingston Seed Co., Columbus, OH 43216) purified over a Percoll gradient as previously described (Bruce et *al.*, 1994). Intact pea chloroplasts were isolated and suspended in import buffer (50 mM Hepes/KOH; 330 mM sorbitol; pH 8.0) at a concentration of 1 mg chlorophyll mL^{-1}.

VI.15.4. IMPORT ASSAYS

Import assays were performed essentially as described in Tripp et *al.*, (2007). All reactions contained: 100 μL chloroplasts (1 mg chlorophyll/mL), 4 mM Mg-ATP/IB final concentration, and 100 μL radio-

labeled precursor proteins to a final total volume of 300 µL. Reactions were incubated for 30 minutes at room temperature, under room light. After import, the reactions were divided into two 100 µL aliquots. One aliquot did not receive Trypsin treatment [(-) control] and intact chloroplasts were directly recovered by centrifugation through a 40% Percoll cushion. The second aliquot was incubated with Trypsin for 30 minutes on ice. After quenching with Trypsin Inhibitor, intact chloroplasts were again recovered by centrifugation through a 40% Percoll cushion, lysed and then fractionated into a total soluble (S) and total membrane fraction (P). All fractions were analyzed by SDS-PAGE and then subjected to fluorography and exposed to X-ray film (Eastman, Kodak, Rochester, NT, USA).

VI.16. REPRODUCIBILITY OF EXPERIMENTS AND STATISTICAL ANALYSES

In most of the cases, unless stated otherwise, the data shown in this thesis resulted from a single biological experiment and were similar in three biologically independent experiments. At least three samples in µg.g-1 fresh weight (FW) were analysed for metabolic experiments and the data represent the mean ±SD (SD=standard deviation). Bacterial numbers values represent mean values ±SD of colony forming units (cfu) per square centimetre from at least seven replicate samples, each consisting of three leaf disks. Statistical analyses were performed using two-tailed Student's t test. Asterisks denote statistically significant differences between Psm- (OD 0.005) and $MgCl_2$-samples (***: $P < 0.001$; **: $P < 0.01$; *: $P < 0.05$).

VII. REFERENCES

Aarts, N., Metz, M., Holub, E., Staskawicz, B.J., Daniels, M.J. and Parker, J.E. (1998). Different requirements for EDS1 and NDR1 by disease resistance genes define at least two R gene-mediated signaling pathways in Arabidopsis. *Proc. Natl. Acad. Sci. USA* **95**, 10306-10311.

Acharya, B.R. and Assmann, S.M. (2009). Hormone interactions in stomatal function. *Plant Molecular Biology* **69**: 451–462.

Akman Gunduz, E. and Douglas, A.E. (2009). Symbiotic bacteria enable insect to use a nutritionally inadequate diet. *Proc Biol Sci 276*: 987-991.

Alonso, J.M., Stepanova, A.N., Leisse, T.J., Kim, C.J., Chen, H., Shinn, P., Stevenson, D.K., Zimmerman, J., Barajas, P., Cheuk, R., Gadrinab, C., Heller, C., Jeske, A., Koesema, E., Meyers, C.C., Parker, H., Prednis, L., Ansari, Y., Choy, N., Deen, H., Geralt, M., Hazari, N., Hom, E., Karnes, M., Mulholland, C., Ndubaku, R., Schmidt, I., Guzman, P., Aguilar-Henonin, L., Schmid, M., Weigel, D., Carter, D.E., Marchand, T., Risseeuw, E., Brogden, D., Zeko, A., Crosby, W.L., Berry, C.C. and Ecker, J.R. (2003). Genome-wide insertional mutagenesis of *Arabidopsis thaliana*. *Science* **301**: 653-657.

Amir, R., Hacham, Y. and Galili, G. (2002) Cystathionine gamma-synthase and threonine synthase operate in concert to regulate carbon flow towards methionine in plants. *Trends Plant Sci* **7**: 153–156 **.**

Anderson, J.W. (1990). Sulfur Metabolism in plants. *The biochemistry of plants* **16**: 327-381.

Arabidopsis Genome Initiative (2000). Analysis of the genome sequence of the flowering plant *Arabidopsis thaliana*. *Nature* **408**: 796-815.

Arruda, P., Kemper, E.L., Papes, F. and Leite, A. (2000). Regulation of lysine catabolism in higher plants. *Trends Plant Sci.* **5**: 324-330.

Asai, T., Tena, G., Plotnikova, J., Willmann, M.R., Chiu, W.-L., Gómez-Gómez, L., Boller, T., Ausubel, F.M., and Sheen, J. (2002). MAP kinase signaling cascade in Arabidopsis innate immunity. *Nature* **415**: 977–83.

Attaran, E., Zeier, T.E., Griebel, T. and Zeier, J. (2009). Methyl salicylate production and jasmonate signaling are not essential for systemic acquired resistance in Arabidopsis. *Plant Cell* **21**: 954–71.

Axtell, M.J. and Staskawicz, B.J. (2003). Initiation of RPS2-specified disease resistance in Arabidopsis is coupled to the AvrRpt2-directed elimination of RIN4. *Cell* **112**: 369–377.

Barends, T.R.M., Dunn, M.F. and Schlichting, I. (2008). Tryptophan synthase, an allosteric molecular factory. *Curr. Opin. Chem. Biol.* **12**: 593–60.

Bartsch, M., Gobbato, E., Bednarek, P., Debey, S., Schultze, J.L., Bautor, J. and Parker, J. (2006). Salicylic Acid – Independent ENHANCED DISEASE SUSCEPTIBILITY1 Signaling in Arabidopsis Immunity and Cell Death Is Regulated by the Monooxygenase FMO1 and the Nudix Hydrolase NUDT7. *Plant Cell* **18**: 1038–1051.

Baxter, C.J., Redestig, H., Schauer, N., Repsilber, D., Patil, K.R., Nielsen, J., Selbig, J., Liu, J., Fernie, A.R. and Sweetlove, L.J. (2007). The metabolic response of heterotrophic Arabidopsis cells to oxidative stress. *Plant Physiol.* **143**: 312–25.

Bechtold, N., Ellis, J. and Pelletier, G. (1993). *In planta Agrobacterium*-mediated gene transfer by infiltration of adult *Arabidopsis thaliana* plants. *C. R. Acad. Sci. Paris, Life Sciences* **316**: 1194-1199.

Beckers, G.J., Jaskiewicz, M., Liu, Y., Underwood, W.R., He, S.Y., Zhang, S. and Conrath, U. (2009). Mitogen-activated protein kinases 3 and 6 are required for full priming of stress responses in *Arabidopsis thaliana*. *Plant Cell* **21**: 944–953.

Bednarek, P., Schneider, B., Svatoš, A., Oldham, N.J. and Hahlbrock, K. (2005). Structural complexity, differential response to infection, and tissue specificity of indolic and phenylpropanoid secondary metabolism in Arabidopsis roots*. Plant Physiol.* **138**: 1058-1070.

Benjamini, Y. and Hochberg, Y. (1995). Controlling the false discovery rate – a practical and powerful approach to multiple testing. *Journal of the Royal Statistical Society Series B-Methodological* **57**: 289-300.

Binder, S., Knill, T. and Schuster, J. (2007). Branched-chain amino acid metabolism in higher plants. *Physiologia Plantarum* **129**: 68–78.

Binder, S. (2010). Branched-Chain Amino Acid Metabolism in *Arabidopsis thaliana*. *Arabidopsis Book* **8**: e0137.

Bleecker, A.B., Estelle, M.A., Somerville, C. and Kende, H. (1988). Insensitivity to ethylene conferred by a dominant mutation in *Arabidopsis thaliana*. *Science* **241**: 1086–1089.

Bleecker, A.B. and Kende, H. (2000). Ethylene: A gaseous signal molecule in plants. *Annu Rev Cell Dev Biol.* **16**: 1–18.

Block, A. and Alfano, J.R. (2011). Plant targets for *Pseudomonas syringae* type III effectors: Virulence targets or guarded decoys? *Curr Opin Microbiol* **14**: 39–46.

Blume, B., Nürnberger, T., Nass, N. and Scheel, D. (2000). Receptor-mediated increase in cytoplasmic free calcium required for activation of pathogen defense in parsley. *Plant Cell* **12**: 1425–1440.

Boller, T. (1995). Chemoperception of microbial signals in plant cells. *Annu. Rev. Plant Physiol. Plant Mol. Biol.* **46**: 189–214.

Boller. T. and Felix, G. (2009). A renaissance of elicitors: Perception of microbe-associated molecular patterns and danger signals by pattern-recognition receptors. *Annu Rev Plant Biol.* **60**: 379–406

Bonardi, V. and Dangl, J.L. (2012). How complex are intracellular immune receptor signaling complexes? *Frontiers in Plant Science* **3**: 1-9.

Bowling, S.A., Clarke, J.D., Liu, Y., Klessig, D.F. and Dong, X. (1997). The *cpr5* mutant of Arabidopsis expresses both NPR1-dependent and NPR1-independent resistance. *Plant Cell* **9**: 1573–84.

Bräutigam, A., Kajala, K., Wullenweber, J., Sommer, M., Gagneul, D., Weber, K.L., Carr, K.M., Gowik, U., Mass, J., Lercher, M.J., Westhoff, P., Hibberd, J.M. and Weber, A.P.M. (2011). An mRNA blueprint for C4 photosynthesis derived from comparative transcriptomics of closely related C3 and C4 species. *Plant Physiology* **155**: 142-156.

Brenner, E.D., Martinez-Baboza, N., Clark, A.P., Liang, Q.S., Stevenson, D. and Coruzzi, G.M. (2000). Arabidopsis mutants resistant to S(+)-beta-methyl-alpha, beta-iaminopropionic acid, a cycad-derived glutamate receptor agonist. *Plant Physiol.* **124**: 1615-1624.

Brodersen, P., Petersen, M., Bjørn Nielsen, H., Zhu, S., Newman, M.A., Shokat, K.M., Rietz, S., Parker, J. and Mundy, J. (2006). Arabidopsis MAP kinase 4 regulates salicylic acid- and jasmonic acid/ethylene-dependent responses via EDS1 and PAD4. *Plant J.* **47**: 532–546.

Broquist, H.P. (1991). Lysine-pipecolic acid metabolic relationships in microbes and mammals. *Annu. Rev. Nutr.* **11**: 435–48.

Browse, J. (2009). Jasmonate passes muster: a receptor and targets for the defense hormone. *Annu. Rev. Plant Biol.* **60**: 183-205.

Bruce, B.D. (1998). The role of lipids in plastid protein transport. *Plant Mol. Biol.* **38**: 223-246.

Bruce, B.D. (2001). The paradox of plastid transit peptides: conservation of function despite divergence in primary structure. *Biochim. Biophys. Acta* **1541**: 2–21.

Bryan, J.K. (1990). Advances in the biochemistry of amino acid biosynthesis. In *The Biochemistry of Plants*, J. Miflin, ed (New York, NY: Academic Press), pp. 403–452.

Büttner, D, He, S.Y. (2009). Type III protein secretion in plant pathogenic bacteria. *Plant Physiol* **150**: 1656–1664.

Callaway, A., Liu, W., Andrianov, V., Stenzler, L., Zhao, J., Wettlaufer, S., Jayakumar, P. and Howell, S.H. (1996). Characterization of cauliflower mosaic virus (CaMV) resistance in virus-resistant ecotypes of Arabidopsis. *Mol. Plant-Microbe Interact.* **9**: 810-818.

Cameron, R.K., Dixon, R.A. and Lamb, C.J. (1994) Biologically induced systemic acquired resistance in Arabidopsis thaliana. *Plant J.* **5**: 715–725.

Cameron, R.K., Paiva, N.L., Lamb, C.J. and Dixon, R.A. (1999). Accumulation of salicylic acid and *PR-1* gene transcripts in relation to the systemic acquired resistance (SAR) response induced by *Pseudomonas syringae* pv. *tomato* in Arabidopsis. *Physiol. Mol. Plant Pathol.* **55:** 121–130.

Canet, J.V., Dobon, A., Roig, A. and Tornero, P. (2010b). Structure-function analysis of npr1 alleles in Arabidopsis reveals a role for its paralogs in the perception of salicylic acid. *Plant Cell Environ.* **33**: 1911-1922.

Cao, H,, Bowling, S.A., Gordon, S. and Dong, X. (1994). Characterization of an Arabidopsis mutant that is nonresponsive to inducers of systemic acquired resistance. *Plant Cell* **6**: 1583-1592.

Cao, H., Glazebrook, J., Clarke, J.D., Volko, S. and Dong, X. (1997). The Arabidopsis NPR1 gene that controls systemic acquired resistance encodes a novel protein containing ankyrin repeats. *Cell* **88**: 57–63.

Cao, H., Li, X. and Dong, X. (1998). Generation of broad-spectrum disease resistance by overexpression of an essential regulatory gene in systemic acquired resistance. *Proc. Natl. Acad. Sci. USA* **95**: 6531–6536.

Cecchini, N.M., Monteoliva, M.I. and Alvarez, ME. (2011). Proline dehydrogenase contributes to pathogen defense in Arabidopsis. *Plant Physiol.* **155**: 1947-1959.

Century, K.S., Holub, E.B. and Staskawicz, B.J. (1995). NDR1, a locus of Arabidopsis thaliana that is required for disease resistance to both a bacterial and a fungal pathogen. *Proc. Natl. Acad. Sci. USA* **92**: 6597–601.

Champigny, M.J., Isaacs, M., Carella, P., Faubert, J., Fobert, P.R. and Cameron, R.K. (2013). Long distance movement of DIR1 and investigation of the role of DIR1-like during systemic acquired resistance in Arabidopsis. *Frontiers in Plant Science* **4**: 230.

Chaturvedi, R. and Shah, J. (2007). Salicylic acid in plant disease resistance. In Salicylic Acid – A Plant Hormone (Hayat, S. and Ahmad, A., eds). *Dordrecht, The Netherlands: Springer, pp.* 335–370.

Champigny, M.J., Shearer, H., Mohammad, A., Haines, K., Neumann, M., Thilmony, R., He, S.Y., Fobert, P., Dengler, N. and Cameron, R.K. (2011). Localization of DIR1 at the tissue, cellular and subcellular levels during Systemic Acquired Resistance in Arabidopsis using DIR1:GUS and DIR1:EGFP reporters. *BMC Plant Biol.* **11**: 125.

Chanda, B., Xia, Y., Mandal, M.K., Yu, K., Sekine, K.T., Gao, Q.M., Selote, D., Hu, Y., Stromberg, A., Navarre, D., Kachroo, A. and Kachroo P. (2011). Glycerol-3-phosphate is a critical mobile inducer of systemic immunity in plants. *Nature Genetics* **43**: 421–427.

Chang, Y.-F. (1976). Pipecolic acid pathway: the major lysine metabolic route in the rat brain. *Biochemical and Biophysical Research Communications* **69**: 174–180.

Charles, A.K. (1986). Pipecolic acid receptors in rat cerebral cortex. *Neurochem Res.* **11**: 521-5.

Chaturvedi, R., Krothapalli, K., Makandar, R., Nandi, A., Sparks, A., Roth, M.R., Welti, R. and Shah, J. (2008). Plastid omega3-fatty acid desaturase-dependent accumulation of a systemic acquired resistance inducing activity in petiole exudates of *Arabidopsis thaliana* is independent of jasmonic acid. *Plant J.* **54**: 106–17.

Chaturvedi, R., Venables, B., Petros, R.A., Nalam, V., Li, M., Wang, X., Takemoto, L.J. and Shah, J. (2012). An abietane diterpenoid is a potent activator of systemic acquired resistance. *Plant J.* **71**: 161–172.

Chen, H., Wilkerson, C.G., Kuchar, J.A., Phinney, B.S. and Howe, G.A. (2005). Jasmonate-inducible plant enzymes degrade essential amino acids in the herbivore midgut. *Proc. Natl. Acad. Sci. USA* **102**: 19237- 19242.

Chini, A., Fonseca, S., Fernández, G., Adie, B., Chico, J.M., Lorenzo, O., García-Casado, G., López-Vidriero, I., Lozano, F.M., Ponce, M.R., Micol, J.L. and Solano, R. (2007). The JAZ family of repressors is the missing link in jasmonate signaling. *Nature* **448**: 666–671.

Chini, A., Boter, M. and Solano, R. (2009a). Plant oxylipins: COI1/JAZs/MYC2 as the core jas- monic acid-signaling module. *FEBS J.* **276:** 4682–4692.

Chrisholm, S.T., Coaker, G., Day, B. and Staskawicz, B.J. (2006). Host-microbe interactions: shaping the evolution of the plant immune response. *Cell* **124**: 803–814.

Chang, Y.F. (1976). Pipecolic acid pathway: the major lysine metabolic route in the rat brain. *Biochem. Biophys. Res. Commun.* **8**: 174-80.

Chuang, D.T., Chuang, J.L. and Wynn, R.M. (2006). Lessons from genetic disorders of branched-chain amino acid metabolism. *J. Nutr.* **136**: 243S-249S.

Clarke, J.D., Volko, S.M., Ledford, H., Ausubel, F.M. and Dong, X.N. (2000). Roles of salicylic acid, jasmonic acid, and ethylene in *cpr*-induced resistance in Arabidopsis. *Plant Cell* **12**: 2175-2190.

Clough, S.J. and Bent, A.F. (1998). Floral dip: a simplified method for Agrobacterium-mediated transformation of *Arabidopsis thaliana. Plant J.* **16:** 735-43.

Cohen, Y.R. and Gisi, U. (1994). Systemic translocation of 14C-DL-3-aminobutyric acid in tomato plants in relation to induced resistance against *Phytophthora infestans. Physiol. Mol. Plant Pathol.* **45**: 441-456.

Cohen, Y.R. (2002). β-aminobutyric acid-induced resistance against plant pathogens. *Plant Dis*. **86**: 448- 457.

Conrath, U. (2011). Molecular aspects of defense priming. Trends Plant Sci. **16**: 524–31.

Consonni, C., Bednarek, P., Humphry, M., Francocci, F., Ferrari, S., Harzen, A., Ver Loren van Themaat, E. and Panstruga, R. (2010). Tryptophan-derived metabolites are required for antifungal defense in the Arabidopsis mlo2 mutant. *Plant Physiol.* **152**: 1544–61.

Coppinger, P., Repetti, P.P., Day, B., Dahlbeck, D., Mehlert, A. and Staskawicz, B.J. (2004). Overexpression of the plasma membrane-localized NDR1 protein results in enhanced bacterial disease resistance in *Arabidopsis thaliana. Plant J.* **40**, 225-237.

Coruzzi, G.M., and Last, R.L. (2000). Amino acids. In Biochemistry and Molecular Biology of Plants, Buchanan, R.B., Gruissem, W., and Jones, R., eds (Rockville, MD: Am. Soc. Plant Physiol. Press) pp. 358–410

Cunha da, L., McFall, A.J. and Mackey, D. (2006). Innate immunity in plants: a continuum of layered defenses. *Microbes Infect.* **8**: 1372-1381.

Curien, G., Laurencin, M., Robert-Genthon, M. and Dumas, R. (2007). Allosteric monofunctional aspartate kinases from Arabidopsis. *The FEBS Journal* **274**: 164–176.

van Damme. M., Andel. A., Huibers. R.P., Panstruga. R., Weisbeek. P.J. and van den Ackerveken. G. (2005). Identification of Arabidopsis loci required for susceptibility to the downy mildew pathogen *Hyaloperonospora parasitica*. **18**: 583–592.

van Damme, M., Zeilmaker, T., Elberse, J., Andel, A., de Sain-van der Velden, M. and van den Ackerveken, G. (2009). Downy mildew resistance in Arabidopsis by mutation of HOMOSERINE KINASE. *Plant Cell* **21**: 2179–89.

Dancis, J. and Cox, R.P. (1989). Errors of lysine metabolism. In *The Metabolic Basis of Inherited Diseases*, ed. E.R. Scriver, A.L. Beaudet, W.S. Sly, D. Valde, 665-70. New York: McGraw-HilL 6th ed.

Dean, J.V. and Mills, J.D. (2004). Uptake of salicylic acid 2-O-β-D-glucose into soybean tonoplast vesicles by an ATP-binding cassette transporter-type mechanism. *Physiol Plant.* **120**: 603–12.

Dean, J.V, Mohammed, L. and Fitzpatrick, T. (2005). The formation, vacuolar localization, and tonoplast transport of salicylic acid glucose conjugates in tobacco cell suspension cultures. *Planta* **221**: 287–96.

Dean, J.V. and Delaney, S.P. (2008). Metabolism of salicylic acid in wild-type, ugt74f1 and ugt74f2 glucosyltransferase mutants of *Arabidopsis thaliana. Physiol. Plant.* **132**: 417–25.

DebRoy, S., Thilmony, R., Kwack, Y.-B., Nomura, K., and He, S.Y. (2004). A family of conserved bacterial effectors inhibits salicylic acid-mediated basal immunity and promotes disease necrosis in plants. *Proc. Natl. Acad. Sci. USA* **101**: 9927–32.

Delaney, T.P., Uknes, S., Vernooij, B., Friedrich, L., Weymann, K., Negrotto, D., Gaffney, T., Gut-Rella, M., Kessmann, H., Ward, E. and Ryals, J. (1994). A central role of salicylic acid in plant disease resistance. *Science* **266**: 1247-1250.

Delaney, T.P., Friedrich, L. and Ryals, J.A. (1995). Arabidopsis signal transduction mutant defective in chemically and biologically induced disease resistance. *Proc Natl Acad Sci USA* **92**: 6602-6606.

Dempsey, D.A., Pathirana, M.S., Wobbe, K.K. and Klessig, D.F. (1997). Identification of an Arabidopsis locus required for resistance to turnip crinkle virus. *Plant J.* **11**: 301-311.

Dempsey, D.A., Shah, J. and Klessig, D.F. (1999). Salicylic acid and disease resistance in plants. *Crit. Rev. Plant Sci.* **18**: 547–75.

Dempsey, D.A., Vlot, A.C., Wildermuth, M.C. and Klessig, D.F. (2011). Salicylic Acid biosynthesis and metabolism. *Arabidopsis Book* **9**: e0156.

Dempsey, D.A. and Klessig, D.F. (2012). SOS - too many signals for systemic acquired resistance? *Trends Plant Sci.* **17**: 538–45.

Despres, C., DeLong, C., Glaze, S., Liu, E. and Fobert, P.R. (2000). The Arabidopsis NPR1/NIM1 protein enhances the DNA binding activity of a subgroup of the TGA family of bZIP transcription factors. *Plant Cell* **12**: 279–290.

Diebold, R., Schuster, J., Däschner, K. and Binder, S. (2002). The branched- chain amino acid transaminase gene family in Arabidopsis encodes plastid and mitochondrial proteins. *Plant Physiol* **129**: 540-550.

Dong, X. (1998). SA, JA, ethylene, and disease resistance in plants. *Curr. Opin. Plant Biol.* **1**: 316–323.

Dong, X. (2004). NPR1, all things considered. *Curr. Opin. Plant Biol.* **7**: 547–52.

Douglas, A.E. (1998). Nutritional interactions in insect-microbial symbioses: aphids and their symbiotic bacteria Buchnera. *Ann. Rev. Ent.* 43: 17-37.

Dow, M., Newman, M. A. and von Roepenack, E. (2000). The induction and modulation of plant defense responses by bacterial lipopolysaccharides*. Annu. Rev. Phytopathol.* **38**: 241–261.

Durner, J. and Klessig, D.F. (1995). Inhibition of ascorbate peroxidase by salicylic acid and 2,6-dichloroisonicotinic acid, two inducers of plant defense responses. *Proc.Natl. Acad. Sci.USA* **92**: 11312–16**.**

Durner, J. and Klessig, D.F. (1996). Salicylic acid is a modulator of tobacco and mammalian catalases. *Journal of Biochemistry* **271**: 28492–28501.

Durner, J., Shah, J. and Klessig, D.F. (1997). Salicylic acid and disease resistance in plants. *Trends in Plant Science* **2**: 266–274.

Durrant, W.E. and Dong, X. (2004) Systemic acquired resistance. *Annu. Rev. Phytopathol.* **42**: 185–209.

Eberhard, J., Ehrler, T.T., Epple, P., Felix, G., Raesecke, H.R., Amrhein, N. and Schmid, J. (1996). Cytosolic and plastidic chorismate mutase isozymes from *Arabidopsis thaliana*: molecular characterization and enzymatic properties. *Plant J.* **10**: 815–21.

Elthon, T.E. and Stewart, C.R. (1981). Submitochondrial location and electron transport characteristics of enzymes involved in proline oxidation*. Plant Physiol* **67**: 780–784.

Fabro, G., Kovács, I., Pavet, V., Szabados, L. and Alvarez, M.E. (2004). Proline accumulation and AtP5CS2 geneactivation are induced by plant-pathogen incompatible interactions in Arabidopsis*. Mol. Plant- Microbe Interact.* **17**: 343-350.

Facchini, P.J., Huber-Allanach, K.L. and Tari, L.W. (2000). Plant aromatic L-amino acid decarboxylases: Evolution, biochemistry, regulation, and metabolic engineering applications. *Phytochemistry* **54**: 121- 138.

Facchini, P.J., Bird, D.A. and St-Pierre, B. (2004) Can Arabidopsis make complex alkaloids? *Trends Plant Sci.* **9**: 116-122.

Falk, A., Feys, B.J., Frost, L.N., Jones, J.D., Daniels, M.J. and Parker, J.E. (1999). EDS1, an essential component of R gene-mediated disease resistance in Arabidopsis has homology to eukaryotic lipases. *Proc Natl Acad Sci USA* **96**: 3292–3297.

Fariduddin, Q., Hayat, S. and Ahmad A. (2003). Salicylic acid influences net photosynthetic rate, carboxylation efficiency, nitrate reductase activity, and seed yield in *Brassica juncea. Photosynthetica* **41**: 281–284.

Felix, G., Regenass, M. and Boller, T. (1993). Specific perception of subnanomolar concentrations of chitin fragments by tomato cells. Induction of extracellular alkalinization, changes in protein phosphorylation, and establishment of a refractory state. *Plant J.* **4**: 307–316.

Felix, G., Duran, J. D., Volko, S. and Boller, T. (1999). Plants have a sensitive perception system for the most conserved domain of bacterial flagellin. *Plant J.* **18**: 265–276.

Ferrari, S., Plotnikova, J.M., De Lorenzo, G. and Ausubel, F.M. (2003). Arabidopsis local resistance to *Botrytis cinerea* involves salicylic acid and camalexin and requires EDS4 and PAD2, but not SID2, EDS5 or PAD4. *Plant J.* **35**: 193–205.

Ferrari, S., Galletti, R., Denoux, C., De Lorenzo, G., Ausubel, F.M. and Dewdney, J. (2007). Resistance to *Botrytis cinerea* induced in Arabidopsis by elicitors is independent of salicylic acid, ethylene, or jasmonate signaling but requires PHYTOALEXIN DEFICIENT3. *Plant Physiol.* **144**: 367-379.

Feys, B.J., Moisan, L.J., Newman, M.-A., and Parker, J.E. (2001). Direct interaction between the Arabidopsis disease resistance signaling proteins, EDS1 and PAD4. *EMBO J.* **20**: 5400-5411.

Feys, B.J., Wiermer, M., Bhat, R.A., Moisan, L.J., Medina-Escobar, N., Neu, C., Cabral, A. and Parker, J.E. (2005). Arabidopsis SENESCENCE-ASSOCIATED GENE101 stabilizes and signals within an ENHANCED DISEASE SUSCEPTIBILITY1 complex in plant innate immunity. *Plant Cell* **17**: 2601-2613.

Fletcher, S.A., Rhodes, D. and Csonka, L.N. (2001). Analysis of effects of osmoprotectants on the high osmolality-dependant induction of increased thermotolerance in *Salmonella typhimurium*. *Food Microbiol.* **18:** 345– 354.

Flor, H.H. (1956). The complementary genetic systems in flax and flax rust. *Adv Genet* **8**: 29-54.

Fonseca, S., Chini, A., Hamberg, M., Adie, B., Porzel, A., Kramell, R., Miersch, O., Wasternack, C. and Solano, R. (2009b). (+)-7-iso- Jasmonoyl-L-isoleucine is the endogenous bioactive jasmonate. *Nat. Chem. Biol.* **5**: 344-350.

Forouhar, F., Yang, Y., Kumar, D., Chen, Y., Fridman, E., Park, S.W., Chiang, Y., Acton, T.B., Montelione, G.T., Pichersky, E., Klessig, D.F., and Tong, L. (2005). Structural and biochemical studies identify tobacco SABP2 as a methyl salicylate esterase and implicate it in plant innate immunity. *Proc. Natl. Acad. Sci. USA* **102**: 1773–8.

Fritz-Laylin, L.K., Krishnamurthy, N., Tör, M., Sjölander, K.V. and Jones, J.D.G. (2005). Phylogenomic analysis of the receptor-like proteins of rice and Arabidopsis. *Plant Physiol.* **138**: 611-623.

Froehlich, J. (2011). In *Chloroplast Research in Arabidopsis*: Methods and Protocols, R. Paul Jarvis (ed.), Volume I, *Methods in Molecular Biology*, Vol. 774, DOI 10.1007/978-1-61779-234-2_21, **774**: 351–367.

Fu, Z.Q., Yan, S., Saleh, A., Wang, W., Ruble, J., Oka, N., Mohan, R., Spoel, S.H., Tada, Y., Zheng, N. and Dong, X. (2012). NPR3 and NPR4 are receptors for the immune signal salicylic acid in plants. *Nature* **486**: 228–32.

Fu, Z.Q. and Dong, X. (2013). Systemic acquired resistance: turning local infection into global defense. Annu. Rev. *Plant Biol.* **64**: 839–63.

Fujioka, S., Sakurai, A.,Yamaguchi, I., Murofushi, N.,Takahashi, N., Kaihara, S. and Takimoto A. (1987) Isolation and identification of L-pipecolic acid and nicotinamide as flower-inducing substances in Lemna. *Plant and Cell Physiology* **28**: 995–1003.

Fujioka, S. and Sakurai, A. (1997). Conversion of lysine to L-pipecolic acid induces flowering in *Lemna paucicostata* 151. *The Plant Cell Physiology* **38**: 1278–1280

Gaffney, T., Friedrich, L., Vernooij, B., Negrotto, D., Nye, G., Uknes, S., Ward, E., Kessmann, H. and Ryals, J. (1993). Requirement of salicylic acid for the induction of systemic acquired resistance. *Science* **261**: 754–56.

Galili, G., Tang, G., Zhu, X., and Gakiere, B. (2001). Lysine catabolism: a stress and development super-regulated metabolic pathway. *Curr Opin Plant Biol* **4:** 261–266.

Galili, G. (2002). New insights into the regulation and functional significance of lysine metabolism in plants. *Annu. Rev. Plant Biol.* **53**: 27-43.

Gao, Q.-M., Kachroo, A. and Kachroo, P. (2014). Chemical inducers of systemic immunity in plants. *Journal of Experimental Botany* **65**: 1849–1855.

García, A.V., Blanvillain-Baufumé, S., Huibers, R.P., Wiermer, M., Li, G., Gobbato, E., Rietz, S. and Parker, J.E. (2010). Balanced nuclear and cytoplasmic activities of EDS1 are required for a complete plant innate immune response. *PLoS Pathogens* **6**: e1000970.

Garcion, C. and Métraux, J.-P. (2006). Salicylic acid. *In Plant Hormone Signaling,* **24:** 229–255. Oxford: Blackwell Publishing Ltd.

Garcion, C., Lohmann, A., Lamodière, E., Catinot, J., Buchala, A., Doermann, P. and Métraux, J.-P. (2008). Characterization and biological function of the *ISOCHORISMATE SYNTHASE2* gene of Arabidopsis. *Plant Physiol.* **147**: 1279–87.

Garweg G., von Rehren D. and Hintze U. (1980). L-Pipecolate formation in the mammalian brain. Regional distribution of D1-pyrroline-2-carboxylate reductase activity. **J. *Neurochem.* 35**: 616–621.

Gawroński, P., Górecka, M., Bederska, M., Rusaczonek, A., Ślesak, I., Kruk, J. and Karpiński, S. (2013). Isochorismate synthase 1 is required for thylakoid organization, optimal plastoquinone redox status, and state transitions in *Arabidopsis thaliana. J Exp Bot.* **64**: 3669-79.

Glawischnig, E. (2007). Camalexin. *Phytochemistry* **68**: 401-406.

Glazebrook, J. and Ausubel, F. M. (1994). Isolation of phytoalexin-deficient mutants of *Arabidopsis thaliana* and characterization of their interactions with bacterial pathogens. *Proc Natl Acad Sci USA* 91(**19**): 8955–8959.

Glazebrook, J., Rogers, E.E. and Ausubel, F.M. (1996). Isolation of Arabidopsis mutants with enhanced disease susceptibility by direct screening. *Genetics* **143**: 973-982.

Glazebrook, J., Zook, M., Mert, I.F., Kagan, I., Rogers, E.E., Crute, I.R., Holub, E.B., Hammerschmidt, R., and Ausubel, F.M. (1997). Phytoalexin-deficient mutants of Arabidopsis reveal that PAD4 encodes a regulatory factor and that four PAD genes contribute to downy mildew resistance. *Genetics*: 381–392.

Glazebrook, J., Chen, W., Estes, B., Chang, H.-S., Nawrath, C., Métraux, J.-P., Zhu, T. and Katagiri, F. (2003). Topology of the network integrating salicylate and jasmonate signal transduction derived from global expression phenotyping. *Plant J.* **34**: 217-228.

Glazebrook, J. (2005) Contrasting mechanisms of defense against biotrophic and necrotrophic pathogens. *Annu Rev Phytopathol* **43**: 205–227.

Goda, H., Sasaki, E., Akiyama, K., Maruyama-Nakashita, A., Nakabayashi, K., Li, W., Ogawa, M., Yamauchi, Y., Preston, J., Aoki, K., Kiba, T., Takatsuto, S., Fujioka, S., Asami, T., Nakano, T., Kato, H., Mizuno, T., Sakakibara, H., Yamaguchi, S., Nambara, E., Kamiya, Y., Takahashi, H., Hirai, M.Y., Sakurai, T., Shinozaki, K., Saito, K., Yoshida, S. and Shimada, Y. (2008). The AtGenExpress hormone and chemical treatment data set: experimental design, data evaluation, model data analysis and data access. *Plant J.* **55**: 526–542.

Göhre, V. and Robatzek, S. (2008). Breaking the barriers: Microbial effector molecules subvert plant immunity. *Annu Rev Phytopathol.* **46**: 189–215.

Gómez-Gómez, L., Felix, G. and Boller, T. (1999). A single locus determines sensitivity to bacterial flagellin in *Arabidopsis thaliana. Plant J.* **18**: 277–284.

Gómez-Gómez, L. and Boller, T. (2000). FLS2: an LRR receptor-like kinase involved in the perception of the bacterial elicitor flagellin in Arabidopsis. *Mol. Cell* **5**: 1003–1011.

Goyer, A., Johnson, T.L., Olsen, L.J., Collakova, E., Shachar-Hill, Y., Rhodes, D. and Hanson, A.D. (2004). Characterization and metabolic function of a peroxisomal sarcosine and pipecolate oxidase from Arabidopsis. *J. Biol. Chem.* **279**: 16947–53.

Granado, J., Felix, G. and Boller, T. (1995). Perception of fungal sterols in plants: subnanomolar concentrations of ergosterol elicit extracellular alkalinization in tomato cells. *Plant Physiol.* **107**: 485–490.

Grant, M., Brown, I., Adams, S., Knight, M., Ainslie, A. and Mansfield, J. (2000). The RPM1 plant disease resistance gene facilitates a rapid and sustained increase in cytosolic calcium that is necessary for the oxidative burst and hypersensitive cell death. *Plant J* **23**: 441–450.

Griebel, T. and Zeier, J. (2008). Light regulation and daytime dependency of inducible plant defenses in Arabidopsis: Phytochrome signaling controls systemic acquired resistance rather than local defense. *Plant Physiol.* **147**: 790–801.

Griebel, T. and Zeier, J. (2010). A role for beta-sitosterol to stigmasterol conversion in plant-pathogen interactions. *Plant J.* **63**: 254–68.

Gruner, K., Griebel, T., Návarová, H., Attaran, E. and Zeier, J. (2013). Reprogramming of plants during systemic acquired resistance. *Front. Plant Sci.* **4**: 252.

Gunes, A., Inal, A., Alpaslan, M., Eraslan, F., Bagci, E.G and Cicek, N. (2007). Salicylic acid induded changes on some physiological parameters symptomatic for oxidative stress and mineral nutrition in maize (*Zea mays* L.) grown under salinity. *Journal of Plant Physiology* **164**: 728–736.

Gutiérrez-Coronado, M.A., Trejo-López, C. and Larqué-Saavedra, A. (1998). Effects of salicylic acid on the growth of roots and shoots in soybean. *Plant Physiology and Biochemistry* **36**: 563–565.

Hacham, Y., Song, L., Schuster, G. and Amir, R. (2007). Lysine enhances methionine content by modulating the expression of S-adenosylme-thionine synthase. *Plant J.* **51**: 850-861.

Halkier, B.A. and Gershenzon, J. (2006). Biology and biochemistry of glucosinolates. *Annu. Rev. Plant Biol.* **57**: 303-333.

Hallen, A., Cooper, A.J.L., Jamie, J.F., Haynes, P. and Willows, R.D. (2011). Mammalian forebrain ketimine reductase identified as μ-crystallin; potential regulation by thyroid hormones. *J. Neurochem.* **118**: 379–87.

Hammerschmidt, R. (1999a). Induced disease resistance: how do induced plants stop pathogens? *Physiol. Mol. Plant Pathol.* **55**: 77-84.

Hammerschmidt, R. (1999b). PHYTOALEXINS: What Have We Learned After 60 Years? *Annu. Rev. Phytopathol.* **37**: 285-306.

Hansen, B.G., Kliebenstein, D.J. and Halkier, B. (2007). Identification of a flavin-monooxygenase as the S-oxygenating enzyme in aliphatic glucosinolate biosynthesis in Arabidopsis. *Plant J.* **50**: 902–10.

Hanson, J. R. (2009). Diterpenoids. *Nat. Prod. Rep.* **26**: 1156–1171.

Hennig, J., Malamy, J., Grynkiewicz, G., Indulski, J. and Klessig, D.F. (1993). Interconversion of the salicylic acid signal and its glucoside in tobacco. *Plant J.* **4**: 593–600.

Hernandez, J.M., Feller, A., Morohashi, K., Frame, K. and Grotewold, E. (2007). A basic helix-loop-helix domain of maize R links transcriptional regulation and histone modifications by recruitment of an EMSY-related factor. *Proc. Natl Acad. Sci. USA* **104:** 17222–17227.

Hilfiker, O., Groux, R., Bruessow, F., Kiefer, K., Zeier, J. and Reymond, P. (2014). Insect eggs induce a systemic acquired resistance in Arabidopsis. *Plant J.* doi: 10.1111/tpj.12707. [Epub ahead of print]

Holuigue, L., Salinas, P., Blanco, F., and Garretón, V. (2007). Salicylic acid and reactive oxygen species in the activation of stress defense genes. In *Salicylic Acid - A Plant Hormone,* ed. S. Hayat, A. Ahmad **8**: 197–246. Netherlands: Springer

Huang T, Jander, G. and de Vos, M. (2011). Non-protein amino acids in plant defense against insect herbivores: Representative cases and opportunities for further functional analysis. *Phytochemistry* **72**: 1531-1537.

Hudson, A.O., Singh, B.K., Leustek, T. and Gilvarg, C. (2006). An LL-diaminopimelate aminotransferase defines a novel variant of the lysine biosynthesis pathway in plants. *Plant Physiol.* **140**: 292-301.

Huffaker, A., Pearce, G., Ryan, C.A. (2006). An endogenous peptide signal in Arabidopsis activates components of the innate immune response. *Proc Natl Acad Sci USA* **103**: 10098–10103.

Huot, B., Yao, J., Montgomery, B.L. and He, S.Y. (2014). Growth-defense tradeoffs in plants: A balancing act to optimize fitness. *Mol. Plant* **7**: 1267–1287.

Hutzler, J. and Dancis, J. (1968). Conversion of lysine to saccharopine by human tissue. *Biochim. Biophys. Acta* **158**: 62-69.

Idänheimo, N., Gauthier, A., Salojärvi, J., Siligato, R., Brosché, M., Kollist, H., Mähönen, A.P., Kangasjärvi, J. and Wrzaczek, M. (2014). The *Arabidopsis thaliana* cysteine-rich receptor-like kinases CRK6 and CRK7 protect against apoplastic oxidative stress. *Biochem. Biophys. Res. Commun.* **445**: 457–62.

Jagadeeswaran, G., Raina, S., Acharya, B.R., Maqbool, S.B., Mosher, S.L., Appel, H.M., Schultz, J.C., Klessig, D.F. and Raina, R. (2007). Arabidopsis GH3-like defense gene 1 is required for accumulation of salicylic acid, activation of defense responses and resistance to *Pseudomonas syringae*. *Plant J.* **51**: 234-246.

Jakab, G., Cottier, V., Toquin, V., Rigoli, G., Zimmerli, L., Metraux, J.-P. and Mauch-Mani, B. (2001). β-Aminobutyric acid-induced resistance in plants. *Eur. J. Plant Pathol.* **107**: 29-37.

Jander, G. and Joshi, V. (2009). Aspartate-Derived Amino Acid Biosynthesis in *Arabidopsis thaliana*. *Arabidopsis Book* **7**: e0121.

Jander, G. and Joshi, V. (2010) Recent progress in deciphering the biosynthesis of aspartate-derived amino acids in plants. *Molecular Plant* **3**: 54–65**.**

Jarvis, P. and Robinson, C. (2004). Mechanisms of protein import and routing in chloroplasts. *Curr. Biol.* **14**: R1064–77.

Jaskiewicz, M., Conrath, U. and Peterhänsel, C. (2011). Chromatin modification acts as a memory for systemic acquired resistance in the plant stress response. *EMBO Rep.* **12**: 50–55.

Jing, B., Xu, S., Xu, M., Li, Y., Li, S., Ding, J. and Zhang, Y. (2011). Brush and spray: a high-throughput systemic acquired resistance assay suitable for large-scale genetic screening. *Plant Physiol.* **157**: 973–80.

Jirage, D., Tootle, T.L., Reuber, T.L., Frost, L.N., Feys, B.J., Parker, J.E., Ausubel, F.M. and Glazebrook, J. (1999). *Arabidopsis thaliana* PAD4 encodes a lipase-like gene that is important for salicylic acid signaling. *Proc. Natl. Acad. Sci. USA* **96**: 13583–8.

Joshi, V., Laubengayer, K.M., Schauer, N., Fernie, A.R. and Jander, G. (2006). Two Arabidopsis threonine aldolases are nonredundant and compete with threonine deaminase for a common substrate pool. *Plant Cell* **18**: 3564–3575.

Jung, H.W., Tschaplinski, T.J., Wang, L., Glazebrook, J., Greenberg, J.T. (2009). Priming is systemic plant immunity. *Science* **324**: 89–91.

Kaplan, F., Kopka, J., Haskell, D.W., Zhao, W., Schiller, K.C., Gatzke, N., Sung, D.Y. and Guy, C.L. (2004). Exploring the temperature-stress metabolome of Arabidopsis. *Plant Physiol.* **136**: 4159-4168.

Katsir, L., Schilmiller, A. L., Staswick, P. E., He, S. Y. and Howe, G. A. (2008). COI1 is a critical component of a receptor for jasmonate and the bacterial virulence factor coronatine. *Proc. Natl. Acad. Sci. USA* **105**: 7100–7105.

Keith, B., Dong, X., Ausubel, F. and Fink, G. (1991) Differential induction of 3-deoxy-D-arabino-heptulosonate 7-phosphate synthase genes in *Arabidopsis thaliana* by wounding and pathogenic attack. *Proc. Natl. Acad. Sci. USA* **88**: 8821–25*.*

Keegstra, K. (1989). A new hypothesis for the mechanism of protein translocation into chloroplasts. In: Briggs W (ed) *Photosythesis*, pp. 347–357. Alan R. Liss, New York

Kim, T.W. and Wang, Z.Y. (2010). Brassinosteroid signal transduction from receptor kinases to transcription factors. *Annual Review of Plant Biology* **61**: 681–704.

Kinkema, M., Fan, W. and Dong, X. (2000). Nuclear localization of NPR1 is required for activation of *PR* gene expression. *Plant Cell* **12**: 2339–50.

Kishor, K.P., Sangam, S., Amrutha, R., Sri Laxmi, P., Naidu, K., Rao, K., Rao, S., Reddy, K., Theriappan, P. and Sreenivasulu N. (2005). Regulation of proline biosynthesis, degradation, uptake and transport in higher plants: its implications in plant growth and abiotic stress tolerance. *Curr Sci* **88**: 424-438.

Klessig, D.F. and Malamy, J. (1994). The salicylic acid signal in plants. *Plant Mol. Biol.* **26**: 1439–58.

Kloek, A.P., Verbsky, M.L., Sharma, S.B., Schoelz, J.E., Vogel, J., Klessig, D.F. and Kunkel, B.N. (2001). Resistance to *Pseudomonas syringae* conferred by an *Arabidopsis thaliana coronatine-insensitive* (*coi1*) mutation occurs through two distinct mechanisms. *Plant J.* **26**: 509–22.

Knill, T., Schuster, J., Reichelt, M., Gershenzon, J., Binder, S. (2008). Arabidopsis branched-chain aminotransferase 3 functions in both amino acid and glucosinolate biosynthesis. *Plant Physiol.* **146**: 1028-1039.

Koch, M., Vorwerk, S., Masur, C., Sharifi-Sirchi, G., Olivieri, N. and Schlaich, N.L. (2006). A role for a flavin-containing mono-oxygenase in resistance against microbial pathogens in Arabidopsis. *Plant J.* **47**: 629–39.

Koo, Y.J., Kim, M.A., Kim, E.H., Song, J.T. and Jung, C., Moon, J.K., Kimm, J.H., Seo, H.S., Song, S.I., Kim, J.K., Lee, J.S., Cheong, J.J. and Choi, Y.D. (2007). Overexpression of salicylic acid carboxyl methyltransferase reduces salicylic acid-mediated pathogen resistance in *Arabidopsis thaliana*. *Plant Mol. Biol.* **64**: 1–15.

Kovácik, J., Grúz, J., Backor, M., Strnad, M. and Repcák M. (2009). Salicylic acid-induced changes to growth and phenolic metabolism in Matricaria chamomilla plants. *Plant Cell Reports* **28**: 135–143.

Kovács-Bogdán, E., Soll, J. and Bölter, B. (2010). Protein import into chloroplasts: the Tic complex and its regulation. *Biochim. Biophys. Acta* **1803**: 740–7.

Krieg, N.R. and Holt, J.G. (1984). eds. *Bergey's Manual of systematic Bacteriology* Vol. I. Baltimore: Williams & Wilkins, 254–6.

Krol, E., Mentzel, T., Chinchilla, D., Boller, T., Felix, G., Kemmerling, B., Postel, S., Arents, M., Jeworutzki, E., Al-Rasheid, K.A., Becker, D. and Hedrich, R. (2010). Perception of the Arabidopsis danger signal peptide 1 involves the pattern recognition receptor AtPEPR1 and its close homologue AtPEPR2. *J Biol Chem* **285**(18): 13471–13479.

Kugler, F., Graneis, S., Schreiter, P.P.Y., Stintzing, F.C. and Carle, R. (2006). Determination of free amino compounds in betalainic fruits and vegetables by gas chromatography with flame ionization and mass spectrometric detection. *J. Agric. Food Chem.* **54**: 4311-4318.

Kunze, G., Zipfel, C., Robatzek, S., Niehaus, K., Boller, T. and Felix, G. (2004). The N terminus of bacterial elongation factor Tu elicits innate immunity in Arabidopsis plants. *Plant Cell* **16**: 3496-3507.

Kuroda, T. and Tsuchiya, T. (2009). Multidrug efflux transporters in the MATE family. *Biochim. Biophys. Acta.* **1794**: 763-768.

Kutchan, T.M. (1995). Alkaloid biosynthesis: the basis for metabolic engineering of medicinal plants. *Plant Cell* **7**:1059–70.

La Camera, S., Gouzerh, G., Dhondt, S., Hoffmann, L., Frittig, B., Legrand, M., and Heitz, T. (2004). Metabolic reprogramming in plant innate immunity: the contributions of phenylpropanoid and and oxylipin pathways. *Immunol. Rev.* **198**: 267–284.

La Camera, S., L'haridon, F., Astier, J., Zander, M., Abou-Mansour, E., Page, G., Thurow, C., Wendehenne, D., Gatz, C., Métraux, J.-P. and Lamotte, O. (2011). The glutaredoxin ATGRXS13 is required to facilitate *Botrytis cinerea* infection of *Arabidopsis thaliana* plants. *Plant J.* **68**: 507–19.

Lam, H.M., Chiu, J., Hsieh, M.H., Meisel, L., Oliveira, I.C., Shin, M. and Coruzzi, G. (1998). Glutamate-receptor genes in plants. *Nature* **396**:125-126.

Laporte, D., Olate, E., Salinas, P., Salazar, M., Jordana, X. and Holuigue, L. (2012). Glutaredoxin GRXS13 plays a key role in protection against photooxidative stress in Arabidopsis. *J. Exp. Bot.* **63**: 503–15.

Lascombe, M., Larue, R.Y., Marion, D. and Blein, J. (2008). The structure of "'defective in induced resistance '" protein of *Arabidopsis thaliana*, DIR1, reveals a new type of lipid transfer protein. *Protein Sci.* **17**: 1522–1530.

Lawton, M.P., Cashman, J.R, Cresteil, T., Dolphin, C.T., Elfarra, A.A., Hines, R.N., Hodgson, E., Kimura T., Ozols J. and Phillips I.R. (1994). A nomenclature for the mammalian flavin-containing monooxygenase gene family based on amino acid sequence identities. *Arch. Biochem. Biophys.* **308**: 254–257.

Lee, M., and Leustek, T. (1999). Identification of the gene encoding homoserine kinase from *Arabidopsis thaliana* and characterization of the recombinant enzyme derived from the gene. *Arch. Biochem. Biophys.* **372**: 135–142.

Lee, M.W., Lu, H., Jung, H.W. and Greenberg, J.T. (2007). A key role for the Arabidopsis WIN3 protein in disease resistance triggered by *Pseudomonas syringae* that secrete AvrRpt2. *Mol. Plant-Microbe Interact.* **20**: 1192-1200.

Lotze, M.T., Zeh, H.J., Rubartelli, A., Sparvero, L.J., Amoscato, A.A., Washburn, N.R., DeVera, M.E., Liang, X., Tör, M. and Billiar, T. (2007). The grateful dead: damage-associated molecular pattern molecules and reduction/oxidation regulate immunity. *Immunol. Rev.* **220**: 60-81.

Lorenc-Kukula, K., Chaturvedi, R., Roth, M., Welti, R. and Shah, J. (2012). Biochemical and Molecular-Genetic Characterization of SFD1's Involvement in Lipid Metabolism and Defense Signaling. *Front. Plant Sci.* **3**: 26.

Li, J., Brader, G. and Palva, E.T. (2004). The WRKY70 transcription factor: a node of convergence for jasmonate-mediated and salicylate- mediated signals in plant defense. *Plant Cell* **16**: 319–331.

Li, J., Hansen, B.G., Ober, J., Kliebenstein, D.J. and Halkier, B.A. (2008). Subclade of flavin-monooxygenases involved in aliphatic glucosinolate biosynthesis. *Plant Physiol.* **148**: 1721–33.

Li, L., Yu, X., Thompson, A., Guo, M., Yoshida, S., Asami, T., Chory, J. and Yin, Y. (2009). Arabidopsis MYB30 is a direct target of BES1 and cooperates with BES1 to regulate brassinosteroid-induced gene expression. *Plant J.* **58**: 275–286.

Liu, J., Elmore, J.M., Fuglsang, A.T., Palmgren, M.G., Staskawicz, B.J. and Coaker. G. (2009). RIN4 functions with plasma membrane H+ -ATPases to regulate stomatal apertures during pathogen attack. *PLoS Biol.* **7**: e1000139.

Liu, J., Elmore, J.M., Lin, Z.-J.D. and Coaker, G. (2011a). A receptor-like cytoplasmic kinase phosphorylates the host target RIN4, leading to the activation of a plant innate immune receptor. *Cell Host Microbe* **9**: 137-146.

Liu, P.P., Bhattacharjee, S., Klessig, D.F. and Moffett, P. (2010). Systemic acquired resistance is induced by R gene-mediated responses independent of cell death. *Molecular Plant Pathology* **11**: 155–160.

Liu, P.P., von Dahl, C.C. and Klessig, D.F. (2011). The extent to which methyl salicylate is required for signaling systemic acquired resistance is dependent on exposure to light after infection. *Plant Physiol.* **157**: 2216-26.

Liu, Z., Wu, Y., Yang, F., Zhang, Y., Chen, S., Xie, Q., Tian, X. and Zhou, J.M. (2013). BIK1 interacts with PEPRs to mediate ethylene- induced immunity. *Proc Natl Acad Sci USA* **110**: 6205–6210.

Luna, E., Bruce, T.J.A., Roberts, M.R., Flors, V. and Ton, J. (2012). Next generation systemic acquired resistance. *Plant Physiol.* **158**: 844–853.

Luna, E., van Hulten, M., Zhang, Y., Berkowitz, O., López, A., Pétriacq, P., Sellwood, M.A., Chen, B., Burrell, M., van de Meene, A., Pieterse C.M.J., Flors, V. and Ton, J. (2014). Plant perception of β-aminobutyric acid is mediated by an aspartyl-tRNA synthetase. *Nat. Chem. Biol.* **10**: 450–6.

Macheroux, P., Schmid, J., Amrhein, N. and Schaller A. (1999). A unique reaction in a common pathway: mechanism and function of chorismate synthase in the shikimate pathway. *Planta* **207**: 325–34.

Maeda, H., Shasany, A.K., Schnepp, J., Orlova, I., Taguchi, G., Cooper, B.R., Rhodes, D., Pichersky, E. and Dudareva, N. (2010). RNAi suppression of Arogenate Dehydratase 1 reveals that phenylalanine is synthesized predominantly via the arogenate pathway in petunia petals. *Plant Cell* **22**: 832–49.

Maeda, H., Yoo, H. and Dudareva, N. (2011). Prephenate aminotransferase directs plant phenylalanine biosynthesis via arogenate. *Nat. Chem. Biol.* **7**: 19–21.

Maeda, H. and Dudareva, N. (2012). The shikimate pathway and aromatic amino acid biosynthesis in plants. *Annu. Rev. Plant Biol.* **63**: 73-105.

Maekawa, T., Kufer, T.A. and Schulze-Lefert, P. (2011). NLR functions in plant and animal immune systems: so far and yet so close. *Nature Immunology* **12**: 817–826.

Malamy, J., Carr, J.P., Klessig, D.F. and Raskin, I. (1990). Salicylic acid: a likely endogenous signal in the resistance response of tobacco to viral infection. *Science* **250**: 1002–4.

Maldonado, A.M., Doerner, P., Dixon, R.A., Lamb, C.J. and Cameron, R.K. (2002). A putative lipid transfer protein involved in systemic resistance signaling in Arabidopsis. *Nature* **419**:399–403.

Maleck, K., Levine, A., Eulgem, T., Morgan, A., Schmid, J., Lawton, K.A., Jeffery, L. and Dietrich, R.A. (2000). The transcriptome of *Arabidopsis thaliana* during systemic acquired resistance. *Nature Genetics* **26**: 403-410

von Malek, B., van der Graaff, E., Schneitz, K. and Keller, B. (2002). The Arabidopsis male-sterile mutant *dde2-2* is defective in the allene oxide synthase gene encoding one of the key enzymes of the jasmonic acid biosynthesis pathway. *Planta* **216**: 187-92.

Mamer, O.A. and Reimer, M.L. (1992). On the mechanisms of the formation of L-alloisoleucine and the 2-hydroxy-3-methylvaleric acid stereoisomers from L-isoleucine in maple syrup urine disease patients and in normal humans. *Journal of Biological Chemistry* **267**: 22141–22147.

Mao, P., Duan, M., Wie, C. and Li, Y. (2007). WRKY62 transcription factor acts downstream of cytosolic NPR1 and negatively regulates jasmonate-responsive gene expression. *Plant Cell Physiol.* **48**:833–42.

Mateo, A., Funck, D., Mühlenbock, P., Kular, B., Mullineaux, P.M. and Karpinski, S. (2006). Controlled levels of salicylic acid are required for optimal photosynthesis and redox homeostasis. *Journal of Experimental Botany* **57**: 1795–1807.

Mateo, A., Mühlenbock, P., Rusterucci, C., Chang, C.C., Miszalski, Z., Karpinska, B., Parker, J.E., Mullineaux, P.M. and Karpisnki, S. (2004). LESION SIMULATING DISEASE1 is required for acclimation to conditions that promote excess excitation energy. *Plant Physiology* **136**: 2818–2830.

Matsui, A., Ishida, J., Morosawa, T, Mochizuki, Y., Kaminuma, E., Endo, T.A., Okamoto, M., Nambara, E., Nakajima, M., Kawashima, M., Satou, M., Kim, J.M., Kobayashi, N., Toyoda, T., Shinozaki, K. and Sek, M. (2008). Arabidopsis transcriptome analysis under drought, cold, high-salinity and ABA treatment conditions using a tiling array. *Plant Cell Physiol* **49**: 1135-1149.

Matysik, J., Bhalu, B. and Mohanty, P. (2002). Molecular mechanisms of quenching of reactive oxygen species by proline under stress in plants. *Curr. Sci.* **82**: 525–532.

Mauch, F., Mauch-Mani, B. and Boller, T. (1988). Antifungal hydrolases in pea tissue. *Plant Physiol.* **2**: 936–942.

Melotto, M., Underwood, W., Koczan, J., Nomura, K. and He S.Y. (2006). Plant stomata function in innate immunity against bacterial invasion. *Cell* **126**: 969–980.

Mert-Türk, F., Bennett, M.H., Mansfield, J.W. and Holub, E.B. (2003). Camalexin accumulation in *Arabidopsis thaliana* following abiotic elicitation or inoculation with virulent or avirulent *Hyaloperonospora parasitica*. *Physiol. Mol. Plant Pathol.* **62**: 137-145.

Métraux, J.P., Signer, H., Ryals, J., Ward, E., Wyss-Benz, M., Gaudin, J., Raschdorf, K., Schmid, E., Blum, W. and Inverardi, B.(1990). Increase in salicylic acid at the onset of systemic acquired resistance in cucumber. *Science* **250**:1004–1006.

Mishina, T.E. and Zeier, J. (2006). The Arabidopsis flavin-dependent monooxygenase FMO1 is an essential component of biologically induced systemic acquired resistance. *Plant Physiol.* **141**: 1666–1675.

Mishina, T.E. and Zeier, J. (2007). Pathogen-associated molecular pattern recognition rather than development of tissue necrosis contributes to bacterial induction of systemic acquired resistance in Arabidopsis. *Plant J.* **50**: 500–13.

Misra, N. and Saxena, P. (2009). Effect of salicylic acid on proline metabolism in lentil grown under salinity stress. *Plant Science* **177**: 181-189.

Mobley, E.M., Kunkel, B.N., Keith, B. (1999). Identification, characterization and comparative analysis of a novel chorismate mutase gene in *Arabidopsis thaliana*. *Gene* **240**: 115–23.

Monaghan, J. and Zipfel, C. (2012). Plant pattern recognition receptor complexes at the plasma membrane. *Current Opinion in Plant Biology* **15**: 349–357.

Moore, A.L., Albury, M.S., Crichton, P.G. and Affourtit, C. (2002). Function of the alternative oxidase: is it still a scavenger? *Trends in Plant Science* **7**: 478–481.

Morrison, R.I. (1953). The isolation of L-pipecolinic acid from *Trifolium repens*. *Biochem. J.* **53**: 474-478.

Mota, L.J. and Cornelis, G.R. (2005). The bacterial injection kit: type III secretion systems. *Ann Med.* **37**: 234–249.

Mou, Z., Fan, W. and Dong X. (2003). Inducers of plant systemic acquired resistance regulate NPR1 function through redox changes. *Cell* **113**: 935–44.

Moulin, M., Deleu, C., Larher, F. and Bouchereau, A. (2006). The lysine-ketoglutarate reductase-saccharopine dehydrogenase is involved in the osmo-induced synthesis of pipecolic acid in rapeseed leaf tissues. *Plant Physiol. Biochem.* **44**: 474–82.

Mourad, G. and King, J. (1995). L-O-Methylthreonine-resistant mutant of Arabidopsis defective in isoleucine feedback regulation. *Plant Physiol.* **107**: 43–52.

Mousavi, S.A.R., Chauvin, A., Pascaud, F., Kellenberger, S., and Farmer, E.E. (2013). GLUTAMATE RECEPTOR-LIKE genes mediate leaf-to-leaf wound signaling. *Nature* **500**: 422–6.

Mühlenbock, P., Szechynska-Hebda, M., Plaszczyca, M., Baudo, M., Mateo, A., Mullineaux, P.M., Parker, J.E., Karpińska, B. and Karpiński, S. (2008). Chloroplast signaling and LESION SIMULATING DISEASE1 regulate crosstalk between light acclimation and immunity in Arabidopsis. *The Plant Cell* **20**: 2339–2356.

Murthy, S.N. and Janardanasarma, M.K. (1999). Identification of L-amino acid/L-lysine alpha-amino oxidase in mouse brain. *Mol. Cell. Biochem.* **197**: 13–23.

Muskett, P.R., Kahn, K., Austin, M.J., Moisan, L.J., Sadanandom, A., Shirasu, K., Jones, J.D. and Parker, J.E. (2002). Arabidopsis RAR1 exerts rate-limiting control of R gene-mediated defenses against multiple pathogens. *The Plant Cell* **14**: 979–992.

Nambara, E., Kawaide, H., Kamiya, Y. and Naito, S. (1998). Characterization of an *Arabidopsis thaliana* mutant that has a defect in ABA accumulation: ABA-dependent and ABA-independent accumulation of free amino acids during dehydration. *Plant Cell Physiol.* **39**: 853-858.

Nandi, A., Krothapalli, K., Buseman, C.M., Li, M., Welti, R., Enyedi, A. and Fab, S.S.I. (2003). Arabidopsis *sfd* mutants affect plastidic lipid composition and suppress dwarfing, cell death, and the enhanced disease resistance phenotypes resulting from the deficiency of a fatty acid desaturase. *Plant Cell.***15**: 2383-98.

Nandi, A., Welti, R. and Shah, J. (2004). The *Arabidopsis thaliana* dihydroxyacetone phosphate reductase gene *SUPPRESSOR OF FATTY ACID DESATURASE DEFICIENCY1* is required for glycerolipid metabolism and for the activation of systemic acquired resistance. *Plant Cell* **16**: 465–477.

Nardini, M., Ricci, G., Caccuri, A. M., Solinas, S. P., Vesci, L. and Cavallini, D. (1988a). Purification and characterization of a ketimine-reducing enzyme. *Eur. J. Biochem.* **173**: 689–694.

Návarová, H., Bernsdorff, F.E.M., Döring, A.-C. and Zeier, J. (2012). Pipecolic acid, an endogenous mediator of defense amplification and priming, is a critical regulator of inducible plant immunity. *Plant Cell* **24**: 5123–41.

Navarro, L., Zipfel, C., Rowland, O., Keller, I., Robatzek, S., Boller, T. and Jones, J.D.G. (2004). The transcriptional innate immune response to flg22. Interplay and overlap with *Avr* gene-dependent defense responses and bacterial pathogenesis. *Plant Physiol.* **135**: 1113–28.

Nawrath, C., Heck, S., Parinthawong, N. and Métraux, J.P. (2002). EDS5, an essential component of salicylic acid-dependent signaling for disease resistance in Arabidopsis, is a member of the MATE transporter family. *Plant Cell* **14**: 275–86.

Nawrath, C. and Métraux, J.P. (1999). Salicylic acid induction-deficient mutants of Arabidopsis express *PR-2* and *PR-5* and accumulate high levels of camalexin after pathogen inoculation. *Plant Cell* **11**: 1393–404.

Ndamukong, I., Abdallat, A.A., Thurow, C., Fode, B., Zander, M., Weigel, R. and Gatz, C. (2007). SA-inducible Arabidopsis glutaredoxin interacts with TGA factors and suppresses JA-responsive *PDF1.2* transcription. *Plant J.* **50**: 128–139.

Nelson, B.K., Cai, X. and Nebenführ, A. (2007). A multicolored set of *in vivo* organelle markers for co-localization studies in Arabidopsis and other plants. *Plant J.* **51**: 1126-36.

Nie, H., Wu, Y., Yao, C. and Tang D. (2011). Suppression of edr2-mediated powdery mildew resistance, cell death and ethylene-induced senescence by mutations in ALD1 in Arabidopsis. *J Genet Genomics.* **38**: 137-48. doi: 10.1016/j.jgg.2011.03.001.

Nikiforova, V., Freitag, J., Kempa, S., Adamik, M., Hesse, H. and Hoefgen, R. (2003). Transcriptome analysis of sulfur depletion in *Arabidopsis thaliana*: interlacing of biosynthetic pathways provides response specificity. *Plant J.* **33**: 633-650.

Niyogi, K.K. and Fink, G.R. (1992). Two anthranilate synthase genes in Arabidopsis: defense-related regulation of the tryptophan pathway. *Plant Cell* **4**: 721–33.

Nobuta, K., Okrent, R.A., Stoutemyer, M., Rodibaugh, N., Kempema, L., Wildermuth, M.C. and Innes, R.W. (2007). The GH3 acyl adenylase family member PBS3 regulates salicylic acid-dependent defense responses in Arabidopsis. *Plant Physiol.* **144**: 1144-1156.

Noutoshi, Y., Okazaki, M., Kida, T., Nishina, Y.,Morishita, Y.,Ogawa, T., Suzuki, H., Shibata, D., Jikumaru, Y., Hanada, A., Kamiya, Y. and Shirasu, K. (2012). Novel plant immune- priming compounds identified via high-throughput chemical screening target salicylic acid glucosyl- transferases in Arabidopsis. *Plant Cell* **24:** 3795–3804.

Nürnberger, T. and Scheel, D. (2001). Signal transmission in the plant immune response. *Trends Plant Sci.* **6**: 372–9.

O'Connell R.J. and Panstruga R. (2006). Tête à tête inside a plant cell: Establishing compatibility between plants and biotrophic fungi and oomycetes. *New Phytologist* **171**: 699–718.

Okrent, R. a, Brooks, M.D. and Wildermuth, M.C. (2009). Arabidopsis GH3.12 (PBS3) conjugates amino acids to 4-substituted benzoates and is inhibited by salicylate. *J. Biol. Chem.* **284**: 9742–54.

Olszak, B., Malinovsky, F.G., Brodersen, P., Grell, M., Giese, H., Petersen, M. and Mundy, J. (2006). A putative flavin-containing monooxygenase as a marker for certain defense and cell death pathways. *Plant Sci.* **170**: 614–623.

Oort, A. J. P. and Van Andel, O. M. (1960). Aspects in chemotherapy. *Mededel. Opz. Gent.* **25**: 961-992.

Östin, A., Kowalyczk, M., Bhalerao, R.P. and Sandberg, G. (1998) Metabolism of indole-3-acetic acid in Arabidopsis. *Plant Physiol.* **118**: 285-296.

Ouyang, J., Shao, X. and Li, J. (2000). Indole-3-glycerol phosphate, a branchpoint of indole-3-acetic acid biosynthesis from the tryptophan biosynthetic pathway in *Arabidopsis thaliana. Plant J.* **24**: 327–33.

Pálfi, G. and Dézsi, L. (1968) Pipecolic acid as an indicator of abnormal protein metabolism in diseased plants. *Plant and Soil* **29**: 285–291.

Pallas, J.A., Paiva, N.L., Lamb, C. and Dixon, R.A. (1996).Tobacco plants epigenetically suppressed in phenylalanine ammonia-lyase expression do not develop systemic acquired resistance in response to infection by tobacco mosaic virus. *Plant J.* **10**: 281–93

Pancheva T.V., Popova L.P. and Uzunova A.N. (1996). Effects of salicylic acid on growth and photosynthesis in barley plants. *Journal of Plant Physiology* **149**: 57–63**.**

Park, S.-W., Kaimoyo, E., Kumar, D., Mosher, S. and Klessig, D.F. (2007). Methyl salicylate is a critical mobile signal for plant systemic acquired resistance. *Science* **318**: 113–16

Park, J.-E., Park, J.-Y., Kim, Y.-S., Staswick, P.E., Jeon, J., Yun, J., Kim, S.-Y., Kim, J., Lee, Y.-H. and Park, C.-M. (2007). GH3-mediated auxin homeostasis links growth regulation with stress adaptation response in Arabidopsis. *J. Biol. Chem.* **282**: 10036–46.

Parre, E., Ghars, M.A., Leprince, A.S., Thiery, L., Lefebvre, D., Bordenave, M., Richard, L., Mazars, C., Abdelly, C. and Savouré, A. (2007). Calcium signaling via phospholipase C is essential for proline accumulation upon ionic but not nonionic hyperosmotic stresses in Arabidopsis. *Plant Physiol* **144**: 503–512.

Pauwels, L., Barbero, G.F., Geerinck, J., Tilleman, S., Grunewald, W., Pérez, A.C., Chico, J.M., Bossche, R.V., Sewell, J., Gil, E., García-Casado, G., Witters, E., Inzé,

D., Long, J.A., De Jaeger, G., Solano, R. and Goossens, A. (2010). NINJA connects the co-repressor TOPLESS to jasmonate signaling. *Nature* **464**: 788–791.

Payton, C.W. and Chang, Y.F. (1982). Δ1-piperideine-2-carboxylate reductase of Pseudomonas putida. *J. Bacteriol.* **149**: 864–871.

Peleman, J., Boerjan, W., Engler, G., Seurinck, J., Botterman, J., Alliotte, T., Van Montagu, M. and Inze, D. (1989a). Strong cellular preference in the expression of a housekeeping gene of *Arabidopsis thaliana* encoding S-adenosylmethionine synthetase. *Plant Cell* **1**: 81-93.

Peleman, J., Saito, K., Cottyn, B., Engler, G., Seurinck, J., Van Montagu, M. and Inze, D. (1989b). Structure and expression analyses of the S-adenosylmethionine synthetase gene family in *Arabidopsis thaliana*. Gene **84**: 359-369.

Petersen, M., Brodersen, P. Naested, H., Andreasson, E., Lindhart, U., Johansen, B., Nielsen, H.B., Lacy, M., Austin, M.J., Parker, J.E., Sharma, S.B., Klessig, D.F., Martienssen, R., Mattsson, O., Jensen, A.B. and Mundy, J. (2000). Arabidopsis map kinase 4 negatively regulates systemic acquired resistance. *Cell* **103**: 1111–1120.

Perl, A., Shaul, O. and Galili G. (1992). Regulation of lysine synthesis in transgenic potato plants expressing a bacterial dihydrodipicolinate synthase in their chloroplasts. *Plant Mol Biol.* **64**: 3669-79.

Pieterse, C.M.J., Van Wees, S.C.M., Hoffland, E., van Pelt, J. and Van Loon, L.C. (1996). Systemic resistance in Arabidopsis induced by biocontrol bacteria is independent of salicylic acid accumulation and pathogenesis-related gene expression. Plant Cell **8**: 1225–37.

Pieterse, C.M.J., Van der Does, D., Zamioudis, C., Leon-Reyes, A., and Van Wees, S.C.M. (2012). Hormonal modulation of plant immunity. *Annu. Rev. Cell Dev. Biol.* **28**: 489-521.

Petrakis P. L. and Greenberg D. M. (1965). Studies on L-Proline: NAD(P)+-Oxidoreductase of Hog Kidney. *Biochim. Biophys. Acta* **99**: 78–95.

Plecko, B., Hikel, C., Korenke, G.C., Schmitt, B., Baumgartner, M., Baumeister, F., Jakobs, C., Struys, E., Erwa, W. and Stöckler-Ipsiroglu, S. (2005). Pipecolic acid as a diagnostic marker of pyridoxine-dependent epilepsy. *Neuropediatrics* **36**: 200–205.

Pommerrenig, B., Feussner, K., Zierer, W., Rabinovych, V., Klebl, F., Feussner, I. and Sauer, N. (2011). Phloem-specific expression of Yang cycle genes and identification of novel Yang cycle enzymes in Plantago and Arabidopsis. *Plant Cell* **23**: 1904–19.

Pozo, M. J., Verhage, A., García-Andrade, J., García, J.M. and Azcón-Aguilar C. (2009). Priming plant defenses against pathogens by arbuscular mycorrhizal fungi. In Mycorrhizas: Functional Processes and Ecological Impact (Azcón-Aguilar, C. et *al.*, eds), pp. 137–149.

Radwanski, E.R. and Last, R.L. (1995). Tryptophan biosynthesis and metabolism: biochemical and molecular genetics. *Plant Cell* **7**: 921–34.

Rao, M.V., Paliyath, G., Ormrod, D.P., Murr, D.P. and Watkins, C.B. (1997). Influence of salicylic acid on H_2O_2-production, oxidative stress, and H_2O_2-metabolizing enzymes. *Plant Physiology* **115:** 137–149.

Rauhut, T. and Glawischnig, E. (2009). Evolution of camalexin and structurally related indolic compounds. *Phytochemistry* **70**: 1638-1644.

Rasmussen, J.B., Hammerschmidt, R. and Zook, M.N. (1991). Systemic induction of salicylic acid accumulation in cucumber after inoculation with *Pseudomonas syringae* pv. *syringae*. *Plant Physiol.* **97**: 1342–47.

Rate, D.N. and Greenberg, J.T. (2001). The Arabidopsis *aberrant growth and death2* mutant shows resistance to *Pseudomonas syringae* and reveals a role for NPR1 in suppressing hypersensitive cell death. *Plant J.* **27**: 203–11.

Verslues, P.J., Stewart, C.R. and Hack, E. (1989). Pyrroline-5-carboxylate reductase is in Pea (*Pisum sativum* L.) leaf chloroplasts. *Plant Physiol* **91**: 581–586.

Reuber, B.E., Karl, C., Reimann, S.A., Mihalik, S.J. and Dodt, G. (1997). Cloning and functional expression of a mammalian gene for a peroxisomal sarcosine oxidase. Journal of Biological Chemistry **272**: 6766–6776.

Reumann, S., Quan, S, Aung, K., Yang, P., Manandhar-Shrestha, K., Holbrook, D., Linka, N., Switzenberg, R., Wilkerson, C.G., Weber, A.P.M., Olsen, L.J. and Hu, J. (2009). In-depth proteome analysis of Arabidopsis leaf peroxisomes combined with in vivo subcellular targeting verification indicates novel metabolic and regulatory functions of peroxisomes. *Plant Physiol.* **150**: 125-143.

Ribot, C., Zimmerli, C., Farmer, E.E., Reymond, P. and Poirier, Y. (2008). Induction of the Arabidopsis *PHO1H10* gene by 12-oxo-phyto-dienoic acid but not jasmonic acid via a CORONATINE INSENSITIVE1- dependent pathway. *Plant Physiol.* **147**: 696-706.

Rietz, S., Stamm, A., Malonek, S., Wagner, S., Becker, D., Medina-Escobar, N., Vlot, A.C., Feys, B.J., Niefind, K. and Parker, J.E. (2011). Different roles of Enhanced Disease Susceptibility1 (EDS1) bound to and dissociated from Phytoalexin Deficient4 (PAD4) in Arabidopsis immunity. *New Phytol.* **191**: 107-119.

Rivas-San Vicente, M. and Plasencia, J. (2011). Salicylic acid beyond defense: its role in plant growth and development. *J. Exp. Bot.* **62**: 3321–38.

Ritacco, F. V, Graziani, E.I., Summers, M.Y., Zabriskie, M., Yu, K., Bernan, V.S., Carter, G.T., Zabriskie, T.M., and Greenstein, M. (2005). Production of novel rapamycin analogs by precursor-directed biosynthesis. *Appl. Environ. Microbiol.* **71**: 1971–1976.

Robert-Seilaniantz, A., Grant, M. and Jones, J.D. (2011). Hormone crosstalk in plant disease and defense: more than just jasmonate-salicylate antagonism. *Annu. Rev. Phytopathol.* **49**: 317–343.

Robinson, M.D., McCarthy, D.J. and Smyth, G.K. (2010). edgeR: a Bioconductor package for differential expression analysis of digital gene expression data. *Bioinformatics* **26**: 139-140.

Roetschi, A., Si-Ammour, A., Belbahri, L., Mauch, F. and Mauch-Mani, B. (2001). Characterization of an Arabidopsis-Phytophthora pathosystem: resistance requires a functional PAD2 gene and is independent of salicylic acid, ethylene and jasmonic acid signaling. *Plant J.* **28**: 293–305.

Rogers, E.E. and Ausubel, F.M. (1997). Arabidopsis enhanced disease susceptibility mutants exhibit enhanced susceptibility to several bacterial pathogens and alterations in PR-1 gene expression. *Plant Cell* **9**: 305-316.

Romeis, T., Piedras, P., and Jones, J.D. (2000). Resistance gene-dependent activation of a calcium-dependent protein kinase in the plant defense response. *Plant Cell* **12**: 803–16.

Romero, R.M., Roberts, M.F. and Phillipson, J.D. (1995). Anthranilate synthase in microorganisms and plants. *Phytochemistry* **39**:263–76.

Roosens, N.H., Thu, T.T., Iskandar, H.M. and Jacobs, M.(1998). Isolation of the ornithine-d-aminotransferase cDNA and effect of salt stress on its expression in *Arabidopsis thaliana*. *Plant Physiol* **117**: 263– 271.

Ross, A., Yamada, K., Hiruma, K., Yamashita-Yamada, M., Lu, X., Takano, Y., Tsuda, K. and Saijo, Y. (2014). The Arabidopsis PEPR pathway couples local and systemic plant immunity. *EMBO J.* **33**: 62–75.

Rothstein, M. and Miller, L. (1954). The conversion of lysine to pipecloc acid in the rat. *J Biol Chem.* **(2)**: 851-8

von Saint Paul, V., Zhang, W., Kanawati, B., Geist, B., Faus-Keßler, T., Schmitt-Kopplin, P. and Schäffner A. (2011) The Arabidopsis glucosyltransferase UGT76B1 conjugates isoleucic acid and modulates plant defense and senescence. *The Plant Cell* **23**, 4124–4145.

Sauter, M., Lorbiecke, R., Ouyang, B., Pochapsky, T.C. and Rzewuski, G. (2005). The immediate-early ethylene response gene OsARD1 encodes an acireductone dioxygenase involved in recycling of the ethylene precursor S-adenosylmethionine. *Plant J.* **44**: 718–29.

Schaller, A. and Stintzi, A. (2009). Enzymes in jasmonate biosynthesis – structure, function, regulation. *Phytochemistry* **70**: 1532–1538.

Scheel, D. (1998). Resistance response physiology and signal transduction. *Curr. Opin. Plant Biol.* **1**: 305–310.

Schlaich, N.L. (2007). Flavin-containing monooxygenases in plants: looking beyond detox. *Trends Plant Sci.* **12**: 412–8.

Schlenk, D. (1998). Occurrence of flavin-containing monooxygenases in non-mammalian eukaryotic organisms. *Comp. Biochem. Physiol. C: Pharmacol. Toxicol. Endocrinol.* **121**: 185–195.

Schmelz, E.A., Engelberth, J., Tumlinson, J.H., Block, A. and Alborn, H.T. (2004). The use of vapor phase extraction in metabolic profiling of phytohormones and other metabolites. *Plant J.* **39**: 790-808.

Schuhegger, R., Nafisi, M., Mansourova, M., Petersen, B.L., Olsen, C.E., Svatos, A., Halkier, B.A. and Glawischnig, E. (2006). CYP71B15 (PAD3) catalyzes the final step in camalexin biosynthesis. *Plant Physiol.* **141**: 1248–54.

Serrano, M., Wang, B., Aryal, B., Garcion, C., Abou-Mansour, E., Heck, S., Geisler, M., Mauch, F., Nawrath, C. and Métraux, J.-P. (2013). Export of salicylic acid from the chloroplast requires the multidrug and toxin extrusion-like transporter EDS5. *Plant Physiol.* **162**: 1815–21.

Seskar, M., Shulaev, V. and Raskin, I. (1998). Endogenous methyl salicylate in pathogen-inoculated tobacco plants. *Plant Physiol.* **116**: 387–92.

Shah, J., Tsui, F. and Klessig, D.F. (1997). Characterization of a salicylic acid-insensitive mutant (sai1) of *Arabidopsis thaliana* identified in a selective screen utilizing the SA-inducible expression of the *tms2* gene. *Mol Plant Microbe Interact* **10**: 69-78.

Shah, J., Kachroo, P., Nandi, A. and Klessig,D. F. (2001).A recessive mutation in the Arabidopsis *SSI2* gene confers SA- and NPR1-independent expression of *PR* genes and resistance against bacterial and oomycete pathogens. *Plant J.* **25**: 563–574.

Shah, J. and Zeier, J. (2013). Long-distance communication and signal amplification in systemic acquired resistance. *Front. Plant Sci.* **4**: 30.

Shah, J., Chaturvedi, R., Chowdhury, Z., Venables, B. and Petros, R. (2014). Signaling by small metabolites in systemic acquired resistance. *Plant J.***79:** 645–658.

Shakirova, F.M., Sakhabutdinova, A.R., Bezrukova, V., Fatkhutdinova, R.A. and Fatkhutdinova, D.R. (2003). Changes in the hormonal status of wheat seedlings induced by salicylic acid and salinity. Plant *Science* **164**: 317–322.

Shahjee, H.M., Banerjee, K. and Ahmad, F. (2002). Comparative analysis of naturally occurring L-amino acid osmolytes and their D-isomers on protection of *Escherichia coli* against environmental stresses. *J Biosci* **27**: 515–520.

Sheard, L.B., Tan, X., Mao, H.B., Withers, J., Ben-Nissan, G., Hinds, T.R., Kobayashi, Y., Hsu, F.F., Sharon, M., Browse, J., He, S.Y., Rizo, J., Howe, G.A. and Zheng, N. (2010). Jasmonate perception by inositol-phosphate-potentiated COI1-JAZ co-receptor. *Nature* **468**: 400-U301.

Shen, B., Li, C. and Tarczynski, M.C. (2002). High free-methionine and decreased lignin content result from a mutation in the Arabidopsis S-adenosyl-L-methionine synthetase 3 gene. *Plant J.* **29**: 371–380.

Shiu, S.H. and Bleecker, A.B. (2001). Receptor-like kinases from Arabidopsis form a monophyletic gene family related to animal receptor kinases. *Proc. Natl. Acad. Sci. USA* **98**: 10763-10768.

Smith, K.D., Andersen-Nissen, E., Hayashi, F., Strobe, K., Bergman, M.A., Barrett, S.L., Cookson, B.T. and Aderem, A. (2003). Toll-like receptor 5 recognizes a conserved site on flagellin required for protofilament formation and bacterial motility. *Nature Immunol.* **4**: 1247–1253.

Sobolev, V., Edelman, M., Dym, O., Unger, T., Albeck, S., Kirma, M. and Galili, G. (2013). Structure of ALD1, a plant-specific homologue of the universal diaminopimelate aminotransferase enzyme of lysine biosynthesis. *Acta Crystallogr. Sect. F. Struct. Biol. Cryst. Commun.* **69**: 84–9.

Song, J.T., Lu, H. and Greenberg, J.T. (2004a). Divergent roles in *Arabidopsis thaliana* development and defense of two homologous genes, *ABERRANT GROWTH AND DEATH2* and *AGD2-LIKE DEFENSE RESPONSE PROTEIN1*, encoding novel aminotransferases. *Plant Cell* **16**: 353-366.

Song, J.T., Lu, H., McDowell, J.M., and Greenberg, J.T. (2004b). A key role for ALD1 in activation of local and systemic defenses in Arabidopsis. *Plant J.* **40**: 200–12.

Song, J.T., Koo, Y.J., Seo, H.S., Kim, M.C., Choi, Y.D. and Kim, J.H. (2008). Overexpression of *AtSGT1*, an Arabidopsis salicylic acid glucosyltransferase, leads to increased susceptibility to *Pseudomonas syringae. Phytochemistry* **69**: 1128–34.

Song, W.-Y., Choi, K.S., Kim, D.Y., Geisler, M., Park, J., Vincenzetti, V., Schellenberg, M., Kim, S.H., Lim, Y.P., Noh, E.W., Lee, Y. and Martinoia, E. (2010). Arabidopsis PCR2 is a zinc exporter involved in both zinc extrusion and long-distance zinc transport. *Plant Cell* **22**: 2237–52.

Siehl, D.L. (1999). The biosynthesis of tryptophan, tyrosine, and phenylalanine from chorismate. *In Plant Amino Acids: Biochemistry and Biotechnology, ed. BK Singh,* pp. *171–204. New York: Marcel Dekker.*

Singh, B.K., Lonergan, S.G. and Conn, E.E. (1986). Chorismate mutase isoenzymes from selected plants and their immunological comparison with the isoenzymes from Sorghum bicolor. *Plant Physiol.* **81**: 717–22.

Singh, B.K. (1999). Biosynthesis of valine, leucine and isoleucine. In BK Singh, ed, Plant amino acids: Biochemistry and biotechnology. *Marcel Dekker, New York*, pp 227-247.

Singh, B.K. and Shaner, D.L. (1995). Biosynthesis of branched chain amino acids: From test tube to field. *Plant Cell* **7**: 935-944.

Slaymaker, D.H., Navarre, D.A., Clark, D., del Pozo, O., Martin, G.B. and Klessig, D.F. (2002). The tobacco salicylic acid-binding protein 3 (SABP3) is the chloroplast carbonic anhydrase, which exhibits antioxidant capacity and plays a role in the hypersensitive response. *Proc. Natl. Acad. Sci. USA* **99**: 11640–11645.

Smirnoff, N. and Cumbes, Q.J. (1989). Hydroxyl radical scavenging activity of compatible solutes. *Phytochemistry* **28**: 1057–1060.

Spoel, S.H., Koornneef, A., Claessens, S.M.C., Korzelius, J.P., Van Pelt, J.A., Mueller, M.J., Buchala, A.J., Métraux, J.P., Brown, R., Kazan, K., Van Loon, L.C., Dong, X. and Pieterse, C.M. (2003). NPR1 modulates cross-talk between salicylate- and jasmonate-dependent defense pathways through a novel func- tion in the cytosol. *Plant Cell* **15**: 760– 70.

Spoel, S.H., Johnson, J. S. and Dong, X.N. (2007). Regulation of trade-offs between plant defenses against pathogens with different lifestyles. *Proc. Natl. Acad. Sci. USA* **104**: 18842–18847.

Spoel, S.H., Mou, Z., Tada, Y., Spivey, N.W., Genschik, P. and Dong, X.N. (2009). Proteasome-mediated turnover of the transcription coactivator NPR1 plays dual roles in regulating plant immunity. *Cell* **137**: 860–72.

Spoel, S.H. and Dong, X.N. (2012) How do plants achieve immunity? Defense without specialized immune cells. *Nat. Rev. Immunol.* **12**: 89–100.

Staswick, P.E. (2009). The tryptophan conjugates of jasmonic and indole-3-acetic acids are endogenous auxin inhibitors. Plant Physiol. **150**: 1310-1321.

Sticher, L., Mauch-Mani, B. and Métraux, J.P. (1997) Systemic acquired resistance. *Annual Review of Phytopathology* **35**: 235–270.

Stuttmann, J., Hubberten, H., Rietz, S., Kaur, J., Muskett, P., Guerois, R., Bednarek, P., Hoefgen, R. and Parker, J.E. (2011). Perturbation of Arabidopsis amino acid metabolism causes incompatibility with the adapted biotrophic pathogen *Hyaloperonospora arabidopsidis. The Plant Cell* **23**: 2788–2803.

Sun, Y., Li, L., Macho, A.P., Han, Z., Hu, Z., Zipfel, C., Zhou, J.M. and Chai, J. (2013). Structural basis for flg22-induced activation of the Arabidopsis FLS2-BAK1 immune complex. *Science* **342**: 624-8.

Swarbreck, D., Wilks, C., Lamesch, P., Berardini, T.Z., Garcia-Hernandez, M., Foerster, H., Li, D., Meyer, T., Muller, R., Ploetz, L., Radenbaugh, A., Singh, S., Swing, V., Tissier, C., Zhang, P. and Huala, E. (2008). The Arabidopsis Information Resource (TAIR): gene structure and function annotation. *Nucleic Acids Research* **36**: D1009-D1014.

Székely, G., Abraham, E., Cseplo, A., Rigo, G., Zsigmond, L., Csiszar, J., Ayaydin, F., Strizhov, N., Jasik, J., Schmelzer, E., Koncz, C. and Szabados, L. (2008). Duplicated

P5CS genes of Arabidopsis play distinct roles in stress regulation and developmental control of proline biosynthesis. *Plant J.* **53**:11–28.

Szoke, A., Miao, G.H., Hong, Z. and Verma, D.P.S. (1992). Subcellular location of D1-pyrroline-5-carboxylate reductase in root/nodule and leaf of soybean. *Plant Physiol* **99**: 1642–1649.

Tada, Y., Spoel, S.H., Pajerowska-Mukhtar, K., Mou, Z.L., Song, J.Q., Wang, C., Zuo, J.R. and Dong, X.N. (2008). Plant immunity requires conformational charges of NPR1 via S-nitrosylation and thioredoxins. *Science* **321**: 952–956.

Taylor, W.R. (2000) A deeply knotted protein structure and how it might fold. *Nature* **406**: 916-919.

Taylor, N.L., Heazlewood, J.L., Day, D.A. and Millar, A.H. (2004). Lipoic acid-dependent oxidative catabolism of α- keto acids in mitochondria provides evidence for branched-chain amino acid catabolism in Arabidopsis. *Plant Physiol.* **134**: 838-848.

Thatcher, L.F., Manners, J.M. and Kazan, K. (2009). *Fusarium oxysporum* hijacks COI1-mediated jasmonate signaling to promote disease development in Arabidopsis. *Plant J.* **58**:927–39.

Thimm, O., Blasing, O., Gibon, Y., Nagel, A., Meyer, S., Kruger, P., Selbig, J., Muller, L.A., Rhee, S.Y. and Stitt, M. (2004). MAPMAN: a user-driven tool to display genomics data sets onto diagrams of metabolic pathways and other biological processes. *Plant J.* **37**: 914-939.

Thines, B., Katsir, L., Melotto, M., Niu, Y., Mandaokar, A., Liu, G.H., Nomura, K., He, S.Y., Howe, G.A. and Browse, J. (2007). JAZ repressor proteins are targets of the SCFCO11 complex during jasmonate signaling. *Nature* **448**: 661-U662.

Thomma, B.P., Eggermont, K., Penninckx, I.A., Mauch-Mani, B., Vogelsang, R., Cammue, B.P. and Broekaert, W.F. (1998). Separate jasmonate- dependent and salicylate-dependent defense-response pathways in Arabidopsis are essential for resistance to distinct microbial pathogens. *Proc. Natl. Acad. Sci. USA* **95**:15107–11.

Thomma, B.P., Nelissen, I., Eggermont, K. and Broekaert, W.F. (1999). Deficiency in phytoalexin production causes enhanced susceptibility of *Arabidopsis thaliana* to the fungus *Alternaria brassicicola*. *Plant J.* **19**: 163–17.

Thordal-Christensen, H. (2003). Fresh insights into processes of nonhost resistance. *Curr. Opin. Plant Biol.* **6**: 351–357.

Thulke, O.U. and Conrath, U. (1998). Salicylic acid has a dual role in the activation of defense-related genes in parsley. *Plant J.* **14**: 35–42.

Tintor, N., Ross, A., Kanehara, K., Yamada, K., Fan, L., Kemmerling, B., Nürnberger, T., Tsuda, K. and Saijo, Y. (2013). Layered pattern receptor signaling via ethylene and endogenous elicitor peptides during Arabidopsis immunity to bacterial infection. *Proc Natl Acad Sci USA* **110**: 6211–6216.

Ton, J. and Mauch-Mani, B. (2004). β-amino-butyric acid-induced resistance against necrotrophic pathogens is based on ABA-dependent priming for callose. *Plant J.* **38**: 119-130.

Trapp, S. and Croteau, R. (2001). Defensive resin biosynthesis in conifers. *Annu. Rev. Plant Physiol. Plant Mol. Biol* **52**: 689–724.

Traw, M.B. and Bergelson, J. (2003). Interactive effects of jasmonic acid, salicylic acid, and gibberellin on induction of trichomes in Arabidopsis. *Plant Physiology* **133**: 1367–1375.

Tripp, J., Inoue, K., Keegstra, K. and Froehlich JE. (2007). A novel serine/proline-rich domain in combination with a transmembrane domain is required for the insertion of AtTic40 into the inner envelope membrane of chloroplasts. *Plant J.* **52**: 824-838.

Tsuda. K., Sato, M., Stoddard, T., Glazebrook, J. and Katagiri, F. (2009) Network properties of robust immunity in plants. *PLoS Genet* **5**(12): e1000772.

Tzin, V. and Galili, G. (2010) New insights into the shikimate and aromatic amino acids biosynthesis pathways in plants*. Mol Plant* **3**: 956-972.

Uppalapati, S. R., Ishiga, Y.,Wangdi, T., Kunkel, B. N., Anand, A., Mysore, K. S. and Bender, C.L. (2007). The phytotoxin coronatine contributes to pathogen fitness and is required for suppression of salicylic acid accumulation in tomato inoculated with *Pseudomonas syringae* pv. *tomat*o DC3000. Mol. *PlantMicrobe Interact.* **20**: 955–965.

Urano, K., Maruyama, K, Ogata, Y., Morishita, Y., Takeda, M., Sakurai, N., Suzuki, H., Saito, K., Shibata, D., Kobayashi, M., Yamaguchi-Shinozaki, K. and Shinozaki, K. (2009). Characterization of the ABA-regulated global responses to dehydration in Arabidopsis by metabolomics. *Plant J.* **57**: 1065-1078.

Uzunova, A.N. and Popova, L.P. (2000). Effect of salicylic acid on leaf anatomy and chloroplast ultrastructure of barley plants. *Photosynthetica* **38**: 243–250.

Verbruggen, N., Villarroel, R. and Van Montagu, M. (1993). Osmoregulation of a pyrroline-5-carboxylate reductase gene in *Arabidopsis thaliana. Plant Physiol.* **103**: 771–781.

Verbruggen, N. and Hermans, C. (2008). Proline accumulation in plants: a review. *Amino Acids* **35**: 753-759.

Vernooij, B., Friedrich, L., Morse, A., Reist, R., Kolditz-Jawhar, R., Ward, E., Uknes, S., Kessmann, H. and Ryals, J. (1994). Salicylic acid is not the translocated signal responsible for inducing systemic acquired resistance but is required in signal transduction. *Plant Cell* **6**: 959–65.

Vernooij, B., Friedrich, L., Goy, P.A., Saub, T., Kessmann, H. and Ryals, J. (1995). 2,6-Dichloroisonicotinic acid-induced resistance to pathogens without the accumulation of salicylic acid. *Mol. Plant-Microbe Interact.* **8**: 228–34.

Veronese, P., Chen, X., Bluhm, B., Salmeron, J., Dietrich, R. and Mengiste, T. (2004). The BOS loci of Arabidopsis are required for resistance to *Botrytis cinerea* infection. *Plant J.* **40**: 558-574.

Verslues, P.E. and Bray, E.A. (2006). Role of abscisic acid (ABA) and *Arabidopsis thaliana* ABA-insensitive loci in low water potential-induced ABA and proline accumulation. *J Exp Bot* **57**: 201– 212.

Vlot, A.C., Dempsey, D.A. and Klessig, D.F. (2009). Salicylic acid, a multifaceted hormone to combat disease. *Annu Rev Phytopath* **47**: 177–206.

Vogel-Adghough, D., Stahl, E., Návarová, H. and Zeier, J. (2013). Pipecolic acid enhances resistance to bacterial infection and primes salicylic acid and nicotine accumulation in tobacco. *Plant Signal. Behav.* **8**: e26366 1–9.

Vogt, T. (2010). Phenylpropanoid biosynthesis. *Mol. Plant* **3**: 2–20.

Volko, S.M., Boller, T. and Ausubel, F.M. (1998). Isolation of new Arabidopsis mutants with enhanced disease susceptibility to *Pseudomonas syringae* by direct screening. *Genetics* **149**: 537-548.

Wang, D., Amornsiripanitch, N. and Dong, X.N. (2006). A genomic approach to identify regulatory nodes in the transcriptional network of systemic acquired resistance in plants. *PLoS Pathog.* **2:** 1042-1050.

Wang, D., Weaver, N.D., Kesarwani, M. and Dong, X.N. (2005). Induction of protein secretory pathway is required for systemic acquired resistance. *Science* **308**: 1036–40.

Wang, D., Pajerowska-Mukhtar, K., Culler, A.H. and Dong, X.N. (2007). Salicylic acid inhibits pathogen growth in plants through repression of the auxin signaling pathway. *Curr. Biol.* **17**: 1784-1790.

Wang, L., Mitra, R.M., Hasselmann, K.D., Sato, M., Lenarz-Wyatt, L., Cohen, J.D., Katagiri, F., and Glazebrook, J. (2008). The genetic network controlling the Arabidopsis transcriptional response to *Pseudomonas syringae* pv. *maculicola*: roles of major regulators and the phytotoxin coronatine. *Mol. Plant-Microbe Interact.* **21**: 1408-1420.

Wang, L., Tsuda, K., Sato, M., Cohen, J.D., Katagiri, F. and Glazebrook, J. (2009). Arabidopsis CaM Binding Protein CBP60g contributes to MAMP-induced SA accumulation and is involved in disease resistance against *Pseudomonas syringae*. *PLoS Pathog.* **5**: e1000301.

Wang, L., Tsuda, K., Truman, W., Sato, M., Nguyen, L.V., Katagiri, F. and Glazebrook, J. (2011). CBP60g and SARD1 play partially redundant critical roles in salicylic acid signaling. *Plant J.* **67**: 1029-1041.

Wang, K. L., Li, H. and Ecker, J. R. (2002). Ethylene biosynthesis and signaling networks. *Plant Cell* **14**: (Suppl.), S131–S151.

Ward, E.R., Uknes, S.J., Williams, S.C., Dincher, S.S., Wiederhold, D.L., Alexander, D.C., Ahl-goy, P., Métraux, J., Ryals, J.A. and Carolina, N. (1991). Coordinate gene

activity in response to agents that induce systemic acquired resistance. *Plant Cell* **3**: 1085–1094.

Ward, J.L., Forcat, S., Beckmann, M., Bennett, M., Miller, S.J., Baker, J.M., Hawkins, N.D., Vermeer, C.P., Lu, C., Lin, W., Truman, W.M., Beale, M.H., Draper, J., Mansfield, J.W., Grant, M. (2010). The metabolic transition during disease following infection of *Arabidopsis thaliana* by *Pseudomonas syringae* pv. *tomato*. *Plant J.* **63**: 443–457.

Warren, R.F., Merritt, P.M., Holub, E. and Innes, R.W. (1999). Identification of three putative signal transduction genes involved in R-gene specified disease resistance in Arabidopsis. *Genetics* **152**: 401-412.

Wasternack, C. (2007). Jasmonates: an update on biosynthesis, signal transduction and action in plant stress response, growth and development. *Ann. Bot.* **100**: 681-697.

White, RF. (1979) Acetylsalicylic acid (Aspirin) induces resistance to tobacco mosaic virus in tobacco. *Virology* **99**: 410-412.

Wickwire, B.M., Harris, C.M., Harris, T.M. and Broquist, H.P. (1990). Pipecolic acid biosynthesis in *Rhizoctonia leguminicola. J. Biol. Chem.* **265**: 14742–14747.

Wiermer, M., Feys, B.J. and Parker, J.E. (2005). Plant immunity: the EDS1 regulatory node. *Curr. Opin. Plant Biol.* **8**: 383-389.

Wildermuth, M.C., Dewdney, J., Wu, G. and Ausubel, F.M. (2001). Isochorismate synthase is required to synthesize salicylic acid for plant defense. *Nature* **414**: 562–565.

Withers, J., Yao, J., Mecey, C., Howe, G. A., Melotto, M. and He, S.Y. (2012). Transcription factor-dependent nuclear localization of a transcriptional repressor in jasmonate hormone signaling. *Proc. Natl. Acad. Sci. USA* **109**: 20148– 20153.

Witte, C.-P., Noël, L.D., Gielbert, J., Parker, J.E. and Romeis, T. (2004). Rapid one-step purification from plant material using the eight-amino acid StrepII epitope. *Plant Mol Biol.* **55**: 135-47.

Wittek, F., Hoffmann, T., Kanawati, B., Bichlmeier, M., Knappe, C., Wenig, M., Schmitt-Kopplin, P., Parker, J.E., Schwab, W. and Vlot, C. (2014). Arabidopsis ENHANCED DISEASE SUSCEPTIBILITY1 promotes systemic acquired resistance via azelaic acid and its precursor 9-oxo nonanoic acid. *J. Exp. Bot.*: doi:10.1093/jxb/eru331, 1–13.

Wu, B., Zhang, B., Feng, X., Rubens, J.R., Huang, R., Hicks, L.M., Pakrasi, H.B. and Tang, Y.J. (2009). Alternate isoleucine synthesis pathway in cyanobacterial species. Microbiology **156**: 596–602.

Wu, Y., Zhang, D., Chu, J.Y., Boyle, P., Wang, Y., Brindle, I.D., De Luca, V. and Despres, C. (2012) The Arabidopsis NPR1 protein is a receptor for the plant defense hormone salicylic acid. *Cell Rep.* **1**: 639–647.

Xie, D. X., Feys, B. F., James, S., Nieto- Rostro, M. and Turner, J. G. (1998). COI1: an Arabidopsis gene required for jasmonate-regulated defense and fertility. *Science* **280**: 1091–1094.

Xie, D. (2002). The SCF(COI1) ubiquitin-ligase complexes are required for jasmonate response in Arabidopsis. *Plant Cell* **14**: 1919–1935.

Xu, L., Liu, F., Lechner, E., Genschik, P., Crosby, W.L., Ma, H., Peng, W., Huang, D. and von Malek, B., van der Graaff, E., Schneitz, K. and Keller, B. (2002). The Arabidopsis male-sterile mutant *dde2-2* is defective in the ALLENE OXIDE SYNTHASE gene encoding one of the key enzymes of the jasmonic acid biosynthesis pathway. *Planta*, **216**: 187–192.

Xu, X., Chen, C., Fan, B. and Chen, Z. (2006). Physical and Functional Interactions between and WRKY60 Transcription Factors. *Plant Cell* **18**: 1310–1326.

Yamada, K., Lim, J., Dale, J.M., Chen, H., Shinn, P., Palm, C.J., Southwick, A.M., Wu, H.C., Kim, C., Nguyen, M., Pham, P., Cheuk, R., Karlin-Newmann, G., Liu, S.X., Lam, B., Sakano, H., Wu, T., Yu, G., Miranda, M., Quach, H.L., Tripp, M., Chang, C.H., Lee, J.M., Toriumi, M., Chan, M.M., Tang, C.C., Onodera, C.S., Deng, J.M., Akiyama, K., Ansari, Y., Arakawa, T., Banh, J., Banno, F., Bowser, L., Brooks, S., Carninci, P., Chao, Q., Choy, N., Enju, A., Goldsmith, A.D., Gurjal, M., Hansen, N.F., Hayashizaki, Y., Johnson-Hopson, C., Hsuan, V.W., Iida, K., Karnes, M., Khan, S., Koesema, E., Ishida, J., Jiang, P.X., Jones, T., Kawai, J., Kamiya, A., Meyers, C.,

Nakajima, M., Narusaka, M., Seki, M., Sakurai, T., Satou, M., Tamse, R., Vaysberg, M., Wallender, E.K., Wong, C., Yamamura, Y., Yuan, S., Shinozaki, K., Davis, R.W., Theologis, A. and Ecker, J.R. (2003) Empirical analysis of transcriptional activity in the Arabidopsis genome. *Science* **302**: 842-846.

Yamaguchi, Y., Huffaker, A., Bryan, A.C., Tax, F.E. and Ryan, C.A. (2010). PEPR2 is a second receptor for the Pep1 and Pep2 peptides and contributes to defense responses in Arabidopsis. *Plant Cell* **22**: 508–522.

Yan, J., Zhang, C., Gu, M., Bai, Z., Zhang, W., Qi, T., Cheng, Z., Peng, W., Luo, H., Nan, F., Wang, Z. and Xie, D. (2009). The arabidopsis CORONATINE INSENSITIVE1 protein is a jasmonate receptor. *Plant Cell* **21**: 2220- 2236.

Yan, Y.X., Stolz, S., Chetelat, A., Reymond, P., Pagni, M., Dubugnon, L. and Farmer, E.E. (2007). A downstream mediator in the growth repression limb of the jasmonate pathway. *Plant Cell* **19**: 2470-2483.

Yang, S.F. and Hoffman, N.E. (1984). Ethylene biosynthesis and its regulation in higher plants. *Annu Rev Plant Physiol.* **35**: 155–189.

Yatsu, L. and Boynton, D. (1959). Pipecolic acid in leaves of strawberry plant as influenced by treatments affecting growth. *Science* **130**: 864–865.

Yip, W.-K. and Yang, S.F. (1988). Cyanide metabolism in relation to ethylene production in plant tissues. *Plant Physiol.* **88**: 473–476.

Yu, K., Soares, J.M., Mandal, M.K., Wang, C., Chanda, B., Gifford, A.N., Fowler, J.S., Navarre, D., Kachroo, A. and Kachroo, P. (2013). A feedback regulatory loop between G3P and lipid transfer proteins DIR1 and AZI1 mediates azelaic-acid-induced systemic immunity. *Cell Reports* **3**: 1266–1278.

Zander, M., Chen, S., Imkampe, J., Thurow, C. and Gatz, C. (2012). Repression of the *Arabidopsis thaliana* jasmonic acid/ethylene-induced defense pathway by TGA-interacting glutaredoxins depends on their C-terminal ALWL motif. *Mol. Plant* **5**: 831–840.

Zabriskie, T.M. and Jackson, M.D. (2000). Lysine biosynthesis and metabolism in fungi. *Nat. Prod. Rep.* 17: 85–97.

Zacharius, R.M., Thompson, J.F. and Steward F.C. (1952). The detection, isolation and identification of (-)-pipecolic acid as a constituent of plants. *J. Am. Chem. Soc.* **74**: 2949-2949.

Zeier, J., Pink, B., Mueller, M.J. and Berger, S. (2004). Light conditions influence specific defense responses in incompatible plant-pathogen interactions: uncoupling systemic resistance from salicylic acid and PR-1 accumulation. *Planta* **219**: 673–683.

Zeier, J. (2013). New insights into the regulation of plant immunity by amino acid metabolic pathways. *Plant. Cell Environ.* doi: 10.1111/pce.12122.

Zhang, Y., Tessaro, M.J., Lassner, M. and Li, X. (2003) Knockout analysis of Arabidopsis transcription factors TGA2, TGA5, and TGA6 reveals their redundant and essential roles in systemic acquired resistance. *Plant Cell* **15**: 2647–2653.

Zhang, Y., Xu, S., Ding, P., Wang, D., Cheng, Y.T., He, J., Gao, M., Xu, F., Li, Y., Zhu, Z., Li, X. and Zhang, Y. (2010). Control of salicylic acid synthesis and systemic acquired resistance by two members of a plant-specific family of transcription factors. *Proc. Natl. Acad. Sci. USA* **107**: 18220–5.

Zhang, Z., Li, Q., Li, Z., Staswick, P.E., Wang, M., Zhu, Y. and He, Z. (2007). Dual regulation role of GH3.5 in salicylic acid and auxin signaling during Arabidopsis-*Pseudomonas syringae* interaction. *Plant Physiol.* **145**: 450–64.

Zhang, Z., Lenk, A., Andersson, M.X., Gjetting, T., Pedersen, C., Nielsen, M.E., Newman, M.A., Hou, B.H., Somerville, S.C. and Thordal-Christensen, H. (2008). A lesion-mimic syntaxin double mutant in Arabidopsis reveals novel complexity of pathogen defense signaling. *Mol Plant.* **3**: 510-27. doi: 10.1093/mp/ssn011.

Zhao, J.M. and Last, R.L. (1996). Coordinate regulation of the tryptophan biosynthetic pathway and indolic phytoalexin accumulation in Arabidopsis. *Plant Cell* **8**: 2235-2244.

Zhao, J.M., Williams, C.C. and Last, R.L. (1998). Induction of Arabidopsis tryptophan pathway enzymes and camalexin by amino acid starvation, oxidative stress, and an abiotic elicitor. *Plant cell* **10**: 359-370.

Zhao, Y., Christensen, S.K., Fankhauser, C., Cashman, J.R., Cohen, J.D., Weigel, D. and Chory, J. (2001). A role for flavin monooxygenase-like enzymes in auxin biosynthesis. *Science* **291**: 306–9.

Zhou, N., Tootle, T.L., Tsui, F., Klessig, D.F. and Glazebrook, J. (1998). PAD4 functions upstream from salicylic acid to control defense responses in Arabidopsis. *Plant Cell* **10**: 1021–30.

Zhou, N., Tootle, T.L., and Glazebrook, J. (1999). Arabidopsis PAD3, a gene required for camalexin biosynthesis, encodes a putative cytochrome P450 monooxygenase. *Plant Cell* **11**: 2419–28.

Zimmerli, L., Jakab, G., Metraux, J.P. and Mauch-Mani, B. (2000). Potentiation of pathogen-specific defense mechanisms in Arabidopsis by beta-aminobutyric acid. *Proc. Natl. Acad. Sci. USA.* **97**: 12920–5.

Zimmerli, L., Métraux, J.-P. and Mauch-Mani, B. (2001). β-Aminobutyric acid-induced protection of Arabidopsis against the necrotrophic fungus *Botrytis cinerea*. *Plant Physiol.* **126**: 517-523.

Zimmermann, S., Nürnberger, T., Frachisse, J.M., Wirtz, W., Guern, J., Hedrich, R. and Scheel, D. (1997). Receptor-mediated activation of a plant Ca^{2+}-permeable ion channel involved in pathogen defense. *Proc. Natl. Acad. Sci. USA* **94**: 2751–5.

Zipfel, C., Robatzek, S., Navarro, L., Oakeley, E.J., Jones, J.D.G., Felix, G., and Boller, T. (2004). Bacterial disease resistance in Arabidopsis through flagellin perception. *Nature* **428**: 764–767.

Zipfel, C. (2013). Combined roles of ethylene and endogenous peptides in regulating plant immunity and growth. *Proc. Natl. Acad. Sci. USA* **110**: 5748–9.

Zoeller, M., Stingl, N., Krischke, M., Fekete, A., Waller, F., Berger, S. and Mueller, M.J. (2012). Lipid profiling of the Arabidopsis hypersensitive response reveals specific lipid peroxidation and fragmentation processes: biogenesis of pimelic and azelaic acid. *Plant Physiol.* **160**: 365–78.

VIII. ABBREVIATIONS

AAA	Aromatic amino acids
AABA	α-amino butyric acid
ABA	Abscisic acid
ABI	Abscisic acid insensitive
AGD	ABERRANT GROWTH AND CELL DEATH
ALD	AGD2-LIKE DEFENSE RESPONSE PROTEIN
AM	Ante Meridiem
AOC	ALLENE OXIDE CYCLASE
AOS	ALLENE OXIDE SYNTHASE
Avr	avirulence
ARD	ACIDOREDUCTONE DIOXYGENASE
AzA	Azelaic acid
AZI	AZELAIC ACID INDUCED
BABA	β-aminobutyric acid
BAK	Brassinosteroid insensitive1-associated kinase
BCAA	Branched-chain amino acids
BCAT	BRANCHED-CHAIN AMINOTRANSFERASE
BOS	BOYTRITIS SUSCEPTIBLE
bp	Base pair
BRI	BRASSINOSTEROID-INSENSITIVE
BSMT	Salicylic acid/benzoic acid carboxyl methyltransferase
BTH	Benzo (1,2,3) thiadiazole-7-carbothioic acid S-methyl ester
°C	Celcius
CC	coiled-coil
cDNA	complementary DNA
CDPK	CALCIUM DEPENDENT PROTEIN KINASE
cfu	colony forming units
CoA	coenzym A
COI	Coronatine insensitive
Col	Columbia
CPR	CONSTITUTIVE EXPRESSION OF PR GENES
CRK	Receptor-like protein kinase
c_T	cycle threshold
DA	Dehydroabietinal
DAMP	Damage-associated molecular patterns
DAP-AT	Diaminopimelate aminotransferase
DHDPS	DIHYDRODIPICOLINATE SYNTHASE
DIR	DEFECTIVE IN INDUCED RESISTANCE
DND	DISEASE NO DEATH
dpi	day post inoculation
EEE	Excess excitation energy
EDR	ENHANCED DISEASE RESISTANCE
EDS	ENHANCED DISEASE SUSCEPTIBILITY
EDTA	Ethylen-diamine tetra-acetic acid
EFR	ELONGATION FACTOR TU RECEPTOR

EF-Tu	Elongation factor Tu
EIN	ETHYLENE INSENSITIVE
EMS	Ethylmethane sulphonate
ET	Ethylene
ETI	effector-triggered immunity
FLS2	FLAGELLIN SENSING 2
FMO1	FLAVIN-DEPENDENT MONOOXYGENASE 1
FW	fresh weight
GABA	γ-amino butyric acid
G3P	glycerol-3-phosphate
gDNA	genomic DNA
GFP	green fluorescent protein
GRXS	Glutaredoxin
GST	Gluthathione S-transferase
h	hour
HL	High light
HMW	High molecular weight
Hpa	*Hyaloperonospora arabidopsidis*
hpi	hours post inoculation
HR	hypersensitive response
IAA	indole acetic acid, auxin
IBI	BABA-INDUCED DISEASE IMMUNITY
ICS1	ISOCHORISMATE SYNTHASE 1
IEM	Inner envelope membrane
IMS	Intermembrane space
INA	2,6-dichloro-isonicotinic acid
IR	Induced resistance
ISR	Induced systemic resistance
JA	jasmonic acid
JA-Ile	(+)-7-iso-jasmonoyl-L-isoleucine
JAZ	JASMONATE ZIM DOMAIN
LKR	LYSINE KETOGLUTARATE REDUCTASE
LL	Low light
LMW	Low molecular weight
LPS	lipopolysaccharides
LRR	leucine-rich repeat
LSD	LESION SIMULATING DISEASE
M	mol.l^{-1}
MAMP	microorganism-associated molecular patterns
MAP	mitogen-activated protein
MAPK/MPK	mitogen activated protein kinase
MeJA	methyl jasmonate
MeSA	methyl salicylate
MES	MeSA esterase
min	minute
mRNA	messenger RNA
NahG	salicylate hydroxylase

NB	nucleotide-binding site domain
NB-LRR	nucleotide-binding – leucine rich repeats
NDR1	NON RACE SPECIFIC DISEASE RESISTANCE 1
NLS	Nuclear localization sequence
NO	Nitric oxide
NPR1	NON-EXPRESSOR OF PR GENES1
NPQ	Non-photochemical quenching
OEM	outer envelope membrane
ONA	9-oxononanoic acid
PAD	PHYTOALEXIN DEFICIENT
PAL	phenylalanine ammonia-lyase
PAMP	pathogen-associated molecular patterns
PBS3	AvrPphB SUSEPTIBLE 3
PCR	polymerase chain reaction
PDF	PLANT DEFENSIN
PEPR	PEP Receptor
PEX	Petiole exudate
Pip	Pipecolic acid
PM	Post meridiem
PR	pathogenesis-related
PRR	pattern recognition receptors
PS	Photosystem
Psm	*Pseudomonas syringae* pv. *maculicola* ES4326
Psm(avrRpm1)	*Psm* carrying the avirulence gene pLAFR3::*avrRpm1*
Pst	*Pseudomonas syringae* pv. *tomato* DC3000 *AvrRpm1*
PTI	PAMP-triggered immunity
qRT-PCR	quantitative RT-PCR
R	resistance
RIN	RPM1-INTERACTING PROTEIN
RK	receptor kinase
RLP	receptor-like proteins
ROS	reactive oxygen species
RuBisCo	ribulose-1,5-bisphosphate carboxylase/oxygenase
s	second
SA	salicylic acid
SABP	SA BINDING PROTEIN
SAG	SA O-β-glucoside
SAGT	SA glucosyltransferases
SAMT	SA methyltransferase1
SAR	systemic acquired resistance
SARD	SAR-Deficient
SD	standard deviation
SDH	SACCHAROPINE DEHYDROGENASE
SFD	SUPPRESSOR OF FATTY ACID DESATURASE DEFICIENCY
SGE	Salicyloyl glucose ester
SID	Salicylic acid induction deficient
SOX/PIPOX	SARCOSINE OXIDASE/PIPECOLATE OXIDASE

SYP	SYNTAXIN OF PLANTS
TAE	tris-acetate-ethylenediamine tetraacetic acid
TAT	TYROSINE AMINOTRANSFERASE
TCA	tricarbocylic acid
T-DNA	transposable DNA
TIC	Translocon at the inner envelope membrane of chloroplasts
TIR	toll, interleukin 1R and resistance
TLR	Toll-like receptor
TMV	tobacco mosaic virus
TOC	Translocon at the outer envelope membrane of chloroplasts
T3SS	Type-III secretion system
YFP	Yellow fluorescent protein

IX. ADDENDUM

IX.1. VECTOR MAPS

http://www.addgene.org/vector-database/2393/

https://www.promega.co.uk

pEarleyGate 100
11,649 bp

(92) AseI
Eco53kI (101)
SacI (103)
Acc65I (407)
KpnI (411)
FspAI (521)
AarI (585)
AfeI (758)
(11,412) BclI*
(11,281) PsiI
(10,955) BspHI
(10,532) EcoRV
BstBI (1770)
StuI (1868)
PshAI (2467)
PaeR7I - TliI - XhoI (2654)
lac UV5 promoter
BspEI (3105)
NcoI (3410)
BbvCI (3834)
SrfI (3980)
BstXI (4097)
AvrII (4369)
XbaI (4379)
PacI (4392)
SpeI (4404)
MfeI (4708)
BstEII (4980)
AhdI (5110)
SbfI (5135)
HindIII (5143)
(5356) PmeI
PvuI (5269)
(8797) EcoNI
(8488) BmtI
(8484) NheI
(8368) BsiWI
(9273) PluTI
(9271) SfoI
(9270) NarI
(9269) KasI
KanR
ori
bom
pVS1 RepA
pVS1 StaA
LB T-DNA repeat
RB T-DNA repeat
MAS terminator
MAS promoter
CaMV 35S promoter
attR1
CmR
attR2
ccdB
OCS terminator

http://www.snapgene.com/resources/plasmid_files/plant_vectors/

pEarleyGate 104
12,505 bp

(12,268) BclI*
(12,137) PsiI
(11,811) BspHI
(11,388) EcoRV
AseI (92)
FspAI (521)
AarI (585)
AfeI (758)
StuI (1868)
PshAI (2467)
PspXI (2654)
BbvCI (4691)
SrfI (4837)
BstXI (4954)
XbaI (5235)
PacI (5248)
SpeI (5260)
MfeI (5564)
BstEII (5836)
AhdI (5966)
SbfI (5991)
PvuI (6125)
(6212) PmeI
(9653) EcoNI
(9344) BmtI
(9340) NheI
(9224) BsiWI
(10,129) PluTI
(10,127) SfoI
(10,126) NarI
(10,125) KasI
KanR
ori
bom
pVS1 RepA
pVS1 StaA
LB T-DNA repeat
RB T-DNA repeat
MAS terminator
MAS promoter
CaMV 35S promoter
TMV Ω
EYFP
lac UV5 promoter
attR1
CmR
attR2
ccdB
OCS terminator

http://www.snapgene.com/resources/plasmid_files/plant_vectors/

The pIVEX 1.4 WG vector map (3287 bp) showing: Pvu II (530), T7-Promotor, Hin dIII (739), 5′-Enhancer (748-803), Start, Linker + Histag (826-8), Factor Xa (861-872), Ksp I (873), Not I (873), Pac I (884), Nde I (890), Nco I (896), Sal I (905), Xho I (910), Sac I (921), Pst I (926), Xma I (928), Sma I (930), Bam HI (932), Stop, 3′-Enhancer (957-1199), Eco RI (1212), Pvu II (1304), Pvu I (1335), f1 (-) ori, cal (2268), Ampi, I (2380).

Legend:
- Open reading frame
- Origin of replication
- Other gene
- Promoter
- Selectable marker
- Terminator
- Unique restriction site

The pENTR/D-TOPO vector map (2580 bp) showing: pBR322 origin, AlwNI 2166, rrnB_T2 term, rrnB_T1 term, HincII 502, HpaI 502, AvaI 561, AvrI 561, ApaI 568, NotI 673, attL1 other, attL2 other, T7 prom, EcoRV 818, NruI 1057, ORF_1 rf(2), kan2 marker.

X. CURRICULUM VITAE

Personal Information:

Name of birth: Friederike Elisabeth Maria Bernsdorff

Date and place of birth: May 4, 1984, Eutin, Germany

Nationality: German

Education:

7/2011 – 10/2014	**PhD thesis – Düsseldorf (GERMANY)**
3/2008 – 1/2010	**Master of Science – Kiel (GERMANY)** Faculty of Agricultural Sciences at the Christian-Albrechts-University of Kiel
10/2003 – 5/2007	**Bachelor of Science – Kiel (GERMANY)** Faculty of Agricultural Sciences at the Christian-Albrechts-University of Kiel

Research Experience:

7/2011 – 10/2014	**PhD project/Scientific Assistant – Düsseldorf (GERMANY)** Title of work: "Role of amino acids in plant stress resistance" Group of Prof. Dr. Jürgen Zeier at the Institute for Molecular Ecophysiology of Plants, Department of Biology, Heinrich Heine University of Düsseldorf
4/2013 - 10/2013	**Research stay at the Michigan State University – East Lansing (MI, USA)** Group of Prof. Dr. Sheng Yang He, Department of Plant Biology, Howard Hughes Medical Institute-Gordon and Betty Moore Foundation, Michigan State University, East Lansing, Michigan 48824
2/2010 – 6/2011	**Scientific Assistant – Kiel (GERMANY)** Institute for Molecular Phytopathology of the Christian-Albrechts-University of Kiel in the BMBF project „KMU Innovativ – ScleroRes: New ways to increase the resistance of rapeseed (*Brassica napus*) against *Sclerotinia sclerotiorum*"
5/2009-1/2010	**Master thesis – Kiel (GERMANY)** "Sequence, structure and functional analysis of resistance gene analogs (RGA) of wild beet (*Patellifolia procumbens*) and sugar beet lines", Institute for Phytopathology/ Dept. of Molecular Phytopathology of the Christian-Albrechts-University of Kiel
2008/2009	**Graduate Assistant – Kiel (GERMANY)** Institute for Phytopathology/ Dept. of Molecular Phytopathology of the Christian-Albrechts-University of Kiel

2008	**Graduate Assistant – Kiel (GERMANY)** Institute for Grasland and Organic farming: "Plants for health: production of plants with enriched bioactive substances"
5/2007 – 9/2007	**Research stay at the Centro Internacional de la Papa (CIP) – Lima (PERU)** Identification and characterization of entomopathogenic nematode isolates from different sites of the Peruvian Andes
11/2006-5/2007	**Bachelor thesis – Kiel (GERMANY)** "Influence of the bacterial density on the DJ-recovery of *Steinernema feltiae* and *Steinernema carpocapsae*". Institute for Phytopathology/ Dept. of Biotechnology of the Christian-Albrechts-University of Kiel
2006	**Graduate Assistant – Kiel (GERMANY)** Institute for Phytopathology/ Dept. of Biotechnology of the Christian-Albrechts-University of Kiel: „*Bacillus thuringiensis* spp. *israelensis* and entomopathogenic nematodes as biological control agents against the pest *Tipula paludosa* on grasslands"
2005	**Graduate Assistant – Kiel (GERMANY)** Institute for Phytopathology of the Christian-Albrechts-University of Kiel: „Prognosis of Fusarium attack of flowering winter wheat for a disease control in line with demand"

Scholarships:

Since 7/2011	PhD scholarship of the iGRAD Plant graduate school – Düsseldorf (GERMANY) Group of Prof. Dr. Jürgen Zeier at the Institute for Molecular Ecophysiology of Plants, Department of Biology, Heinrich Heine University of Düsseldorf
5/2010	Scholarship of the Robert-Bosch-Foundation – Chongqing (P.R. CHINA) Visit to the Rapeseed Research Centre Southwest University of BeiBei in line with the joint-project "Sustainable Partners – Partners for Sustainability", Chongqing, P.R. China
5/2009 – 6/2009	DAAD-Scholarship – Hangzhou (P.R. CHINA) PPP-program at the Institute of Bioinformatics / Institute of Crop Science, Department of Agronomy, College of Agriculture and Biotechnology, Zheijiang University of Hangzhou
9/2007 – 3/2008	ERASMUS-Scholarship – Ghent (BELGIUM) Master program "Tropical Agriculture" at the University of Ghent, Belgium
5/2007 – 9/2007	Scholarship of the Deutsche Gesellschaft für Technische Zusammenarbeit (GTZ) – Lima (PERU) Research stay at the Centro Internacional de la Papa (CIP)

Poster Presentations:

MPMI 2014, Rhodes, Greece: "Pipecolic acid regulates systemic acquired resistance via SA-dependent and independent pathways." Bernsdorff, F., Döring A.-C., Gruner K., Bräutigam A. and Zeier J.

Plant Biology 2013, Providence, Rhode Island, USA: "Interplay of pipecolic acid and salicylic acid in the induction of plant systemic acquired resistance and defense priming." Bernsdorff F. and Zeier J.

30th New Phytologist Symposium: Immunomodulation by plant-associated organisms, Fallen Leaf Lake, California, USA: "Amino acid metabolism in plant pathogen resistance." Bernsdorff F., Návarová H. and Zeier J.,

Oral Presentations:

2014 iGRAD Plant Retreat: Haus Overbach in Jülich, Germany

2013 iGRAD Plant Symposium/Retreat: Bad Neuenahr-Ahrweiler, Germany

2012 iGRAD Plant Joint Symposium/Retreat Düsseldorf, Germany

2011 iGRAD Plant Symposium/Retreat Traben-Trabach, Germany

COST 872 Fourth Annual Meeting: Exploiting genomics to understand plant-nematode interactions, Lisbon, Portugal

Publications:

Bernsdorff, F., Döring, A.-C., Gruner, K., Bräutigam, A. and Zeier, J. Pipecolic acid orchestrates plant systemic acquired resistance and defense priming via salicylic c acid-dependent and independent pathways, *in prep.*

Návarová H., **Bernsdorff** F., Döring A.-C. and Zeier J. (2012) Pipecolic acid, an endogenous mediator of defense amplification and priming, is a critical regulator of inducible plant immunity, Plant Cell 24: 5123-5141.

Rietz S., **Bernsdorff** F.E.M. and Cai D. (2012) Members of the germin-like protein family in Brassica napus are candidates for the initiation of an oxidative burst that impedes pathogenesis of Sclerotinia sclerotiorum. Journal of Experimental Botany, 63(15):5507-19

Workshops:

3/2013   PC based analysis and presentation of biological data' - Organizer: Institute for Plant Biochemistry (HHU), Dr. Andrea Bräutigam

1/2013   'Research Paper' - iGRAD workshop in Transferable Skills

12/2012	iGRAD-Plant workshop: Advanced methods in plant science: 'Studying Protein-Protein Interaction via FRET' - Organizer: Institute for Developmental Genetics (HHU), Prof. Dr. Rüdiger Simon
5/2012	iGRAD-Plant workshop in Advanced Methods in Plant Science: 'Wheat germ cell-free expression system for protein purification' - Organizer: Institute for Plant Biochemistry (HHU), Dr. Nicole Linka
3/2012	'Fundamentals of Project Management for Doctoral Researchers' - iGRAD workshop in Transferable Skills
11/2011	'Presenting Science I – comprehensive, competent and convincing' - iGRAD workshop in Transferable Skills
7/2011	'Introduction into Good Scientific Pratice' - iGRAD workshop

XI. ACKNOWLEDGEMENT

XII. ERKLÄRUNG

Erklärung gemäß der Promotionsordnung vom 06.12.2013

der Mathematisch-Naturwissenschaftlichen Fakultät

der Heinrich-Heine Universität Düsseldorf

Hiermit erkläre ich, die vorgelegte Arbeit mit dem Titel „On the role of amino acids in plant disease resistance: Interplay between pipecolic acid and salicylic acid in plant systemic acquired resistance" eigenständig angefertigt und keine anderen als die von mir angegebenen Quellen und Hilfsmittel verwendet zu haben. Diese Dissertation hat weder in gleicher noch ähnlicher Form einer anderen Institution vorgelegen. Ich habe bisher keine erfolglosen Promotionsversuche unternommen.

Düsseldorf, den

(Friederike Elisabeth Maria Bernsdorff)